Thermogenesis and fuel selection during cold exposure: Tissue-specific metabolism and cold-acclimation.

DENIS BLONDIN
M.Sc., University of Ottawa, 2008

Thesis submitted to the
Faculty of Graduate and Postdoctoral Studies
in partial fulfillment of the requirements
for the Doctorate in Philosophy - Human Kinetics

School of Human Kinetics
Faculty of Healthy Sciences
University of Ottawa

THESIS ABSTRACT

The focus of this thesis was to further elucidate the tissues and metabolic processes contributing to heat production during cold exposure, examine the interaction between the primary thermogenic organs and investigate the plasticity of these processes following a cold-acclimation protocol. The manuscripts contained within the thesis describe how this was accomplished. First, we began by examining the role of brown adipose tissue (BAT) in producing heat in adult humans. Prior to 2009, this tissue was considered metabolically irrelevant following infancy. However, our first manuscript showed that in fact this tissue can contribute to metabolic heat production during cold exposure but to an extent that varies from person to person, with some individuals relying predominantly on BAT to produce heat whereas others relied on shivering muscles. We then proceeded to examine the interaction and contribution of these two tissues in producing heat and clearing circulating substrates, such as glucose and fatty acids. In the process we also investigated the energy storing and dissipation relationship between white and brown adipose tissue. There were suggestions in the literature that perhaps the mechanisms that lead to white adipose tissue dysfunctions in obese and diabetic individuals may be shared with brown adipose tissue, explaining the apparent scarcity of this tissue in those populations. What was clear in this second manuscript, was that such a relationship is very plausible but, in addition, the thermogenic and substrate handling potential of skeletal muscle far exceeds the capacity from BAT and may be a more viable target to assist in the treatment of these metabolic diseases. The two final manuscripts focused on describing the potential for both BAT and skeletal muscle to change its phenotype in response to four weeks of daily cold exposure. The first of these two manuscripts investigated the plasticity of BAT and its subsequent effect on shivering and whole body energy metabolism, when exposed to a temperature that is slightly warmer than the temperature participants were acclimatized. Although BAT increased in volume and oxidative metabolism, its potential to alter whole body responses were not evident. Consequently, we explored the possibility that perhaps a colder thermal challenge was required in order to provoke the necessary response that demonstrates the thermogenic potential of this tissue. In this final manuscript, we found that even at colder temperatures, shivering intensity remained the same after a four week cold acclimation intervention, but that simply its onset and the skin temperature threshold to trigger detectable levels of shivering were shifted later in the acute cold exposure period. Interestingly, by taking muscle biopsy samples during these colder thermal challenges,

we were able to identify that skeletal muscle had also altered its phenotype over the four weeks, by reducing the cold-induced mitochondrial uncoupling that was apparent in the non-acclimated participants. This suggested that perhaps the simultaneous changes that occurred in BAT and skeletal muscle were neutralized when examining whole-body measurements, which resulted in no detectable changes in whole body heat production following a four-week cold acclimation. What we discovered in the end was that, indeed, BAT is thermogenically relevant in adult humans and under mild cold conditions its thermogenic contribution compared to shivering muscles varies tremendously between individuals. Further, both BAT and skeletal muscle demonstrated tremendous plasticity as a result of daily cold exposure. However, what was also clear is that both the contribution of BAT thermogenesis to whole body heat production and the ability to clear circulating substrates is quite limited when compared to skeletal muscle. Combined, the findings from this thesis provided indications that BAT may play a more local thermoregulatory role and perhaps clear circulating substrates sufficiently to manage small amounts of substrates in circulation, but unlikely to be sufficiently potent to reverse the effects of diabetes and obesity, where excessive levels of substrates are present.

ACKNOWLEDGEMENTS

When taking on the challenge of pursuing a doctorate, a number of factors have to be considered. Aside from the obvious variables such as: (1) do I enjoy research enough, (2) am I passionate about my topic, (3) am I driven enough to overcome the inevitable fluctuations in emotions and challenges; we must also consider the support network we surround ourselves with. It is this support network who will push you and motivate you to continue driving beyond those difficult moments and who will celebrate and acknowledge your successes along the way. I have many individuals to thank for their support. Some had more transient inputs while others provided consistent and regular support. There is no person that I owe more gratitude to than my beloved wife, Jesse Arnup Blondin. We have both had to make many sacrifices to allow me to complete this thesis, but there is no doubt that Jesse has had to sacrifice the most. It is thanks to her relentless support, love, encouragement, and discipline that I was able to complete this thesis. Her ability to provide continual support, despite having completed her own Master's in the process and given birth to our little Charlotte is what makes her that much more remarkable. I can't express adequately enough just how important you were to the process of my completing this thesis. The love that you and Charlotte continually show are what energizes me to continue moving forward on all those long days where I am driving back and forth from Sherbrooke. Along with the support from Jesse, was the encouragement and guidance provided by her mother, Dr. Katherine Arnup. I never would have had the confidence to pursue graduate studies without the guidance and encouragement of Dr. Arnup. Her accomplishments often drove me to remain focused and disciplined. In the process, she also provided tremendous support for both Jesse and I by taking loving care of Charlotte, so that we could continue to grow our relationship as a couple.

The home support I received represents but a portion of the overall guidance and encouragement I needed to complete this thesis. Dr. François Haman, has provided the most important contribution to my professional development as a researcher. As both my Master`s and Doctorate thesis supervisor, François has been providing me with guidance, support and encouragement for 7½ years. It is thanks to his patience, enthusiasm, and commitment to helping others that I have been able to not only complete my Master`s, upon originally abandoning it, but to then go on and pursue a doctorate. Through the process, François has given me the liberty to let my interests direct my focus, which has provided me with the opportunities to make mistakes so that I can ultimately succeed. François, your drive and enthusiasm has provided me with the confidence and perseverance to overcome some of the challenges we've faced over the past few years. It hasn't been easy for either of us, but it is because of your overwhelming support that I was able to look past those challenges and remain focused on our research. I feel that we've been able to make a significant impact in the scientific literature and I look forward to seeing these collaborations grow.

Finally, I'd like to thank my colleagues and mentors. I've had the fortunate opportunity to collaborate with a great team at the University of Sherbrooke and Laval University. I'm grateful for all the support provided by our exceptional nurses, Diane Lessard and Caroll-Lynn Thibodeau, our phenomenal PET technician, Éric Lavallée and our laboratory technician Frédérique Frisch. It is thanks to their help that we were able to navigate through the challenging REB process for a multi-institutional study such as this, their incredible perseverance to ensure that our cold acclimation study could be completed as quickly as possible and their warm, welcoming and charming personalities that we were able to do it all having a lot of fun in the process. Thank you to Dr. Christophe Noll, Margaret Kunach, Hans Tingelstad, Olivier Mantha

and Dr. Julie Martin for providing critical feedback, assisting in the execution of some of the projects and for being just as eager to get involved. I'd like to also acknowledge the guidance afforded to me by my future post-doctoral supervisor, Dr. André Carpentier. I've learned a tremendous amount about the importance of staying focused on the scientific process and scientific rigor and about the most fruitful was of navigating through the political components of academia and research through our brief conversations. Although only tid-bits of information, they have already proven to be quite valuable in my decision making process and my processing of information. Thank you to Dr. Céline Aguer, Dr. Taryn Taylor and Dr. Bert Taylor for agreeing to and taking the risk of being involved in the muscle biopsy portion of this study. This portion never would have been possible without your help. At the start of this PhD, the thought of performing biopsies was but a dream, but it all came together thanks to your enthusiasm regarding the potential results this study could bring. Finally, I'd like to especially acknowledge my dear colleague Dr. Sébastien Labbé. Thank you for being patient with me as I learned the challenging PET methodologies. You have provided more than simply guidance and support in learning the various software and models. Your drive, exceptional work habits and outstanding research performance have served as important motivation for me of what is possible if you are ambitious and determined enough to use all the resources around you .

TABLE OF CONTENTS

LIST OF TABLES

ARTICLE I

ARTICLE II

ARTICLE III

ARTICLE IV

LIST OF FIGURES

INTRODUCTION

ARTICLE I

ARTICLE II

ARTICLE III

ARTICLE IV

DISCUSSION AND CONCLUSION

APPENDICES

1. INTRODUCTION

1. INTRODUCTION

As endotherms, humans exposed to a compensable cold environment can remain homeothermic by producing sufficient heat to counteract the rate of heat loss. Under such conditions, this rate of heat production ($\dot{H}$) can increase by as much as five times the basal levels without modifying core temperature (Eyolfson *et al.*, 2001; Haman *et al.*, 2007). Since heat production (thermogenesis) is a by-product of the combustion of substrates and inefficiencies in biochemical reactions, it occurs within various tissues throughout the body. The sum of these metabolic processes represents whole body heat production. While under basal conditions the contribution of the major oxygen-consuming organs to this metabolic heat production is relatively well known, the partitioning of heat production among these tissues during a cold stress remains to be elucidated. A common assumption has been that the cold-induced rise in energy expenditure is almost entirely attributable to shivering muscles. It is unlikely that the rise in energy use during a cold stress is a process that is additive to the basal metabolic rate. Rather, the heat producing processes involved at rest are likely modulated during a cold stress thus repartitioning the sources of heat production and are subsequently supplemented by voluntary and/or involuntary sources of heat production. The voluntary sources include exercise-induced thermogenesis while shivering thermogenesis (ST) and cold-induced non-shivering thermogenesis (NST) are involuntary contributors. When exercise is not possible, activation of NST and ST is essential for maintaining a thermal balance. To date, very little is known about the respective contribution of NST and ST to $\dot{H}$. If animal models are any indication, these metabolic processes demonstrate significant plasticity to adapt to environmental stressors. This is evidenced by the various adaptations to chronic cold exposure demonstrated in rodents (Cannon & Nedergaard, 2004), monkeys (Steegman *et al.*, 2002) and various other

mammals (Chaffee & Roberts, 1971; Hohtola, 2004). Whether the potential for similar adaptations is preserved in humans remains to be investigated. **The focus of this thesis is to further elucidate the tissues and mechanisms contributing to heat production during cold exposure, examine the interaction between the primary thermogenic organs and elucidate the plasticity of these processes following a cold-acclimation protocol.** This will be accomplished by:

1) *Characterizing brown adipose tissue (BAT) metabolism and its contribution to cold-induced NST.*
2) *Characterizing the interaction between skeletal muscle and BAT derived thermogenesis and fuel selection and their influence on whole body metabolism.*
3) *Examining the plasticity of both skeletal muscle and BAT and their effects on the whole body thermal responses and energy metabolism under two different thermal conditions.*

Results from these studies will help to further clarify the role of tissue-specific metabolism on whole body heat production and oxidative fuel selection when exposed to a mild cold and to determine the plasticity of these mechanisms. Given the increasing evidence demonstrating the therapeutic benefits of cold exposure, these studies are crucial for understanding the extent to which these mechanisms can be modulated to improve processes that are otherwise dysregulated (eg. lipid metabolism in obese and glycemia in type 2 diabetes).

1.1. Temperature regulation - acute cold exposure in humans.

Historically, humans have relied primarily on behavioural strategies such as building or seeking shelter, wearing clothing or mastering fire to counteract environmental cold stresses (Steegman *et al.*, 2002; Wells & Stock, 2007). Among non-behavioural mechanisms of cold defence are the energetically costly (in ascending order of cost) vasoconstriction to conserve heat, NST, ST and exercise. Normothermia, environmental conditions whereby core temperature (T_{core}) can be defended, can be maintained within a large range of ambient temperatures by relying on these non-behavioural mechanisms of cold defence. Although exercise provides the greatest increase in thermogenic rate, reaching values 15 to 20 times above the resting metabolic rate (RMR), it also has its associated risks and is not always advisable under a cold stress [reviewed in (Castellani *et al.*, 2010)]. Consequently, there is a greater reliance on superficial vasomotor activity, ST and NST to maintain a thermal balance.

Much of our understanding regarding the central neural pathways involved in these involuntary thermoregulatory responses are derived from the use of transsynaptic retrograde tracing techniques using pseudorabies virus, direct electrical brain stimulation or pharmocological stimulation and inhibition of neural pathways in various animal models. Only recently have functional magnetic resonance imaging (fMRI) (Davis *et al.*, 1998; Kanosue *et al.*, 2002; McAllen *et al.*, 2006) and positron emission tomography coupled with computed tomography (PET/CT) been used to map the thermoregulatory centres of the human brain (Casey *et al.*, 1996; Egan *et al.*, 2005). As demonstrated in **Figure 1**, the thermoregulatory system consists of a sensory afferent axis, an integration centre and an efferent pathway.

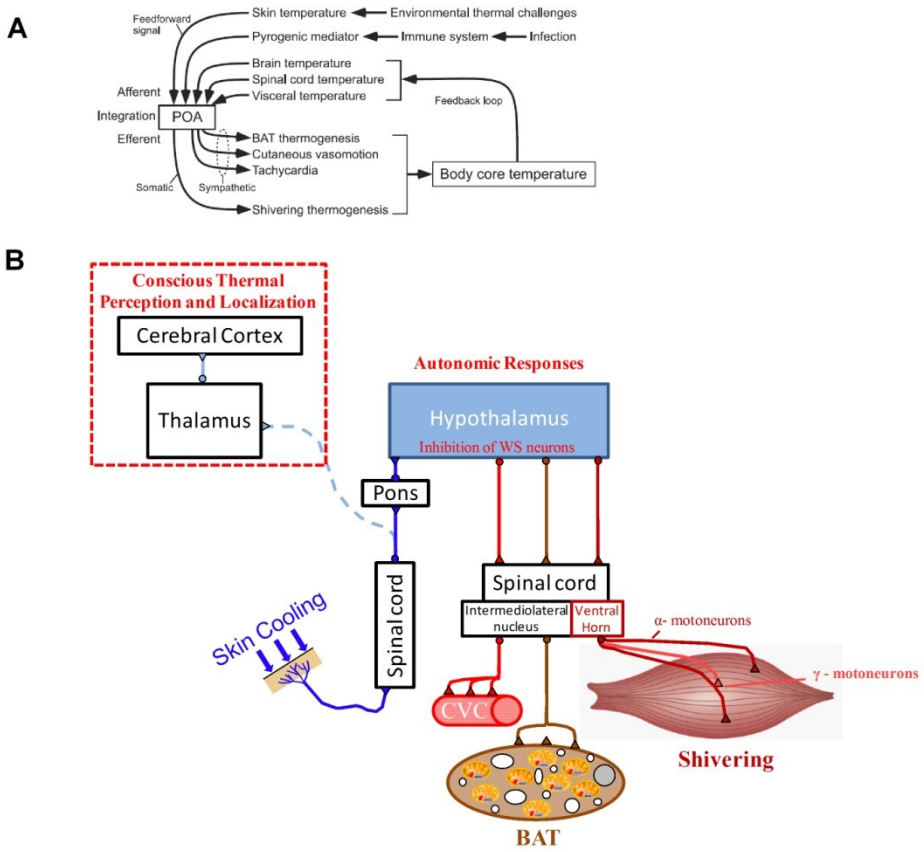

Figure 1. Conceptual demonstration of feedforward and feedback input of the thermoregulatory system (A) and the neural networks that make up the somatosensory and autonomic pathways (B). Adapted from Morrison (2011) and Nakamura (2011).

Cooling the skin activates the temperature-sensitive transient receptor ion channels (termed thermoTRP), expressed in free nerve endings located in the dermis and epidermis (Wang *et al.*, 1990; Hilliges *et al.*, 1995). This stimulation, conveys thermal afferent information through the spinal cord, to the thalamus and cerebral cortex for the conscious perception and localization of changes in temperature (Davis *et al.*, 1998; Egan *et al.*, 2005) as well as to the thermoregulatory centre located in the preoptic area of the hypothalamus to activate homeostatic cold-defence responses (Egan *et al.*, 2005). Interestingly, the spinothalamocortical pathway that is involved in temperature perception does not mediate the autonomous thermoregulatory responses (Morrison, 2011). The feed-forward response resulting from skin cooling, whereby cold defence effectors

are activated prior to changes in T_{core}, ensure that thermoregulatory responses are activated before the environmental thermal challenge can elicit such an influence on T_{core}. The threshold skin temperature that triggers each cold-defence effector may vary depending upon the effector, with shivering, for example, demonstrating a lower threshold than BAT and cutaneous vasoconstriction (CVC) in rodents (Nakamura, 2011). A number of thermoTRPs have been identified, each sensitive to a relatively narrow and distinct range of temperatures but collectively detect a span of temperatures ranging from innocuous to noxious (painful) (Schepers & Ringkamp, 2010). In addition to being found subcutaneously, thermoTRPs are also expressed among afferent nerve fibers located in the abdomen/viscera, spinal cord and hypothalamus, with this afferent input providing feedback on the present thermal state which may potentiate responses of some but not all thermoeffectors (McAllen *et al.*, 2010). Both the peripheral and central cold-sensitive receptors exhibit a vigorous increase in nerve impulse activity upon a decrease in ambient or skin temperate followed by a steady-state continuous discharge when the temperature is held constant (Darian-Smith *et al.*, 1973; Campero *et al.*, 2001), demonstrating an acute habituation effect. Both the dynamic and steady-state firing patterns can also be seen in the activation of the effector responses to an innocuous cold stimulus, whereby upon cooling shivering electromyography increases dramatically, before stabilizing to a lower amplitude (Imbeault *et al.*, 2013).

The preoptic area of the hypothalamus is recognized as the thermoregulatory centre in that it integrates afferent signals and initiates autonomic thermoregulatory responses such as skin vasomotor responses, BAT stimulation and shivering during cold exposure. In ambient conditions, warm-sensitive neurons in the preoptic area are tonically active to suppress thermogenic thermoeffectors. This tonic discharge is reduced by skin cooling thereby

disinhibiting thermoeffector neurons that drive these cold-defence responses. Neural output from raphé pallidus/arcuate nucleus in the medulla appears to increase as a function of decreases in skin temperature (McAllen *et al.*, 2006) in humans. Interestingly, despite the common afferent input, cold-defence thermoeffectors are controlled largely independently of one another and activated in parallel but possibly at different threshold temperatures suggesting that their interactions may simply be by-products of the afferent feedback received. For example, following the neural relay of the medullary raphé, activated sympathetic premotor neurons provide excitatory input to sympathetic preganglionic neurons in the intermediolateral nucleus to drive BAT stimulation and CVC responses, while premotor neurons in this same medullary region provide excitatory input to somatomotor neurons in the ventral horn which excite the alpha (α) and gamma (γ) motoneurons required for shivering (Nakamura, 2011). Consequently, rather than having complementary functions, there is evidence to suggest redundancies in the thermoregulatory system.

Of final note, understanding the thermoregulatory network in play when designing investigations is critical in ensuring that desired outcomes are likely to be met and that appropriate interpretations are made. With the recent surge in investigations examining the BAT function in humans, a trend has developed in the application of cold air exposure (19°C) combined with intermittently putting legs of the participant on blocks of ice (Saito *et al.*, 2009; Yoneshiro *et al.*, 2011) or in ice water (Virtanen *et al.*, 2009; Orava *et al.*, 2011; Orava *et al.*, 2013). There are two important limitations to such a strategy. First, the unintended consequence of applying legs on blocks of ice or in ice water is the stimulation of pain sensitive receptors (nocireceptors). When stimulated these receptors, in addition to signaling a painful cold sensation, stimulate afferent fibers which normally would be sensitive to heat stimuli, which

explains this hot or burning sensation. As a consequence, such an extreme cold may have an inhibitory or blunting effect on the cold-evoked thermoeffectors, such as BAT stimulation (Schepers & Ringkamp, 2010). Second, different brain activation patterns have previously been observed between conditions of local cooling (hand cooling) compared to whole-body cooling (Craig *et al.*, 2000; Egan *et al.*, 2005). These limitations could explain the high variability in BAT activation in these studies compared to the near 100% BAT activation found in studies simply applying cold air (van Marken Lichtenbelt *et al.*, 2009; Vijgen *et al.*, 2011; Vosselman *et al.*, 2012) or a liquid-perfused garment (Ouellet *et al.*, 2012).

1.2. Cold-induced metabolic heat production.

Although progress has been made in characterizing the thermoregulatory neural circuits in humans, little is known regarding the interaction between the cold-defence thermoeffectors. For example, the current knowledge on the respective contribution of NST and ST to total heat production during cold exposure has largely been limited to animal models. While the energy costs of maintaining a thermal balance under basal conditions and the organs contributing to this balance is relatively well characterized (**Figure 2**), much less is known about their respective contributions under cold conditions requiring an increased thermogenic rate. Further, for reasons still unknown, involuntary forms of thermogenesis are limited to ~40% of maximal oxygen consumption [~25 $kj \cdot kg^{-1} \cdot min^{-1}$ or ~5 times resting metabolic rate (X RMR)] (Eyolfson *et al.*, 2001); a value at least 3-times lower than the maximal aerobic capacity. It has been suggested that, like rodents and other mammals, BAT and skeletal muscle are likely the most significant contributors to cold-induced thermogenesis *via* mitochondrial uncoupling in BAT (Cannon & Nedergaard, 2004) or both uncoupling and ATPase-related mechanisms in the muscle (Himms-

Hagen, 2004; Silva, 2006; Wijers *et al.*, 2008). The metabolic activity of other organs, such as the liver and heart, may also be upregulated to support these processes. The following section will focus primarily on describing what is currently known regarding shivering and non-shivering forms of cold-induced thermogenesis.

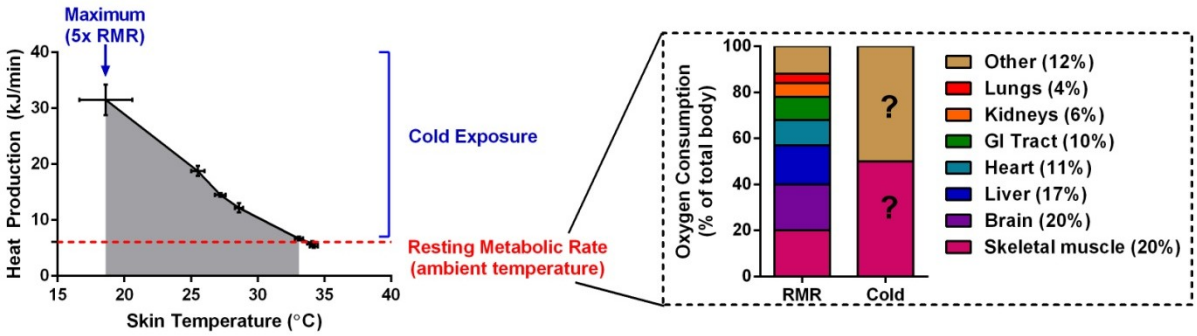

Figure 2. Representation of the relationship between mean skin temperature ($\overline{T}_{skin}$) and metabolic heat production (left panel) and the partitioning of this heat production at rest (right panel). Left panel: Core temperature (T_{core}) can be defended through vasomotor activity, up to a given ambient or skin temperature threshold. Following which, metabolic heat production increases as a function of skin temperature, up to a maximum increase of 5x the resting metabolic rate under passive conditions relying on non-exercising means of heat production. Data from Haman *et al.* (2002; 2005; 2007) and Ouellet *et al.*, (2012). Right Panel: Partitioning of whole body oxygen consumption among major oxygen-consuming organs of body under resting (RMR) and cold conditions. RMR data from Rolfe & Brown, (1997).

1.2.1 Shivering thermogenesis. Shivering has often been considered an ancillary component of cold-induced thermogenesis (Himms-Hagen, 2004; Morrison, 2011). In many mammals, including likely humans, the involuntary, rhythmic muscle contractions of ST is the final thermoregulatory mechanism to be activated during cold exposure given its high energy cost and its effect on motor control/locomotion (Morrison, 2011). The neural mechanisms involved in inducing and regulating ST is still relatively unknown, but as described previously (see **1.1. Temperature regulation - acute cold exposure in humans**), is regulated by feedfoward signaling from skin thermoreceptors (Tanaka *et al.*, 2006; Nakamura & Morrison, 2008; McAllen *et al.*, 2010). In brief, upon exposure to a compensable cold challenge peripheral

thermal afferents are relayed to the hypothalamus, resulting in a disinhibition of warm-sensitive neurons in the preoptic area, which then leads to the excitation of shivering-promoting neurons in the reticulospinal tract. At this point in the descending pathway, the spinal circuit becomes much less clear. The most common hypothesis is that γ-motoneurons are activated as a reflex response to skin cooling prior to any changes in core temperature, which may then activate the stretch reflex, resulting in an increase in α-motoneuron activity (and subsequent silencing of γ-motoneurons) (Meigal, 2002; Tanaka *et al.*, 2006). The early activation of γ-motoneurons is manifested as the thermoregulatory muscle tone observed early in a mild cold exposure and may potentiate the stretch reflex, on which shivering is dependent upon (McAllen *et al.*, 2010). The rhythmicity, shivering intensity and pattern have all been suggested to be determined locally in the spinal cord (Perkins, 1945; Tanaka *et al.*, 2006). The activation of neurons in the reticulospinal tract, which in primates excites motoneurons primarily of proximal muscles and to a smaller extent distal muscles (Shapovalov, 1972; Davidson & Buford, 2004; Riddle *et al.*, 2009), also suggest that proximal muscle groups may be preferentially recruited over distal muscle groups during ST; proximal muscle group activation being only observable non-invasively using nuclear imaging techniques, has never been attempted.

Using electromyography (EMG) methodologies, two distinct patterns have been identified in individual shivering muscles based on differences in intensity [2-5 vs. 7-15 % of maximal voluntary contraction (%MVC)] and rate of occurrence (8-10 vs. 0.1-0.2 Hz) (Israel & Pozos, 1989; Haman *et al.*, 2004a), which are associated to the recruitment of specific motor units. An example of an EMG signal from a shivering muscle is presented in **Figure 3**. In brief, continuous, low-intensity shivering (2-5% MVC, 8-10 Hz), commonly referred to as thermoregulatory muscle tone, is associated with the recruitment of low-threshold type I motor units

(specialized for lipid use), while high-intensity bursts (7-15% MVC, 0.1-0.2 Hz) are associated with high-threshold type II motor units (fast-glycolytic, specialized for CHO use) (Meigal, 2002). This shivering pattern appears to vary between individuals and seems to be strongly associated to fuel selection (Haman *et al.*, 2004b).

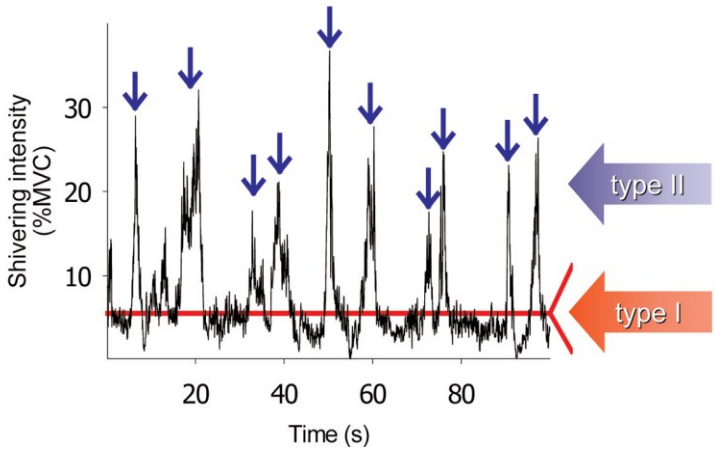

Figure 3. Example of EMG signal of shivering muscle. Low-intensity, continuous shivering is represented by the red horizontal line, and high intensity, burst shivering is indicated by the blue arrows. Figure from Haman *et al.,*(2005).

1.2.2. Cold-induced NST. Since heat production is a by-product of both the inefficiency of ATP production and ATP utilization, muscle contractions are not always necessary to produce heat. Given the energetic cost and associated limitations to sustaining ST, establishing the contribution of NST to total $\dot{H}$ and examining means of increasing its role in various degrees of cold exposure is required. Cold-induced NST may come from multiple sources in various tissues. The predominant sources of cold-induced NST have been suggested to come from either an ATPase-related mechanism of thermogenesis, consumers of ATP such as what is used to maintain ion gradients, or thermogenic mechanisms resulting from uncoupled oxidative phosphorylation [reviewed in (Rolfe & Brown, 1997; Himms-Hagen, 2004; Silva, 2006)]. Some have suggested that cold-induced NST occurs predominantly in skeletal muscle *via*: (1) futile calcium (Ca^{2+}) cycling resulting from the leakage of Ca^{2+} from the sarcoplasmic reticulum,

which may be mediated by increased thyroxine 5'-deiodinase type 2 (TD2) activity in the muscle (Himms-Hagen, 2004) and/or (2) cold-induced mitochondrial uncoupling (Wijers *et al.*, 2008). The mechanism of the latter remains unclear. According to the investigation from Wijers *et al.* (2008), the authors suggested that because the protein content of the uncoupling protein isoform found in skeletal muscle (UCP3) did not increase, the mitochondrial uncoupling must not be mediated by this protein. However, a cold-induced up-regulation in UCP3-mediated proton leakage may still be present without changing protein content. A recent investigation has shown that UCP3-mediated proton leakage is activated by reactive oxygen species production, which elicits a negative feedback loop to mitigate further ROS production (Mailloux *et al.*, 2011). It remains unclear whether this same mechanism is evoking the cold-induced proton leakage observed previously. With skeletal muscle representing ~40% of total body mass and uncoupled respiration accounting for ~20-40 % of respiration in skeletal muscle at rest (Rolfe & Brown, 1997), the potential for this mechanism to contribute significantly to cold-induced thermogenesis is intriguing to investigate.

Another location of cold-induced NST is found in BAT through mitochondrial uncoupling. With BAT volume estimated at ~130 cm^3 in lean men at a density of 0.9 g/ cm^3 (van Marken Lichtenbelt *et al.*, 2009) and the metabolic rate of this tissue estimated at 1.7 mL O_2 per g of tissue per min (Rothwell & Stock, 1983), the maximal stimulation of this tissue alone could contribute up to 25% of cold-induced thermogenesis (Haman *et al.*, 2010). Until recently, this tissue was considered to be only present in significant volume and activity in infants. This was despite necropsy studies indicating that this tissue persisted, albeit in fewer sites and smaller volumes, in adult humans but its presence appeared to decrease with age (Heaton, 1972). Preliminary epidemiological studies, where retrospective analysis of PET/CT scans for cancer

diagnosis were conducted, showed a relatively low prevalence of spontaneous BAT activity in adult humans (5-10% of population studied; (Au-Yong *et al.*, 2009; Cypess *et al.*, 2009; Ouellet *et al.*, 2011)). In 2009, seminal papers describing the presence of functional BAT in adult humans were published (Cypess *et al.*, 2009; van Marken Lichtenbelt *et al.*, 2009; Virtanen *et al.*, 2009), which triggered an increase in studies examining this tissue in humans. Significant progress has since been made in characterizing its developmental origin (Sharp *et al.*, 2012; Wu *et al.*, 2012), function (Ouellet *et al.*, 2012; Vosselman *et al.*, 2013) and distribution (Ouellet *et al.*, 2011; Cypess *et al.*, 2013). Recent studies have demonstrated that most BAT depots in humans exhibit molecular signatures and histological features resembling the inducible brown adipocytes (known as beige, brown-in-white or brite) clustered within white adipose tissue depots of cold-exposed rodents (Sharp *et al.*, 2012; Wu *et al.*, 2012) but may also contain classical BAT (Cypess *et al.*, 2013; Jespersen *et al.*, 2013). The differentiation of both the classical and beige/brite brown adipocytes (Wu *et al.*, 2012; Schulz *et al.*, 2013; Yin *et al.*, 2013) and its activation (van Marken Lichtenbelt *et al.*, 2009; Virtanen *et al.*, 2009; Ouellet *et al.*, 2012) appear to be largely mediated by a sympathetic input. To date, the most potent and effective sympathetic stimulator of BAT differentiation and activation in humans has been cold exposure, as most sympathomimetics applied *in vivo* have shown little to no effect on BAT activation (Cypess *et al.*, 2012; Vosselman *et al.*, 2012; Carey *et al.*, 2013). The large BAT mass and activity in patients with pheochromocytomas [catecholamine-secreting tumors; (Ricquier *et al.*, 1982; Lean *et al.*, 1986)] and in individuals chronically exposed to the cold (Huttunen *et al.*, 1981) suggests that this tissue can be developed with the appropriate stressor (sympathetic stimulation) and when stimulated for prolonged or intermittent periods. In addition, very recent investigations have demonstrated that relative BAT glucose uptake as assessed by increased ^{18}F-

fluorodeoxyglucose (^{18}FDG) standard uptake value (SUV) with PET can be increased by repeated cold exposure in humans (van der Lans *et al.*, 2013; Yoneshiro *et al.*, 2013). Whether the increased volume of glucose uptake observed is a result of proliferation of classical brown adipocytes, a *de novo* recruitment of brite adipocytes from white adipose tissue precursors (Wu *et al.*, 2012) or simply a direct interconversion of mature white adipocytes into a brown adipocyte phenotype or "*browning*" (Frontini *et al.*, 2013; Rosenwald *et al.*, 2013), is unclear. The use of ^{18}FDG uptake has allowed investigators to simply establish the presence of BAT and some have estimated the extent of its activity and contribution to the thermogenic rate by the degree of ^{18}FDG uptake. However, ^{18}FDG uptake is a marker of glucose uptake and, in absolute terms, does not accurately reflect the metabolic rate of BAT, given that only 10% of total BAT metabolism is supported by glucose (Ma & Foster, 1986). Other PET tracers may be more appropriate to characterize BAT metabolism in humans, such as the fatty acid analogue, 14(R,S)-^{18}fluoro-6-thia-heptadecanoic acid (^{18}FTHA), ^{11}C-acetate (a marker of Krebs cycle activity), or ^{15}O-oxygen to measure tissue respiration. Each tracer, however, has its own strengths and limitations, which will be further discussed in **1.6.3. PET nuclear imaging**. Of relevance here is that both ^{18}FDG and ^{18}FTHA uptake may be influenced by either substrate availability or utilization rate, whereas ^{11}C-acetate or ^{15}O-oxygen are not affected by either (Klein *et al.*, 2001).

Finally, studies conducted using the rodent model have provided valuable insight on the metabolic and thermogenic potential of BAT and the possible cross-talk that may occur between it and other organs. For example, BAT in rodents has been shown to play an important role in the post-prandial clearing of triglyceride-rich lipoproteins (to the extent comparable to the liver; (Bartelt *et al.*, 2011), when transplanted into the visceral cavity can improve glucose metabolism and insulin sensitivity in a dose-dependent manner; (Stanford *et al.*, 2013) and can be activated

by adrenergic-independent mechanisms (Villarroya & Vidal-Puig, 2013). These findings have shown the prospective therapeutic potential of this tissue. However, much work remains to be done to confirm whether similar mechanisms are present in humans.

1.3. Skeletal muscle - brown adipose tissue interaction

An important recent trend has shown important interactions between skeletal muscle and BAT. Although it is unequivocal that BAT is a vestigial organ of thermoregulatory importance, increasingly, evidence is surfacing demonstrating the metabolic consequences of its high thermogenic capacity. With locomotion and motor control being the primary function of skeletal muscle, relieving this organ from thermoregulatory functions is clearly of great importance. Prior to describing the interactions recently described in the scientific literature, it is important to recognize the context in which this interaction may be important. First, epidemiological studies examining the prevalence of spontaneous ^{18}FDG uptake in BAT have consistently demonstrated that diabetes status and BMI are negatively associated to the presence of BAT (Saito *et al.*, 2009; Ouellet *et al.*, 2011). Under acute cold stimulation, BAT ^{18}FDG uptake is lower in obese (Orava *et al.*, 2013) and morbidly obese (Vijgen *et al.*, 2011; Vijgen *et al.*, 2012) compared to lean individuals and is more insulin resistant in obese compared to lean individuals (Orava *et al.*, 2013). Although, further evidence is required to validate these findings, since interpretation of these findings have been somewhat contentious, in rodents, BAT has been shown to defend against diet-induced obesity, improve glucose homeostasis and hyperlipidemia and play an important role in postprandial energy partitioning (Cannon & Nedergaard, 2004; Bartelt *et al.*, 2011; Stanford *et al.*, 2013). Type 2 diabetes is also characterized by a dysregulation of postprandial substrate partitioning and metabolic inflexibility of plasma lipid fluxes in white

adipose tissue, which tends to result in the overexposure of lean tissues to fatty acids. This ultimately influences cardiac function (Labbe *et al.*, 2012) and impairs substrate handling in liver and skeletal muscles (Labbe *et al.*, 2011). All these dysfunctions can lead back to the impairments in both cathecholamine-induced nonesterified fatty acid mobilization and insulin-stimulated storage of meal fatty acids in WAT. Consistent with the impairments currently seen in BAT of obese individuals, there is a suggestion that resistance to both insulin-mediated storage of dietary fatty acids and catecholamine-mediated lipolysis of intracellular triglycerides may be generalized to both BAT and WAT, with the resulting dysregulation of energy storage and utilization thus contributing to the overexposure of lipids in lean tissues (Grenier-Larouche *et al.*, 2012). The consequence of this with regards to thermoregulation, is a greater reliance on skeletal muscle to produce heat due to the potential dysfunction of BAT. However, the relationship between BAT and skeletal muscle in thermoregulation and metaboregulation, has never been examined.

Two recent papers have begun shedding some light on the relationship between these highly thermogenic organs. The first was an investigation from Wu *et al.* (2012), which identified a novel myokine released following exercise after a 10-week endurance exercise intervention, which when exogenously administered to rats induced a browning of subcutaneous fat. This myokine, named Irisin, is cleaved and secreted into circulation as a portion of the membrane protein fibronectin type III domain containing 5 (FNDC5), with the expression of FNDC5 stimulated by an exercise-induced increased expression of the transcriptional co-activator PPAR-γ co-activator-1 α (PGC1-α). Irisin in turn, when administered exogenously to rats acted on white adipocytes in culture and subcutaneous fat depots *in vivo* to induce a *browning* of white adipose tissue (*ie.* display a brown adipocyte phenotype within a white

adipocyte depot). Interestingly, irisin-induced *browning* was never confirmed in the older, obese individuals (> 60 years old) taking part in exercise intervention and has since received much criticism in the literature. However, this study did provide some insight into the possible skeletal muscle-brown adipose tissue interaction that from an evolution perspective would seem to represent a positive adaptation to reduce the thermoregulatory function of skeletal muscle.

The second investigation that has provided valuable insight on the interaction between these highly thermogenic tissue is that of Yin *et al.* (2013). Lineage-tracing experiments have shown that brown adipocytes are derived from at least two types of developmental lineages. Classical brown adipocytes are derived from a myoblastic lineage [*Myf-5* positive myoblast precursors; (Seale *et al.*, 2008)], whereas the brown adipocytes found in clusters within white adipose depots (known as *brown-in-white* or *brite*) are derived from *Myf-5* negative progenitor cells, similar to white adipocytes (Petrovic *et al.*, 2010). Yin *et al.* (2013) showed that microRNA-133, expressed in adult satellite cells, plays a critical role regulating the brown adipogenic or myogenic commitment of these cells. More importantly, they found that cold exposure represses the expression of microRNA-133, inducing an increase in satellite cell-derived brown adipocytes which appeared to be greatest in intercostal, paraspinal and upper back muscles (central muscles) compared to limb muscles. This effect may not be incidental and may be linked to the cold-defence neural pathways that are stimulated during cold exposure. Together, these two studies combined with the recent studies in rodents and examining the pathophysiology of type 2 diabetes (T2D) have lead to many questions regarding the interaction between skeletal muscle and BAT which warrant further investigation.

1.4. Fueling thermogenesis during cold exposure

The thermogenic mechanisms described above are fuelled by the combustion of carbohydrates (CHO), lipids and proteins. Our current understanding of fuel selection during cold exposure suggests that the contribution of each fuel is influenced by differences in shivering intensity (Haman *et al.*, 2005; Haman *et al.*, 2007), variations in muscle fiber recruitment as indicated by the burst shivering rate (Haman *et al.*, 2004b) and changes in the size of CHO reserves prior to cold exposure (Martineau & Jacobs, 1989; Young *et al.*, 1989; Haman *et al.*, 2004c). In non-acclimatized men fasted overnight for 12-14 h, exposure to a moderate cold stress (<2.5 X RMR) results in the oxidation of CHO, lipids and proteins contributing ~40%, 50% and 10 % of total heat production respectively (Haman *et al.*, 2002; Haman *et al.*, 2005). As the cold stress increases (2.5-3.8 X RMR) the relative contribution of CHO utilization to total $\dot{H}$ increases to as high as 62% while the lipid contribution falls to ~35% of $\dot{H}$ (Haman *et al.*, 2005; Haman *et al.*, 2007). This shift in substrate utilization is linked to differences in muscle fibre recruitment. For example, a study by Haman *et al.* (2004b) demonstrated a high variability in fuel selection between participants during a cold exposure inducing moderate-intensity shivering. This high variability was attributed to differences in shivering pattern/muscle fibre recruitment, as those demonstrating a greater reliance on lipids recruited predominantly more type I (oxidative fibres) compared to those relying more on CHO who recruited predominantly type II (glycolytic fibres). To date, only the partitioning of CHO utilization has been examined during cold exposure, while very little is known regarding lipid metabolism. Results from studies examining the importance of CHO reserves have indicated that muscle glycogen always provides most of the glucose required to sustain CHO oxidation (~75-80% of total CHO oxidation) whereas the contribution of plasma glucose remains constant at ~20-25% regardless of shivering intensity (Haman *et al.*, 2005), muscle fiber recruitment (Haman *et al.*, 2004a), or the status of

glycogen reserves (Haman *et al.*, 2004c). With lipids providing the most abundant energy source and characterized by its high energy density (energy per gram), there is tremendous value in further examining the role of this substrate and its various sources during cold exposure.

A number of questions remain regarding fuel selection during cold exposure. If highly metabolically active tissues are contributing to the increased thermogenic rate during a cold stress, to what extent are their substrate utilization reflected in the whole body measurements? Would their contribution explain the differences in the whole body fuel selection pattern observed between exercise and cold-induced thermogenesis of the same metabolic rate? Further research is required to clarify: (1) the role of tissue-specific metabolism to whole body fuel selection, (2) whether the recruitment of specific muscle groups are contributing to this fuel selection pattern and (3) how these two are modulated over a wide range of cold stresses.

1.5. Adaptation, acclimatization and acclimation to cold

As a preface to this section, it is important to define and distinguish the following three terms: adaptation, acclimatization and acclimation. Although all apparently similar and often used interchangeably, each term carries very important distinctions. Adaptation refers to genotypic characteristics having evolved through natural selection to favour survival in a particular environment (IUPS Thermal Commission, 2001). Acclimatization refers to physiological changes naturally occurring as a result of the natural climate in which the organism is exposed to (e.g. seasonal, geographical, working conditions) (IUPS Thermal Commission, 2001). Finally, acclimation refers to physiological changes induced experimentally. The distinctions are not only important as means of establishing operational definitions, but because

the physiological changes that occur through acclimatization can often help explain some of the physiological changes evoked through acclimation.

Humans chronically or repeatedly exposed to a cold stress exhibit modified physiological responses to a cold stimulus. These responses can even differ as a result of living or working in cold environments (cold-acclimatized) versus experimentally-induced cold exposures (cold-acclimated). Some of the modified physiological responses commonly observed are either: metabolic, insulative, or hypothermic in nature or a combination of these. A metabolic adjustment refers to an increase in cold-induced heat production which is often accompanied by higher skin temperatures but a normal core temperature (T_{core}). To our knowledge such adjustments have only been found in certain populations living in cold conditions (e.g. Hammel *et al.*, 1959; Elsner *et al.*, 1960; Hart *et al.*, 1962) and thus are likely genetic adaptations or related to differences in physical characteristics (ie. morphology, fitness) or dietary factors between this population and the control comparison group. Insulative adjustments are characterized by lower skin temperatures and a normal metabolic response and T_{core}. Similar to the metabolic adjustments, this type of response has only been observed in a coastal tribe of Northern Australia (Scholander *et al.*, 1958) and traditional Korean and Japanese Ama divers (Hong, 1973). An example of hypothermic adjustments to repeated cold exposure is presented in **Figure 4**. In brief, this adjustment is characterized by a fall in core temperature, due to a lower metabolic response to the same skin temperature or rate of heat loss.

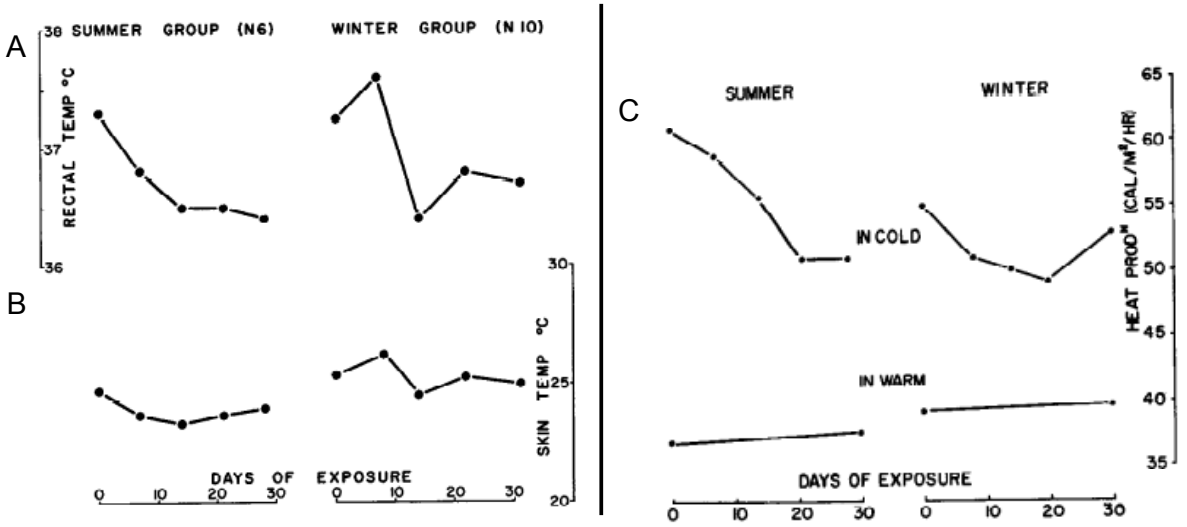

Figure 4. Rectal temperature (T_{re}; *panel A*), $\overline{T}_{skin}$ (*panel B*) and metabolic rate in relative to body surface area (*panel C*) during 120 min of cold air exposure (13.5°C) before (Pre-Acclimation) and after (Post-Acclimation) 31 days of cold air exposure (6 days/week for 8hrs/day @ 11.8-13.5°C). Figure from Davis *et al.* (1961).

To date, the results and interpretation of results from cold acclimation studies (ie. experimentally induced cold exposure) are quite contradictory. While some have demonstrated a 17% decrease in $\dot{H}$ (Hesslink *et al.*, 1992), others have demonstrated either a slight ~10% increase in $\dot{H}$ (Bittel, 1987) or no change (Young *et al.*, 1986). Both Young *et al.* (1986) and Bittel (1987) observed significantly lower mean skin temperatures ($\overline{T}_{skin}$) following their cold-acclimation protocols, but one study found a lower T_{core} post-acclimation (Young *et al.*, 1986) and was thus considered an insulative-hypothermic acclimation (**Figure 5**), while the other did not and was thus considered a metabolic-insulative acclimation (Bittel, 1987) (**Figure 6**). The insulative-hypothermic acclimation pattern is the most often observed response with the majority of cold-acclimation studies reporting similar findings (Lapp & Gee, 1967; Golden & Tipton, 1988; Janský *et al.*, 1996; Stocks *et al.*, 2001). This may simply be an unavoidable consequence of conducting these investigations during periods when participants are considered least acclimatized to the cold, in

late summer. During such studies, the influence of the cold stress combined with the heat stress during the day seems to elicit similar cold-acclimation patterns as that observed in primitive people living in temperate weather who experience cold nights and hot days [see Young, (1996) for review].

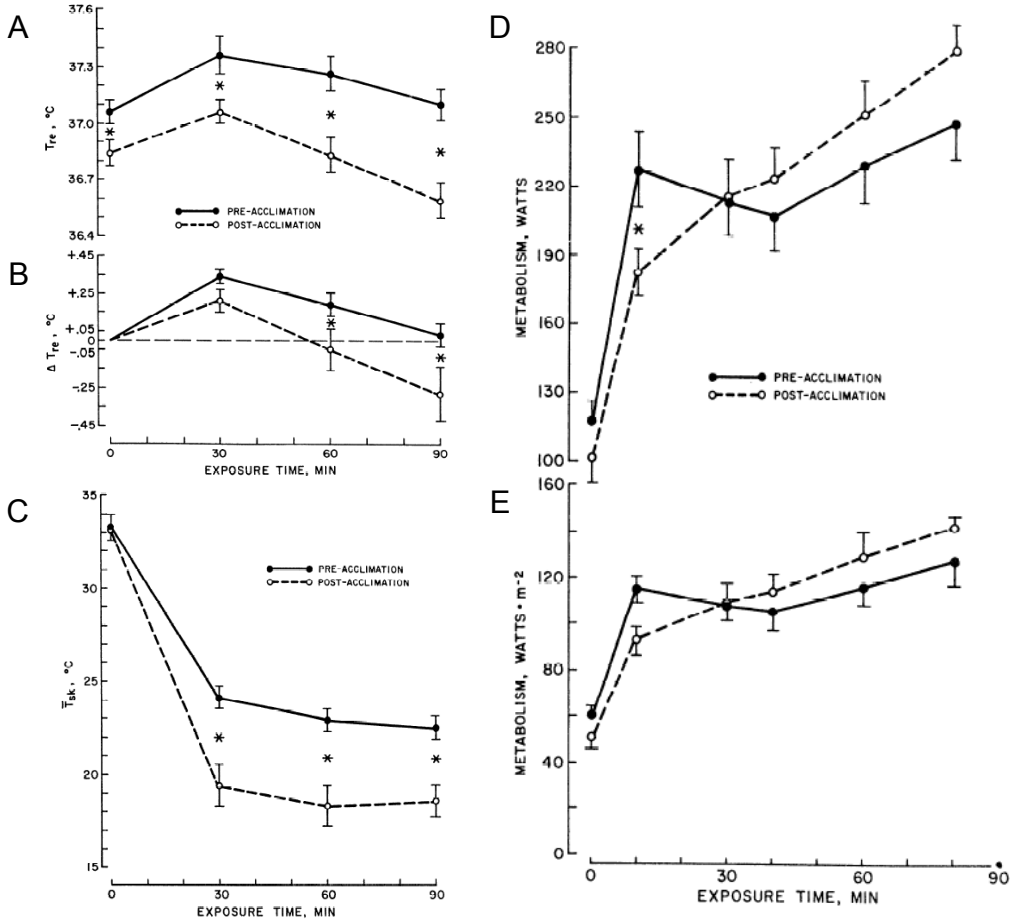

Figure 5. T_{re} (*panel A*), change in T_{re} (ΔT_{re}; *panel B*), $\overline{T}_{skin}$ (*panel C*) and metabolic rate in absolute (*panel D*) and relative to body surface area (*panel E*) during 90 min of cold air exposure (5°C) before (Pre-Acclimation) and after (Post-Acclimation) 5 weeks of repeated cold water immersions (5 days/week for 90 min @ 18 °C). Figure from Young *et al.*(1986).

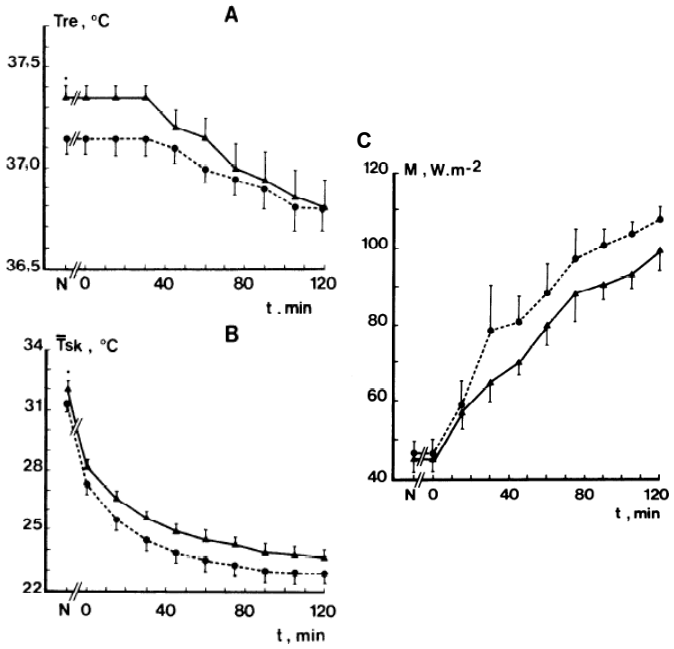

Figure 6. T_{re} (*panel A*), $\overline{T}_{skin}$ (*panel B*) and metabolic rate in relative to body surface area (*panel C*) during 120 min of cold air exposure (10°C) before (Pre-Acclimation) and after (Post-Acclimation) 2 months of cold water immersion (5 consecutive days/week for 1-3 hrs/day @ 10-15°C). Figure from Bittel (1987).

The divergent thermoregulatory adjustments exhibited in response to experimentally induced cold-acclimation may be related in part to differences in acclimation protocols; 30 min twice daily at 4.4ºC for 8 weeks (Hesslink *et al.*, 1992), 90 min 5 days a week for 5 weeks in 18°C water (Young *et al.*, 1986) and 60-180 min for 4 to 5 days per week depending on individual tolerance in 10-15ºC water for 8 weeks (Bittel, 1987). In this previous work, the main focus was placed on changes in $\dot{H}$ measured from changes in rates of oxygen consumption. Consequently, no information is currently available on whole-body changes in ST and NST. It is likely that changes in the respective contribution of ST and NST to total $\dot{H}$ can occur without modifying rates of oxygen consumption. To date only one study has provided semi-quantitative information on shivering activity from cold-acclimation and their findings support such a hypothesis. Six

unacclimated men were exposed to 12-14°C air, 8h/day for 31 consecutive days and found that mean shivering activity fell to 80% of pre-acclimation values, without observable changes in $\dot{H}$ (Davis, 1961). By definition this implies an increase in cold-induced NST. Further research is needed to confirm this hypothesis as well as determine whether such a change can occur with shorter intermittent periods of cold exposure. If rodent models are any indication (Wiesinger *et al.*, 1990), it is plausible for such an acclimation to induce similar physiological alterations and for a full transition towards a nearly complete reliance on NST to occur within 4 weeks [**Figure 7**; (Cannon & Nedergaard, 2004)]. Given the 30% increase in plasma norepinephrine (NE) concentration observed during an acute cold stress test, following a five week acclimation protocol (Young *et al.*, 1986), this increased NST may come from increased BAT activity which, if intermittently exposed to NE, may have also increased in volume and capacity. A recent study has shown that exposure to 15-16°C cold air for six hours per day for 10 consecutive days could increase the volume of metabolically active BAT by 27% in women and 38% in men (van der Lans *et al.*, 2013). It remains unclear whether the oxidative capacity of this tissue has also changed.

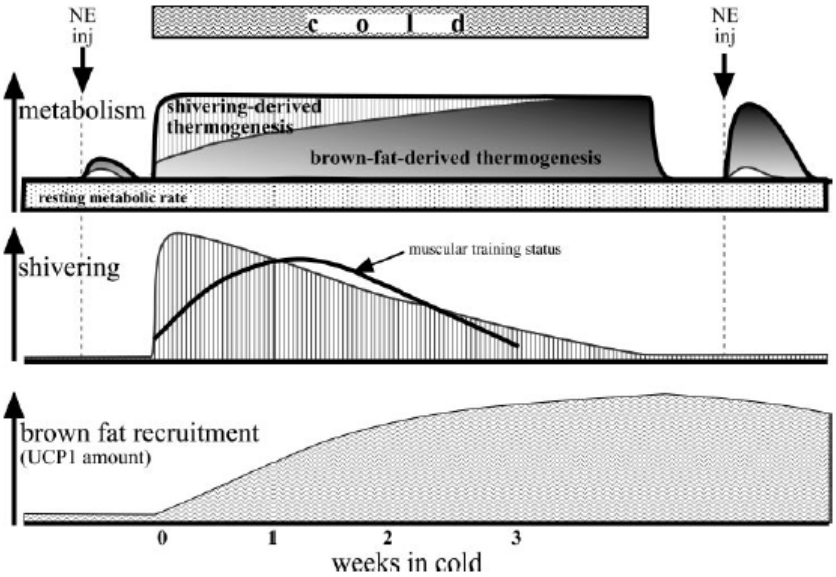

Figure 7.
Hypothetical sketch of metabolic responses to acute and chronic cold, based on an experimental rodent. Figure from Cannon & Nedergaard (2004).

1.6. Measuring metabolism from whole-body to organs.

Traditionally, estimating whole body to tissue-specific metabolism has required a range of techniques which have also varied in their level of complexity and invasiveness. These techniques have varied from indirect calorimetry to more invasive techniques such as arterial and venous catheterization techniques to measure arterio-venous metabolite gradients. This section will aim to describe some of the techniques used in the present thesis which include: indirect calorimetry, stable and radioactive isotope methodologies and PET imaging.

1.6.1. Indirect calorimetry. Whole body metabolic rate and fuel selection will be quantified by indirect calorimetry, using flow-through respirometry. The rates of oxygen consumption ($\dot{V}O_2$) and carbon dioxide production ($\dot{V}CO_2$) will be calculated using the following equations derived by Brown et al. (1984) adapted for its application with a canopy:

(1) Correction for the dilution effect of water vapour pressure (P_w) on fractions of O_2 (F_{O2}) and CO_2 (F_{CO2}) and the flow rate ($\dot{F}$) of the air being drawn:

$$F_{O2}' = F_{O2} \times P_b/(P_b - P_w) \quad (1)$$

$$F_{CO2}' = P_{CO2} \times P_b/(P_b - P_w) \quad (2)$$

$$\dot{F}' = \dot{F} \times (P_b - P_w)/P_b \quad (3)$$

P_b, barometric pressure

(2) A background baselining technique, developed by Sable Systems International, described in Melanson *et al.* (2010), was then applied to correct for analyser drift.

(3) The following respirometry equations were then applied:

$$\dot{V}O_2 = \dot{F}' \times \left(\frac{(FO2') - 0.2095 \times (PCO2')}{(1 - 0.2095)}\right) \quad (4)$$

$$\dot{V}CO_2 = \dot{F}' \times \left(\frac{(PCO2') - 0.0005 \times (PO2')}{(1 - 0.0005)}\right) \quad (5)$$

This approach allows for a constant measurement and subsequent correction for the dilution effect of water vapor pressure on $\dot{V}O_2$ and $\dot{V}CO_2$ and ensures that all variables are measured and accounted for in the calculation of $\dot{V}O_2$ and $\dot{V}CO_2$, without making any assumptions. $\dot{V}O_2$ and $\dot{V}CO_2$ will be subsequently used to quantify whole body substrate utilization and total thermogenic rate.

Total protein (RP_{ox}), carbohydrate (RC_{ox}) and lipid (RF_{ox}) oxidation rates (in g/min) will be calculated as follows:

$$RP_{ox}\,(g/min) = 2.9 \text{ x } UREA_{urine}\,(g/min) \quad (6)$$

$$RC_{ox}\,(g/min) = 4.59\,\dot{V}CO_2\,(l/min) - 3.23\,\dot{V}O_2\,(l/min) \quad (7)$$

$$RF_{ox}\,(g/min) = -1.70\,\dot{V}CO_2\,(l/min) + 1.70\,\dot{V}O_2\,(l/min) \quad (8)$$

where urinary urea excretion ($UREA_{urine}$) is measured in urine collected in ambient conditions and again at the end of cold exposure, and $\dot{V}CO_2$ (l/min) and $\dot{V}O_2$ (l/min) corrected for the volumes of O_2 and CO_2 corresponding to protein oxidation (1.010 and 0.843 l/g, respectively). Energy potentials of 16.3 kJ/g (CHO), 40.8 kJ/g (lipids), and 19.7 kJ/g (proteins) will be used to calculate the relative contributions of each fuel to the total thermogenic rate (Elia, 1991; Péronnet & Massicotte, 1991).

1.6.2. Stable and radioactive tracers. A number of stable and radioactive tracers will be used over the course of the investigations that make up this thesis. Tracers are biological

compounds that contain one or many atoms that are isotopes of the atoms that make up the native/naturally occurring compound. These isotopes are low in natural abundance, which allows for the fate of a labelled-compound to be easily monitored continuously. In particular, these tracers will allow us to determine whole body rates of appearance and disappearance of labelled molecules. The three most commonly used isotopes in human studies include carbon-13 (^{13}C), deuterium (^{2}H) and tritium (^{3}H); the latter being a radioactive isotope. Although radioactive, ^{3}H tends to be used preferentially above other radioactive isotopes, such as carbon-14 (^{14}C), due to its relatively shorter half-life and final destination/incorporation in human tissues which renders it much safer in comparison. For example, the half-life of ^{3}H is 12.32 years, however it is often cleared from the human body within 7 to 14 days under the form of water, be it through urine, perspiration, respiration or other water-eliminating processes. In contrast, ^{14}C has a half-life of ~5730 years and in many instances, when metabolized to form $^{14}CO_2$ can be exchanged with the bone CO_2 compartment (Poyart *et al.*, 1975) where it becomes trapped for an indefinite period.

In the investigations presented here, three tracers will be described. They include: [3-^{3}H]-glucose, [U-^{13}C]-palmitate and [1,2-^{13}C]-sodium acetate. Whole body plasma glucose and non-esterified fatty acid (NEFA) kinetics will be quantified using a primed continuous infusion of [3-^{3}H]-glucose and [U-^{13}C]-palmitate. [U-^{13}C]-palmitate infusion will be preceded by an intravenous (IV) bolus of [1-^{13}C]-sodium bicarbonate to prime the bicarbonate pool (Wolfe & Chinkes, 2005). During protocol A of **Article #1**, [1,2-^{13}C]-sodium acetate will be infused intravenously, preceded by a bolus of [1-^{13}C]-sodium bicarbonate, to determine the acetate retention factor which will correct for the fixation of ^{13}C into products of the tricarboxylic acid cycle prior to the recovery of expired $^{13}CO_2$ during protocol B of **Article #1,** when [U-^{13}C]-palmitate oxidation will be quantified (Sidossis *et al.*, 1995). Subsequently the rate of

appearance ($Ra_{glucose}$, Ra_{NEFA}) and disappearance ($Rd_{glucose}$, Rd_{NEFA}) of these substrates will be calculated using Steele's non-steady state equations (Steele, 1959):

$$Ra = \frac{F - V[(C_2 + C_1)/2][(E_2 - E_1)/(t_2 - t_1)]}{(E_2 + E_1)/2} \quad (9)$$

$$Rd = Ra - V \times \left(\frac{C_2 - C_1}{t_2 - t_1} \right) \quad (10)$$

where F is the infusion rate ($\mu mol \cdot kg^{-1} \cdot min^{-1}$), V is the distribution volume for glucose or palmitate [162.5 or 90 ml/kg respectively; (Carpentier *et al.*, 2001)], C_1 and C_2 are the glucose or palmitate concentrations (mmol/l) at *time 1* (t_1) and *2* (t_2) respectively, E_2 and E_1 are the plasma glucose or palmitate enrichments at *time 1* and *2*, respectively.

Plasma palmitate oxidation ($Rox_{palmitate}$) will also be quantified through breath $^{13}CO_2$ enrichment during [U-^{13}C]-palmitate infusion, corrected for the fractional recovery of ^{13}C in expired CO_2 observed after the infusion of labelled acetate (Sidossis *et al.*, 1995).

$Rox_{palmitate}$ will be determined using the equations:

$$Rox_{palmitate} = (\dot{V}CO_2 \times R_{exp}) / (F_{[U\text{-}13C]palmitate} \times 16 \times k) \quad (11)$$

where $\dot{V}CO_2$ is expressed in micromoles per lean body mass per minute, R_{exp} is the isotopic enrichment of expired CO_2, $F_{[U\text{-}13C]palmitate}$ is the palmitate tracer infusion rate ($\mu mol \cdot kg^{-1} LBM \cdot min^{-1}$), 16 is the number of carbon atoms in palmitate and *k* is the fractional recovery of ^{13}C in expired CO_2, observed after the infusion of labelled acetate, which is calculated as:

$$k = (\dot{V}CO_2 \times R_{exp}) / (F_{[1,2\text{-}13C]acetate} \times 2) \quad (12)$$

where $F_{[1,2\text{-}13C]acetate}$ is the [1,2-^{13}C]-sodium acetate infusion rate.

Total plasma NEFA oxidation will be calculated by dividing palmitate oxidation rates by the fractional contribution of plasma palmitate to total plasma NEFA concentration.

1.6.3. PET nuclear imaging. PET is a medical imaging technique which has traditionally been used in oncology to detect and classify the stage of malignant tumors as well as for radiation therapy. In metabolic research, it is more commonly being used as a non-invasive means of quantifying tissue-specific substrate uptake and metabolism. As the name implies, the basis of its utilization revolves around the use of positron-emitting radionucleotides (^{11}C, ^{13}N, ^{15}O, ^{18}F), which are produced using a cyclotron. Once injected, the positron (positive electron) will travel through matter, losing energy along the way, and once having lost enough energy will be annihilated with a nearby electron and yield two gamma photons emitting 511 keV (511 000 electron volts) of energy that are emitted 180° from one another and detected simultaneously by scintillators (Turkington, 2001). These scintillation detectors make up the ring seen in **Figure 8**.

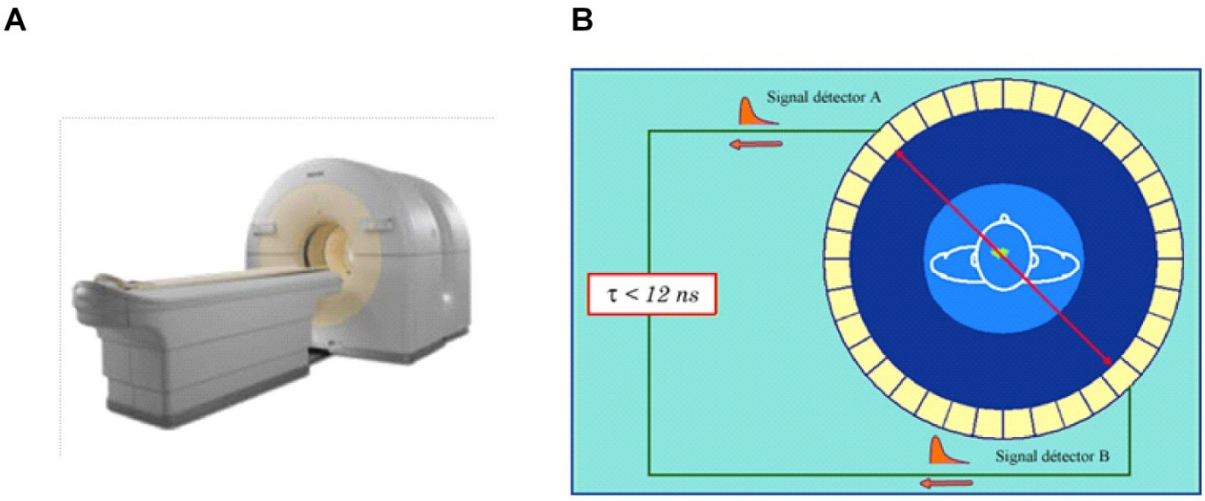

Figure 8. (A) Philips Gemini TF PET/CT scanner. CT and PET cameras can be seen in 1st and 2nd ring, respectively. Each ring offers an axial field of view for image acquisition of up to 18 cm. (B) Gamma photons emitted during positron annihilation are detected by scintillators, structured as a ring (figure from http://www.laradioactivite.com).

The accumulation of these gamma rays allows for the construction of tomographic cross-sections of the participant and, using reconstruction algorithms, creates a three-dimensional image. These images are then used to delimit regions of interest for a tissue of interest to determine the metabolic activity within. PET images are then combined with x-ray computed tomography (CT) images, usually acquired prior to the PET scan, to correlate the anatomical location with the spatial distribution of the metabolic activity detected by PET.

In the investigations presented in this thesis, both static and dynamic PET image acquisition will be used. The static acquisition allows for the whole body bio-distribution of the radio-tracer being given to be determined. This is demonstrated in the left panel of **Figure 9**, where the bio-distribution of a fluorine-18 (^{18}F) glucose analogue (^{18}FDG) and long chain fatty acid analogue (^{18}FTHA) can be seen (metabolism of each described in ***1.6.3.1 and 1.6.3.2***, respectively).

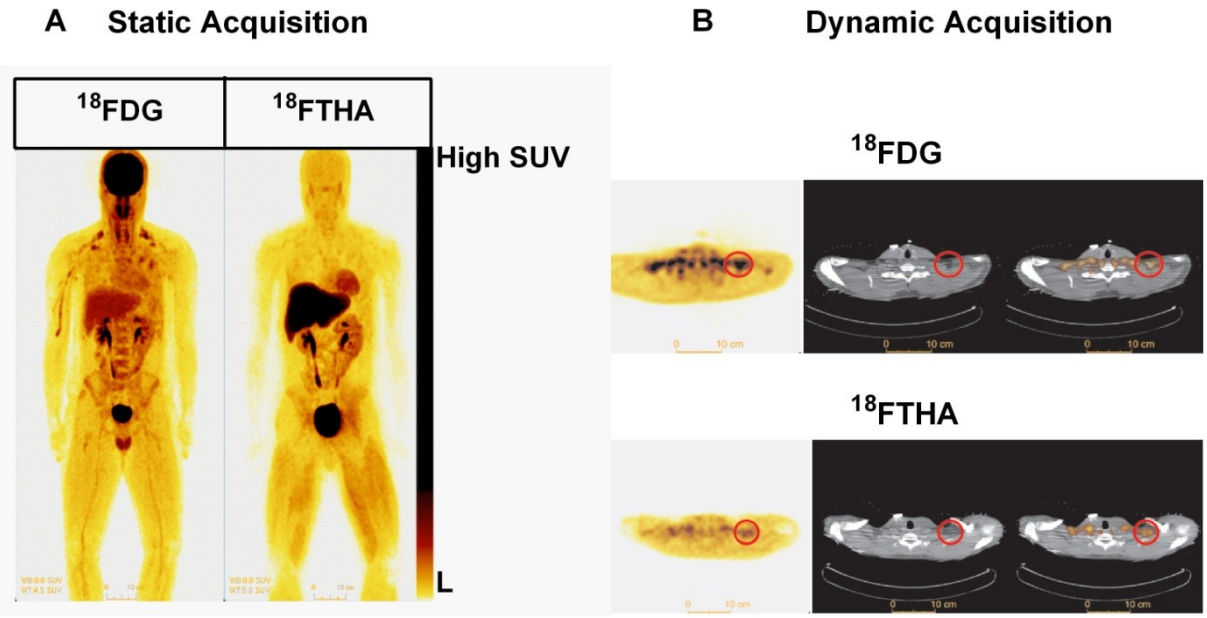

Figure 9. (A) Static PET acquisition of a fluorine-18 labelled glucose analogue (^{18}FDG) and long chain fatty acid analogue (^{18}FTHA). (B) Low-dose (40 mAS) computed tomography scan (left panel), dynamic PET scan (middle panel) and PET/CT fused image (right panel) centred at the cervicothoracic junction. Image represents a single slice and a single frame (single time point). Red circle represents BAT deposit.

In each instance, the radio-labelled tracer was injected 60 - 75 minutes prior to these scans being taken. These images represent the accumulation of the respective tracer over the course of post-injection period, presented as a mean value of pixels (or mean standard uptake value; mean SUV) according to the following equation:

$$\text{Standard Uptake Value (SUV)} = C_{tissue}/(\text{radioactivity injected/kg body weight}) \quad (13)$$

where C_{tissue} represents tissue concentration (in kBq/mL of tissue) of the defined region of interest.

Dynamic acquisitions allow for the time-dependent uptake of the radio-labelled tracer to be determined, in order to quantify the flux of substrates entering the tissue and in some instances its metabolism once taken up by the tissue. The dynamic acquisition can be broken down into various time sequences depending on the radio-isotope being infused and the modeling being applied (see Patlak linearization model presented in **Figure 10**). For example, using ^{18}FDG or ^{18}FTHA, a 40-minute dynamic PET acquisition is performed with an image (frame) captured at the following intervals, sequentially: 12 images at 10 second intervals, 8 images at 30 second intervals, 6 images at 90 second intervals and the final 5 images at 300 second intervals. As this model clearly illustrates, the uptake of the radio-isotope can be followed from the moment it reaches the aortic arch to when it is distributed to the rest of the body to the tissue of interest. Recent advances in PET modeling has allowed for arterial input functions, derived from repeated arterialized blood sampling, to be replaced with image-derived input functions (Croteau *et al.*, 2010), which eliminates the additional stress on participants and provides a more accurate reflection of the isotope distribution. In brief, regions of interest are drawn on the aortic arch and the tissues of interest, within the field of view available (see **Figure**

9B). These regions of interest are then copied to each frame, which represent a particular time point and can be used to create time-radioactivity curves.

1.6.3.1. 2-deoxy-2-[^{18}F]-fluoro-D-glucose (^{18}FDG). ^{18}FDG is a fluorine-18-labelled glucose analogue, that is very commonly used in nuclear medicine and metabolic investigations for the purpose of detecting neoplastic pathologies as well as examine glucose metabolism in the brain, heart and various other tissues. As a fluorine-18-labelled molecule, its half-life is 110 min. The metabolic fate of ^{18}FDG follows the same fate as other deoxyglucose tracers. ^{18}FDG is transported in a cell through the same transporters as glucose. Once transported ^{18}FDG is phosphorylated by hexokinase to form ^{18}FDG-6-phosphate. ^{18}FDG-6-phosphate does not participate any further in glycolysis and is subsequently irreversibly trapped within the cell and accumulates in proportion to the glycolytic rate (Phelps, 2000). Non-phosphorylated ^{18}FDG can return to the circulation and be taken up elsewhere. Arterial plasma and tissue time-radioactivity curves can be created by drawing regions of interest on the aortic arch and tissues of interest, respectively (as previously described). These curves are then analyzed using the Patlak linearization method (Patlak *et al.*, 1983). This model is only interested in the end outcome of ^{18}FDG accumulation within the cell and does not distinguish between the number of intracellular compartments in which it might exchange with. The slope of the plot in the graphical analysis is equal to the tissue glucose extraction constant of ^{18}FDG (K_i, in min^{-1} of ^{18}FDG). This represents the amount of glucose extracted by the tissue, relative to what it sees and is corrected for tissue density. Other multi-compartmental models may also be applied to distinguish between these pools, but are beyond the scope of this thesis. The product of the fractional extraction (K_i) and arterial plasma glucose concentration yields the net glucose uptake of the tissue of interest (K_m, in μmol of glucose·mL of tissue^{-1}·min^{-1}). The arterial plasma glucose concentration is corrected

for the differences in the transport and phosphorylation between glucose and ^{18}FDG [1.2 in skeletal muscle and 1.0 in other tissues; (Kelley *et al.*, 1999)].

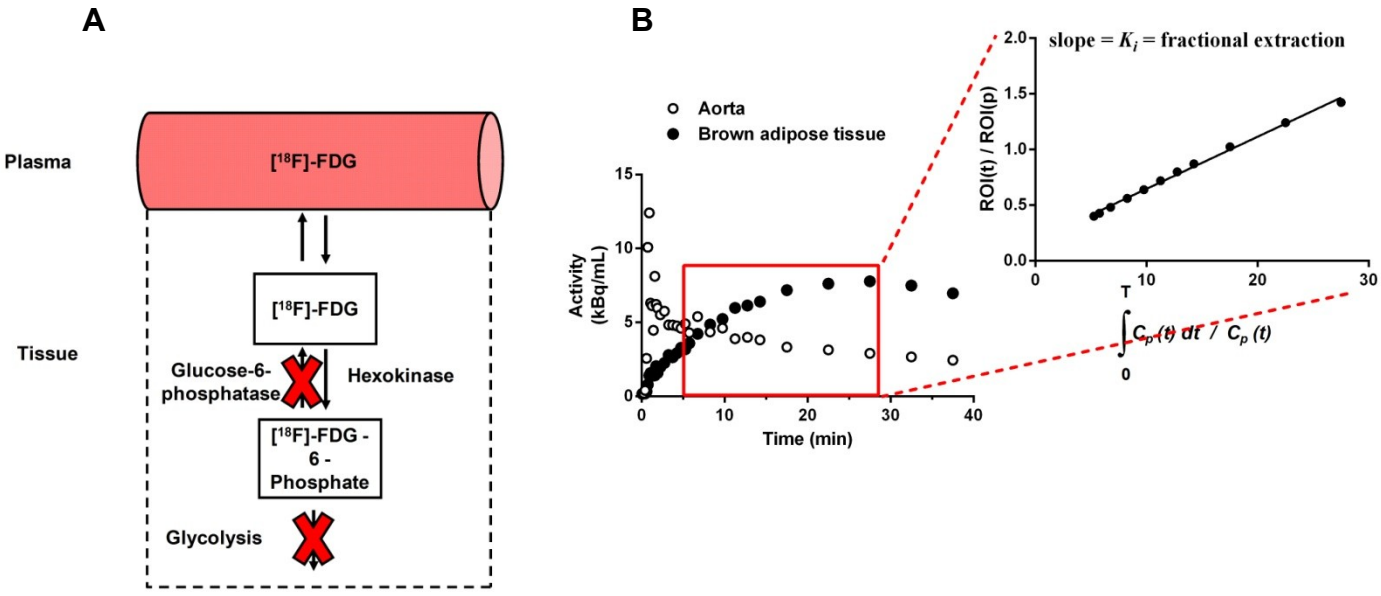

Figure 10. (A) Metabolic fate of ^{18}FDG. Adapted from (Phelps, 2000). (B) Time-activity curve representing aorta and brown adipose tissue ^{18}FDG activity (left panel). Patlak linearization graphical analysis (right panel) applying the equations of Patlak *et al.* (1983). ROI (t), represents region of interest of the tissue of interest (BAT here); ROI (p), represents region of interest of the arterial plasma.

1.6.3.2. [^{18}F]-fluoro-6-thia-heptadecanoic acid (^{18}FTHA). ^{18}FTHA is an ^{18}F-labelled long chain fatty acid analogue with a thioether on the 6th carbon (see **Figure 11**). Like other fatty acids, it is found bound to albumin in the plasma and must ultimately disassociate from albumin to enter a cell. Once taken up by tissues it is activated by acyl-CoA synthetase and transported within the mitochondria where it undergoes the initial steps of β-oxidation. Following the formation of the first two acetyl CoA, the remaining part of the fatty acid chain is trapped within the mitochondria as further oxidation is blocked at its sulfur heteroatom located at the sixth carbon of the fatty acid chain (DeGrado *et al.*, 2000). ^{18}FTHA may also be incorporated into complex lipids, such as phospholipids and triglycerides (DeGrado *et al.*, 1991).

The esterification of ^{18}FTHA into triglycerides is much less than non-labelled NEFA, which is compensated by its incorporation into diacylglycerides and phospholipids (Ci *et al.*, 2006). The metabolic fate of ^{18}FTHA also appears to be tissue-specific. For instance, in a study conducted in pigs, 89% of myocardial ^{18}FTHA uptake entered the mitochondria compared to only 36% in muscle [consistent with humans; (Kelley *et al.*, 1993)], which suggests that the uptake and retention of this radio-isotope represents β-oxidation in the heart but NEFA uptake in skeletal muscle (Takala *et al.*, 2002). Similar to ^{18}FDG, Patlak linearization graphical analysis is applied using the equations of Patlak *et al.* (1983) to determine the fractional extraction of ^{18}FTHA by the delimited tissue (K_i, in min^{-1} of ^{18}FTHA). The fractional extraction of ^{18}FTHA is then multiplied by the arterial plasma NEFA concentration, corrected using a lumped constant of 1.0 as the actual value is unknown in humans, to obtain the net ^{18}FTHA uptake (K_m, in μmol of NEFA·mL of tissue^{-1}·min^{-1}).

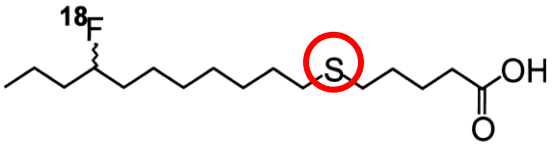

Figure 11. 14(R,S)-[^{18}F]-fluoro-6-thia-heptadecanoic acid

1.6.3.3. 1-^{11}C-acetate. As a carbon-11-labelled radio-tracer, ^{11}C-acetate offers a number of great advantages compared to the tracers previously described, particularly in research examining BAT metabolism *in vivo* in humans. This is a tracer that has been used to investigate myocardial blood flow and as an index of myocardial oxygen consumption since the 1980's (Pike *et al.*, 1982; Brown *et al.*, 1989), but increasingly, it is being applied to investigate the perfusion or oxidative metabolism of other tissues [e.g. brain (Wyss *et al.*, 2009) and kidney (Hussain *et al.*, 2009)]. The primary advantage of this radiotracer is that in some tissues it can serve as an

excellent marker of tricarboxylic acid cycle (TCA) activity and a surrogate to oxidative metabolism, since its product, acetyl CoA, is the final common pathway for all the major oxidative fuels that enter the TCA and the TCA is tightly coupled to oxygen consumption. Indeed, in the heart, the only major metabolic pathway for acetate once converted to acetyl CoA is to enter the TCA cycle where it is readily oxidized to form two molecules of CO_2 (Buxton *et al.*, 1988). In other tissues, the metabolic fate of ^{11}C-acetate may also include incorporation into lipids, where it can subsequently decay over time, production of ketones or, once in the TCA cycle, the rapid conversion to amino acids which are then taken up again by the TCA cycle (Klein *et al.*, 2001). The clearance of ^{11}C radioactivity in highly metabolically active tissues may appear biphasic at times, as demonstrated in the multi-compartmental kinetics model found in **Figure 12B.** Here we see an early rapid decay (k_1 or Phase 1 in **Figure 12B**) followed by a slower decay (k_2 or Phase 2 in **Figure 12B**). The former is a result of the decarboxylation of ^{11}C-acetate-derived citrate (if the C-6 carbon of citrate is labelled with ^{11}C) or α-ketoglutarate (if the C-1 carbon is labelled with ^{11}C), which only occurs in the second cycle of the TCA, whereas the latter results from the late decarboxylation of α-ketoglutarate following an exchange with glutamate (Klein *et al.*, 2001). However, often a more simple mono-exponential fitting provides a more valid index of oxidative metabolism since the α-ketoglutarate exchange with glutamate may be negligible (as illustrated in **Figure 12C**). In conditions where TCA cycle activity is low, the time-activity curve will simply be represented by a slow decay of the ^{11}C, which suggests that it has been incorporated into lipids.

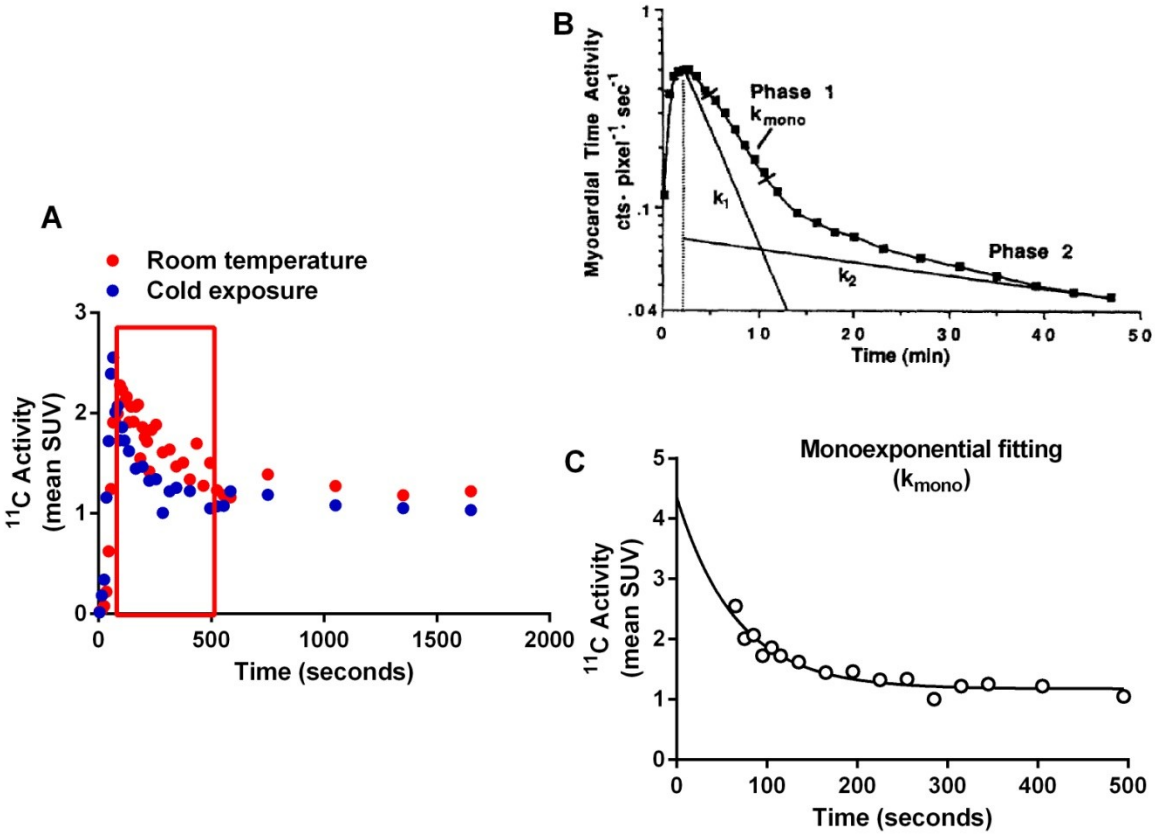

Figure 12. (A) Example of a ^{11}C-acetate time-activity curve for BAT following an intravenous injection of ~185 MBq of ^{11}C-acetate, injected at room temperature and again during cold exposure. (B) Determination of tissue oxidative activity is performed by modeling the two decay constants for a two-phase decay [figure adapted from Armbrecht *et al.* (1989)] or (C) a mono-exponential decay from the peak tissue activity.

Another advantage of this tracer is that its uptake and metabolism is not influenced by the metabolic state of the tissue, unlike the previous two PET tracers described. The main limitation of ^{11}C-acetate relates to its relatively short half-life. With a 20.3 min half-life, only the kinetics of tissues located within the 18 cm PET field of view chosen can be investigated for a single injection of ^{11}C-acetate, since 20-30 min is required to obtain the time-activity curve required to model the metabolic activity. This limits the ability to compare the oxidative metabolism of various tissues simultaneously or examine the bio-distribution of this tracer, since whole body static scans require 40-50 minutes to complete (representing two half-lives of the tracer).

Consequently, careful consideration is required when planning studies using ^{11}C-acetate. The shorter half-life, does offer some advantages, by reducing the exposure to radioactivity and allowing for the serial use of multiple ^{11}C-labelled substrates such as palmitate, glucose or acetoacetate.

1.6.3.4. ^{15}O-oxygen ($H_2{}^{15}O$, $C^{15}O$, $^{15}O_2$). Although not used in the investigations presented in this thesis, it is important to distinguish the use of this tracer compared to ^{11}C-acetate. Similar to ^{11}C-acetate, oxygen-15(^{15}O)-labelled molecules are used to measure tissue perfusion ($H_2{}^{15}O$) (Orava *et al.*, 2011; Orava *et al.*, 2013) and tissue metabolic rate ($^{15}O_2$) (Muzik *et al.*, 2012). Tissue blood volume can also be measured using either ^{11}C-labelled or ^{15}O-labelled carbon monoxide (^{11}CO or C^{15}O, respectively). However, the greatest distinction between these two tracers are their half-lives. As previously described, the half-life of ^{11}C is 20.3 minutes. Since the half-life of ^{15}O-labelled oxygen is 124 seconds, the timing of its utilization is of greater importance and contains very important temporal limitations and requires very specialized set-ups. Consequently, the production of these particular radioisotopes must be produced on-site by a radiochemist with the use of a cyclotron contained within or near the PET scanning room. In addition, although tissue metabolic rate can be quite valuable, often only $H_2{}^{15}O$ is used to measure perfusion and subsequently interpreted to represent the metabolic rate of the tissue. While strong correlations between tissue perfusion and tissue-specific metabolic rate or substrate utilization/extraction may be found, there are a number of conditions where such correlations are not evident, such as under insulin stimulation [see Orava *et al.* (2011) for example].

2. RESEARCH QUESTIONS AND HYPOTHESES

2.1 Specific aims

The focus of this thesis is to further elucidate the tissues and processes contributing to heat production during cold exposure, examine the interaction between the primary thermogenic organs and elucidate the plasticity of these processes following a cold-acclimation protocol. This will be accomplished by:

1) Characterizing BAT metabolism and its effect on whole body metabolism by:
    a. Quantifying whole body heat production and tissue-specific glucose and fatty acid metabolism and oxidative metabolism using nuclear imaging techniques (PET/CT).
    b. Examine their effect on whole body thermal responses and shivering activity using EMG.

2) Characterizing the interaction between BAT- and skeletal muscle-derived thermogenesis and their influence on whole body metabolism by:
    a. Examining the relationship between whole-body sympathetically induced lipolysis and BAT metabolism.
    b. Examining the thermoregulatory relationship between BAT and skeletal muscles.
    c. Examining the relationship of BAT and skeletal muscle in the handling of circulating glucose.
    d. Map the muscle activation pattern using the complementary techniques of EMG and PET/CT.

3) Examining the plasticity of both skeletal muscle and BAT and their effects on the whole body thermal responses and energy metabolism under two different thermal conditions.

   At a temperature warmer than the acclimation temperature:

   a. Examine the changes to the volume of metabolically active BAT and its oxidative capacity and
   b. The effects of these changes on shivering and muscle metabolism, using EMG and PET/CT.

   At a temperature colder than the acclimation temperature:

   a. Establish the temporal changes in the thermoregulatory responses resulting from daily cold exposure, particularly whole body heat production and shivering intensity.
   b. Determine whether the electromyographic pattern of muscle recruitment or the recruitment of particular muscle groups were modulated as a result of daily cold exposure
   c. Examine the consequent effects on substrate metabolism.

2.2. Hypotheses

During cold exposure, thermogenic and thermolytic responses are recruited to maintain a thermal balance. We expect that, during a mild cold exposure, highly metabolically active tissues such as brown adipose tissue will provide a significant contribution to metabolic heat production and the utilization of circulating glucose and fatty acids. Given the suspected central neural pathways implicated in shivering, we also expect that deeper proximally located muscles will be preferentially recruited for ST. We expect individuals demonstrating greater BAT stimulation will elicit a lower whole body shivering intensity and reduced burst shivering activity, subsequently diminishing whole body CHO utilisation. Further, we expect a continuous low-intensity shivering pattern to predominate but this should not have any consequences on the uptake of glucose or fatty acids given their respective dependences on contraction-stimulated transport into skeletal muscle. Finally, we expect that whole body oxygen consumption will remain the same following 4 weeks of intermittent cold-exposure but whole body shivering intensity and muscle burst activity will decrease as a result of an increased volume and oxidative capacity of BAT, subsequently reducing whole body CHO utilisation. We hypothesize that the plasticity demonstrated by BAT will be more greatly manifested during a thermal challenge that is colder than the acclimation temperature.

3. ARTICLES

3.1 Article I

Final accepted version of article published in Journal of Clinical Investigations, 122 (2): 545-552, 2012 (Appendix C)

Brown adipose tissue oxidative metabolism contributes to energy expenditure during acute cold exposure in humans

Véronique Ouellet [1], Sébastien M. Labbé [2], Denis P. Blondin [3], Serge Phoenix [2,4], Brigitte Guérin [4], François Haman [3], Eric E. Turcotte [4], Denis Richard [1], André C. Carpentier [2]

[1] Centre de recherche de l'Institut universitaire de cardiologie et de pneumologie de Québec, Université Laval, Quebec City, Quebec, Canada; [2] Department of Medicine, Centre de recherche clinique Etienne-Le Bel, Université de Sherbrooke, Sherbrooke , Quebec, Canada; [3] Unité de recherche sur la nutrition et le métabolisme, Montfort Hospital, University of Ottawa, Ottawa, Ontario, Canada; [4] Department of Nuclear Medicine and Radiobiology, Université de Sherbrooke, Québec, Canada.

Abstract

Recent studies using PET with ^{18}F-fluorodeoxyglucose (^{18}FDG) have shown the presence of brown adipose tissue (BAT). Whether BAT contributes to cold-induced non-shivering thermogenesis has however not been proven in adult humans. Using PET with ^{11}C-acetate, ^{18}FDG and ^{18}F-fluoro-thiaheptadecanoic acid (^{18}FTHA, a fatty acid tracer), BAT oxidative metabolism, glucose and nonesterified fatty acid (NEFA) turnover were quantified in six healthy men under controlled cold exposure condition designed to minimize shivering. Upon cold exposure, we showed significant NEFA uptake in addition to glucose uptake. We demonstrated significant cold-induced activation of oxidative metabolism in BAT, but not in adjoining skeletal muscles and subcutaneous adipose tissue. This was associated with a 1.8-fold increase in total energy expenditure. We found a significant inverse relationship between BAT volume of activity and shivering and significant increase in BAT radio-density, indicating reduced BAT triglyceride content. The present study demonstrates that BAT represents a non-shivering thermogenesis effector in humans.

Introduction

Brown adipose tissue (BAT) is a specialized tissue whose function is to produce heat (Cannon & Nedergaard, 2004; Richard & Picard, 2011). Its thermogenic capacity is such that it allows mammals to live below thermoneutral condition without having to rely on shivering muscles. The exceptional thermogenic potential of BAT is conferred by abundant well-developed mitochondria comprising uncoupling protein 1 (UCP1), a protein uncoupling mitochondrial respiration from adenosine-5′-triphosphate (ATP) synthesis (Richard & Picard, 2011). BAT is highly vascularized and richly innervated by terminal fibers of the postganglionic neurons of the sympathetic nervous system (Cannon & Nedergaard, 2004; Sell *et al.*, 2004; Richard & Picard, 2011).

Positron emission tomography / computed tomography (PET/CT) scanning investigations using ^{18}F-fluorodeoxyglucose (^{18}FDG) have revealed symmetrical cervical, supra-clavicular metabolically active fat depots, which were suggested by Hany and colleagues to represent brown adipose tissue (Hany *et al.*, 2002; Cypess *et al.*, 2009; Saito *et al.*, 2009; Virtanen *et al.*, 2009). These fat depots comprise sympathetically innervated multilocular adipocytes expressing UCP1 (Zingaretti *et al.*, 2009), the ultimate marker of brown fat cells. The magnitude of ^{18}FDG uptake by BAT was reported to increase with exposure to low temperature, to be higher in women than men, and to decrease with age and body fat mass (Cohade *et al.*, 2003; Garcia *et al.*, 2006; Kim *et al.*, 2008; Cypess *et al.*, 2009; Saito *et al.*, 2009; Zingaretti *et al.*, 2009; Ouellet *et al.*, 2011). These observations tend to support a germane BAT participation to energy expenditure (Cannon & Nedergaard, 2010; Enerback, 2010; Richard & Picard, 2011). As these observations have only been based on ^{18}FDG uptake, however, the studies carried out so far in

humans have only allowed speculative conclusions regarding the oxidative capacity/activity of BAT.

The present study was thus designed to determine whether BAT is metabolically active and contributes to cold-induced non-shivering thermogenesis in humans. Using PET with ^{11}C-acetate (to determine tissue oxidative activity), ^{18}FDG (a glucose analogue) and ^{18}F-fluoro-thiaheptadecanoic acid (^{18}FTHA, a fatty acid tracer), BAT oxidative metabolism, glucose and nonesterified fatty acid (NEFA) uptake were quantified in adult humans subjected to cold exposure conditions designed to minimize shivering.

Results

Six healthy men aged from 23 to 42 years, with a BMI of 23.7 to 31.0 kg/m^2 and taking no medication participated in the present study protocols (**Figure 1**). During cold exposure, average skin temperature was reduced by 3.8 ± 0.4°C without change in core body temperature, and VO_2, VCO_2 and resting energy expenditure increased ~1.8-fold (**Table 1**). Plasma glucose, triglycerides, triiodothyronine, thyroxin, thyroid-stimulating hormone, cortisol or ACTH levels did not change significantly with cold exposure, whereas NEFA levels and NEFA rate of appearance in blood increased significantly (**Table 1**). By design, shivering was controlled and minimized to 1.6 ± 0.5% (range 1.1 to 2.4%) of maximal voluntary contraction as continuously recorded by electromyography (EMG) in 4 large muscle groups known to contribute significantly to shivering during cold exposure (Haman *et al.*, 2004a; Haman *et al.*, 2004b; Haman *et al.*, 2010).

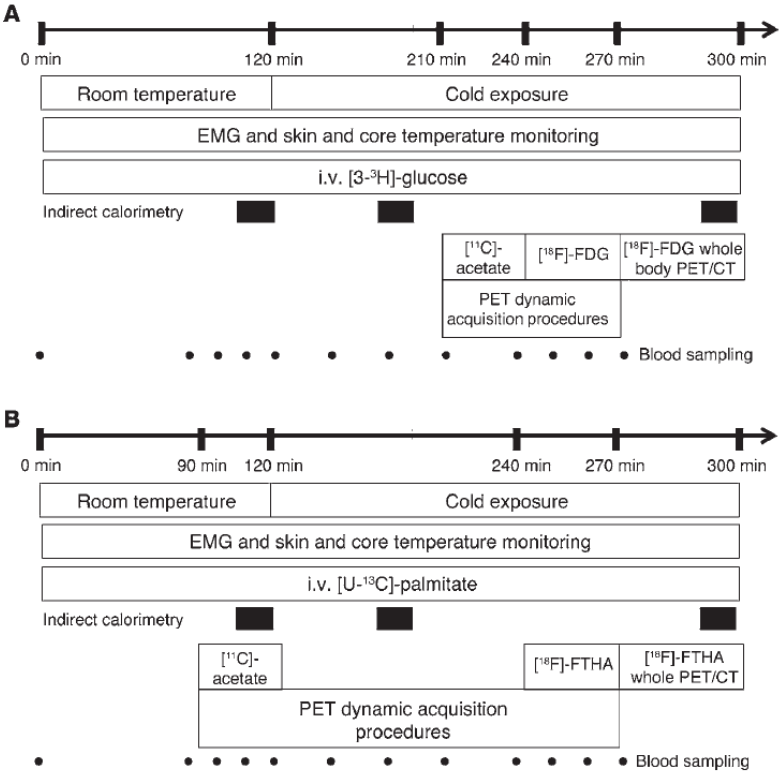

Figure 1

Study protocols. **(A)** Measurement of plasma glucose turnover and brown adipose tissue ^{11}C-acetate and ^{18}F-fluorodeoxyglucose uptake during acute cold exposure. **(B)** Measurement of plasma nonesterified fatty acid turnover and brown adipose tissue ^{18}F-fluoro-thiaheptadecanoic acid during acute cold exposure and brown adipose tissue ^{11}C-acetate uptake at room temperature. CT: computed tomography; EMG: electromyography; FDG: fluorodeoxyglucose; FTHA: fluoro-6-thia-heptadecanoic acid; PET: positron emission tomography.

Table 1

Average body temperatures, indirect calorimetry, circulating metabolites and hormones and plasma glucose and NEFA appearance rates at ambient temperature (warm) and during cold exposure (cold).

		1	**2**	**3**	**4**	**5**	**6**	**Mean ± SEM**
Skin T° (°C)	warm	32.9	33.1	32.6	34.2	33.1	32.7	33.1 ± 0.2
	cold	28.2	30.5	28.5	30.7	29.2	28.2	29.6 ± 0.4*
Core T° (°C)	warm	37.0	37.0	37.4	37.0	36.6	36.6	37.0 ± 0.1
	cold	36.4	36.4	37.4	36.8	36.2	36.7	36.6 ± 0.2
VO_2 (l/min)	warm	0.318	0.346	0.356	0.375	0.386	0.441	0.370 ± 0.017
	cold	0.563	0.661	0.473	0.615	0.678	0.923	0.652 ± 0.062*
VCO_2 (l/min)	warm	0.275	0.302	0.320	0.324	0.310	0.390	0.320 ± 0.016
	cold	0.503	0.643	0.431	0.497	0.535	0.893	0.584 ± 0.068*
TEE (kcal/min)	warm	1.54	1.69	1.75	1.82	1.85	2.15	1.80 ± 0.08
	cold	2.76	3.29	2.33	2.95	3.24	4.59	3.19 ± 0.31*
Glucose (mmol/l)	warm	3.7	4.4	4.1	3.3	4.2	4.0	4.0 ± 0.2
	cold	3.8	4.5	3.7	3.9	4.2	3.9	4.0 ± 0.1

$Ra_{glucose}$ (µmol/min)	warm	ND	ND	ND	ND	ND	ND	ND
	cold	950	957	1,133	1,703	3,661	556	1,493 ± 460
Insulin (pmol/l)	warm	65	67	74	53	45	125	71 ± 11
	cold	69	62	45	57	62	84	63 ± 5
TG (mmol/l)	warm	0.88	0.87	1.52	0.69	0.49	1.15	0.93 ± 0.15
	cold	0.89	0.78	1.61	0.62	0.57	1.06	0.92 ± 0.16
NEFA (µmol/l)	warm	366	352	645	689	311	484	474 ± 66
	cold	475	535	805	897	476	677	644 ± 73*
Ra_{NEFA} (µmol/min)	warm	708	ND	740	845	759	813	773 ± 25
	cold	901	ND	937	1,011	884	1,278	1,002 ± 72*
TSH (IU/l)	warm	0.91	1.59	0.87	2.21	1.72	0.97	1.38 ± 0.22
	cold	0.91	1.66	0.80	2.17	1.59	0.93	1.34 ± 0.22
Free T3 (pmol/l)	warm	5.3	4.6	5.2	5.9	5.7	6.1	5.5 ± 0.2
	cold	5.0	4.6	5.2	6.0	5.5	6.2	5.4 ± 0.2
Free T4 (pmol/l)	warm	18.3	18.1	17.1	16.5	16.2	17.2	17.2 ± 0.4
	cold	18.6	18.9	17.6	15.8	16.7	17.8	17.5 ± 0.5

Cortisol (nmol/l)	warm	216	277	184	237	274	257	241 ± 15
	cold	256	284	197	255	269	302	260 ± 15
BAT K_i ^{18}FDG	warm	ND	ND	ND	ND	ND	ND	ND
	cold	0.013	0.009	0.009	0.019	0.011	0.027	0.015 ± 0.003
BAT K_i ^{18}FTHA	warm	ND	ND	ND	ND	ND	ND	ND
	cold	0.018	0.013	0.015	0.022	0.020	0.023	0.018 ± 0.002

Values from all participants at ambient temperature (between times 80 and 120 min) and during cold exposure (between times 180 and 300 min) were averaged from both protocols (no difference between protocol A and B), except for $Ra_{glucose}$ and Ra_{NEFA} that were only determined in protocol A and B, respectively, at isotopic steady state enrichment (between times 100 and 120 min and times 280 and 300 min). * $P < 0.05$ by Wilcoxon test. BAT: supraclavicular brown adipose tissue; FDG: fluorodeoxyglucose; FTHA: fluoro-6-thia-heptadecanoic acid; K_i: fractional uptake rate; ND: not determined; NEFA: nonesterified fatty acids; Ra: rate of appearance; T3: triiodothyronine; T4: thyroxine; TEE: total energy expenditure; TSH: thyroid-stimulating hormone.

^{18}FDG uptake during the cervico-thoracic dynamic PET/CT acquisition upon cold exposure of one representative participant is shown in **Figure 2A**. During cold exposure, fractional uptake (K_i) of ^{18}FDG (**Figure 2B**) was higher in supraclavicular BAT compared to trapezius and deltoid muscles and subcutaneous adipose tissue but not compared to the *longus colli* (a small muscle located on the anterior surface of the cervical spine, between the atlas and the third dorsal vertebra). Net tissue glucose uptake (K_m) (**Figure 2C**) was higher in BAT *vs.* subcutaneous adipose tissue, trapezius and deltoid, but not compared to the *longus colli*. Whole body ^{18}FDG uptake in one of the participants at the end of the protocol is shown in **Figure 2D**. BAT mean total volume of activity was 168 ± 56 ml (range 31 to 329 ml) based on ^{18}FDG uptake. Glucose uptake by BAT amounted to 10.8 ± 4.5 µmol/min (range 1.3 to 28.7 µmol/min). Given a plasma glucose appearance rate of 1,493 ± 460 µmol/min, BAT glucose uptake accounted for 1.3 ± 0.8 % of plasma glucose turnover (range 0.04 to 5.2 %).

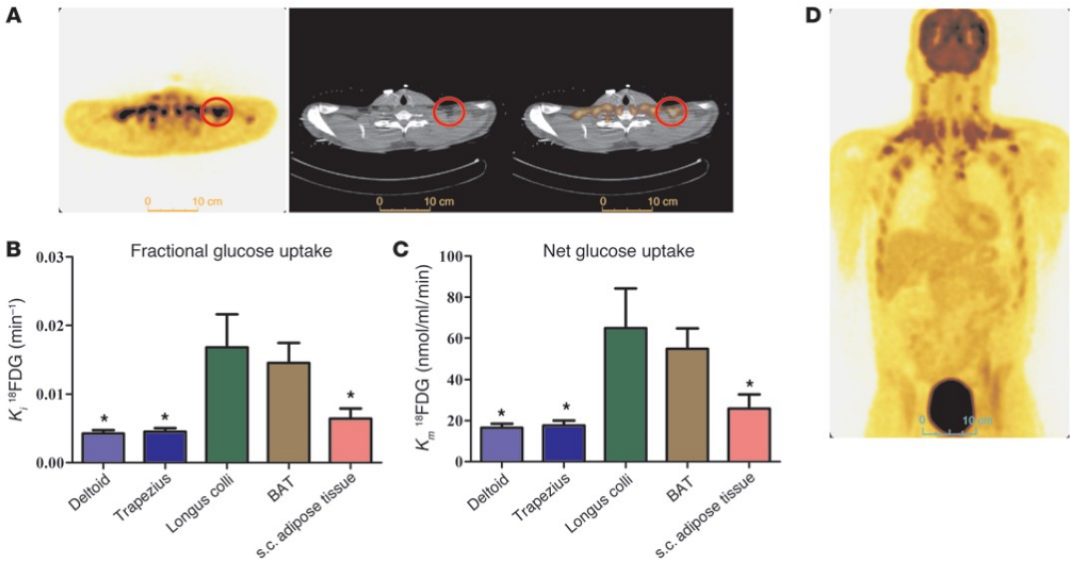

Figure 2
Tissue glucose uptake. (**A**) Transversal computed tomography (left panel), positron emission tomography (right panel) and fusion scan (middle panel) views of the cervico-thoracic junction in one of the participants. The red circle denotes supraclavicular brown adipose tissue. (**B**) Fractional (K_i) and (**C**) net (K_m) glucose uptake in cervico-thoracic tissues. (**D**) Coronal view (postero-anterior projection) of whole body ^{18}FDG uptake during cold exposure. * denotes ANOVA with Dunnett's post-hoc test $P < 0.05$ *vs.* brown adipose tissue. BAT: brown adipose tissue; FDG: fluorodeoxyglucose; SC: subcutaneous.

^{18}FTHA uptake during the cervico-thoracic dynamic PET/CT acquisition upon cold exposure of one representative participant is shown in **Figure 3A**. During cold exposure, fractional uptake (K_i) of ^{18}FTHA (**Figure 3B**) and net tissue NEFA uptake (K_m) (**Figure 3C**) were significantly higher in supraclavicular BAT compared to subcutaneous adipose tissue, trapezius and deltoid but not different from that of the *longus colli*. Whole body ^{18}FTHA uptake at the end of the protocol in one of the participants is shown in **Figure 3D**. NEFA uptake by BAT amounted to 2.3 ± 0.8 µmol/min (range 0.3 to 4.4 µmol/min). Given a plasma NEFA appearance rate of 1,002 ± 72 µmol/min, BAT NEFA uptake accounted for approximately 0.25 ±0.08 % of plasma NEFA turnover (range 0.04 to 0.44 %).

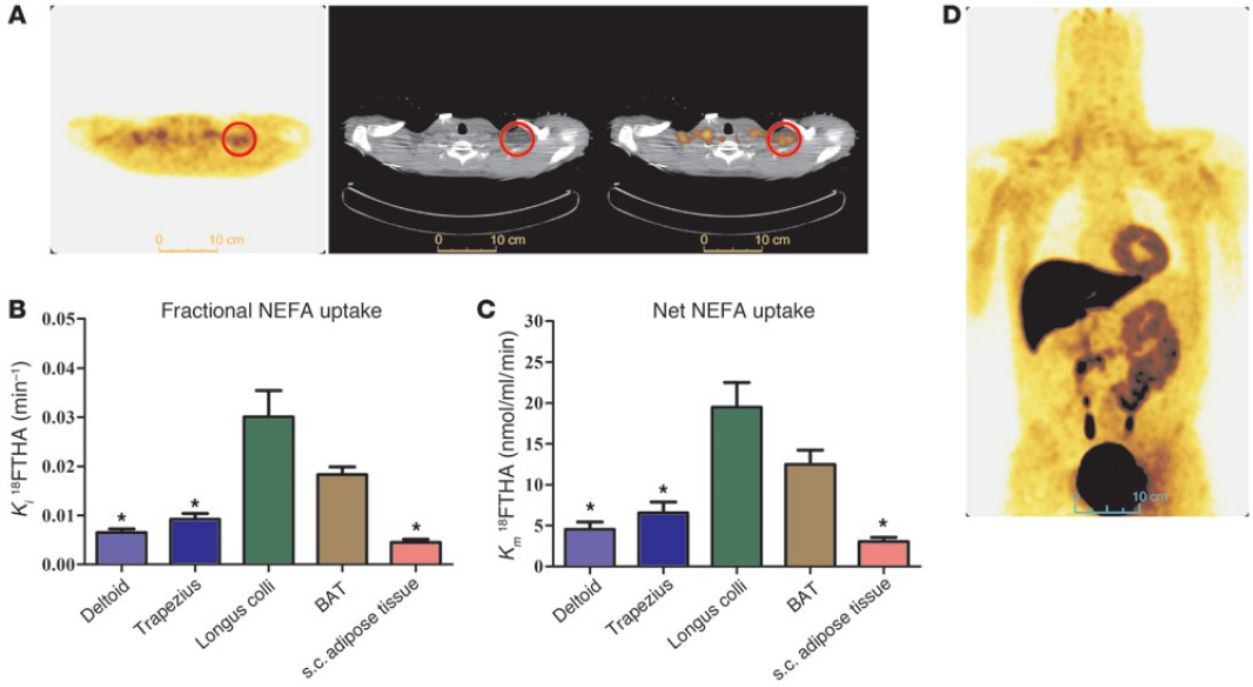

Figure 3

Tissue nonesterified fatty acid uptake. (**A**) Transversal computed tomography (left panel), positron emission tomography (right panel) and fusion scan (middle panel) views of the cervico-thoracic junction in one of the participants. The red circle shows supraclavicular brown adipose tissue. (**B**) Fractional (K_i) and (**C**) net (K_m) nonesterified fatty acid uptake in cervico-thoracic tissues. (**D**) Coronal view (postero-anterior projection) of whole body ^{18}FTHA uptake during cold exposure. * denotes ANOVA with Dunnett's post-hoc test $P < 0.05$ *vs.* brown adipose tissue. BAT: brown adipose tissue; NEFA: nonesterified fatty acid; FTHA: fluoro-6-thia-heptadecanoic acid; SC: subcutaneous.

After IV injection of ^{11}C-acetate, blood ^{11}C radioactivity over time was not significantly different during cold exposure compared to room temperature (**Figure 4A**). BAT (**Figure 4B**), but not subcutaneous adipose tissue (**Figure 4C**) ^{11}C radioactivity was increased throughout exposure to cold. The *longi colli* (**Figure 4D**) and sternocleidomastoids (not shown) were the only cervical and upper thoracic muscles that displayed significant cold-induced increase in ^{11}C radioactivity over time. ^{11}C radioactivity over time in trapezius and deltoids are shown in **Figure 4E and 4F**, respectively. The area under the curve (AUC) of tissues ^{11}C radioactivity, a marker of tissue oxidative and/or non-oxidative metabolism (acetate retention) was elevated in BAT and *longus colli*. The monoexponential decay slope from tissue peak ^{11}C activity (^{11}C-acetate k), a valid surrogate of tissue oxidative metabolism (Brown *et al.*, 1987; Ng *et al.*, 1994), was however increased in BAT in all participants (**Figure 4G**) but not in *longus colli* (**Figure 4H**), demonstrating that the former tissue plays an important role in cold-induced non-shivering thermogenesis whereas the latter tissue mostly retained acetate in non-oxidative pathways. BAT CT radio-density (in Hounsfield units) increased in all participants (by 17 ± 5%, range 6 to 41%, P = 0.03) (**Figure 4I**) whereas WAT radio-density did not change (3 ± 5%, P = 1.00). **Supplemental Figure 1** shows actual PET, CT and fusion images of the integrated tissue activity in the neck and upper chest area from dynamic list-mode acquisitions at room temperature and during cold exposure in one of the participants.

There was a significant inverse correlation between BAT volume of activity and shivering expressed as % of voluntary maximal contraction (Spearman r = -0.89, P = 0.03) (**Supplemental Figure 2**). We found no other significant correlations between BAT volume of activity and energy expenditure (**Supplemental Table**), although our small sample size severely limits the power of these analyses.

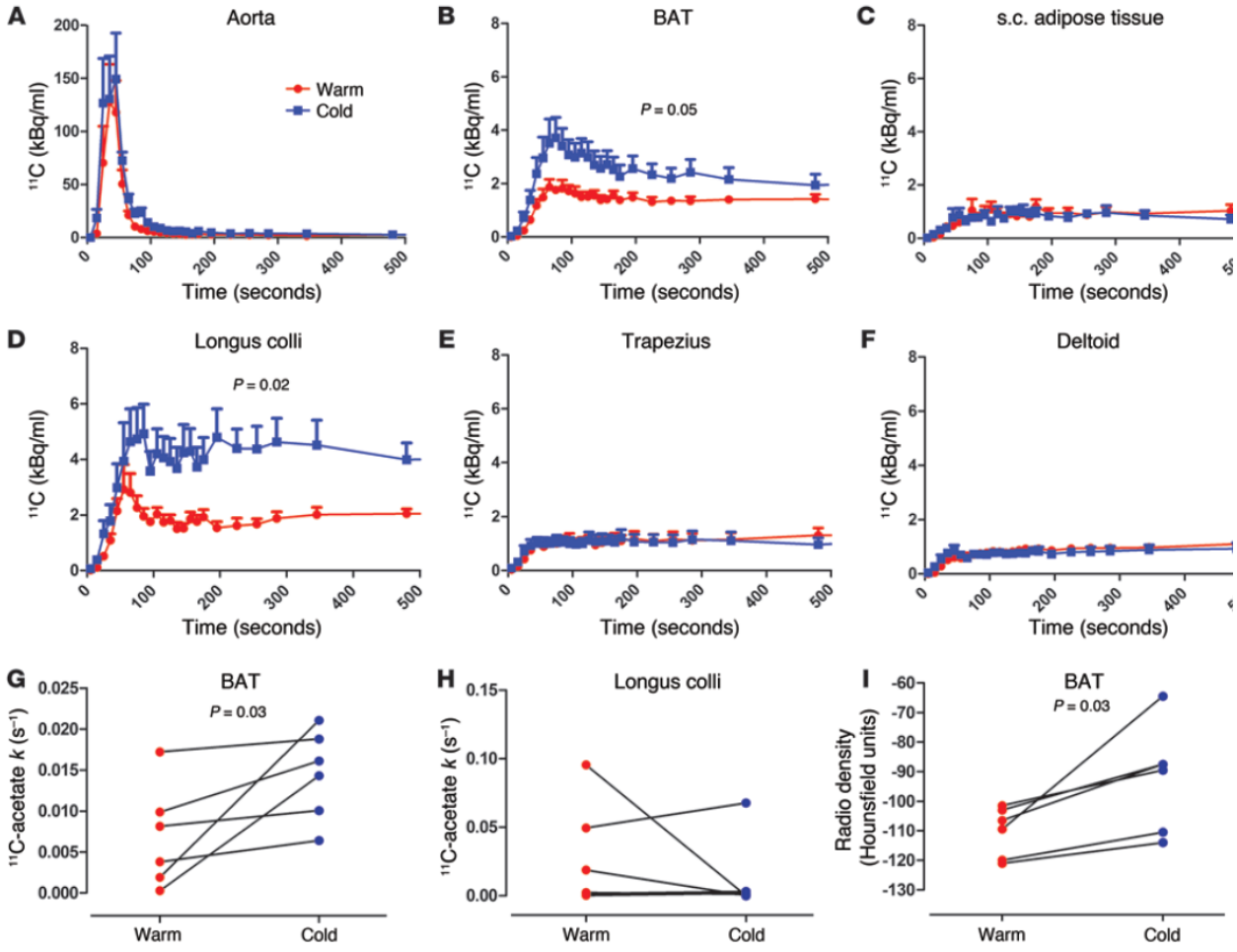

Figure 4

^{11}C-acetate kinetics. ^{11}C time-radioactivity curves over the first 500 seconds of acquisition after ^{11}C-acetate injection at room temperature (in red) and during cold exposure (in blue) in (**A**) blood in the aorta, (**B**) supraclavicular brown adipose tissue, (**C**) subcutaneous adipose tissue, (**D**) *longus colli*, (**E**) trapezius and (**F**) deltoid. ^{11}C time-radioactivity curves were different during cold exposure vs. at room temperature in BAT (two-way ANOVA $P = 0.05$, interaction with time $P < 0.001$) and in *longi colli* (two-way ANOVA $P = 0.02$, interaction with time $P < 0.001$), but not in other organs. Monoexponential decay slope from peak tissue ^{11}C activity (^{11}C-acetate k) in (**G**) supraclavicular brown adipose tissue and (**H**) *longus colli*. (**I**) Brown adipose tissue radio-density by computed tomography. BAT: brown adipose tissue; SCAT: subcutaneous adipose tissue.

Discussion

Based on ^{11}C-acetate tissue kinetics the present results demonstrate significant cold-induced activation of BAT oxidative metabolism in all subjects studied under well-controlled cold exposure conditions designed to minimize shivering. We also determined, for the first time in vivo in humans that plasma NEFA uptake is increased in cold-activated BAT compared to resting skeletal muscles and subcutaneous adipose tissues.

A cold-induced total BAT glucose uptake averaging 10.8 ± 2.9 μmol/min lies within the range reported by Virtanen et al. (Virtanen *et al.*, 2009). In addition, the present results demonstrate the ability of human BAT to also increase its NEFA uptake during cold exposure. Whole body ^{18}FTHA uptake at the end of the protocol predicts a NEFA uptake by BAT amounting to 2.3 ± 0.8 μmol/min (range 0.3 to 4.4 μmol/min). One limitation of our experimental design was the impossibility to assess ^{18}FDG and ^{18}FTHA BAT uptake at ambient temperature given the complexity of design and acceptable limits of radiation exposure of research participants. However, significant BAT glucose and NEFA uptake is not detectable in the vast majority of individuals at ambient temperature (Labbe *et al.*, 2011; Ouellet *et al.*, 2011). In rodents, the contribution from glucose and NEFA uptake has proved to be a relatively small fraction of total BAT metabolism during acute cold-induced thermogenesis compared to intracellular brown adipocyte triglycerides (Ma & Foster, 1986). Also, we did not assess BAT utilization of fatty acids from circulating lipoproteins, another potential source of BAT energy substrates (Bartelt *et al.*, 2011). However, unlike what has been observed in mice in the latter study, we did not find any reduction in circulating triglycerides in the present study (**Table 1**). Assuming a volume of distribution of 0.45 dl/kg of body weight (Carpentier *et al.*, 2001) with an average body weight of 80.7 kg and a plasma triglyceride level of 0.93 mmol/l (82 mg/dl), mean

total circulating triglyceride content is estimated at approximately 3 g in the participants of the present study. As the half-life of circulating triglycerides during fasting (mostly VLDL) is relatively long (approximately 2 hours, i.e. a fractional clearance rate of 0.5/h – (Carpentier *et al.*, 2001)) compared to the length of cold exposure in the present study, it is very unlikely that the pool of circulating triglycerides, even if it was fully utilized, could account for the 250 extra kcal of energy expenditure observed (i.e. approximately 28 g of triglycerides). It is also noteworthy that our subjects were not, in contrast to the mice in Bartelt's study (Bartelt *et al.*, 2011), adapted to a temperature below thermoneutrality, which may render BAT adipocytes more prepared to clear circulating glucose and lipid.

The six subjects of the present study all exhibited increases in BAT metabolism upon cold exposure, albeit to various degrees. The variability in the response occurred despite application of a cold exposure protocol that not only restricted shivering but also dictated the strength of the cold response from strict body and skin temperature monitoring and indirect calorimetry measurements. Such variation would seem to be accounted for by inter-individual differences in BAT capacity (volume). The wide inter-individual difference in detectable BAT volume of activity (from to 31 to 329 ml) observed in young healthy men in the present study suggests that unknown factors may modulate BAT volume and thermogenic capacity in addition to age, gender, body mass index, and diabetes (Richard *et al.*, 2010). Furthermore, we found a significant inverse relationship between BAT volume of activity and shivering. Interestingly, BAT precursor cells are present in supra-clavicular fat independent of the presence or not of spontaneous ^{18}FDG uptake (Lee *et al.*, 2011). Of note, a very recent publication demonstrated cold-induced increased blood flow in BAT that was associated with increased energy

expenditure (Orava *et al.*, 2011). The latter is consistent with the present results which demonstrate cold-induced BAT thermogenesis in humans.

Our demonstration of BAT oxidative metabolism with trivial rates of plasma glucose and NEFA utilization, and rapid increase in BAT radio-density during cold exposure is suggestive of increased intracellular triglyceride utilization as the main source of energy for BAT thermogenesis. Intracellular triglycerides are the main fuel to sustain BAT energy metabolism during cold exposure in animal models (Aherne & Hull, 1966; Baba *et al.*, 2010; Richard & Picard, 2011). In room temperature-acclimated rats, short-term acute exposure to cold has been reported to lead to a near-complete depletion of BAT lipid (Baba *et al.*, 2010). A similar depletion of BAT lipid has been reported at necropsy in newborn infants and adults who died from hypothermia (Aherne & Hull, 1966). Intracellular brown adipocyte triglycerides represent half of the brown adipocyte volume (Aherne & Hull, 1966). From a mass of 168 g (the average BAT mass seen in the present study), one can predict a BAT fat content of ~84 g. Mobilization of one third of that lipid reserve (28 g), which seems possible based on previous investigations (Baba *et al.*, 2010), would be sufficient to account for the extra energy (250 ± 45 kcal) expended during the 3-hour period of cold exposure in the present study. Although the 80% increase in TEE that we observed during acute cold exposure appears important, it is therefore very likely that BAT thermogenesis accounted for an important fraction of this increase in TEE. Future studies will need to determine the contribution of intracellular triglycerides to BAT thermogenesis.

In addition, we cannot exclude the contribution of other tissues to cold-induced thermogenesis. We recorded increased glucose, NEFA and acetate uptake in the *longus colli*. Nonetheless, the observation that significant cold-induced increase in ^{11}C-acetate oxidative

metabolism was only seen in BAT demonstrates a significant role of this tissue in the non-shivering thermogenic response to cold. The limited field-of-view of our PET/CT scanner (18 cm length) during dynamic acquisitions prevents us from assessing oxidative metabolism from the ^{11}C-acetate method in other internal organs such as the heart and other deep central muscles that might have been activated by cold. Despite the low number of subjects studied, this due to the complexity of our measurements, we are nonetheless confident that our findings apply to other populations since they were very consistent. Finally, it is not possible to exclude an effect of the 2-hour daily time difference in ^{11}C-acetate injection between the two protocols in the present study. To our knowledge, the effect of nycthemeral cycle on BAT metabolism has not been previously studied in humans.

The present findings support a role of BAT for non-shivering thermogenesis in humans with intracellular triglycerides as the main source of energy for this process, as observed in rodents. However, it remains to be demonstrated whether chronic and frequent bouts of cold exposure may contribute to increase BAT capacity and/or activity and may be a viable adjunct therapeutic strategy to other lifestyle interventions to prevent or treat obesity and its metabolic complications. It is also possible that energy substrate uptake by BAT could be substantially increased once intracellular triglyceride stores are depleted and/or BAT is fully cold adapted as recently shown in rodents (Bartelt *et al.*, 2011). Quantitative assessment of the contribution of intracellular triglyceride oxidation in BAT thermogenesis awaits further methodological developments.

In summary, the present study demonstrates that a cold-exposure stimulus designed to minimize muscle-mediated shivering thermogenesis enhances BAT oxidative metabolism as well as glucose and NEFA uptake in adult humans. The enhanced BAT activity was associated with a

1.8-fold increase in whole body energy expenditure. We found a significant inverse relationship between BAT volume of activity and shivering and a significant increase in BAT radio-density within 3 hours of cold exposure, indicating rapid reduction in BAT triglyceride content. The present results demonstrate that BAT is undoubtedly involved in non-shivering thermogenesis in humans.

Methods

Protocols A and B are 4.5-hour metabolic tests performed in random order, within an average of 20 days of each other (range 7 to 36 days) and designed to assess whole body and BAT-specific energy substrate turnover and oxidation and energy expenditure at room temperature (~25ºC, time 0 to 120 min) and during acute exposure to cold (time 120 to 270 min) (**Figure 1**). Participants were instrumented and fitted with a liquid-conditioned tube suit (Allen-Vanguard Inc.). Following the room temperature period (time 0 to 120 min), the liquid-conditioned tube suit was perfused with ~18°C water using a temperature and flow-controlled circulation bath (Endocal, NESLAB and Model 200-00, Micropump Inc.). Briefly, the same suit was used for all subjects to maintain consistent tubing density. In addition, the flow and temperature of water through the suit was produced with the same cooling bath. Based on pilot experiments, we determined that circulating water in the suit at 18°C minimized overt shivering in healthy participants while achieving a significant reduction in skin temperature of at least 2.5°C. We did not try to avoid the slight but significant increase in EMG activity observed during the experiments. Therefore, EMG activity could slightly differ between individuals despite similar cold exposure depending on their degree of non-shivering thermogenesis. This difference in extent of EMG activity thus masked any possibility to discern a correlation between non-shivering thermogenesis and TEE. Change in total heat production was calculated by indirect calorimetry (Vmax29n, Sensormedics) (Carpentier *et al.*, 2005) at room temperature and between times 180 to 200 min and 280 to 300 min (i.e. 60 to 80 min and 160 to 180 min after the beginning of cold exposure). TEE rapidly increased by time 180 to 200 min to ~79% of that recorded between times 280 to 300 min. Only indirect calorimetry and EMG measurements during the latter period are reported. Dry heat loss from the difference between water

temperature entering and exiting the tube suit at a given flow rate was determined (Blondin *et al.*, 2010). Skin and core temperatures were monitored as previously described (Dubois & Dubois, 1916; Hardy & Dubois, 1937). Changes in whole-body heat production, heat loss, core and mean skin temperatures as well as muscle shivering intensity by EMG were determined as previously described (Haman *et al.*, 2004a; Haman *et al.*, 2004b; Haman *et al.*, 2004c; Haman *et al.*, 2005). This protocol achieved consistent skin temperature (difference = -0.2 ± 0.3°C) and energy expenditure (difference 2.2 ± 7.0%) between protocols A and B during cold exposure.

Plasma glucose appearance rate ($Ra_{glucose}$) was determined using a primed continuous infusion (0.33 x 10^6 dpm/min) of [3-^{3}H]-glucose during protocol A (Carpentier *et al.*, 2001) (23). Ra_{NEFA} was measured using IV administration of [U-^{13}C]-palmitate during protocol B using Steele's steady state equation, as previously described (Carpentier *et al.*, 2005; Carpentier *et al.*, 2007). Tissue oxidative metabolism was determined after IV bolus injection of ^{11}C-acetate (~185 MBq) at time 90 min (room temperature) and at time 210 min (i.e. 90 min after onset of cold exposure) followed by 30min list-mode dynamic PET acquisition, preceded by a 40mAs CT acquisition centered at the cervico-thoracic junction, as described (Labbe *et al.*, 2011). Tissue oxidative metabolism index (the rapid fractional tissue clearance of ^{11}C-acetate, k, in sec^{-1}) were estimated from tissue ^{11}C activity over time using monoexponential fit from the time of peak tissue activity (Buck *et al.*, 1991). This method is based on the following assumptions (Klein *et al.*, 2001): 1) acetate enters the Krebs cycle freely after rapid conversion into acetyl-CoA; 2) other acetate metabolic fates (e.g. de novo lipogenesis) are relatively slow compared to the Krebs cycle carbon fluxes; 3) carbon fluxes into the Krebs cycle through acetyl-CoA is directly coupled to the production of reducing equivalents; 4) the Krebs cycle contribution to the production of

reducing equivalents is stable and accounts for approximately two thirds of total production; 5) the production of reducing equivalents is tightly coupled to oxygen consumption.

In protocol A, each participant received an IV bolus of ^{18}F-fluorodeoxyglucose (^{18}FDG) (~185 MBq) at time 240 min (i.e. 2 hours after the onset of cold exposure) with 30 min list-mode dynamic PET acquisition centered at the cervico-thoracic junction to determine tissue glucose uptake using Patlak graphical analysis (Menard *et al.*, 2010). This was followed by a whole body CT scan (16 mAs) to correct for attenuation and for definition of PET regions of interests, followed by a whole body PET acquisition to determine whole body ^{18}FDG uptake. In protocol B, the same procedure was performed but with IV bolus administration of ^{18}Fluoro-6-thia-heptadecanoic acid (^{18}FTHA, ~185 MBq) instead of ^{18}FDG to determine tissue NEFA uptake after correction for plasma metabolites using Patlak linearization (Ci *et al.*, 2006; Menard *et al.*, 2010; Labbe *et al.*, 2011). For dynamic PET acquisitions, mean value of pixels (mean standard uptake value – SUV) for each frame were recorded. Regions of interest were drawn on the aortic arch for blood activity (input functions) and on supraclavicular BAT according to the following criteria: a tissue radio-density between -10 and -100 Hounsfield units and ^{18}FDG uptake during cold exposure of more than 1 SUV unit (Ouellet *et al.*, 2011). We also calculated total BAT volume of activity on whole body scans according to the later criteria, as previously described (Ouellet *et al.*, 2011). The regions of interest were first defined from the transaxial CT slices, then copied to ^{18}FDG, and then to ^{11}C-acetate and ^{18}FTHA image sequences. For whole-body scans, mean values of pixels (mean SUV) for all tissues of interest were recorded. In the cervico-thoracic dynamic sequences, ROI were drawn on the two largest muscles in the field of view (deltoid and trapezius, the latter also being electromyographically recorded), on posterior cervical subcutaneous adipose tissue and on any muscle or tissue structures that showed

significant (> 1 SUV unit) ^{18}FDG uptake during cold exposure. The latter occurred systematically only in small paraspinal muscles of the neck (*longi colli*) within the field of view of dynamic scans.

Statistical Analyses

Data are expressed as mean ± SEM. Wilcoxon test was used to compare characteristics and averaged steady state hormone and metabolite levels between room temperature *vs.* cold exposure. Two-way ANOVA for repeated measures with temperature, time and interaction as the independent variables was used to analyze time and temperature-dependent differences in blood and tissue PET-acquired activities throughout the protocols. ANOVA for repeated measures with Dunnett's post-hoc test were performed to compare fractional and net glucose and NEFA uptake between BAT *vs.* other tissues during cold exposure. Appropriate transformation of variables was performed when normal distribution was not observed for parametric statistical testing. A two-tailed P value < 0.05 was considered significant. All analyses were performed with the GraphPad Prism version 5.00 for Windows (San Diego, CA).

Study approval

Informed written consent was obtained from all participants in accordance with the Declaration of Helsinki and the protocol received approval from the Human Ethics Committee of the *Centre de recherche clinique Etienne-LeBel*.

Acknowledgements

This work was supported by a grant from the Canadian Diabetes Association (OG-3-10-2970-AC) and was performed at the *Centre de recherche clinique Etienne-Le Bel*, a research center funded by the *Fonds de la recherche en santé du Québec* (FRSQ). SML is the recipient of a Canadian Diabetes Association Doctoral Studentship Award. D.R. is the recipient of the CIHR/Merck Frosst Research Chair on Obesity. A.C.C. was the recipient of a FRSQ Senior Scholarship Award and is now the recipient of the CIHR-GlaxoSmithKline Chair in Diabetes.

References

1. Cannon B, and Nedergaard J. Brown adipose tissue: function and physiological significance. *Physiol Rev.* 2004;84(1):277-359.
2. Richard D, and Picard F. Brown fat biology and thermogenesis. *Front Biosci (Landmark Ed).* 2011;16(1233-60.
3. Sell H, Deshaies Y, and Richard D. The brown adipocyte: update on its metabolic role. *Int J Biochem Cell Biol.* 2004;36(11):2098-104.
4. Hany TF, Gharehpapagh E, Kamel EM, Buck A, Himms-Hagen J, and von Schulthess GK. Brown adipose tissue: a factor to consider in symmetrical tracer uptake in the neck and upper chest region. *Eur J Nucl Med Mol Imaging.* 2002;29(10):1393-8.
5. Cypess AM, Lehman S, Williams G, Tal I, Rodman D, Goldfine AB, Kuo FC, Palmer EL, Tseng YH, Doria A, et al. Identification and importance of brown adipose tissue in adult humans. *N Engl J Med.* 2009;360(15):1509-17.
6. Virtanen KA, Lidell ME, Orava J, Heglind M, Westergren R, Niemi T, Taittonen M, Laine J, Savisto NJ, Enerbäck S, et al. Functional brown adipose tissue in healthy adults. *N Engl J Med.* 2009;360(15):1518-25.
7. Saito M, Okamatsu-Ogura Y, Matsushita M, Watanabe K, Yoneshiro T, Nio-Kobayashi J, Iwanaga T, Miyagawa M, Kameya T, Nakada K, et al. High incidence of metabolically active brown adipose tissue in healthy adult humans: effects of cold exposure and adiposity. *Diabetes.* 2009;58(7):1526-31.
8. Zingaretti MC, Crosta F, Vitali A, Guerrieri M, Frontini A, Cannon B, Nedergaard J, and Cinti S. The presence of UCP1 demonstrates that metabolically active adipose tissue in the neck of adult humans truly represents brown adipose tissue. *FASEB J.* 2009;23(9):3113-20.
9. Cohade C, Mourtzikos KA, and Wahl RL. "USA-Fat": prevalence is related to ambient outdoor temperature-evaluation with 18F-FDG PET/CT. *J Nucl Med.* 2003;44(8):1267-70.
10. Garcia CA, Van Nostrand D, Atkins F, Acio E, Butler C, Esposito G, Kulkarni K, and Majd M. Reduction of brown fat 2-deoxy-2-[F-18]fluoro-D-glucose uptake by controlling environmental temperature prior to positron emission tomography scan. *Mol Imaging Biol.* 2006;8(1):24-9.
11. Kim S, Krynyckyi BR, Machac J, and Kim CK. Temporal relation between temperature change and FDG uptake in brown adipose tissue. *Eur J Nucl Med Mol Imaging.* 2008;35(5):984-9.
12. Ouellet V, Routhier-Labadie A, Bellemare W, Lakhal-Chaieb L, Turcotte E, Carpentier AC, and Richard D. Outdoor Temperature, Age, Sex, Body Mass Index, and Diabetic Status Determine the Prevalence, Mass, and Glucose-Uptake Activity of 18F-FDG-Detected BAT in Humans. *J Clin Endocrinol Metab.* 2011;96(1):192-9.
13. Cannon B, and Nedergaard J. Metabolic consequences of the presence or absence of the thermogenic capacity of brown adipose tissue in mice (and probably in humans). *Int J Obes (Lond).* 2010;34 Suppl 1(S7-16.
14. Enerback S. Brown adipose tissue in humans. *Int J Obes (Lond).* 2010;34 Suppl 1(S43-6.
15. Haman F, Legault SR, Rakobowchuk M, Ducharme MB, and Weber J-M. Effects of carbohydrate availability on sustained shivering II: relating muscle recruitment to fuel selection. *J Appl Physiol.* 2004;96(41-9.

16. Haman F, Legault SR, and Weber J-M. Fuel selection during intense shivering in humans: EMG pattern reflects carbohydrate oxidation. *J Physiol.* 2004;556(1):305-13.
17. Haman F, Blondin DP, Imbeault M-A, and Maneshi A. Metabolic Requirements of Shivering Humans. *Front Biosci.* 2010;15(Jun 1):1155-68.
18. Brown M, Marshall DR, Sobel BE, and Bergmann SR. Delineation of myocardial oxygen utilization with carbon-11-labeled acetate. *Circulation.* 1987;76(3):687-96.
19. Ng CK, Huang SC, Schelbert HR, and Buxton DB. Validation of a model for [1-11C]acetate as a tracer of cardiac oxidative metabolism. *Am J Physiol.* 1994;266(4 Pt 2):H1304-15.
20. Labbe SM, Croteau E, Grenier-Larouche T, Frisch F, Ouellet R, Langlois R, Guerin B, Turcotte EE, and Carpentier AC. Normal postprandial nonesterified fatty acid uptake in muscles despite increased circulating fatty acids in type 2 diabetes. *Diabetes.* 2011;60(2):408-15.
21. Ma SW, and Foster DO. Uptake of glucose and release of fatty acids and glycerol by rat brown adipose tissue in vivo. *Can J Physiol Pharmacol.* 1986;64(5):609-14.
22. Bartelt A, Bruns OT, Reimer R, Hohenberg H, Ittrich H, Peldschus K, Kaul MG, Tromsdorf UI, Weller H, Waurisch C, et al. Brown adipose tissue activity controls triglyceride clearance. *Nat Med.* 2011;17(2):200-5.
23. Carpentier A, Patterson BW, Uffelman KD, Giacca A, Vranic M, Cattral MS, and Lewis GF. The effect of systemic versus portal insulin delivery in pancreas transplantation on insulin action and VLDL metabolism. *Diabetes.* 2001;50(6):1402-13.
24. Richard D, Carpentier AC, Dore G, Ouellet V, and Picard F. Determinants of brown adipocyte development and thermogenesis. *Int J Obes (Lond).* 2010;34 Suppl 2(S59-66.
25. Lee P, Swarbrick MM, Zhao JT, and Ho KK. Inducible brown adipogenesis of supraclavicular fat in adult humans. *Endocrinology.* 2011;152(10):3597-602.
26. Orava J, Nuutila P, Lidell ME, Oikonen V, Noponen T, Viljanen T, Scheinin M, Taittonen M, Niemi T, Enerback S, et al. Different metabolic responses of human brown adipose tissue to activation by cold and insulin. *Cell Metab.* 2011;14(2):272-9.
27. Aherne W, and Hull D. Brown adipose tissue and heat production in the newborn infant. *J Pathol Bacteriol.* 1966;91(1):223-34.
28. Baba S, Jacene HA, Engles JM, Honda H, and Wahl RL. CT Hounsfield units of brown adipose tissue increase with activation: preclinical and clinical studies. *J Nucl Med.* 2010;51(2):246-50.
29. Carpentier AC, Frisch F, Cyr D, Genereux P, Patterson BW, Giguere R, and Baillargeon JP. On the suppression of plasma nonesterified fatty acids by insulin during enhanced intravascular lipolysis in humans. *Am J Physiol Endocrinol Metab.* 2005;289(5):E849-56.
30. Blondin DP, Dépault I, Imbeault P, Péronnet F, Imbeault M-A, and Haman F. Effects of two glucose ingestion rates on substrate utilization during moderate-intensity shivering. *Eur J Appl Physiol.* 2010;108(2):289-300.
31. Dubois D, and Dubois EF. A formula to estimate the approximate surface area if height and weight be known. *Arch Inter Med.* 1916;17(863-71.
32. Hardy JD, and Dubois EF. Regulation of Heat Loss from the Human Body. *Proc Natl Acad Sci U S A.* 1937;23(12):624-31.
33. Haman F, Péronnet F, Kenny GP, Doucet E, Massicotte D, Lavoie C, and Weber J-M. Effects of carbohydrate availability on sustained shivering I: oxidation of plasma glucose, muscle glycogen and proteins. *J Appl Physiol.* 2004;96(32-40.

34. Haman F, Péronnet F, Kenny GP, Massicotte D, Lavoie C, and Weber J-M. Partitioning oxidative fuels during cold exposure in humans: muscle glycogen becomes dominant as shivering intensifies. *J Physiol.* 2005;566(1):247-56.
35. Carpentier AC, Frisch F, Brassard P, Lavoie F, Bourbonnais A, Cyr D, Giguere R, and Baillargeon JP. Mechanism of insulin-stimulated clearance of plasma nonesterified fatty acids in humans. *Am J Physiol Endocrinol Metab.* 2007;292(3):E693-701.
36. Buck A, Wolpers HG, Hutchins GD, Savas V, Mangner TJ, Nguyen N, and Schwaiger M. Effect of carbon-11-acetate recirculation on estimates of myocardial oxygen consumption by PET. *J Nucl Med.* 1991;32(10):1950-7.
37. Klein LJ, Visser FC, Knaapen P, Peters JH, Teule GJ, Visser CA, and Lammertsma AA. Carbon-11 acetate as a tracer of myocardial oxygen consumption. *Eur J Nucl Med.* 2001;28(5):651-68.
38. Menard SL, Croteau E, Sarrhini O, Gelinas R, Brassard P, Ouellet R, Bentourkia M, van Lier JE, Des Rosiers C, Lecomte R, et al. Abnormal in vivo myocardial energy substrate uptake in diet-induced type 2 diabetic cardiomyopathy in rats. *Am J Physiol Endocrinol Metab.* 2010;298(5):E1049-57.
39. Ci X, Frisch F, Lavoie F, Germain P, Lecomte R, van Lier JE, Benard F, and Carpentier AC. The effect of insulin on the intracellular distribution of 14(R,S)-[18F]Fluoro-6-thia-heptadecanoic acid in rats. *Mol Imaging Biol.* 2006;8(4):237-44.

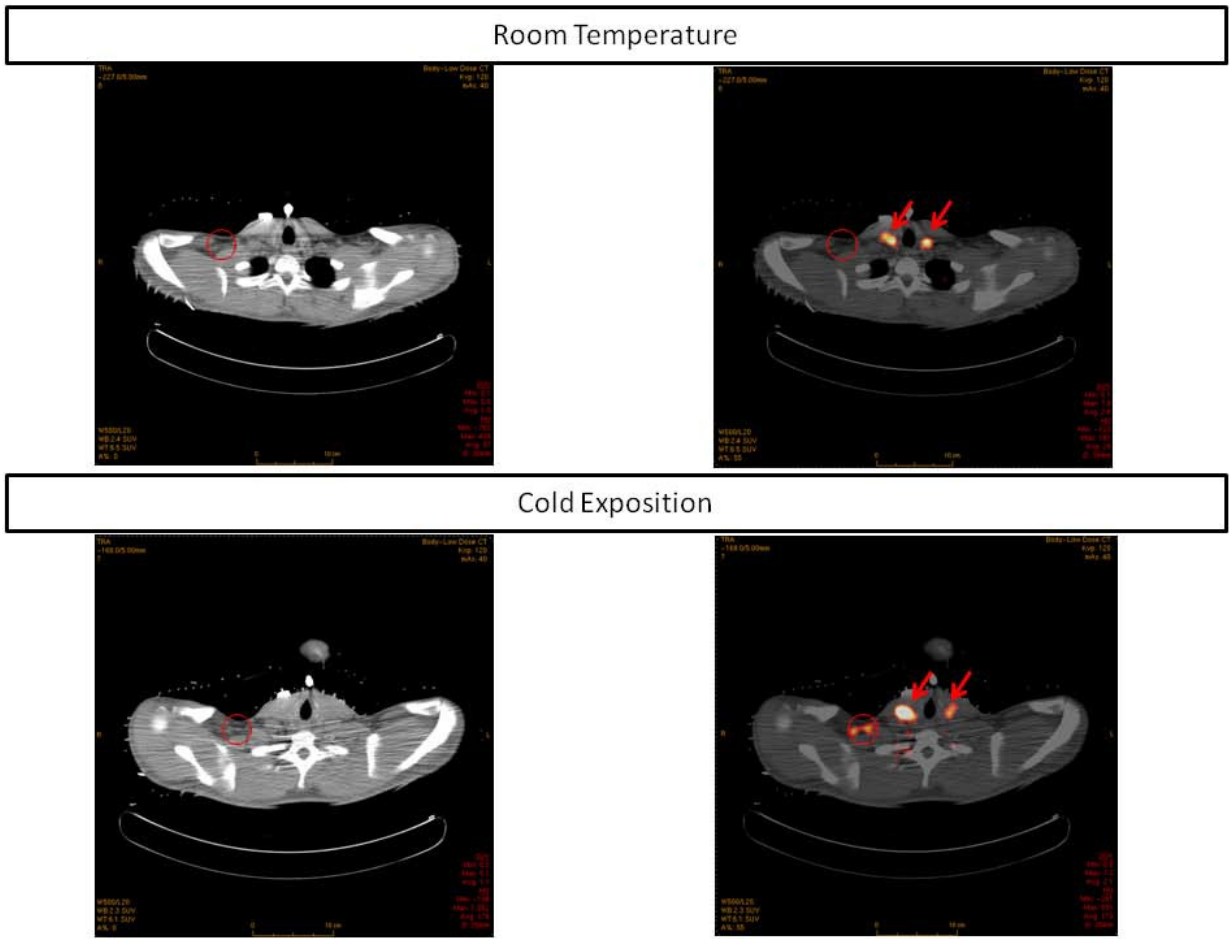

Supplemental Figure 1:

PET (left panels) , CT (middle panels) and fusion images (right panels) of the integrated tissue activity in the neck and upper chest area from dynamic list-mode acquisitions at room temperature (upper row) and during cold exposure (lower row) in one of the participants. The arrow in all frames points to the supraclavicular BAT, showing an increase in ^{11}C-acetate activity in BAT during cold exposure vs. at room temperature.

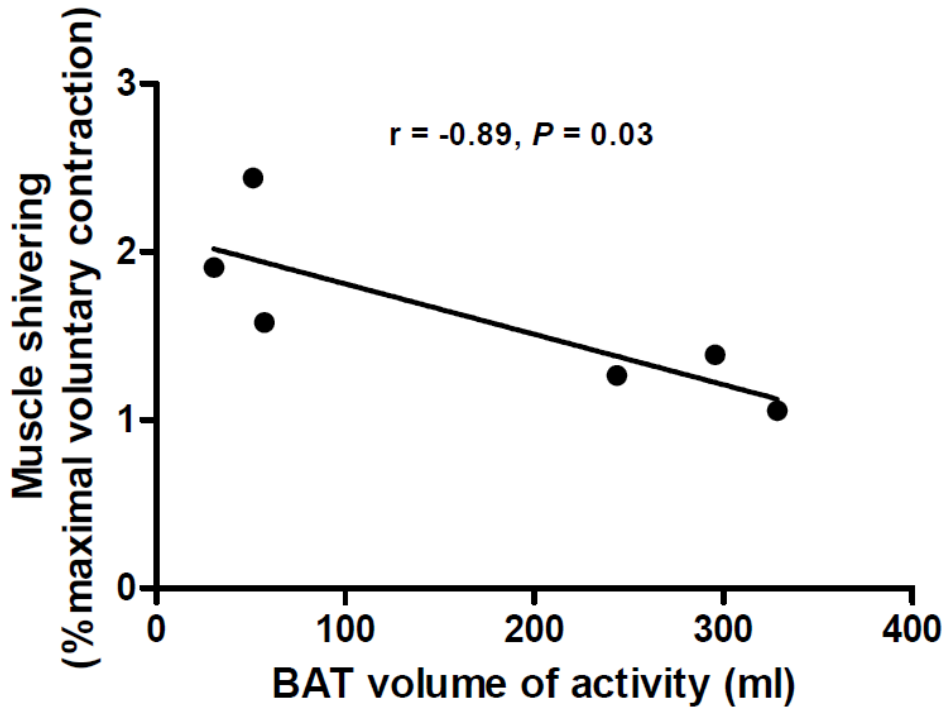

Supplemental Figure 2

Correlation between BAT volume of activity and shivering during cold exposure expressed as % maximal voluntary muscle contraction.

Supplemental Table:

Spearman correlation between brown adipose tissue volume of activity and metabolic parameters

	r	*P*
BAT K_m FDG (nmol/ml/min)	0.66	0.18
BAT K_m FTHA (nmol/ml/min)	0.37	0.50
ΔRa_{NEFA} (μmol/min)	0.50	0.45
ΔTEE (kcal/min)	0.20	0.71
Muscle shivering (% MVC)	-0.89	0.03
ΔBAT ^{11}C-acetate *K*	-0.66	0.18

BAT: brown adipose tissue; Δ: change between cold exposure vs. room temperature; K_m FDG: glucose uptake; K_m FTHA: nonesterified fatty acid uptake; MVC: maximal voluntary contraction; Ra_{NEFA}: nonesterified fatty acid rate of appearance in plasma; TEE: total energy expenditure.

3.2 Article II

Submitted to Journal of Physiology (London).

Relative contribution of brown adipose tissue and skeletal muscles to acute cold-induced metabolic response in healthy men.

Denis P. Blondin[1], Sébastien M. Labbé[2], Serge Phoenix[2,4], Brigitte Guérin[4], Éric E. Turcotte[4], Denis Richard[3], André C. Carpentier[2], François Haman[4].

[1] Department of Medicine, Centre de Recherche du Centre hospitalier universitaire de Sherbrooke, Université de Sherbrooke

[2] Centre de Recherche de l'Institut Universitaire de Cardiologie et de Pneumologie de Québec, Université Laval

[3] Department of Nuclear Medicine and Radiobiology, Université de Sherbrooke, Québec, Canada.

[4] Faculty of Health Sciences, University of Ottawa

Running Head: cold-induced interaction between BAT and skeletal muscle

Word Count: Main Text: 4496

KEY POINTS

- Both BAT and skeletal muscle metabolic activation contribute to energy expenditure upon acute cold exposure in healthy men even if effort is made to minimize the shivering response;
- Activation of adipose tissue intracellular lipolysis is associated with BAT metabolic response upon acute cold exposure in healthy men;
- Although BAT glucose uptake per volume of tissue is important, the bulk of glucose turnover during cold exposure is mediated by skeletal muscle metabolic activation even when shivering is minimized.

ABSTRACT

Cold exposure stimulates the sympathetic nervous system (SNS), triggering the activation of cold-defense responses and mobilizing substrates to fuel the thermogenic processes. Although these processes have been investigated independently, the physiological interaction and coordinated contribution of the tissues involved in producing heat or mobilizing substrates has never been investigated in humans. Using [U-^{13}C]-palmitate and [3-^{3}H]-glucose tracer methodologies coupled with PET using ^{11}C-acetate and ^{18}F-fluorodeoxyglucose (^{18}FDG), we examined the relationship between whole body sympathetically-induced WAT lipolysis and BAT metabolism and mapped the skeletal muscle shivering and metabolic activation pattern during a mild, acute cold exposure designed to minimize shivering response in 12 lean healthy men. Cold-induced increase in NEFA appearance rate was strongly associated with the volume of metabolically active BAT (r = 0.64, P = 0.04), total BAT oxidative metabolism (r = 0.72, P = 0.02) and BAT glucose uptake (r = 0.72, P = 0.02), but not muscle glucose metabolism. Cold-induced increase in whole-body oxygen consumption was not independently associated with BAT volume of activity, BAT oxidative metabolism or muscle metabolism or shivering intensity, but rather, depended on the sum of responses of these two thermogenic tissues. The total glucose uptake was more than one order of magnitude greater in skeletal muscles compared to BAT during cold exposure (675±124 μmol·min^{-1} *vs.* 16±8 μmol·min^{-1}, respectively, P < 0.001). ^{18}FDG uptake demonstrated that deeper, centrally located muscles of the neck, back and inner thigh were the greatest contributors of muscle glucose uptake during cold exposure due to their more important shivering response. In summary, these results demonstrate for the first time that increase in plasma NEFA appearance from WAT lipolysis is closely associated with BAT metabolic activation upon acute cold exposure in healthy men. In humans, muscle glucose utilization during shivering contributes to a much greater extent than BAT to systemic glucose utilization during acute cold exposure.

Key words: energy metabolism; skeletal muscle; brown adipose tissue; cold exposure; adipose tissue intracellular lipolysis.

Abbreviations: BAT, brown adipose tissue; EMG, electromyography; ^{18}FDG, ^{18}F-fluorodeoxyglucose; K_i: fractional uptake; K_m: net uptake; MVC, maximal voluntary contraction; NEFA: nonesterified fatty acids; PET: positron emission tomography; sEMG, surface electromyography; SNS: sympathetic nervous system; Ra: rate of appearance; SUV: standard uptake value; TG, triglycerides; WAT, white adipose tissue

INTRODUCTION

BAT investigations in humans to date have usually reported absence of overt shivering by non-quantitative direct observation and/or subjective report of subjects (van Marken Lichtenbelt *et al.*, 2009; Vijgen *et al.*, 2011; Yoneshiro *et al.*, 2011; Cypess *et al.*, 2012; Muzik *et al.*, 2012; Vijgen *et al.*, 2012). We previously have simultaneously quantified both shivering and BAT activity in healthy men (Ouellet *et al.*, 2012). In the latter study, a significant increase in cold-induced BAT oxidative metabolism was accompanied by limited but detectable level of shivering activity, measured by surface electromyography (sEMG), representing ~2% of a maximal voluntary contraction. The inverse relationship between BAT volume of metabolic activity and shivering activity in the latter study also suggested that cold-stimulated oxidative metabolism is driven by the integration of both shivering and BAT thermogenesis in healthy men. Deeper muscles that are not accessible by sEMG may also contribute significantly to the whole body metabolic response observed during mild, acute cold exposure (Ouellet *et al.*, 2012). However, no quantification of the relative contribution of muscle shivering response vs. BAT metabolic response to circulating energy substrate metabolism has been reported to date.

Sympathetic nervous system (SNS) stimulation by acute cold exposure triggers the activation of cold-defence responses and mobilizes substrates to fuel the thermogenic processes. Given the sympathetic innervation of adipose tissues, cold-mediated SNS activation stimulates β-adrenergic receptor signaling in white adipose tissue (WAT) and brown adipose tissue (BAT), thus activating intracellular lipolysis in both organs. Whereas sympathetic β-adrenergic stimulation of lipolysis in WAT mobilizes NEFA towards thermogenic organs, such as brown adipose tissue (BAT) and shivering skeletal muscles (Ouellet *et al.*, 2012), SNS-mediated lipolysis of intracellular triglycerides (TG) in BAT serves to activate and fuel BAT

thermogenesis (Cannon & Nedergaard, 2004). Regional differences in catecholamine-mediated lipolysis and adrenoreceptor activity across various WAT depots have previously been documented in humans (Leibel & Hirsch, 1987; Mauriege *et al.*, 1987; Wahrenberg *et al.*, 1989; Mauriege *et al.*, 1991). However, it remains unclear whether sympathetically-triggered lipolysis in WAT and BAT thermogenesis are associated or distinct processes in humans.

The aims of this study were 1) to characterize BAT and skeletal muscle glucose metabolism during acute cold exposure and 2) to assess the relationship between BAT, skeletal muscle metabolic responses and total energy expenditure and cold-induced activation of adipose tissue lipolysis in healthy men. We hypothesized that 1) both skeletal muscles and BAT would contribute to energy expenditure and glucose metabolism during acute cold exposure and 2) that cold-induced whole-body lipolysis of WAT would be associated with BAT metabolic response.

MATERIALS AND METHODS

Methods

Ethical approval

Twelve healthy, non-cold acclimatized men aged 24 ± 1 years with a BMI of 25.5 ± 0.8 kg/m^2 were fully informed of the risks and methodologies applied and provided their written consent to participate in this study, in accordance with the Declaration of Helsinki. This study received ethics approval from the Human Ethics Committee of the *Centre de Recherche du Centre hospitalier universitaire de Sherbrooke*. None of the participants were diagnosed with diabetes, based on medical history, repeated assessment of fasting glucose concentration and 75 g oral glucose tolerance test. None were taking any medication, had any current medical condition known to affect lipid levels or insulin sensitivity, or had known cardiovascular or other medical conditions.

Experimental Protocols

All subjects participated in a single metabolic protocol designed to assess whole-body and tissue-specific metabolic rate as well as glucose turnover during an acute cold exposure. The metabolic protocol consisted of a 120 min baseline period at ambient temperature (~25 °C) followed by 180 min of exposure to a mild cold, elicited using a liquid conditioned suit (Three Piece, Allen-Vanguard, Ottawa, ON) perfused with water at 18°C using a temperature and flow-controlled circulation bath (Endocal, NESLAB Model 200–00, Micropump, Vancouver, WA, USA). Experiments were conducted between 7h30 and 15h00, following a 12h fast and 48h without strenuous physical activity. Subjects were asked to follow a two-day standard isocaloric diet based upon a 3-day food record, filled a validated questionnaire for physical activity (Sallis

et al., 1985) and underwent portable arm band accelerometry for 7 days (St-Onge *et al.*, 2007). Upon their arrival in the laboratory, subjects wearing only shorts were weighed and instrumented with autonomous wireless temperature sensors (Thermochron iButton® model DS1922H, Maxim) placed on the forehead, chest, forearm, back of hand, lower back and quadricep to measure mean skin temperature (Palmes & Park, 1947). Surface electromyography electrodes (Delsys, EMG System, USA) were placed on the belly of 8 large muscles known to contribute significantly to shivering during cold exposure (Bell *et al.*, 1992; Haman *et al.*, 2004b; Haman *et al.*, 2005): *m. pectoralis major*, *m. deltoideus, m. trapezius*, *m. sternocleidomastoid, m. rectus abdominis*, *m. rectus femoris, m. vastus medialis* and *m. vastus lateralis*. Participants were then fitted with the liquid-conditioned suit, swallowed a telemetric thermometry capsule to measure core temperature (Vital Sense monitor and Jonah temperature capsule, Mini Mitter Co., Inc., Bend, OR, USA) and performed a series of maximal voluntary contractions (MVC) of each of the 8 muscles being recorded by sEMG for qualibration of the measures. Indwelling catheters were then placed in an antecubital vein in both arms for blood sampling and tracer infusions. Participants were asked to empty their bladder and a primed continuous infusion of [3-^{3}H]-glucose to measure $Ra_{glucose}$ (3.3 x 10^{6} dpm min^{-1} bolus + infusion at 0.33 x 10^{6} dpm min^{-1}) and [U-^{13}C]-palmitate to measure Ra_{NEFA} (1.2 µmol kg^{-1} bolus of [1-^{13}C]-$NaH^{13}CO_3$ + 0.01 µmol kg^{-1} min^{-1} infusion of [U-^{13}C]-palmitate in 100 mL of 25% human serum albumin) were started (time = 0 min) (Carpentier *et al.*, 2001; Carpentier *et al.*, 2005; Carpentier *et al.*, 2007; Ouellet *et al.*, 2012). Whole body and muscle-specific shivering intensity and pattern as well as mean skin and core temperatures were measured continuously from time 90 to 300 min as previously described (Haman *et al.*, 2004b). Only the mean of the final 30 min of the ambient period and final 120 min of the cold exposure are reported. Whole body oxygen consumption (VO_2) and energy

expenditure was determined by indirect respiratory calorimetry (Vmax 29n; Sensormedics) (Haman *et al.*, 2002; Haman *et al.*, 2004c) (Carpentier AC AJP 2005) at room temperature and between times 180 to 200 min and 280 to 300 min (i.e., 60 to 80 min and 160 to 180 min after the beginning of cold exposure).

PET/CT protocol

Participants remained supine in a PET/CT scanner (Philips Gemini GXL; Philips, Eindhoven, The Netherlands) for 120 min at ambient temperature (~25°C). Following this ambient period, the liquid-conditioned suit was perfused with 18°C water for 180 min (between 120 and 300 min) while the participant remained supine in the PET/CT scanner. BAT oxidative metabolism was determined by first performing a CT scan (40 mAs) centered at the cervico-thoracic junction to correct for attenuation and to define PET regions of interest (ROI). At time 210 minutes (*i.e.* 90 minutes after onset of cold exposure), a ~185 MBq bolus of ^{11}C-acetate was injected intravenously, and was followed by a 30 minute list-mode dynamic PET acquisition. This was immediately followed by another regional CT scan (40 mAS) and a ~185 MBq i.v. bolus of ^{18}F-fluorodeoxyglucose (^{18}FDG) at time 240 min (i.e. 120 min after onset of cold exposure) followed by a 40 minute list-mode dynamic PET acquisition. At time 300 min, a whole body CT scan (16 mAs) and whole body static PET acquisition were performed to determine whole body ^{18}FDG organ distribution and tissue standard uptake value (SUV).

PET/CT image analyses

ROI were first defined from the transaxial CT slices, then copied to ^{11}C-acetate and then to ^{18}FDG PET image sequences. For dynamic PET acquisitions, mean value of pixels (mean standard uptake value [SUV]) for each frame was recorded. ROI were drawn on the aortic arch

for blood activity (input functions), the larger skeletal muscles in the field of view (*e.g. m. sternocleidomastoid*, *m. longus colli*, *m. trapezius*, *m. pectoralis major*, *m. deltoideus*), on posterior cervical subcutaneous adipose tissue and on supraclavicular BAT. For whole-body scans, ROI were first defined from the transaxial CT slices and then co-registered to ^{18}FDG image sequences. Mean values of pixels (mean SUV) of ROI were determined bilaterally for BAT, abdominal subcutaneous white adipose tissue (scWAT) and the following muscles: *m. sternocleidomastoid* (SCM), *m. longus colli* (LC), *m. trapezius* (TR), *m. lattissimus dorsi* (LD), *m. pectoralis major* (PM), *m. deltoideus* (DT), *m. biceps brachii* (BB), *m. triceps brachii* (TB), *m.brachioradialis* (BR), *m. erector spinae* (ES), *m.rectus abdominis* (RA), m. psoas *major* (PS), *m. adductor magnus* (AM), *m. gluteus maximus* (GM), *m. biceps femoris* (BF), *m. rectus femoris* (RF), *m. vastus medialis* (VM), *m. vastus lateralis* (VL).

Calculations

The volume of supraclavicular BAT was determined according to the following criteria: a tissue radio density between –30 and –150 Hounsfield units and ^{18}FDG uptake during cold exposure of more than 1.5 SUV unit (Ouellet *et al.*, 2011). BAT total oxidative metabolism index was calculated as the product of the total volume of supraclavicular BAT and BAT oxidative metabolism index. To determine tissue glucose uptake, plasma and tissue time-radioactivity curves were analyzed graphically using the Patlak linearization method (Menard *et al.*, 2010), with the image-derived arterial input function taken from the aortic arch (Croteau *et al.*, 2010). The slope of the plot in the graphical analysis is equal to BAT glucose fractional uptake (K_i in min^{-1}). BAT net glucose uptake (K_m) was then calculated by multiplying K_i by plasma glucose concentration, measured during the PET imaging protocol, which assumes a lump constant value of 1.0 compared with endogenous plasma glucose. BAT oxidative

metabolism index (the rapid fractional tissue clearance of ^{11}C-acetate, *k*, in sec^{-1}) was estimated from BAT ^{11}C activity over time using a monoexponential fit from the time of peak tissue activity (Buck *et al.*, 1991).

Shivering EMG signals were recorded from the following muscle groups: PM, DT, TR, SCM, RA, RF, VM and VL. Raw EMG signals were collected at 1000 Hz, filtered to remove spectral components below 20 Hz and above 500 Hz as well as 60-Hz contamination and related harmonics, and analyzed using custom-designed MATLAB algorithms (Mathworks, Natick, MA). Shivering intensity of individual muscles was determined from root-mean-square (RMS) values calculated from raw EMG. In brief, baseline RMS values ($RMS_{baseline}$: 5 min RMS average measured prior to cold exposure) were subtracted from shivering RMS (RMS_{shiv}) values and RMS values obtained from the maximal voluntary contractions of individual muscles (RMS_{mvc}). Shivering intensity was normalized to RMS_{mvc} by using the following equation:

$$\text{Shivering Intensity (\%MVC)} = \frac{RMS_{shiv} - RMS_{baseline}}{RMS_{mvc} - RMS_{baseline}} \text{ X } 100 \qquad (1)$$

Shivering intensity was determined by using a weighted mean of the shivering intensity of all 8 muscles, as previously described (Haman *et al.*, 2004a).

The muscles identified by PET/CT scanning were grouped into upper body (e.g. SCM, LC, TR, LD, PM, DT, BB, TB, BR, ES, RA) *vs.* lower body (e.g. PS, AM, GM, BF, RF, VM, VL), peripheral (e.g. DT, BB, TB, BR, GM, BF, RF, VM, VL) *vs.* central (e.g. SCM, LC, TR, LD, PM, ES, RA, PS, AM), and deep (e.g. LC, ES, AM, PS,) *vs.* superficial (e.g. SCM, TR, LD, PM, DT, BB, TB, BR, RA, GM, BF, RF, VM, VL). A weighted average of glucose partitioning

(SUV) of the 18 skeletal muscles, which include deep muscles that are inaccessible using surface electromyography, was also used as a shivering metabolic index.

Laboratory assays

Insulin, cortisol, TSH, free T3 and free T4 were measured by specific radioimmunoassays (Linco, St. Charles, MO, and Nichols Institute Diagnostics, San Juan Capistrano, CA). Glucose, total plasma NEFA and triglycerides were measured using colorimetric assays (Wako Industrials and Thermo DMA, respectively). To measure plasma palmitate, linoleate, oleate, and [U-^{13}C]-palmitate enrichment, heptadecanoic acid was added as an internal standard to 100 µl of plasma and mixed with 500 µl of methanol. After centrifugation, the supernatant was filtered and injected on a Hypersil ODS column (5 µm, 4.0 × 125 mm) on an LC/MSD series 1100 (Agilent) with monitoring of ions 279 (C18:2), 281 (C18:1), 255 (C16:0), 271 (C16:0 *M* +16), and 269 (C17, internal standard). Standard curves were generated for C16:0, C18:1, C18:2, and C16:0 *M* +16 enrichment by use of purified standards of known concentration.

Statistical analysis

Data are expressed as mean + SEM. Paired *t*-test was used to compare averaged steady-state mean values of all end-points of interest between room temperature and cold exposure. ANOVA for repeated measures with Bonferroni post-hoc test was used to compare glucose partitioning and shivering intensity between the different tissues or muscles. Spearman correlation was used to determine correlation between variables. A 2-tailed *P* value of less than 0.05 was considered significant. All analyses were performed using SPSS for Windows (version

16.0; SPSS Inc., Chicago IL) or GraphPad Prism version 6.01 for Windows (GraphPad, San Diego, CA).

RESULTS

During cold exposure, average skin temperature and core temperature decreased by 4.5 ± 0.3 °C and 0.4 ± 0.1 °C, respectively, eliciting an 82% increase in energy expenditure (Table 1). By design, whole body shivering intensity was controlled and maintained to 1.6 ± 0.4 % MVC (Table 1). Plasma glucose, insulin and triglyceride concentrations did not change during cold exposure (Table 1), whereas NEFA levels increased by 48% ($P < 0.001$, Figure 1A). This was a result of a cold-induced increase in the R_a of NEFA (Figure 1C), which increased by 41% in the cold (868 ± 71 μmol·min^{-1} in the cold *vs.* 616 ± 60 μmol·min^{-1} at room temperature). The monoexponential decay slope from tissue peak ^{11}C activity (^{11}C-acetate *k*), a surrogate of tissue oxidative metabolism (Brown *et al.*, 1987; Ng *et al.*, 1994), increased 2.3-fold during cold exposure (Figure 1C) which was paralleled by an increase in the radiodensity of BAT (Figure 1D).

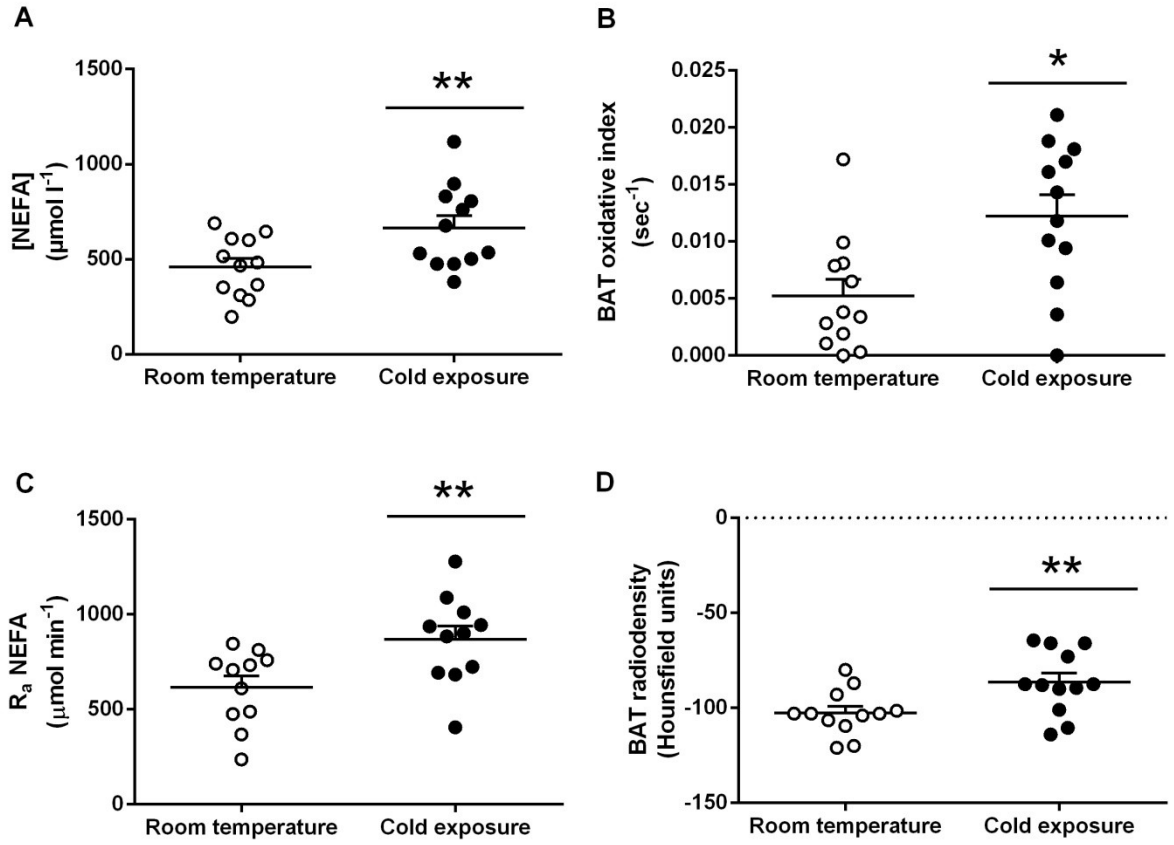

Figure 1. Whole-body NEFA kinetics and BAT lipolysis and oxidative metabolism. Plasma NEFA concentrations (A), BAT monoexponential decay slope from peak ^{11}C activity (BAT ^{11}C-acetate *k;* B), NEFA rate of appearance in circulation (C) and BAT radiodensity at room temperature and during cold exposure (D). Values presented as mean ± SEM (n = 12). * Different from room temperature, $P \leq 0.01$, **, $P \leq 0.001$.

TABLE 1. Core and mean skin temperature, energy expenditure, circulating metabolites and hormones and plasma glucose and NEFA appearance rates.

	Room Temperature	**Cold Exposure**	***P* Value**
Mean skin temperature (°C)	33.1 ± 0.3	28.6 ± 0.3	0.0001
Core temperature (°C)	36.5 ± 0.1	36.1 ± 0.1	0.001
Energy expenditure (kJ min^{-1})	6.7 ± 0.3	12.2 ± 0.8	0.0001
Shivering intensity (% MVC)	-	1.6 ± 0.3	-
Shivering index (mean SUV)	-	0.8 ± 0.1	-
Glucose (mmol l^{-1})	4.4 ± 0.2	4.4 ± 0.2	0.71
$Ra_{glucose}$ (μmol min^{-1})	-	1600 ± 235	-
Insulin (pmol l^{-1})	65.1 ± 7.2	58.1 ± 4.8	0.15
Triglycerides (mmol l^{-1})	1.02 ± 0.23	1.03 ± 0.21	0.98
Cortisol (nmol l^{-1})	285 ± 22	284 ± 20	0.97
TSH (IU l^{-1})	1.95 ± 0.41	1.65 ± 0.29	0.06
Free T4 (pmol l^{-1})	16.7 ± 0.4	17.1 ± 0.4	0.02
Free T3 (pmol l^{-1})	5.7 ± 0.2	5.6 ± 0.2	0.21

Data are expressed as mean ± SEM for steady-state values during the last 30 min at each temperature (n = 12). $Ra_{glucose}$, glucose rate of appearance.

The mean BAT volume of activity represented 117±34 mL (Figure 2A), which when multiplied by the tissue oxidative metabolism provided a more accurate perspective on total BAT oxidative metabolism and demonstrated a 69% increase due to cold exposure (from 0.91±0.47 mL of BAT·^{11}C-acetate sec^{-1} to 1.69 ± 0.59 mL of BAT·^{11}C-acetate sec^{-1}; Figure 2B). During cold exposure, the fractional uptake (K_i; Figure 2C) and net uptake (K_m; Figure 2D) of ^{18}FDG, during the cervicothoracic dynamic PET/CT acquisition, was significantly greater in supraclavicular BAT compared with *m. deltoideus*, *m. trapezius*, and subcutaneous adipose tissue but not compared to the *m. pectoralis major, m. sternocleidomastoid* and *m. longus colli*. A strong association between the relative uptake of ^{18}FDG in BAT (in mean SUV) and both the fractional and net uptake of ^{18}FDG in BAT (Figure 2E-F) suggests that the relative uptake of ^{18}FDG may be a reliable surrogate to estimate net glucose uptake in BAT.

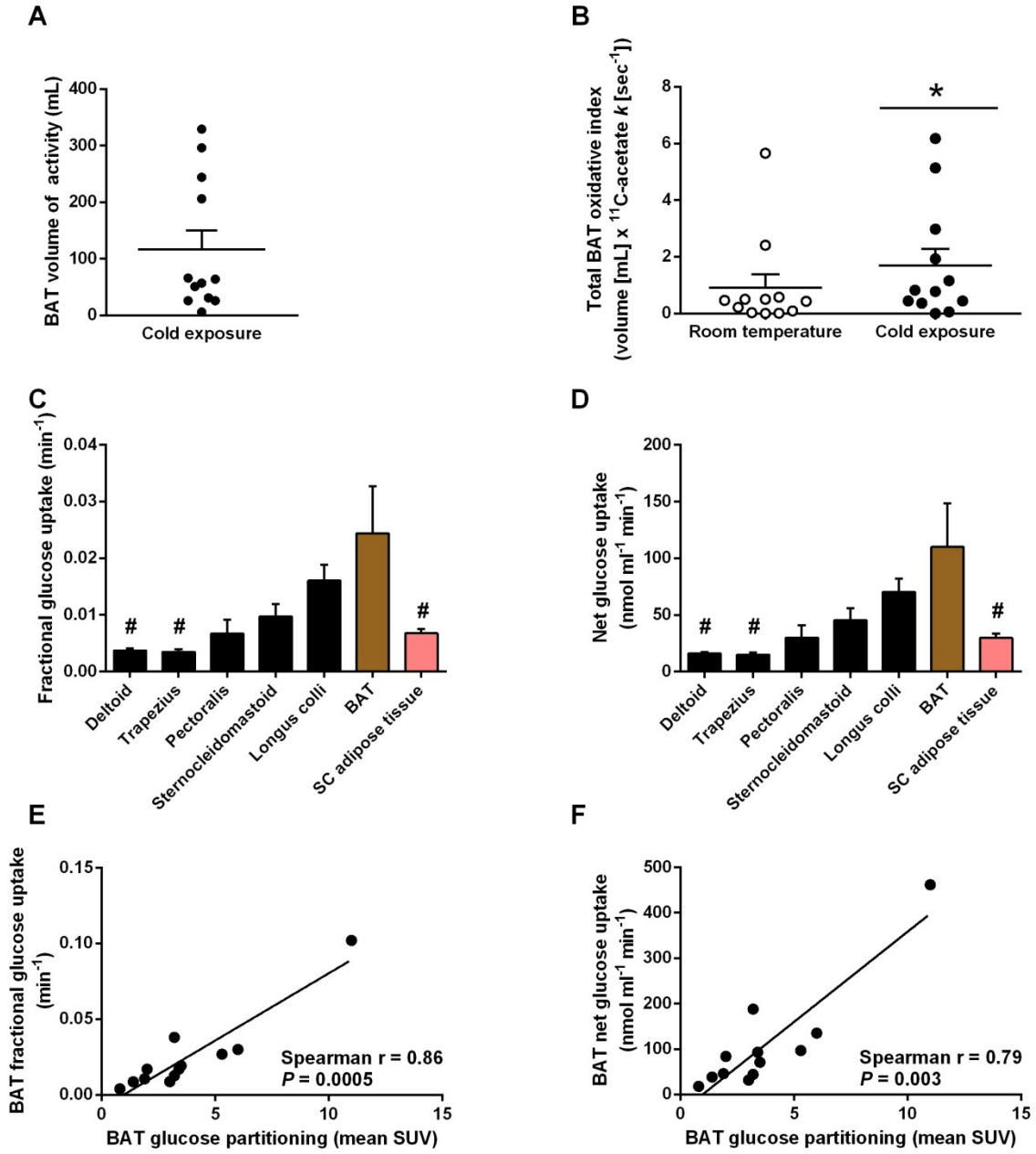

Figure 2. BAT energy metabolism during acute cold exposure. BAT volume of activity (A) during cold exposure. BAT total oxidative metabolism index (B) at room temperature and during cold exposure. Fractional (K_i) (C) and net (K_m) glucose uptake (D) in cervicothoracic tissues. The relationship between the relative uptake of ^{18}FDG in BAT and fractional and net glucose uptake in BAT (E-F). Values presented as mean ± SEM (n = 12). * Different from room temperature, $P \leq 0.01$, $^{\#}$ Different from BAT, $P \leq 0.01$.

To further investigate the relationship between sympathetically-mediated whole body lipolysis and BAT metabolism, we examined the association between the cold-induced changes in the NEFA R_a (Δ R_a NEFA) and BAT volume of activity (Figure 3A), cold-induced total BAT oxidative metabolism (Δ BAT total oxidative metabolism index, Figure 3B) and BAT total glucose uptake (Figure 3C). We found a strong association between the Δ R_a NEFA and the BAT metabolic variables, but no such association between Δ R_a NEFA and cold-induced muscle metabolism (Figures 3D-F).

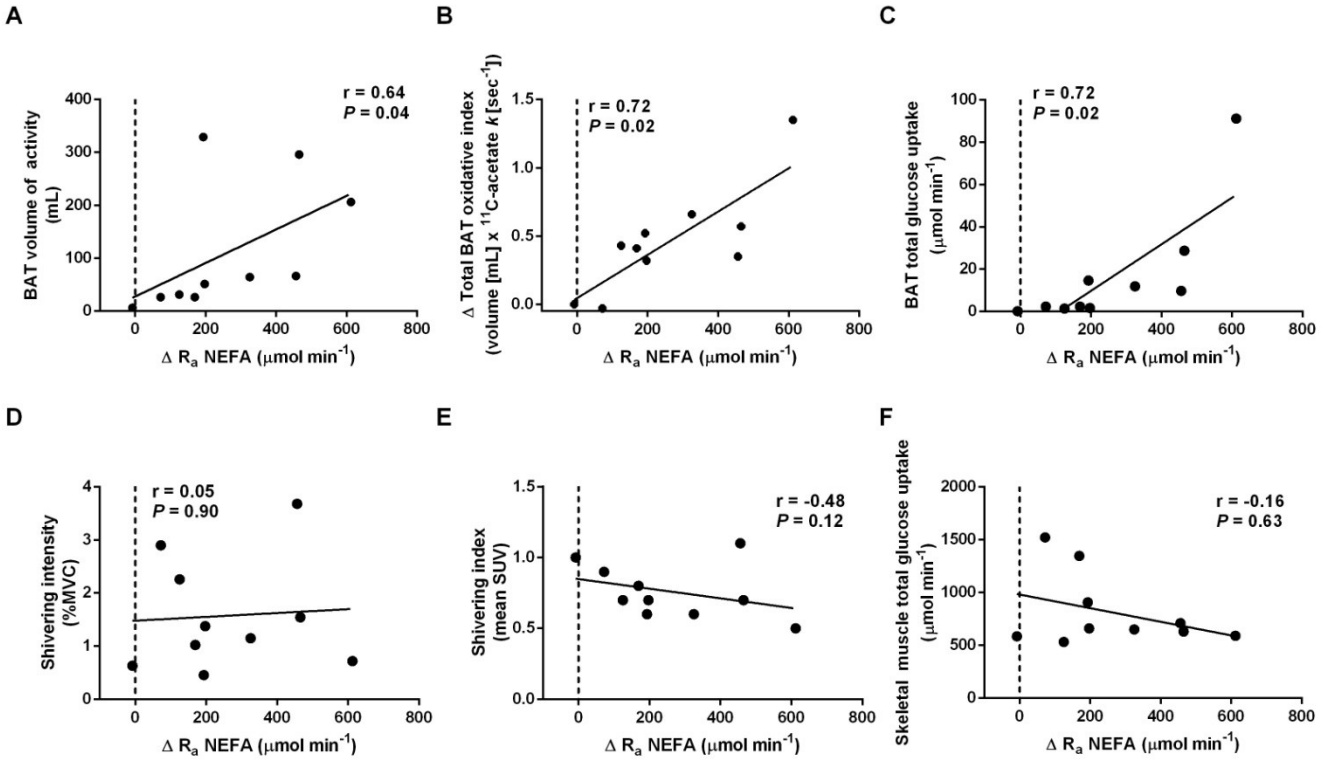

Figure 3. Sympathetic nervous system-mediated WAT lipolysis and BAT and skeletal muscle metabolism. Spearman correlation between whole-body changes in NEFA Ra (Δ R_a NEFA) and BAT volume of activity (A), change in BAT total oxidative metabolism index (B), BAT total glucose uptake (C), shivering intensity (D), PET-determined shivering index (E) and skeletal muscle total glucose uptake (F).

To begin investigating BAT energy metabolism and the role of circulating glucose, we examined the association between ^{18}FDG uptake and the radiodensity of BAT prior to i.v. injection of ^{18}FDG during cold exposure (Figure 4A-B) and cold-induced BAT oxidative metabolism (Figure 4C-D). We found that the radiodensity of BAT prior to i.v. injection of ^{18}FDG during cold exposure was strongly associated with the fractional and net ^{18}FDG uptake (Figure 4A-B). This provides some indications of both the effect of TG content on ^{18}FDG uptake and the possible metabolic fate of the glucose taken up by BAT. That the fractional and net ^{18}FDG uptake did not correlate with the oxidative metabolism of BAT (Figure 4C-D), suggests that it is likely indirectly fueling BAT thermogenesis, *via de novo* lipogenesis.

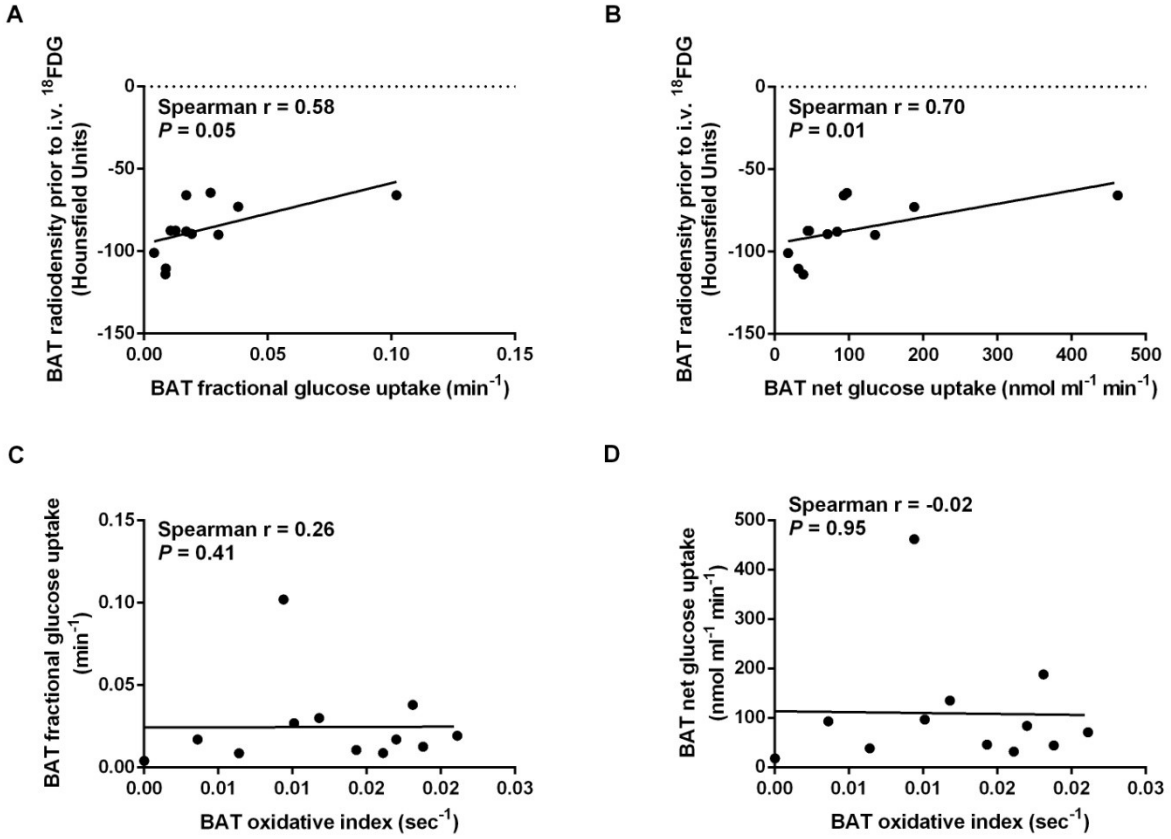

Figure 4. BAT glucose metabolism during cold exposure. Spearman correlation between BAT radiodensity prior to intravenous (i.v.) injection of ^{18}FDG and fractional (A) and net (B) BAT ^{18}FDG uptake. Spearman correlation between BAT monoexponential decay slope from peak ^{11}C activity (BAT ^{11}C-acetate *k*) and BAT fractional (C) and net (D) ^{18}FDG uptake.

The fall in mean skin temperature induced a 1.8-fold increase in VO_2 (Figure 5A; 0.328 ± 0.016 $L \cdot min^{-1}$ to 0.582 ± 0.040 $L \cdot min^{-1}$). No relationship between this change in VO_2 and either shivering intensity (Figure 5D; r = 0.44, P = 0.15), BAT volume of activity (Figure 5E; r = 0.40, P = 0.20) or BAT total oxidative capacity (Figure 5F; r = 0.19, P = 0.57) was identified. Interestingly, no relationship between the shivering intensity and BAT volume of activity or BAT total oxidative metabolism was found either (Figure 5B-C).

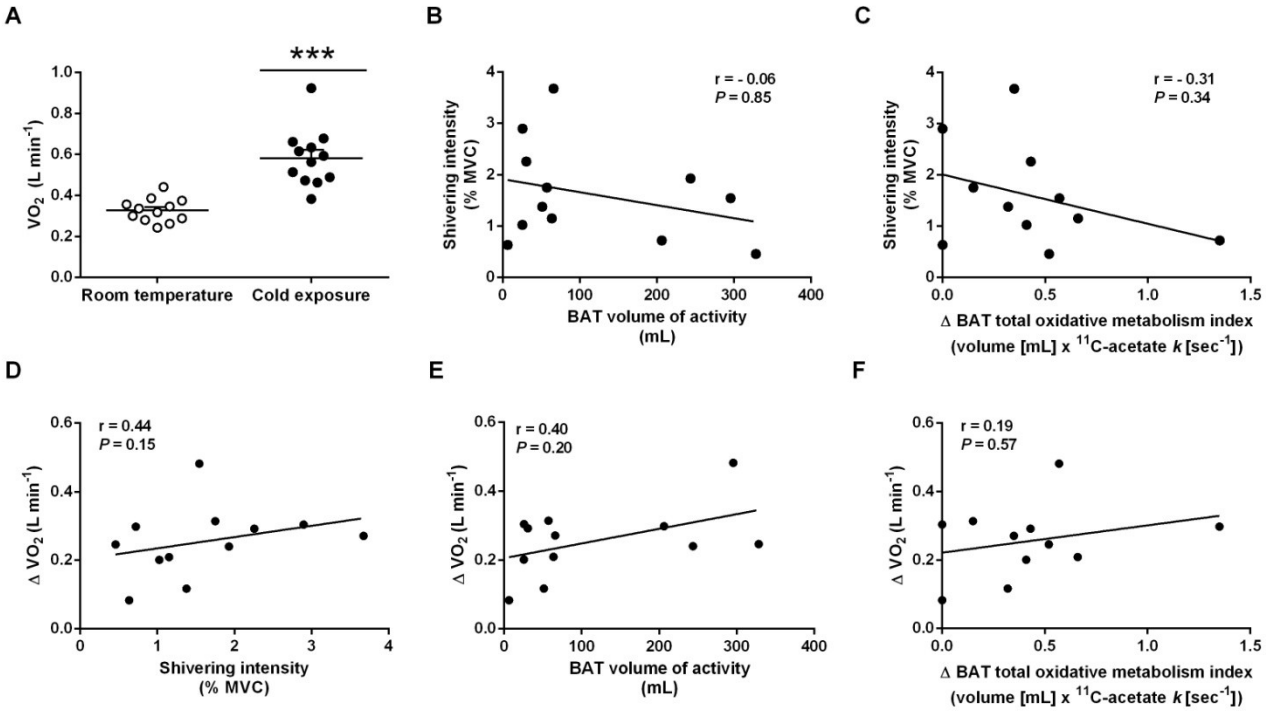

Figure 5. BAT - skeletal muscle thermoregulatory interaction during cold exposure. Oxygen consumption ($\dot{V}O_2$) at room temperature and during cold exposure (values presented as mean ± SEM; A). Spearman correlation between shivering intensity and BAT volume of activity (B) and cold-induced BAT total oxidative capacity (Δ BAT total oxidative metabolism index; C). Spearman correlation between cold-induced change in $\dot{V}O_2$ (Δ $\dot{V}O_2$) and shivering intensity (D), BAT volume of activity (E) and cold-induced BAT total oxidative capacity (F). *** Different from room temperature, $P \leq 0.0001$.

To quantify the contribution of BAT and shivering muscles in clearing circulating glucose, we estimated total glucose uptake and plasma glucose turnover in these two tissues (Figure 6A-B). Total glucose uptake during cold exposure was 42-times greater in skeletal muscle compared to BAT (675±124 μmol·min^{-1} in skeletal muscle *vs.* 16±8 μmol·min^{-1} in BAT). This represented 47±7 % of glucose turnover occurring in muscle compared to 1 ± 1 % in BAT.

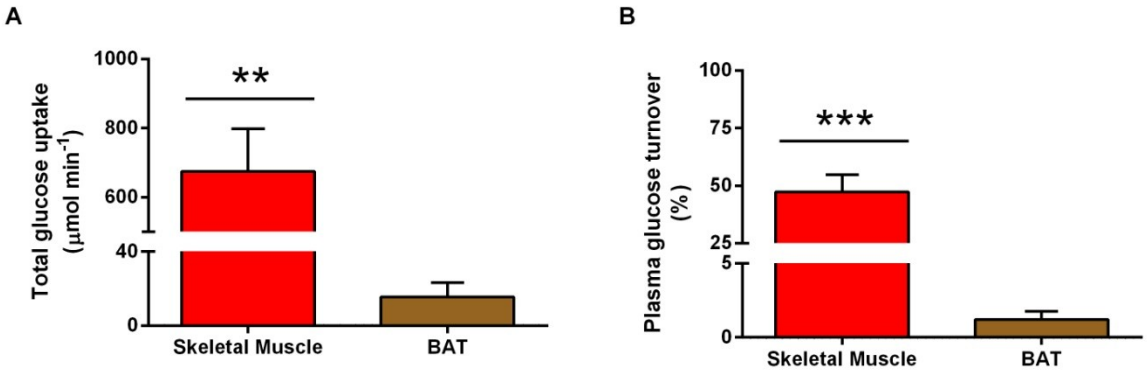

Figure 6. BAT and skeletal muscle metabolic regulatory function during cold exposure. Total glucose uptake (A) and plasma glucose turnover (B) of skeletal muscle (red bar) and BAT (brown bar). Values presented as mean ± SEM (n = 12). **Different from BAT, $P \leq 0.001$, *** $P \leq 0.0001$.

Whole body static PET acquisition showing the relative bio-distribution of ^{18}FDG and is presented in Figure 7A. The relative uptake of ^{18}FDG, as assessed by the mean SUV, varied considerably between muscles and relative to BAT ($P < 0.0001$, between all muscles and BAT). Of the eight muscles that were examined concomitantly by sEMG, the mean SUV of ^{18}FDG was significantly greater in the *m. pectoralis major* relative to *m. vastus lateralis, m. vastus medialis, m. rectus femoris, m. rectus abdominis*, *m.deltoideus* and *m. trapezius* ($P < 0.001$), but not *m.sternocleidomastoid* ($P = 0.76$). The relative uptake of ^{18}FDG between BAT and all skeletal muscles was compared and showed no significant difference between BAT and *m. longus colli*, *m. psoas major* and *m. sternocleidomastoid* (3.72 ± 0.71 vs. 2.80 ± 0.31, 1.73 ± 0.45, 1.44 ± 0.29

mean SUV, respectively, $P > 0.05$). Muscle-dependent differences in shivering intensity were observed ($P < 0.001$) during cold exposure, assessed by sEMG, with *m.pectoralis major* showing greater shivering activity than *m. rectus femoris*, *m. vastus lateralis, m. rectus abdominis, m. vastus medialis* and *m. deltoideus* but not compared *to m. trapezius* and *m. sternocleidomastoid* (Figure 7B). To determine whether the relative uptake of ^{18}FDG could serve as a reliable surrogate to sEMG, we compared the shivering intensity, determined by sEMG, with a shivering index, determined by PET (Figure 7C). We found a positive association between these two variables ($r^2 = 0.36$, $P = 0.04$), with the remaining variability likely explained by the activity of deep muscle groups which are detectable by PET but not by sEMG. Indeed, the relative uptake of ^{18}FDG was significantly greater in centrally located muscles relative to peripheral muscles ($P < 0.0001$) and deep muscles compared to superficial muscle groups ($P < 0.001$), whereas no difference was seen between upper body and lower body muscles ($P = 0.19$; Figure 7D).

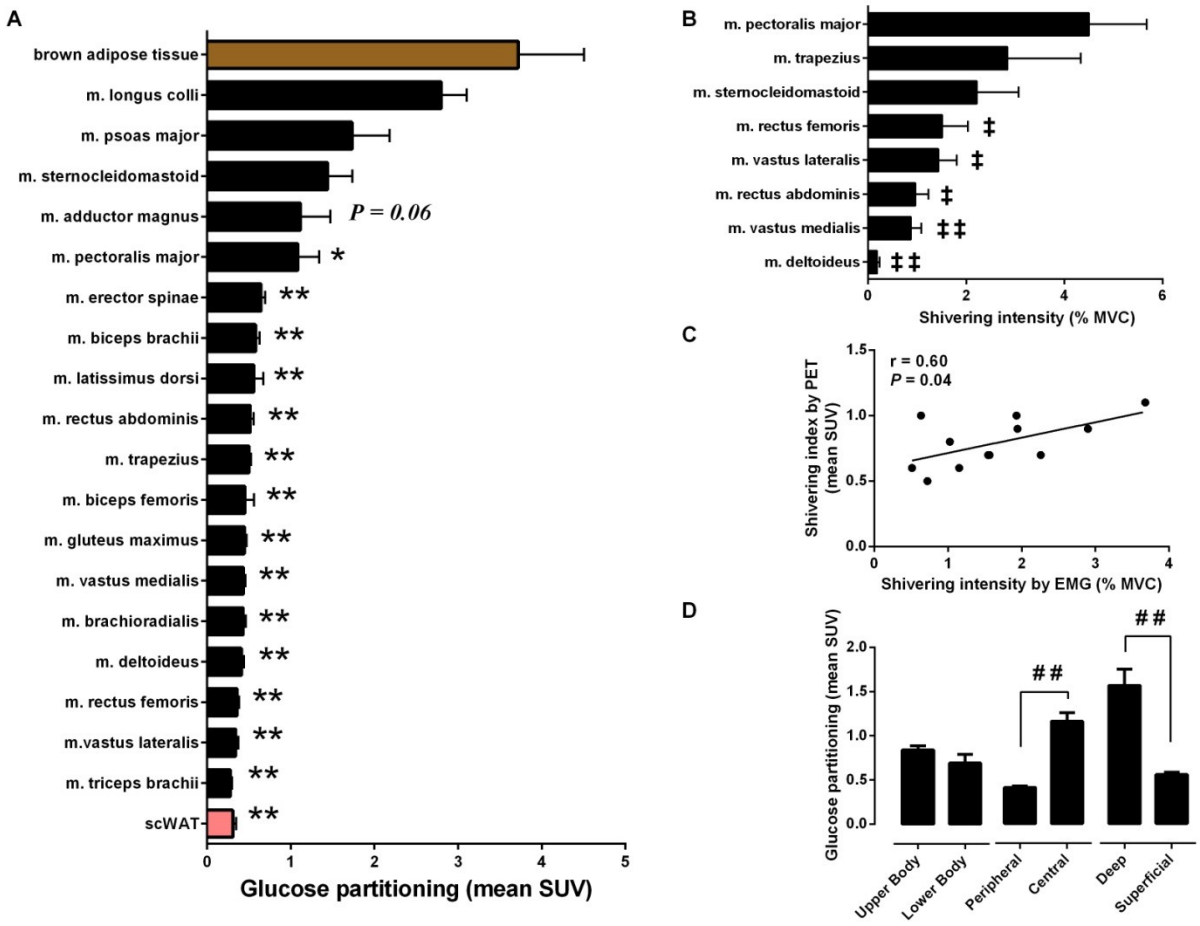

Figure 7. Bio-distribution of glucose and muscle recruitment during cold exposure. Relative uptake of ^{18}FDG in BAT, subcutaneous WAT (scWAT) and skeletal muscles during cold exposure (A,D). Shivering intensity of *m. pectoralis major*, *m. trapezius, m. sternocleidomastoid* (n = 9)*, m. rectus femoris, m. vastus lateralis* (n = 9)*, m. rectus abdominis, m. vastus medialis* (n = 9) and *m. deltoideus* (n = 9)*,* determined by surface EMG (B). Spearman correlation between shivering intensity determined by surface EMG and a shivering index calculated using the relative uptake of ^{18}FDG in skeletal muscles. Values presented as mean ± SEM (n = 12, unless otherwise indicated). *Different from BAT, $P \leq 0.05$, ** $P \leq 0.001$. ‡ Different from *m. pectoralis major*, $P \leq 0.05$, ‡‡ $P \leq 0.001$. ## Significant difference, $P \leq 0.001$.

DISCUSSION

The primary focus of this paper was to examine the inter-relationship between WAT, stimulated BAT and skeletal muscle on whole-body thermogenesis and substrate handling. The current findings establish a direct association between sympathetically-induced WAT lipolysis and BAT metabolism in humans. Additionally, in our lean, healthy cohort, cold-induced thermogenesis was derived from a balanced contribution between BAT and skeletal muscle with the latter providing the greatest thermogenic potential and capacity to regulate whole-body energy homeostasis under these thermal conditions. By mapping the bio-distribution of the positron-emitting glucose analog ^{18}FDG among a series of muscle groups, a pattern of muscle recruitment emerged whereby deep, centrally-located muscles were preferentially recruited over superficial, peripherally-located muscles for thermogenesis. Such a recruitment pattern is not only a reflection of the central efferent pathways involved, but may also be of significance in partially relieving skeletal muscle from its thermoregulatory function in favour of its more essential motor function.

Cold-induced WAT lipolysis and BAT thermogenesis

Sympathetic β-adrenergic stimulation initiates the hydrolysis of intracellular TG in WAT and BAT. In brown adipocytes, the hydrolysed intracellular TG generate fatty acids that serve as both the activator and metabolic substrate fueling BAT thermogenesis. Rodent models have shown regional variations in the sympathetic drive of various adipose depots, which appears to be influenced by the lipolytic stimulus (Brito *et al.*, 2008). Cold exposure elicited the greatest sympathetic drive and thus lipolytic activity, which seemed to be generalized across the various adipose depots (except dorsosubcutaneous WAT) but was most potent in BAT. Although

regional differences in catecholamine-mediated WAT lipolysis and adrenoreceptor activity have been well documented in humans (Leibel & Hirsch, 1987; Mauriege *et al.*, 1987; Wahrenberg *et al.*, 1989; Mauriege *et al.*, 1991), the relationship between sympathetically-triggered lipolysis in WAT and BAT thermogenesis has never been investigated. Here we show that under a mild cold stress, whole-body lipolytic activity increases by 41% and is paralleled by an 86% increase in BAT oxidative metabolism. This sympathetically-stimulated WAT lipolysis was strongly associated with the volume of BAT taking up ^{18}FDG, net ^{18}FDG uptake and most importantly the total oxidative metabolism of BAT. These findings have important implications as they demonstrate that sympathetic nervous system-mediated WAT lipolysis and BAT thermogenesis are closely matched. Obese insulin-resistant individuals exhibit a blunted response to catecholamine-induced lipolysis in WAT (Reynisdottir *et al.*, 1994; Horowitz *et al.*, 1999; Jocken *et al.*, 2008), which is associated with a reduction in cell surface β_2-adrenergic receptor density (Reynisdottir *et al.*, 1994). If such a catecholamine resistance is extended to BAT, this might explain the lower volume of BAT taking up ^{18}FDG (Vijgen *et al.*, 2011) and BAT glucose uptake (Orava *et al.*, 2013) reported in obese individuals, suggesting that this WAT-BAT relationship may play an important part in the development of obesity, lean tissue energy overload and lipotoxicity (Grenier-Larouche *et al.*, 2012). The inability of WAT to properly regulate NEFA fluxes, characteristic of the pathogenesis of type 2 diabetes and obesity (as reviewed in Lewis *et al.*, 2002; Carpentier *et al.*, 2011), combined with a dysregulation in facultative heat production by BAT would place an additional load on other learn organs such as the liver, heart and skeletal muscle to store and dissipate energy. Whether this explains our current understanding of BAT metabolism in obese and diabetic individuals requires further exploring, but the findings from the present study lend some support to this hypothesis.

As previously described, the mechanism by which BAT thermogenesis is both activated and fueled relies upon the lipolysis of intracellular TG. Consistent with our previous findings (Ouellet *et al.*, 2012; Blondin *et al.*, 2014), the cold-induced increases in BAT radio-density in the present study (from -103 ± 3 HU to 86 ± 5 HU) indicate that BAT oxidative metabolism was indeed primarily supported by intracellular TG utilization. That BAT ^{18}FDG uptake was limited to 15.6 ± 7.7 μmol min^{-1}, accounting for 1.2 ±0.6 % of plasma glucose turnover, and was inversely associated with BAT triglyceride content but not associated with BAT oxidative metabolism, indicates that uptake of circulating glucose by BAT is dependent upon intracellular TG content but not the tissue metabolic rate. This suggests that under short-term acute cold exposure circulating glucose may indirectly fuel BAT thermogenesis through the replenishment of intracellular TG pools (*i.e. de novo* lipogenesis). It also demonstrates that ^{18}FDG may be a good marker of BAT *de novo* lipogenesis but not necessarily BAT thermogenesis. That cold-induced thermogenesis and clearance of circulating substrates was only partially explained by BAT metabolism, led us to then investigate the thermoregulatory and metabolic regulatory interaction between shivering skeletal muscle and BAT.

Thermoregulatory BAT - skeletal muscle interaction

A recent surge in mild cold exposure studies have focused on the thermoregulatory and potential metaboregulatory role of stimulated BAT in humans (van Marken Lichtenbelt *et al.*, 2009; Virtanen *et al.*, 2009; Orava *et al.*, 2011; Vijgen *et al.*, 2011; Yoneshiro *et al.*, 2011; Muzik *et al.*, 2012; Ouellet *et al.*, 2012; Vijgen *et al.*, 2012; Vosselman *et al.*, 2012; Muzik *et al.*, 2013). Although the prospect of applying BAT-mediated thermogenesis as a treatment for obesity and its associated diseases appears obvious. The current study demonstrates that skeletal

muscle, even under such a mild cold stimulation, has a similarly effective regulatory role. To begin teasing out the interaction between BAT metabolism and shivering activity as well as their effect on whole body energy metabolism, we examined the association between shivering intensity and the volume of metabolically active BAT as well as its oxidative capacity. Using a robust cooling protocol designed to clamp the skin temperature and consequent thermosensory input, we found that the thermogenic contribution of BAT versus skeletal muscle varied tremendously (Figure 5) as did the shivering activity between individual muscles (Figure 7). In some individuals shivering skeletal muscle had a markedly greater contribution to heat production than BAT, for the same change in metabolic rate (Figure 4). While whole-body shivering intensity, quantified using sEMG, was limited to ~2 % MVC, the shivering activity of individual muscles varied from 0.2 ± 0.1 % MVC in the *m. deltoideus* to as high as 4.5 ± 1.2 % MVC in the *m. pectoralis major.* This clearly indicates that shivering activity was present to varying degrees in this study and was contributing to the cold-induced increase in metabolic rate, even in individuals demonstrating greater BAT oxidative metabolism. Previous investigations have relied on qualitative methods such as visual inspection, self-reporting or experimenter-led inquiries (van Marken Lichtenbelt *et al.*, 2009; Vijgen *et al.*, 2011; Yoneshiro *et al.*, 2011; Vijgen *et al.*, 2012; Vosselman *et al.*, 2012) as well as more quantitative approaches such as the muscle perfusion (Orava *et al.*, 2011; Muzik *et al.*, 2012; Muzik *et al.*, 2013; Orava *et al.*, 2013) and glucose uptake (Orava *et al.*, 2011; Orava *et al.*, 2013) of a single muscle via ^{15}O and ^{18}FDG PET methods to determine muscle activity under similar thermal conditions. In many cases, by experimental design, overt shivering was considered absent or blunted. Indeed, if the sEMG results *of m. deltoideus* are examined (Figure 7), the reference muscle commonly used (Orava *et al.*, 2011; Muzik *et al.*, 2012; Muzik *et al.*, 2013; Orava *et al.*, 2013), a similar absence of

shivering activity would be concluded and would be consistent with previous studies also using sEMG (Meigal *et al.*, 1996; Meigal *et al.*, 1998). However, combined, these studies simply demonstrate that careful consideration should be taken if measuring muscle activity of a single muscle to represent whole-body muscle metabolism as the thermogenic and metabolic contribution of skeletal muscle may be vastly underestimated.

Metaboregulatory BAT - skeletal muscle interaction

There have been a number of promising investigations in rodents demonstrating the effectiveness of BAT in regulating triglyceride clearance (Bartelt *et al.*, 2011), glucose homeostasis and insulin sensitivity (Stanford *et al.*, 2013) and energy balance by dissipating excess energy during cold exposure or excess feeding (Rothwell & Stock, 1979; Feldmann *et al.*, 2009). However, *in vivo* confirmation of these metabolic regulatory functions in humans, has remained less clear. The findings from the present study not only show important thermoregulatory interactions between BAT and shivering muscles, but also demonstrate the metabolic regulatory function of these highly thermogenic tissues. Expanding our investigation of the metabolic interaction between BAT and shivering muscles, we investigated their respective roles in regulating circulating substrates. Although it should come as no surprise, total glucose uptake and plasma glucose turnover were both more than one order of magnitude greater in skeletal muscle compared to BAT in humans acutely exposed to the cold. With BAT mass representing ~1% of total body weight in adult humans compared to the ~42% represented by skeletal muscle (Rolfe & Brown, 1997) combined with the generalized muscle recruitment inherent in shivering, the overall potential for skeletal muscle to clear circulating substrates during cold exposure *via* contraction-mediated pathways is significantly greater. It should be noted, however, that the clearance of circulating substrates by BAT may be greatest either during

more prolonged cold exposures or once cold exposure is concluded. In these contexts, intracellular TG likely deplete and must rely on lipogenesis to replenish TG stores to maintain or re-activate BAT thermogenesis.

Particular muscles were preferentially recruited to produce heat during cold exposure, which would incidentally lead to circulating substrates being channeled preferentially towards these same muscles. Indeed, whether examining individual muscles or grouping them according to their anatomical location, it was clear that under mild cold conditions deep, centrally-located muscles were preferentially recruited and thus clearing plasma glucose to a greater extent than superficial, peripherally-located muscles. This was consistent with previous observations made using surface EMG (Bell *et al.*, 1992) and indications from our previous BAT metabolism investigation (Ouellet *et al.*, 2012), which showed that tissue oxidative and/or nonoxidative metabolism (acetate retention), was elevated in the *m. longus colli* compared to the *m. trapezius* and *m. deltoideus*. The rhythmicity, shivering intensity and pattern have all been suggested to be determined locally in the spinal cord (Perkins, 1945; Tanaka *et al.*, 2006). The activation of neurons in the reticulospinal tract, which in primates excites motoneurons primarily of proximal muscles and to a smaller extent distal muscles (Shapovalov, 1972; Davidson & Buford, 2004; Riddle *et al.*, 2009), also suggest that proximal muscle groups may be preferentially recruited over distal muscle groups during shivering thermogenesis; proximal muscle group activation being only observable non-invasively using nuclear imaging techniques, had never been attempted previously. Given the well documented contraction-stimulated glucose uptake in skeletal muscle (Glatz *et al.*, 2010; Wasserman *et al.*, 2011) and that ^{18}FDG is retained in the cell in proportion to the glycolytic rate (Phelps, 2000; Sharp *et al.*, 2012) we examined the relationship between EMG-derived shivering activity and the relative uptake of ^{18}FDG in the

same skeletal muscles. As would be expected, a strong direct relationship between EMG-determined shivering intensity and the relative uptake of ^{18}FDG was observed (Figure 7), suggesting that the latter could serve as a strong surrogate to EMG-determined shivering intensity.

The apparent preferential muscle recruitment may have important implications in further understanding and targeting the metabolic mechanisms recruited through acute and chronic cold exposure. Recent studies have suggested potential inter-organ interactions between skeletal muscle and BAT (classical or brown-in-white) (Bostrom *et al.*, 2012; Yin *et al.*, 2013; Lee *et al.*, 2014) with the muscle contractions of shivering providing the stimulus for phenotypic changes (Lee *et al.*, 2014). It is intriguing to hypothesize that perhaps these interactions occur directly through specific muscle groups either based on anatomical location. For example, satellite cell-derived brown adipocyte differentiation was observed in intercostal, paraspinal, and back muscles but not the limb muscles of mice exposed to 4°C for 1 week (Yin *et al.*, 2013). While we are still in the early exploration phases in examining this hypothesis, it is worth considering the various muscles recruited and metabolically active under such thermal conditions considering the potential specificity of these mechanisms.

In summary , the findings from this study present an interesting interconnection between WAT, BAT and skeletal muscle. This interaction illustrates how the balance between these tissues could positively influence whole-body energy homeostasis, while also implying that BAT may be susceptible to similar lipolytic dysfunction as WAT in the pathogenesis of obesity and diabetes. The latter would explain the absence or impaired function of cold-induced BAT activity in individuals who are morbidly obese or diabetic (Vijgen *et al.*, 2011; Orava *et al.*, 2013). However, such a fate would result in a greater contribution to heat production from shivering

skeletal muscles, which do not appear to be influenced by the sympathetically-mediated lipolysis and appear to clear and utilize circulating substrates efficiently. Further investigations are required to examine these interactions in these populations.

ACKNOWLEDGEMENTS

The authors would like to acknowledge the excellent technical assistance provided by Diane Lessard, Caroll-Lynn Thibodeau and Éric Lavallée. This work was supported by a grant from the Canadian Diabetes association (OG-3-10-2970-AC) and the Natural Sciences and Engineering Research Council of Canada (NSERC Canada) to FH and was performed at the Centre de recherche clinique Etienne-Le Bel, a research centre funded by the Fonds de la recherché en santé du Québec (FRSQ). DPB is the recipient of the NSERC Postgraduate Scholarship. SML is the recipient of a CIHR Postdoctoral fellowship. DR is the recipient of the CIHR/Merck Frosst Research Chair on Obesity. ACC is currently the recipient of a FRSQ Senior Scholarship Award CIHR/GSK Chair in Diabetes. We also thank the subjects of this study for their collaboration.

REFERENCES

Bartelt A, Bruns OT, Reimer R, Hohenberg H, Ittrich H, Peldschus K, Kaul MG, Tromsdorf UI, Weller H, Waurisch C, Eychmuller A, Gordts PL, Rinninger F, Bruegelmann K, Freund B, Nielsen P, Merkel M & Heeren J. (2011). Brown adipose tissue activity controls triglyceride clearance. *Nat Med* **17,** 200-205.

Bell DG, Tikuisis P & Jacobs I. (1992). Relative intensity of muscular contraction during shivering. *J Appl Physiol* **72,** 2336-2342.

Blondin DP, Labbé SM, Tingelstad HC, Noll C, Kunach M, Phoenix S, Guérin B, Turcotte ÉE, Carpentier AC, Richard D & Haman F. (2014). Increased Brown Adipose Tissue Oxidative Capacity in Cold-Acclimated Humans. *J Clin Endocrinol Metab* **99,** E438-E446.

Bostrom P, Wu J, Jedrychowski MP, Korde A, Ye L, Lo JC, Rasbach KA, Bostrom EA, Choi JH, Long JZ, Kajimura S, Zingaretti MC, Vind BF, Tu H, Cinti S, Hojlund K, Gygi SP & Spiegelman BM. (2012). A PGC1-alpha-dependent myokine that drives brown-fat-like development of white fat and thermogenesis. *Nature* **481,** 463-468.

Brito NA, Brito MN & Bartness TJ. (2008). Differential sympathetic drive to adipose tissues after food deprivation, cold exposure or glucoprivation. *Am J Physiol Regul Integr Comp Physiol* **294,** R1445-1452.

Brown M, Marshall DR, Sobel BE & Bergmann SR. (1987). Delineation of myocardial oxygen utilization with carbon-11-labeled acetate. *Circulation* **76,** 687-696.

Buck A, Wolpers HG, Hutchins GD, Savas V, Mangner TJ, Nguyen N & Schwaiger M. (1991). Effect of carbon-11-acetate recirculation on estimates of myocardial oxygen consumption by PET. *J Nucl Med* **32,** 1950-1957.

Cannon B & Nedergaard J. (2004). Brown adipose tissue: function and physiological significance. *Physiol Rev* **84,** 277-359.

Carpentier A, Patterson BW, Uffelman KD, Giacca A, Vranic M, Cattral MS & Lewis GF. (2001). The effect of systemic versus portal insulin delivery in pancreas transplantation on insulin action and VLDL metabolism. *Diabetes* **50,** 1402-1413.

Carpentier AC, Frisch F, Brassard P, Lavoie F, Bourbonnais A, Cyr D, Giguere R & Baillargeon JP. (2007). Mechanism of insulin-stimulated clearance of plasma nonesterified fatty acids in humans. *Am J Physiol Endocrinol Metab* **292,** E693-701.

Carpentier AC, Frisch F, Cyr D, Genereux P, Patterson BW, Giguere R & Baillargeon JP. (2005). On the suppression of plasma nonesterified fatty acids by insulin during enhanced intravascular lipolysis in humans. *Am J Physiol Endocrinol Metab* **289,** E849-856.

Carpentier AC, Labbé SM, Grenier-Larouche T & Noll C. (2011). Abnormal dietary fatty acid metabolic partitioning in insulin resistance and Type 2 diabetes. *Clinical Lipidology* **6,** 703-716.

Croteau E, Lavallée E, Labbe SM, Hubert L, Pifferi F, Rousseau JA, Cunnane SC, Carpentier AC, Lecomte R & Bénard F. (2010). Image-derived input function in dynamic human PET/CT: methodology and validation with 11C-acetate and 18F-fluorothioheptadecanoic acid in muscle and 18F-fluorodeoxyglucose in brain. *Eur J Nucl Med Mol Imaging* **37,** 1539-1550.

Cypess AM, Chen YC, Sze C, Wang K, English J, Chan O, Holman AR, Tal I, Palmer MR, Kolodny GM & Kahn CR. (2012). Cold but not sympathomimetics activates human brown adipose tissue in vivo. *Proc Natl Acad Sci U S A* **109,** 10001-10005.

Davidson AG & Buford JA. (2004). Motor outputs from the primate reticular formation to shoulder muscles as revealed by stimulus-triggered averaging. *J Neurophysiol* **92,** 83-95.

Feldmann HM, Golozoubova V, Cannon B & Nedergaard J. (2009). UCP1 ablation induces obesity and abolishes diet-induced thermogenesis in mice exempt from thermal stress by living at thermoneutrality. *Cell Metab* **9,** 203-209.

Glatz JFC, Luiken JFP & Bonen A. (2010). Membrane Fatty Acid Transporters as Regulators of Lipid Metabolism: Implications for Metabolic Disease. *Physiol Rev* **90,** 367-417.

Grenier-Larouche T, Labbe SM, Noll C, Richard D & Carpentier AC. (2012). Metabolic inflexibility of white and brown adipose tissues in abnormal fatty acid partitioning of type 2 diabetes. *Int J Obes Supp* **2,** S37-S42.

Haman F, Legault SR, Rakobowchuk M, Ducharme MB & Weber J-M. (2004a). Effects of carbohydrate availability on sustained shivering II: relating muscle recruitment to fuel selection. *J Appl Physiol* **96,** 41-49.

Haman F, Legault SR & Weber J-M. (2004b). Fuel selection during intense shivering in humans: EMG pattern reflects carbohydrate oxidation. *J Physiol* **556,** 305-313.

Haman F, Péronnet F, Kenny GP, Doucet E, Massicotte D, Lavoie C & Weber J-M. (2004c). Effects of carbohydrate availability on sustained shivering I: oxidation of plasma glucose, muscle glycogen and proteins. *J Appl Physiol* **96,** 32-40.

Haman F, Péronnet F, Kenny GP, Massicotte D, Lavoie C, Scott C & Weber J-M. (2002). Effect of cold exposure on fuel utilization in humans: plasma glucose, muscle glycogen, and lipids. *J Appl Physiol* **93,** 77-84.

Haman F, Péronnet F, Kenny GP, Massicotte D, Lavoie C & Weber J-M. (2005). Partitioning oxidative fuels during cold exposure in humans: muscle glycogen becomes dominant as shivering intensifies. *J Physiol* **566,** 247-256.

Horowitz JF, Coppack SW, Paramore D, Cryer PE, Zhao G & Klein S. (1999). Effect of short-term fasting on lipid kinetics in lean and obese women. *Am J Physiol* **276,** E278-284.

Jocken JW, Goossens GH, van Hees AM, Frayn KN, van Baak M, Stegen J, Pakbiers MT, Saris WH & Blaak EE. (2008). Effect of beta-adrenergic stimulation on whole-body and abdominal subcutaneous adipose tissue lipolysis in lean and obese men. *Diabetologia* **51,** 320-327.

Lee P, Linderman JD, Smith S, Brychta RJ, Wang J, Idelson C, Perron RM, Werner CD, Phan GQ, Kammula US, Kebebew E, Pacak K, Chen KY & Celi FS. (2014). Irisin and FGF21 Are Cold-Induced Endocrine Activators of Brown Fat Function in Humans. *Cell Metab* **19,** 302-309.

Leibel RL & Hirsch J. (1987). Site- and sex-related differences in adrenoreceptor status of human adipose tissue. *J Clin Endocrinol Metab* **64,** 1205-1210.

Lewis GF, Carpentier A, Adeli K & Giacca A. (2002). Disordered fat storage and mobilization in the pathogenesis of insulin resistance and type 2 diabetes. *Endocrine reviews* **23,** 201-229.

Mauriege P, Despres JP, Prud'homme D, Pouliot MC, Marcotte M, Tremblay A & Bouchard C. (1991). Regional variation in adipose tissue lipolysis in lean and obese men. *Journal of lipid research* **32,** 1625-1633.

Mauriege P, Galitzky J, Berlan M & Lafontan M. (1987). Heterogeneous distribution of beta and alpha-2 adrenoceptor binding sites in human fat cells from various fat deposits: functional consequences. *European journal of clinical investigation* **17,** 156-165.

Meigal AY, Lupandin YV & Hanninen O. (1996). Head and body positions affect thermoregulatory tonus in deltoid muscles. *J Appl Physiol* **80,** 1397-1400.

Meigal AY, Oksa J, Hohtola E, Lupandin YV & Rintamaki H. (1998). Influence of cold shivering on fine motor control in the upper limb. *Acta Physiol Scand* **163,** 41-47.

Menard SL, Croteau E, Sarrhini O, Gelinas R, Brassard P, Ouellet R, Bentourkia M, van Lier JE, Des Rosiers C, Lecomte R & Carpentier AC. (2010). Abnormal in vivo myocardial energy substrate uptake in diet-induced type 2 diabetic cardiomyopathy in rats. *Am J Physiol Endocrinol Metab* **298,** E1049-1057.

Muzik O, Mangner TJ & Granneman JG. (2012). Assessment of oxidative metabolism in brown fat using PET imaging. *Front Endocrinol* **3,** 15.

Muzik O, Mangner TJ, Leonard WR, Kumar A, Janisse J & Granneman JG. (2013). 15O PET measurement of blood flow and oxygen consumption in cold-activated human brown fat. *J Nucl Med* **54,** 523-531.

Ng CK, Huang SC, Schelbert HR & Buxton DB. (1994). Validation of a model for [1-11C]acetate as a tracer of cardiac oxidative metabolism. *Am J Physiol* **266,** H1304-1315.

Orava J, Nuutila P, Lidell ME, Oikonen V, Noponen T, Viljanen T, Scheinin M, Taittonen M, Niemi T, Enerback S & Virtanen KA. (2011). Different metabolic responses of human brown adipose tissue to activation by cold and insulin. *Cell Metab* **14,** 272-279.

Orava J, Nuutila P, Noponen T, Parkkola R, Viljanen T, Enerbäck S, Rissanen A, Pietiläinen KH & Virtanen KA. (2013). Blunted metabolic responses to cold and insulin stimulation in brown adipose tissue of obese humans. *Obesity* **21,** 2279-2287.

Ouellet V, Labbe SM, Blondin DP, Phoenix S, Guerin B, Haman F, Turcotte EE, Richard D & Carpentier AC. (2012). Brown adipose tissue oxidative metabolism contributes to energy expenditure during acute cold exposure in humans. *J Clin invest* **122,** 545-552.

Ouellet V, Routhier-Labadie A, Bellemare W, Lakhal-Chaieb L, Turcotte E, Carpentier AC & Richard D. (2011). Outdoor Temperature, Age, Sex, Body Mass Index, and Diabetic Status Determine the Prevalence, Mass, and Glucose-Uptake Activity of 18F-FDG-Detected BAT in Humans. *J Clin Endocrinol Metab* **96,** 192-199.

Palmes ED & Park CR. (1947). Thermocouples for the measurement of the surface temperature of the skin. *Fed Proc* **6,** 175.

Perkins JF, Jr. (1945). The role of the proprioceptors in shivering. *Am J Physiol* **145,** 264-271.

Phelps ME. (2000). Positron emission tomography provides molecular imaging of biological processes. *Proc Natl Acad Sci U S A* **97,** 9226-9233.

Reynisdottir S, Ellerfeldt K, Wahrenberg H, Lithell H & Arner P. (1994). Multiple lipolysis defects in the insulin resistance (metabolic) syndrome. *J Clin Invest* **93,** 2590-2599.

Riddle CN, Edgley SA & Baker SN. (2009). Direct and indirect connections with upper limb motoneurons from the primate reticulospinal tract. *J Neurosci* **29,** 4993-4999.

Rolfe DFS & Brown GC. (1997). Cellular energy utilization and molecular origin of standard metabolic rate in mammals. *Physiol Rev* **77,** 731-758.

Rothwell NJ & Stock MJ. (1979). A role for brown adipose tissue in diet-induced thermogenesis. *Nature* **281,** 31-35.

Sallis JF, Haskell WL, Wood PD, Fortmann SP, Rogers T, Blair SN & Paffenbarger RSJ. (1985). Physical activity assessment methodology in the Five-City Project. *Am J Epidemiol* **121,** 91-106.

Shapovalov AI. (1972). Extrapyramidal monosynaptic and disynaptic control of mammalian alpha-motoneurons. *Brain Res* **40,** 105-115.

Sharp LZ, Shinoda K, Ohno H, Scheel DW, Tomoda E, Ruiz L, Hu H, Wang L, Pavlova Z, Gilsanz V & Kajimura S. (2012). Human BAT possesses molecular signatures that resemble beige/brite cells. *PLoS One* **7,** e49452.

St-Onge M, Mignault D, Allison DB & Rabasa-Lhoret R. (2007). Evaluation of a portable device to measure daily energy expenditure in free-living adults. *Am J Clin Nutr* **85,** 742-749.

Stanford KI, Middelbeek RJ, Townsend KL, An D, Nygaard EB, Hitchcox KM, Markan KR, Nakano K, Hirshman MF, Tseng YH & Goodyear LJ. (2013). Brown adipose tissue regulates glucose homeostasis and insulin sensitivity. *J Clin invest* **123,** 215-223.

Tanaka M, Owens NC, Nagashima K, Kanosue K & McAllen RM. (2006). Reflex activation of rat fusimotor neurons by body surface cooling, and its dependence on the medullary raphe. *J Physiol* **572,** 569-583.

van Marken Lichtenbelt WD, Vanhommerig JW, Smulders NM, Drossaerts JM, Kemerink GJ, Bouvy ND, Schrauwen P & Teule GJ. (2009). Cold-activated brown adipose tissue in health men. *N Engl J Med* **360,** 1500-1508.

Vijgen GH, Bouvy ND, Teule GJ, Brans B, Hoeks J, Schrauwen P & van Marken Lichtenbelt WD. (2012). Increase in brown adipose tissue activity after weight loss in morbidly obese subjects. *J Clin Endocrinol Metab* **97,** E1229-1233.

Vijgen GH, Bouvy ND, Teule GJ, Brans B, Schrauwen P & van Marken Lichtenbelt WD. (2011). Brown adipose tissue in morbidly obese subjects. *PLoS One* **6,** e17247.

Virtanen KA, Lidell ME, Orava J, Heglind M, Westergren R, Niemi T, Taittonen M, Laine J, Savisto NJ, Enerbäck S & Nuutila P. (2009). Functional brown adipose tissue in healthy adults. *N Engl J Med* **360,** 1518-1525.

Vosselman MJ, van der Lans AA, Brans B, Wierts R, van Baak MA, Schrauwen P & van Marken Lichtenbelt WD. (2012). Systemic beta-adrenergic stimulation of thermogenesis is not accompanied by brown adipose tissue activity in humans. *Diabetes* **61,** 3106-3113.

Wahrenberg H, Lonnqvist F & Arner P. (1989). Mechanisms underlying regional differences in lipolysis in human adipose tissue. *J Clin Invest* **84,** 458-467.

Wasserman DH, Kang L, Ayala JE, Fueger PT & Lee-Young RS. (2011). The physiological regulation of glucose flux into muscle in vivo. *J Exp Biol* **214,** 254-262.

Yin H, Pasut A, Soleimani VD, Bentzinger CF, Antoun G, Thorn S, Seale P, Fernando P, van Ijcken W, Grosveld F, Dekemp RA, Boushel R, Harper ME & Rudnicki MA. (2013). MicroRNA-133 controls brown adipose determination in skeletal muscle satellite cells by targeting Prdm16. *Cell Metab* **17,** 210-224.

Yoneshiro T, Aita S, Matsushita M, Kameya T, Nakada K, Kawai Y & Saito M. (2011). Brown adipose tissue, whole-body energy expenditure, and thermogenesis in healthy adult men. *Obesity (Silver Spring)* **19,** 13-16.

3.3 Article III

Final accepted version of article published in Journal of Clinical Endocrinology & Metabolism, 99 (3): E438 - 446, 2014 (Appendix D)

Increased brown adipose tissue oxidative capacity in cold-acclimated humans.

Denis P. Blondin[1], Sébastien M. Labbé[2], Hans Christian Tingelstad[1], Christophe Noll[3], Margaret Kunach[3], Serge Phoenix[3,4], Brigitte Guérin[4], Éric E. Turcotte[4], André C. Carpentier[3], Denis Richard[2], François Haman[1].

[1] Faculty of Health Sciences, University of Ottawa, Ottawa, Ontario, Canada.

[2] Centre de Recherche de l'Institut Universitaire de Cardiologie et de Pneumologie de Québec, Université Laval, Quebec City, Quebec, Canada.

[3] Department of Medicine, Centre de Recherche Clinique Etienne-Le Bel, Université de Sherbrooke, Sherbrooke, Quebec, Canada.

[4] Department of Nuclear Medicine and Radiobiology, Université de Sherbrooke, Sherbrooke, Quebec, Canada.

Running Head: Increased BAT volume and activity following cold-acclimation

Key Words: cold-acclimation; energy metabolism; positron emission tomography; brown adipose tissue

Word Count: Main Text: 3,535

Number of tables: 1 Number of figures: 4

Conflict of interest: The authors have declared that no conflict of interest exists related to the content of this manuscript.

ABSTRACT

Context: Recent studies examining brown adipose tissue (BAT) metabolism in adult humans have provided convincing evidence of its thermogenic potential and role in clearing circulating glucose and fatty acids under acute mild-cold exposure. In contrast, early indications suggest that BAT metabolism is defective in obesity and type 2 diabetes (T2D), which may have important pathological and therapeutic implications. Although, many mammalian models have demonstrated the phenotypic flexibility of this tissue through chronic cold exposure, little is known about the metabolic plasticity of BAT in humans.

Objective: To determine whether four weeks of daily cold exposure could increase both the volume of metabolically active brown adipose tissue (BAT) and its oxidative capacity.

Design: Six non-acclimated men were exposed to 10°C, two hours daily for four weeks (5 days/week), using a liquid-conditioned suit. Using electromyography combined with positron emission tomography with ^{11}C-acetate and ^{18}F-fluorodeoxyglucose, shivering intensity and BAT oxidative metabolism, glucose uptake and volume prior to and following four weeks of cold acclimation were examined under controlled acute cold exposure conditions.

Results: The four-week acclimation protocol elicited a 45% increase in BAT volume of activity (from 66±30 to 95±28 mL, $P<0.05$) and a 2.2-fold increase in cold-induced total BAT oxidative metabolism (from 0.725±0.300 to 1.591±0.326 mL·sec^{-1}, $P<0.05$). Shivering intensity was not significantly different pre- compared to post-acclimation (2.1±0.7 *vs* 2.0±0.5 %MVC, respectively). Fractional glucose uptake in BAT increased post-acclimation (from 0.035±0.014 to 0.048±0.012 min^{-1}) while net glucose uptake trended towards an increase as well (from 163±60 to 209±50 nmol·g^{-1}·min^{-1}).

Conclusions: These findings demonstrate that daily cold exposure not only increases the volume of metabolically active BAT, but also increases its oxidative capacity and thus its contribution to cold-induced thermogenesis.

INTRODUCTION

In the four years since the seminal papers describing the presence of functional brown adipose tissue (BAT) in adult humans were published (Cypess *et al.*, 2009; van Marken Lichtenbelt *et al.*, 2009; Virtanen *et al.*, 2009), significant progress has been made in characterizing its developmental origin (Sharp *et al.*, 2012; Wu *et al.*, 2012), function (Ouellet *et al.*, 2012; Vosselman *et al.*, 2013) and distribution (Ouellet *et al.*, 2011; Cypess *et al.*, 2013). As in most mammals, BAT provides an important contribution to thermoregulatory heat production in adult humans (Ouellet *et al.*, 2012). The scarce amount of BAT found in individuals who are overweight or obese (Vijgen *et al.*, 2011; Orava *et al.*, 2013) combined with the large BAT mass and lean phenotype exhibited by patients with pheochromocytoma (catecholamine-secreting tumors) (Ricquier *et al.*, 1982; Lean, 1989) have lead to suggestions that it may also play an important part in energy homeostasis. Whether BAT can be induced to grow or increase its metabolic capacity and consequently be a therapeutic target for obesity and its related complications remains unclear. Evidence from animal models (Cannon & Nedergaard, 2004) and indirect-support from human studies (Huttunen *et al.*, 1981; Vijgen *et al.*, 2012) have suggested an inherent plasticity to this tissue, presenting signs of BAT recruitment. Further, the differentiation of both types of brown adipocytes (classical and beige/brite) (Wu *et al.*, 2012; Schulz *et al.*, 2013; Yin *et al.*, 2013) and its activation (van Marken Lichtenbelt *et al.*, 2009; Virtanen *et al.*, 2009; Ouellet *et al.*, 2012) appear to be largely mediated by a sympathetic input. To date, the most potent and effective sympathetic stimulator of BAT differentiation and activation in humans has been cold exposure, as most sympathomimetics applied *in vivo* have shown little to no effect on BAT activation (Cypess *et al.*, 2012; Vosselman *et al.*, 2012; Carey *et al.*, 2013). Very recent studies have demonstrated that relative BAT glucose uptake as

assessed by increased ^{18}F-fluorodeoxyglucose (^{18}FDG) standard uptake value (SUV) with positron emission tomography (PET) can be increased by repeated cold exposure in humans (van der Lans *et al.*, 2013; Yoneshiro *et al.*, 2013). However, whether BAT oxidative capacity increases with the increase in BAT recruitment has not yet been demonstrated in adult humans. Six healthy, lean men were invited to participate in a four-week cold-acclimation protocol and undergo acute cold exposure studies prior to and following the intervention to determine whether four weeks of daily cold exposure could increase both the volume of metabolically active BAT and its oxidative capacity.

MATERIALS AND METHODS

Experimental Protocol

Six healthy, lean men aged 23 ± 1 years with a BMI of 24.5 ± 1.2 kg/m^2 and body surface area of 2.01 ± 0.04 m^2 participated in two metabolic experimental sessions within a four-week interval designed to assess whole body and tissue-specific metabolism during an acute cold exposure (**Figure 1**). The cold acclimation protocol followed between these two experimental sessions consisted of daily cold exposure lasting two hours where 10°C water was circulated through a liquid conditioned suit (Three Piece, Allen-Vanguard, Ottawa, ON), repeated 5 consecutive days per week for 4 consecutive weeks for a total of 18 acclimation sessions and 2 testing sessions. Participants were asked to maintain their current training regiment and refrain from drinking caffeinated or alcoholic beverages for the duration of the study.

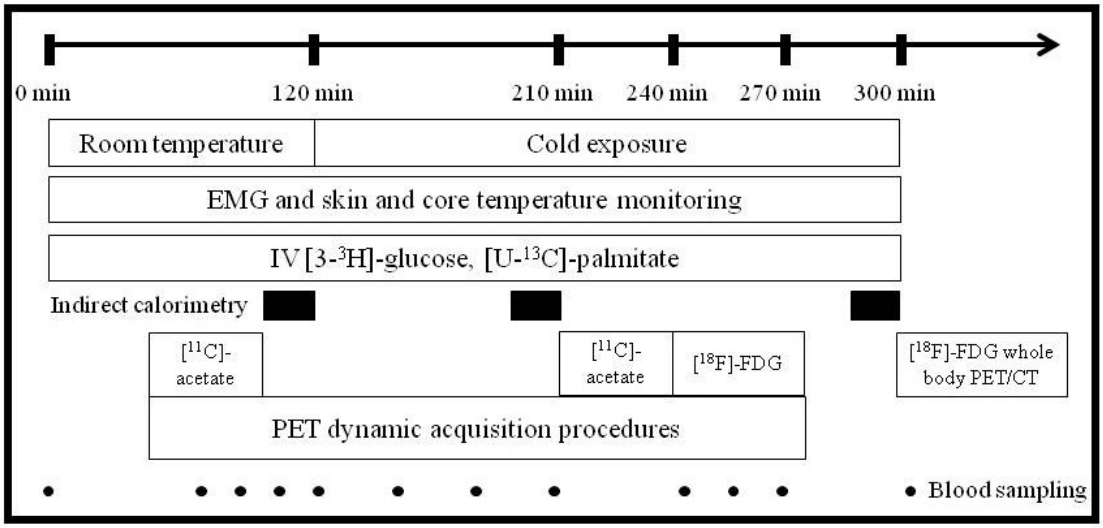

Figure 1. Study protocol.

Each acute cold exposure experimental session consisted of a 120 min baseline period at ambient temperature (~25 °C) followed by 180 min of exposure to a mild cold, elicited using the same liquid conditioned suit. During cold exposure, 18.0°C water was circulated through the suit during the pre-acclimation visit and water at a temperature eliciting the same individualized inlet-outlet temperature difference as the pre-acclimation protocol (16.8±0.1°C) was circulated during the post-acclimation visit using a temperature-controlled circulation bath (Endocal, NESLAB Model 200–00, Micropump, Vancouver, WA, USA). The post-acclimation temperature was adjusted to induce a similar thermogenic rate between the two experimental sessions. The same suit was used for all subjects to maintain consistent tubing density and water flow. Experiments were conducted between 0730 h and 1600 h, following 48h without strenuous physical activity. Upon their arrival in the laboratory, subjects wearing only shorts were weighed and instrumented with 12 autonomous wireless temperature sensors (Thermochron iButton® model DS1922H, Maxim) fixed to the skin to measure mean skin temperature (Hardy & Dubois, 1938) and surface electromyography electrodes (Delsys, EMG System, USA) placed on the belly of 12 muscles. Participants were then fitted with the liquid conditioned suit, ingested a telemetric thermometry capsule to measure core temperature (Vital Sense monitor and Jonah temperature capsule, Mini Mitter Co., Inc., Bend, OR, USA) and performed a series of exercises to estimate the maximal voluntary contraction (MVC) of each of the muscles being measured for shivering activity. Whole body metabolic heat production was determined by indirect respiratory calorimetry (Vmax 29n; Sensormedics) (Haman *et al.*, 2002) at room temperature and between times 180 to 200 min and 280 to 300 min (i.e., 60 to 80 min and 160 to 180 min after the beginning of cold exposure). Whole body and muscle-specific shivering intensity and pattern as well as mean skin and core temperatures were measured continuously

from time 90 to 300 min as previously described (Haman *et al.*, 2004b). Only the means of the final 30 min of the ambient period and final 120 min of the cold exposure are reported. A weighted average of the ^{18}FDG uptake of 18 skeletal muscles, which includes deep muscles that are inaccessible using surface electromyography, was also used as a shivering index to determine whether: 1) shivering activity was modified based on muscle location (superficial *vs.* deep) and 2) ^{18}FDG uptake in skeletal muscles could serve as a viable indicator of whole body shivering activity. Plasma glucose appearance rate ($Ra_{glucose}$) was determined using a primed continuous infusion (0.33 × 106 dpm/min) of [3-^{3}H]-glucose (Carpentier *et al.*, 2001). Ra_{NEFA} was measured using i.v. administration of [U-^{13}C]-palmitate using the Steele steady-state equation, as previously described (Carpentier *et al.*, 2005).

PET/CT protocol

Tissue oxidative metabolism was determined by first performing a CT scan (40 mAs) centered at the cervico-thoracic junction to correct for attenuation and to define PET regions of interest. At time 90 minutes (room temperature) and again at time 210 minutes (i.e., 90 minutes after onset of cold exposure), ~185 MBq of ^{11}C-acetate was injected intravenously followed by 30-minutes list-mode dynamic PET acquisition (24 x 10 s, 12 x 30 s, 4 x 300 s), as previously described (Labbe *et al.*, 2011). Tissue oxidative metabolism index (the rapid fractional tissue clearance of ^{11}C-acetate, k, in s^{-1}) was estimated from tissue ^{11}C activity over time using monoexponential fit from the time of peak tissue activity (Buck *et al.*, 1991). This method is based on the following assumptions (Klein *et al.*, 2001): (a) acetate enters the Krebs cycle freely after rapid conversion into acetyl-CoA; (b) other acetate metabolic fates (e.g., de novo

lipogenesis) are relatively slow compared with the Krebs cycle carbon fluxes; (c) carbon fluxes into the Krebs cycle through acetyl-CoA are directly coupled to the production of reducing equivalents; (d) the Krebs cycle contribution to the production of reducing equivalents is stable and accounts for approximately two thirds of total production; and (e) the production of reducing equivalents is tightly coupled to oxygen consumption. Total oxidative metabolism index of BAT was determined by multiplying k by the total volume of metabolically active BAT, as determined by ^{18}FDG uptake (described below). This calculation was performed to reflect the total oxidative metabolism of BAT located throughout the body, whereas k represents the oxidative metabolism of a particular depot.

To determine tissue glucose uptake, an i.v. bolus of ^{18}FDG (~185 MBq) was given at time 240 minutes (i.e., 2 hours after the onset of cold exposure), with 40-minutes list-mode dynamic PET acquisition (12 x 10 s, 8 x 30 s, 6 x 90 s, 5 x 300 s), followed by a CT scan (40 mAs) centered at the cervicothoracic junction to correct for attenuation and for definition of PET regions of interest. Plasma and tissue time-radioactivity curves were analyzed graphically using the Patlak linearization method (Menard *et al.*, 2010), with the image-derived arterial input function taken from the aortic arch (Croteau *et al.*, 2010). The slope of the plot in the graphical analysis is equal to the tissue glucose extraction constant of ^{18}FDG (K_i in min^{-1}of ^{18}FDG). Tissue net glucose uptake (K_m) was then calculated by multiplying K_i by plasma glucose concentration, measured during the PET imaging protocol, which assumes a lump constant value of 1.0 compared with endogenous plasma glucose. Following cold exposure (at time 300 min), a whole body CT scan (16 mAs) followed by a static whole-body PET acquisition was performed to determine whole body ^{18}FDG organ distribution and tissue standard uptake value (SUV).

PET/CT image analyses

The regions of interest (ROI) were first defined from the transaxial CT slices, then copied to ^{18}FDG and then to ^{11}C-acetate PET image sequences. For dynamic PET acquisitions, mean value of pixels (mean standard uptake value [SUV]) for each frame was recorded. Regions of interest were drawn on the aortic arch for blood activity (input functions), the larger skeletal muscles in the field of view, posterior cervical subcutaneous adipose tissue and on supraclavicular BAT according to the following criteria: a tissue radio density between –30 and –150 Hounsfield units and ^{18}FDG uptake during cold exposure of more than 1.5 SUV unit. Total BAT volume of activity on whole-body scans were also quantified according to the latter criteria.. For whole-body scans, mean values of pixels (mean SUV) for all tissues of interest were recorded.

Statistical analysis

Data are expressed as mean ± SEM. Paired Student's *t* test was used to compare between acute cold exposure experimental sessions. Two-way ANOVA for repeated measures with acclimation status, temperature and their interaction as the independent variables was used to analyze acclimation- and temperature-dependent differences in averaged steady-state hormone and metabolite levels and blood and tissue PET-acquired activities throughout the protocols. Bonferonni's multiple comparisons post-hoc test was used, where applicable. Appropriate transformations of variables were performed when normal distribution was not observed for parametric statistical testing. Pearson correlation coefficients were used to determine correlation between variables. A 2-tailed *P* value of less than 0.05 was considered significant. All analyses were performed using SPSS for Windows (version 16.0; SPSS Inc., Chicago IL) or GraphPad Prism version 6.00 for Windows (GraphPad, San Diego, CA).

Study approval.

Participants were fully informed of the risks and methodologies applied and provided their written consent to participate in this study, in accordance with the Declaration of Helsinki. This study received ethics approval from the Office of Research Ethics and Integrity at the University of Ottawa and the Institutional Review Board for research on humans of the *Centre hospitalier universitaire de Sherbrooke* and *Université de Sherbrooke*.

RESULTS

Effect of cold acclimation on thermal responses and plasma metabolites.

The energy expenditure was individually matched between experimental sessions by maintaining the same difference in inlet and outlet temperature of the water circulating through the cooling garment (Δ 2.8±0.2°C; **Figure 2A**), before and after the four-week cold acclimation. This elicited a similar 1.9-fold increase in thermogenic rate (**Figure 2B**) in the acute cold experimental sessions. Using this approach, the cold stimulus produced by the liquid-conditioned cooling garment evoked a decrease in mean skin temperature that was the same between acute cold exposure sessions (**Figure 2C**). Shivering intensity, which was purposely kept to a minimum, was not significantly different between experimental conditions, whether it was determined electromyographically (**Figure 2D**) or using a weighted average of the ^{18}FDG uptake of 18 skeletal muscles as a shivering index (**Figure 2 E**). The significant relationship between shivering intensity and the shivering index (Pearson $r = 0.66$, $P = 0.02$) suggests that the latter may also represent a good indicator of whole body shivering activity, which includes deep muscles that are inaccessible using surface electromyography (**Figure 2F**).

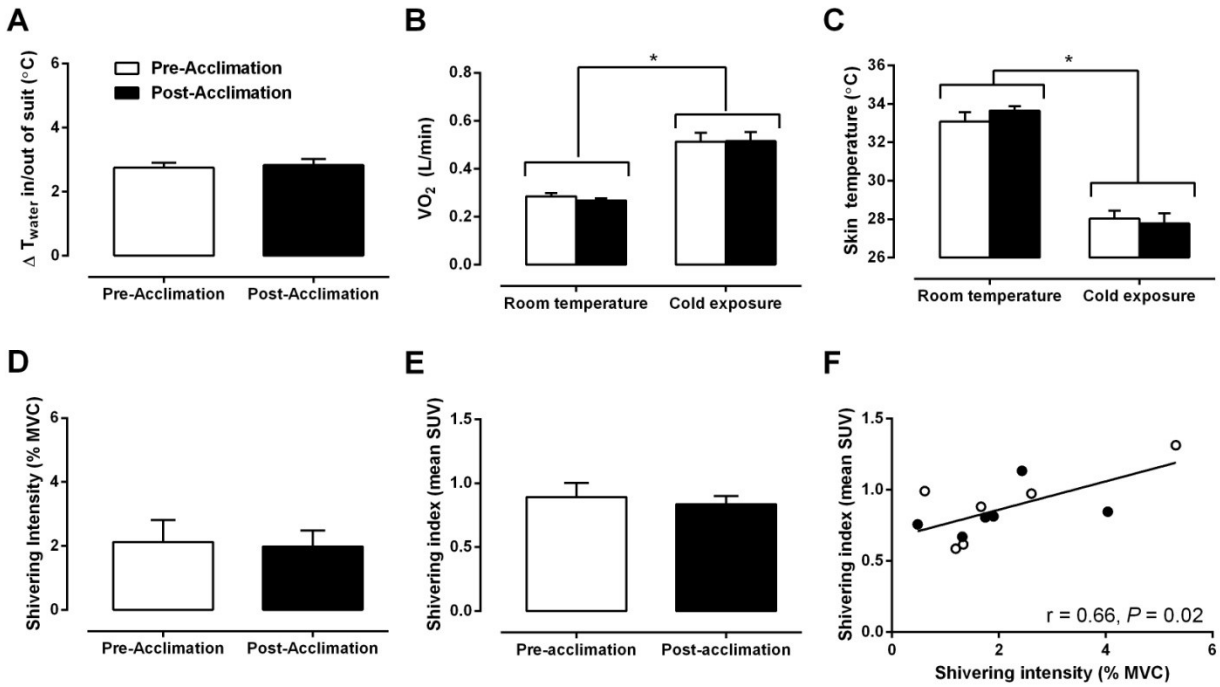

Figure 2. Thermal responses. (**A**)Change in inlet and outlet water temperature of liquid conditioned garment. (**B**) Oxygen consumption ($\dot{V}O_2$) and (**C**) mean skin temperature during room temperature and cold exposure, pre- and post-acclimation. (**D**) Shivering intensity and (**E**) shivering intensity index , pre- and post-acclimation. (**F**) Relationship between mean shivering intensity and shivering intensity index (Pearson r = 0.66, $P = 0.02$). *$P < 0.05$ versus Room temperature, ANOVA with Bonferonni post-hoc test.

To assess the whole body metabolic consequences of daily cold exposure, hormonal and metabolite changes were examined. Insulin, triglycerides (TG), triiodothyronine, thyroxin, ACTH and leptin levels did not change significantly with cold exposure or cold-acclimation (**Table 1**). NEFA rate of appearance, oxidation rate and concentration were similarly increased before and after cold acclimation during acute cold exposure. Only glucose and cortisol concentrations appeared to be influenced by acclimation state, with both being significantly lower post-acclimation compared to pre-acclimation, regardless of temperature exposure. Glucose production rate was not significantly changed after cold acclimation, demonstrating that the reduced glucose level was caused by increased glucose clearance.

Table 1. Hormone and metabolite concentrations at room temperature and cold exposure, pre and post cold acclimation.

	Pre-acclimation		**Post-acclimation**	
	Room temperature	**Cold exposure**	**Room temperature**	**Cold exposure**
Energy expenditure (kcal/min)	1.4 ± 0.1	2.7 ± 0.2*	1.3 ± 0.0	2.5 ± 0.2*
Glucose (mmol/L)	4.8 ± 0.2	4.8 ± 0.1	4.6 ± 0.1$^{\#}$	4.5 ± 0.1$^{\#}$
$Ra_{glucose}$ (µmol/min)	-	1707 ± 166	-	2059 ± 100
Insulin (pmol/L)	67 ± 13	53 ± 8	57 ± 14	53 ± 9
TG (mmol/L)	1.20 ± 0.47	1.13 ± 0.41	0.95 ± 0.36	1.02 ± 0.41
NEFA (µmol/L)	398 ± 53	687 ± 110*	411 ± 69	691 ± 132*
Ra_{NEFA} (µmol/min)	485 ± 71	756 ± 96*	448 ± 111	665 ± 119*
Rox_{NEFA} (µmol/min)	326 ± 77	601 ± 89*	319 ± 65	631 ± 128*
TSH (IU/L)	2.56 ± 0.73	1.96 ± 0.54*	1.98 ± 0.34	1.82 ± 0.47*
Free T3 (pmol/L)	6.0 ± 0.4	5.8 ± 0.4	5.8 ± 0.3	7.0 ± 1.1
Free T4 (pmol/L)	16.2 ± 0.8	16.7 ± 0.7	16.8 ± 0.4	16.0 ± 1.5
ACTH (pmol/L)	4.2 ± 0.7	3.4 ± 0.4	3.8 ± 0.2	3.4 ± 0.4
Cortisol (nmol/L)	374 ± 25	308 ± 37	299 ± 48$^{\#}$	280 ± 27$^{\#}$
Leptin (ng/mL)	2.5 ± 0.9	2.4 ± 1.0	2.6 ± 0.9	2.3 ± 0.7

Values are means ± SEM; n = 6 subjects.

*, different from Room temperature, $P < 0.05$.

$^{\#}$**,** different from Pre-acclimation, , $P < 0.05$.

Daily cold exposure increases BAT volume of activity and fractional glucose uptake

To examine the effect of daily cold exposure on BAT volume, we determined the whole body volume of ^{18}FDG uptake in BAT (i.e. volume of BAT activity) following a whole body PET/CT acquisition, performed immediately upon completing the acute cold exposure. A whole body PET/CT image of a representative participant prior to and following a four-week cold acclimation protocol is shown in **Figure 3A.** Total BAT volume of activity increased by 45% following four weeks of cold acclimation (66 ± 30 mL pre-acclimation *vs.* 95 ± 28 mL post-acclimation; $P = 0.05$; **Figure 3B**). BAT attenuation, determined using computed tomography (CT) and expressed in Hounsfield units (HU), was the same at room temperature and increased to a similar degree in all participants following an acute cold exposure, independent of acclimation status (**Figure 3C)**. To examine cold-stimulated BAT and skeletal muscle quantitative glucose uptake, a cervicothoracic dynamic PET/CT acquisition was performed following the intravenous injection of a bolus of ^{18}FDG during the acute cold exposure. Fractional uptake (K_i) of ^{18}FDG **(Figure 3D)** was significantly greater in supraclavicular BAT compared with the longus colli, sternocleidomastoid, trapezius, pectoralis major and deltoid muscles, as well as subcutaneous adipose tissue. K_i of ^{18}FDG in supraclavicular BAT was significantly greater post-acclimation compared to pre-acclimation to cold (**Figure 3D**). Similarly, net tissue glucose uptake (K_m) (**Figure 3E**) was significantly higher in BAT *vs.* longus colli, sternocleidomastoid, trapezius, pectoralis major and deltoid muscles, as well as subcutaneous adipose tissue. K_m of ^{18}FDG in supraclavicular BAT was not significantly different between acclimation states ($P = 0.08$). Given a total glucose uptake by BAT of 20.1 ± 15.2 μmol/min pre-acclimation and 26.2 ± 11.8 μmol/min post-acclimation ($P = 0.08$) and a plasma glucose appearance of 1707 ± 166 and 2059 ± 100 μmol/min, respectively, BAT glucose uptake accounted for 1.1 ± 0.8 % and 1.4 ± 0.7 % of plasma glucose turnover, respectively. There was a

significant direct relationship between the radiodensity of BAT and the fractional and net glucose uptake by the tissue (Pearson r = 0.71, P = 0.01 and Pearson r = 0.72, P = 0.008, respectively; **Figure 3F** and **G**).

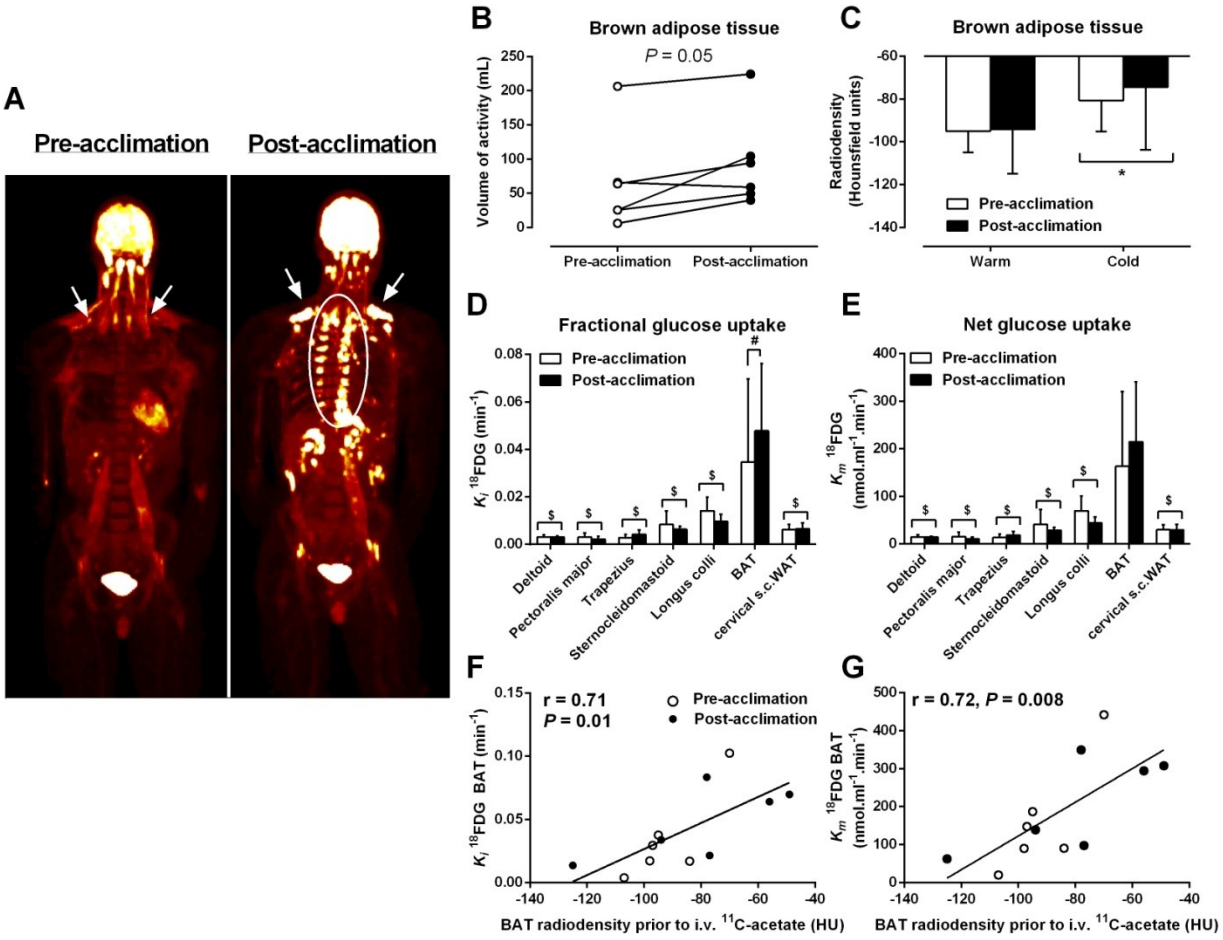

Figure 3. Tissue glucose uptake. (**A**) Coronal view (anterior-posterior projection) of whole-body ^{18}FDG uptake during cold exposure, pre- and post-acclimation. (**B**)Volume of BAT ^{18}FDG activity, pre- and post-acclimation. (**C**) BAT radiodensity by CT during room temperature and cold exposure, pre- and post-acclimation. (**D**) Fractional (K_i) and (**E**) net (K_m) glucose uptake in cervicothoracic tissues. Relationship between BAT radiodensity from CT taken before i.v. ^{11}C-acetate injection in the cold and (**F**) K_i ^{18}FDG (Pearson r = 0.71, P = 0.01) and (**G**) K_m ^{18}FDG (Pearson r = 0.72, P = 0.008). *$P < 0.05$ versus Room temperature, $^{\$}P < 0.005$ versus BAT, $^{\#}P <$ 0.05 versus pre-acclimation, ANOVA with Bonferonni post-hoc test.

Daily cold exposure increases BAT oxidative metabolism.

To investigate the oxidative capacity of cold-stimulated BAT, a cervicothoracic dynamic PET/CT acquisition was performed following the intravenous injection of a bolus of ^{11}C-acetate during the acute cold exposure. Following the i.v. injection of ^{11}C-acetate, BAT ^{11}C radioactivity over time was significantly higher during cold exposure compared to room temperature, both prior to and following a cold acclimation intervention (**Figure 4A and E**). Pectoralis major was the only muscle displaying a significant cold-induced increase in ^{11}C radioactivity over time (**Figure 4C and G**). The monoexponential decay slope from tissue peak ^{11}C activity (^{11}C-acetate *k*), a surrogate of tissue oxidative metabolism (Brown *et al.*, 1987; Ng *et al.*, 1994), increased significantly during cold exposure in BAT (effect of temperature $P = 0.001$; **Figure 4I**), demonstrating an increased in cold-induced oxidative metabolism. The monoexponential decay slope from tissue peak ^{11}C activity was also presented as a function of the total BAT volume of activity to demonstrate the total oxidative metabolism of BAT. The total BAT oxidative metabolism increased significantly in the cold with the increase being significantly greater following the cold acclimation (temperature x acclimation interaction $P = 0.02$; **Figure 4J**).

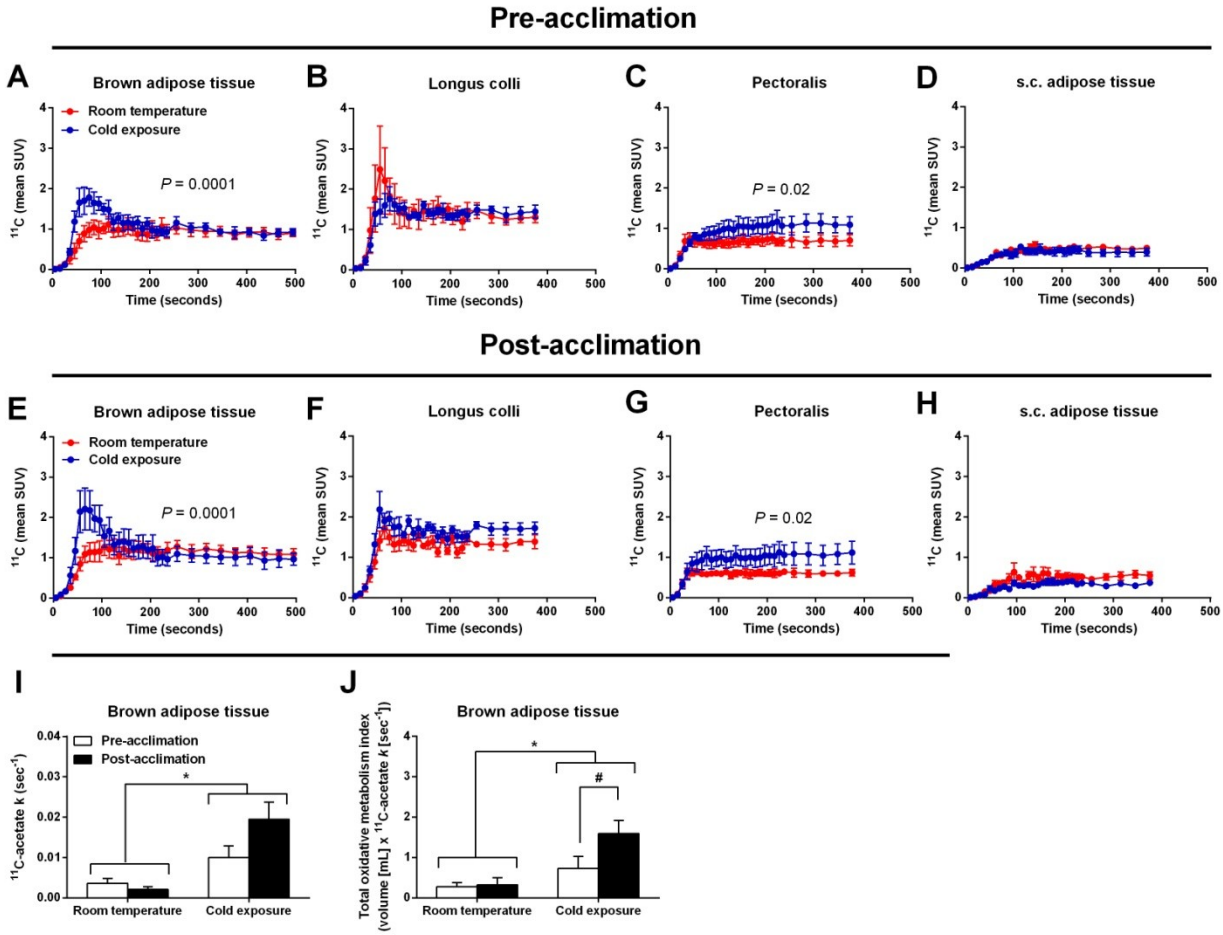

Figure 4. ^{11}C-acetate kinetics. ^{11}C time-radioactivity curves over the first 500 seconds of acquisition after ^{11}C-acetate injection at room temperature (red) and during cold exposure (blue) in BAT (**A** and **E**), Longus colli (**B** and **F**), Pectoralis (**C** and **G**) and cervical subcutaneous white adipose tissue (**D** and **H**) pre-acclimation and post-acclimation. (**I**) Tissue oxidative metabolism index (^{11}C-acetate *k*) in cervicothoracic BAT pre- and post-acclimation. (**J**) Total BAT oxidative metabolism index, pre- and post-acclimation. **P* < 0.05 versus Room temperature, $^{\#}$*P* < 0.05 versus pre-acclimation, ANOVA with Bonferonni post-hoc test.

DISCUSSION

Based on the PET tracers ^{18}FDG and ^{11}C-acetate, this study demonstrates for the first time that daily cold exposure not only increases the volume of metabolically active BAT by 45% but also doubles its cold-induced oxidative capacity in adult humans. Within the ^{11}C-acetate PET acquisition field-of-view including the neck and upper thorax, BAT was the only tissue demonstrating a significant increase in the total oxidative metabolism in the cold with the increase being significantly greater following the cold acclimation. ^{11}C-acetate as PET tracer has proved to be instrumental in assessing BAT (Ouellet *et al.*, 2012) and other tissue metabolism *in vivo* (Klein *et al.*, 2001; van den Hoff *et al.*, 2001; Menard *et al.*, 2010; Labbe *et al.*, 2012).

Thirty years ago, Huttunen *et al.* (Huttunen *et al.*, 1981) described the greater presence of multilocular adipocytes after necropsy in adipose tissue samples excised from the neck region of Finnish outdoor workers exposed to the cold compared to indoor workers. Until recently, this was the only evidence suggesting that chronic cold exposure induces increases in BAT mass in adult humans. However, the hypothesis that chronic cold activation stimulates BAT recruitment *in vivo* in adult humans has only recently explicitly been investigated (van der Lans *et al.*, 2013; Yoneshiro *et al.*, 2013), while the present study was in progress. We and others (van der Lans *et al.*, 2013) have observed that daily exposure to a mild cold, an unequivocal and to date most potent and safe stimulus to activate BAT in humans, does indeed increase whole body BAT volume of activity, as defined by the volume of ^{18}FDG uptake in BAT. Recent studies have demonstrated that most BAT depots in humans exhibit molecular signatures and histological features resembling the inducible brown adipocytes (known as beige, brown-in-white or brite) clustered within white adipose tissue depots of cold-exposed rodents (Sharp *et al.*, 2012; Wu *et al.*, 2012) but may also contain classical BAT (Cypess *et al.*, 2013; Jespersen *et al.*, 2013).

Whether the increased volume of glucose uptake observed herein is a result of proliferation of classical brown adipocytes, a *de novo* recruitment of brite adipocytes from white adipose tissue precursors (Wu *et al.*, 2012) or simply a direct interconversion of mature white adipocytes into a brown adipocyte phenotype or "*browning*" (Frontini *et al.*, 2013; Rosenwald *et al.*, 2013), is unclear. These findings imply that the thermogenic potential of BAT has increased as a result of the four-week cold acclimation. Due to the requirement of using radioactive isotopes to assess BAT metabolism *in vivo* in humans and limits in radioactivity exposure, the time course of both BAT recruitment and atrophy following the end of the intervention are not possible to determine in a within-subject design such as this.

The decreases in BAT radiodensity and the low levels of glucose uptake, averaging 20.1 ± 15.2 and 26.2 ± 11.8 μmol/min, under both experimental cold conditions lends further support to the notion that intracellular triglycerides (TG) are likely the predominant substrate fueling BAT oxidative metabolism in humans. Although intracellular TG depots decrease during the acute cold exposure, the similar radiodensity of BAT observed under unstimulated conditions (e.g. room temperature) pre and post-acclimation would suggest that they replete rapidly following the acute cold exposure. The time-course of this repletion, including the role of BAT in postprandial metabolism requires further investigation and may shed some light on the metabolic regulatory function of BAT. The significant inverse relationship between BAT radiodensity and its fractional and net glucose uptake suggests that, similar to skeletal muscle, circulating substrates may supply and complement the intracellular depots to meet the energy demand under stimulated conditions. The metabolic fate of glucose taken up by BAT has yet to be clearly established in humans. However, with BAT thermogenesis dependent on fatty acids for the activation of UCP1 and as a substrate to fuel thermogenesis (Cannon & Nedergaard,

2004), glucose is likely supplying the carbon backbone for fatty acid synthesis, which can be subsequently oxidized. The reduced concentration of circulating glucose post-acclimation, despite a greater glucose rate of appearance, combined with a trend towards a greater glucose clearance by BAT also suggests that this tissue may play a greater role in glucose metabolism than previously suspected. The detailed characterization of the fuel utilization and substrate handling of this tissue in humans warrants further investigation if is to be further pursued as a therapeutic target for metabolic diseases.

The metabolic impact of the increased BAT oxidative capacity that occurred following repetitive cold exposures may have contributed to an increase in the non-shivering thermogenesis (NST) of our subjects. Nonetheless, our cold acclimation protocol was insufficient to promote the recruitment of BAT-mediated NST to the extent necessary to completely abolish the shivering response (figure 2). More prolonged and/or intense cold-acclimation could be necessary to fully recruit BAT-mediated NST in humans or exposure to a colder acute thermal challenge may be required for BAT-mediated NST to fully manifest. Further, although EMG was monitored in 12 muscle groups, it remains that this method measures superficial electromyographic activity and provides some insight on fiber recruitment and fuel selection. Consequently, it is possible that deeper muscle groups, not accessible by EMG, were most influenced by the changes in BAT-mediated NST or that changes in skeletal muscle bioenergetics were also modified. In the only cold acclimation study quantifying shivering activity in humans, and thus *de facto* NST, 20 days of daily exposure to 12°C (8 hours/day) was required to observe a near abolishment of shivering activity in men previously acclimated to summer conditions (Davis, 1961). It is noteworthy that even in rodents subjected to aggressive cold exposure protocols (often 24 hour-exposure for several days at 4ºC), NST develops

progressively (Nedergaard & Cannon, 2013). In rats, cold exposure leads to an initial (a few hours) increase in BAT thermogenic activity associated with an increase in UCP1 stimulation, which is followed after a few days by a progressive increase in the thermogenic capacity, revealed through increases in UCP1 expression, mitochondriogenesis and brown adipocyte protein contents (Trayhurn *et al.*, 1987). In rats, cold adaptation has been reported to tremendously increase the thermogenic capacity of BAT, which can account for more than 60% of the total heat produced in response to noradrenaline with little contribution from skeletal muscle (Foster & Frydman, 1979). In the present study, since we did not have access to BAT tissue samples, we cannot conclude on the cause of the increase in BAT thermogenic capacity (i.e. increase in expression of UCP1 and accessory thermogenic genes or mitochondriogenesis). Another important limitation of the present study is the inability to assess the relative contribution of BAT and muscle as well as organs such as the heart and liver to total thermogenesis. Nevertheless, based on the present ^{11}C-acetate oxidative metabolism and BAT radiodensity data one can be confident of some contribution of BAT to energy metabolism following four weeks of acclimation, which is in line with evidence showing that human brown adipocytes are metabolically active and share similarities with classic brown adipocytes seen in laboratory rodents (Cypess *et al.*, 2013).

In summary, we showed that total BAT volume of activity increases significantly as a result of repeated controlled daily cold exposure and that this change in mass is paralleled by an increase in BAT oxidative capacity. Therefore, the contribution of BAT to NST must necessarily increase during cold-acclimation in humans.

ACKNOWLEDGEMENTS

The authors would like to acknowledge the excellent technical assistance provided by Diane Lessard, Caroll-Lynn Thibodeau, Maude Gérard, Éric Lavallée and Frédérique Frisch. This work was supported by a grant from the Canadian Diabetes association (OG-3-10-2970-AC) and the Natural Sciences and Engineering Research Council of Canada (NSERC Canada) to FH and was performed at the *Centre de recherche clinique Etienne-Le Bel*, a research centre funded by the *Fonds de la recherche Québec - Santé* (FRQS). DPB is the recipient of the NSERC Postgraduate Scholarship. SML is the recipient of a CIHR Postdoctoral fellowship. DR is the recipient of the CIHR/Merck Frosst Research Chair on Obesity. ACC is the recipient of the CIHR-GSK Chair in Diabetes. We also thank the subjects of this study for their collaboration and Allen-Vanguard Inc. (Kevin Semeniuk) for providing the liquid-conditioned suits.

AUTHOR CONTRIBUTIONS

Conception and design of the experiments: FH, DR, ACC, EET, BG

Collection, analysis and interpretation of data: DPB, SML, HT, CN, MK, SP, FH, EET, DR, ACC, SP

Drafting the article or revising it critically for important intellectual content: DPB, SML, HT, FH, ACC, DR, EET, BG, CN, MK

REFERENCES

1. van Marken Lichtenbelt WD, Vanhommerig JW, Smulders NM, Drossaerts JM, Kemerink GJ, Bouvy ND, Schrauwen P, and Teule GJ. Cold-activated brown adipose tissue in health men. *N Engl J Med.* 2009;360(15):1500-8.
2. Cypess AM, Lehman S, Williams G, Tal I, Rodman D, Goldfine AB, Kuo FC, Palmer EL, Tseng YH, Doria A, et al. Identification and importance of brown adipose tissue in adult humans. *N Engl J Med.* 2009;360(15):1509-17.
3. Virtanen KA, Lidell ME, Orava J, Heglind M, Westergren R, Niemi T, Taittonen M, Laine J, Savisto NJ, Enerbäck S, et al. Functional brown adipose tissue in healthy adults. *N Engl J Med.* 2009;360(15):1518-25.
4. Wu J, Bostrom P, Sparks LM, Ye L, Choi JH, Giang AH, Khandekar M, Virtanen KA, Nuutila P, Schaart G, et al. Beige adipocytes are a distinct type of thermogenic fat cell in mouse and human. *Cell.* 2012;150(2):366-76.
5. Sharp LZ, Shinoda K, Ohno H, Scheel DW, Tomoda E, Ruiz L, Hu H, Wang L, Pavlova Z, Gilsanz V, et al. Human BAT possesses molecular signatures that resemble beige/brite cells. *PLoS One.* 2012;7(11):e49452.
6. Ouellet V, Labbe SM, Blondin DP, Phoenix S, Guerin B, Haman F, Turcotte EE, Richard D, and Carpentier AC. Brown adipose tissue oxidative metabolism contributes to energy expenditure during acute cold exposure in humans. *J Clin invest.* 2012;122(2):545-52.
7. Vosselman MJ, Brans B, van der Lans AA, Wierts R, van Baak MA, Mottaghy FM, Schrauwen P, and van Marken Lichtenbelt WD. Brown adipose tissue activity after a high-calorie meal in humans. *Am J Clin Nutr.* 2013;98(1):57-64.
8. Ouellet V, Routhier-Labadie A, Bellemare W, Lakhal-Chaieb L, Turcotte E, Carpentier AC, and Richard D. Outdoor Temperature, Age, Sex, Body Mass Index, and Diabetic Status Determine the Prevalence, Mass, and Glucose-Uptake Activity of 18F-FDG-Detected BAT in Humans. *J Clin Endocrinol Metab.* 2011;96(1):192-9.
9. Cypess AM, White AP, Vernochet C, Schulz TJ, Xue R, Sass CA, Huang TL, Roberts-Toler C, Weiner LS, Sze C, et al. Anatomical localization, gene expression profiling and functional characterization of adult human neck brown fat. *Nat Med.* 2013;19(5):635-9.
10. Vijgen GH, Bouvy ND, Teule GJ, Brans B, Schrauwen P, and van Marken Lichtenbelt WD. Brown adipose tissue in morbidly obese subjects. *PLoS One.* 2011;6(2):e17247.
11. Orava J, Nuutila P, Noponen T, Parkkola R, Viljanen T, Enerbäck S, Rissanen A, Pietiläinen KH, and Virtanen KA. Blunted metabolic responses to cold and insulin stimulation in brown adipose tissue of obese humans. *Obesity.* 2013;21(11):2279-87.
12. Lean ME. Brown adipose tissue in humans. *Proc Nutr Soc.* 1989;48(2):243-56.
13. Ricquier D, Nechad M, and Mory G. Ultrastructural and biochemical characterization of human brown adipose tissue in pheochromocytoma. *J Clin Endocrinol Metab.* 1982;54(803-7.
14. Cannon B, and Nedergaard J. Brown adipose tissue: function and physiological significance. *Physiol Rev.* 2004;84(1):277-359.
15. Vijgen GH, Bouvy ND, Teule GJ, Brans B, Hoeks J, Schrauwen P, and van Marken Lichtenbelt WD. Increase in brown adipose tissue activity after weight loss in morbidly obese subjects. *J Clin Endocrinol Metab.* 2012;97(7):E1229-33.
16. Huttunen P, Hirvonen J, and Kinnula V. The occurrence of brown adipose tissue in outdoor workers. *Eur J Appl Physiol Occup Physiol.* 1981;46(4):339-45.

17. Schulz TJ, Huang P, Huang TL, Xue R, McDougall LE, Townsend KL, Cypess AM, Mishina Y, Gussoni E, and Tseng YH. Brown-fat paucity due to impaired BMP signalling induces compensatory browning of white fat. *Nature.* 2013;495(7441):379-83.
18. Yin H, Pasut A, Soleimani VD, Bentzinger CF, Antoun G, Thorn S, Seale P, Fernando P, van Ijcken W, Grosveld F, et al. MicroRNA-133 controls brown adipose determination in skeletal muscle satellite cells by targeting Prdm16. *Cell Metab.* 2013;17(2):210-24.
19. Carey AL, Formosa MF, Van Every B, Bertovic D, Eikelis N, Lambert GW, Kalff V, Duffy SJ, Cherk MH, and Kingwell BA. Ephedrine activates brown adipose tissue in lean but not obese humans. *Diabetologia.* 2013;56(1):147-55.
20. Vosselman MJ, van der Lans AA, Brans B, Wierts R, van Baak MA, Schrauwen P, and van Marken Lichtenbelt WD. Systemic beta-adrenergic stimulation of thermogenesis is not accompanied by brown adipose tissue activity in humans. *Diabetes.* 2012;61(12):3106-13.
21. Cypess AM, Chen YC, Sze C, Wang K, English J, Chan O, Holman AR, Tal I, Palmer MR, Kolodny GM, et al. Cold but not sympathomimetics activates human brown adipose tissue in vivo. *Proc Natl Acad Sci U S A.* 2012;109(25):10001-5.
22. van der Lans AAJJ, Hoeks J, Brans B, Vijgen GHEJ, Visser MGW, Vosselman MJ, Hansen J, Jörgensen JA, Wu J, Mottaghy FM, et al. Cold acclimation recruits human brown fat and increases nonshivering thermogenesis. *The Journal of Clinical Investigation.* 2013;123(8):0-.
23. Yoneshiro T, Aita S, Matsushita M, Kayahara T, Kameya T, Kawai Y, Iwanaga T, and Saito M. Recruited brown adipose tissue as an antiobesity agent in humans. *J Clin Invest.* 2013;123(8):3404-8.
24. Hardy JD, and Dubois EF. The technic of measuring radiation and convection. *J Nutr.* 1938;15(461-75.
25. Haman F, Péronnet F, Kenny GP, Massicotte D, Lavoie C, Scott C, and Weber J-M. Effect of cold exposure on fuel utilization in humans: plasma glucose, muscle glycogen, and lipids. *J Appl Physiol.* 2002;93(77-84.
26. Haman F, Legault SR, and Weber J-M. Fuel selection during intense shivering in humans: EMG pattern reflects carbohydrate oxidation. *J Physiol.* 2004;556(1):305-13.
27. Carpentier A, Patterson BW, Uffelman KD, Giacca A, Vranic M, Cattral MS, and Lewis GF. The effect of systemic versus portal insulin delivery in pancreas transplantation on insulin action and VLDL metabolism. *Diabetes.* 2001;50(6):1402-13.
28. Carpentier AC, Frisch F, Cyr D, Genereux P, Patterson BW, Giguere R, and Baillargeon JP. On the suppression of plasma nonesterified fatty acids by insulin during enhanced intravascular lipolysis in humans. *Am J Physiol Endocrinol Metab.* 2005;289(5):E849-56.
29. Labbe SM, Croteau E, Grenier-Larouche T, Frisch F, Ouellet R, Langlois R, Guerin B, Turcotte EE, and Carpentier AC. Normal postprandial nonesterified fatty acid uptake in muscles despite increased circulating fatty acids in type 2 diabetes. *Diabetes.* 2011;60(2):408-15.
30. Buck A, Wolpers HG, Hutchins GD, Savas V, Mangner TJ, Nguyen N, and Schwaiger M. Effect of carbon-11-acetate recirculation on estimates of myocardial oxygen consumption by PET. *J Nucl Med.* 1991;32(10):1950-7.
31. Klein LJ, Visser FC, Knaapen P, Peters JH, Teule GJ, Visser CA, and Lammertsma AA. Carbon-11 acetate as a tracer of myocardial oxygen consumption. *Eur J Nucl Med.* 2001;28(5):651-68.

32. Menard SL, Croteau E, Sarrhini O, Gelinas R, Brassard P, Ouellet R, Bentourkia M, van Lier JE, Des Rosiers C, Lecomte R, et al. Abnormal in vivo myocardial energy substrate uptake in diet-induced type 2 diabetic cardiomyopathy in rats. *Am J Physiol Endocrinol Metab.* 2010;298(5):E1049-57.
33. Croteau E, Lavallée E, Labbe SM, Hubert L, Pifferi F, Rousseau JA, Cunnane SC, Carpentier AC, Lecomte R, and Bénard F. Image-derived input function in dynamic human PET/CT: methodology and validation with 11C-acetate and 18F-fluorothioheptadecanoic acid in muscle and 18F-fluorodeoxyglucose in brain. *Eur J Nucl Med Mol Imaging.* 2010;37(8):1539-50.
34. Brown M, Marshall DR, Sobel BE, and Bergmann SR. Delineation of myocardial oxygen utilization with carbon-11-labeled acetate. *Circulation.* 1987;76(3):687-96.
35. Ng CK, Huang SC, Schelbert HR, and Buxton DB. Validation of a model for [1-11C]acetate as a tracer of cardiac oxidative metabolism. *Am J Physiol.* 1994;266(4 Pt 2):H1304-15.
36. Labbe SM, Grenier-Larouche T, Noll C, Phoenix S, Guerin B, Turcotte EE, and Carpentier AC. Increased myocardial uptake of dietary fatty acids linked to cardiac dysfunction in glucose-intolerant humans. *Diabetes.* 2012;61(11):2701-10.
37. van den Hoff J, Burchert W, Borner AR, Fricke H, Kuhnel G, Meyer GJ, Otto D, Weckesser E, Wolpers HG, and Knapp WH. [1-(11)C]Acetate as a quantitative perfusion tracer in myocardial PET. *J Nucl Med.* 2001;42(8):1174-82.
38. Jespersen NZ, Larsen TJ, Peijs L, Daugaard S, Homoe P, Loft A, de Jong J, Mathur N, Cannon B, Nedergaard J, et al. A classical brown adipose tissue mRNA signature partly overlaps with brite in the supraclavicular region of adult humans. *Cell Metab.* 2013;17(5):798-805.
39. Frontini A, Vitali A, Perugini J, Murano I, Romiti C, Ricquier D, Guerrieri M, and Cinti S. White-to-brown transdifferentiation of omental adipocytes in patients affected by pheochromocytoma. *Biochim Biophys Acta.* 2013;1831(5):950-9.
40. Rosenwald M, Perdikari A, Rulicke T, and Wolfrum C. Bi-directional interconversion of brite and white adipocytes. *Nat Cell Biol.* 2013;15(6):659-67.
41. Davis TRA. Chamber cold acclimatization in man. *J Appl Physiol.* 1961;16(6):1011-5.
42. Nedergaard J, and Cannon B. UCP1 mRNA does not produce heat. *Biochim Biophys Acta.* 2013;1831(5):943-9.
43. Trayhurn P, Ashwell M, Jennings G, Richard D, and Stirling DM. Effect of warm or cold exposure on GDP binding and uncoupling protein in rat brown fat. *Am J Physiol.* 1987;252(2 Pt 1):E237-43.
44. Foster DO, and Frydman ML. Tissue distribution of cold-induced thermogenesis in conscious warm- or cold-acclimated rats reevaluated from changes in tissue blood flow: the dominant role of brown adipose tissue in the replacement of shivering by nonshivering thermogenesis. *Can J Physiol Pharmacol.* 1979;57(3):257-70.

3.4 Article IV

Cold-acclimation in adult humans: transient modulation in the contribution of shivering and non-shivering thermogenesis.

Denis P. Blondin[1], Hans Christian Tingelstad[1], François Haman[1].

[1] Faculty of Health Sciences, University of Ottawa, Ottawa, Ontario, Canada.

Running Head: **Cold-acclimation modulates shivering and non-shivering thermogenesis**

Key Words: cold-acclimation; energy metabolism; shivering; non-shivering thermogenesis

Word Count: Main Text: 5,491 Abstract: 266

Number of tables: **Number of figures:**

Conflict of interest: The authors have declared that no conflict of interest exists related to the content of this manuscript.

ABSTRACT

The thermoregulatory adjustments resulting from chronic cold exposure have shown remarkable variability in humans. The primary goals of this investigation were to: (1) establish the temporal changes in the thermoregulatory responses resulting from daily cold exposure, particularly whole body heat production and shivering intensity; (2) determine whether the electromyographic (EMG) pattern of muscle recruitment or the recruitment of particular muscle groups were modulated as a result of this acclimation intervention; and (3) examine the consequent effects on substrate metabolism. Using simultaneous metabolic and EMG measurements, we quantified the effects of a four-week cold-acclimation intervention on whole body heat production and shivering activity. This particular intervention evoked a hypothermic form of acclimation, such that a greater uncompensated drop in core temperature was presented following four weeks of daily cold exposure. Contrary to expectation, both cold-induced thermogenesis (1629 ± 46 kJ pre-acclimation *vs.* 1595 ± 68 kJ in Week 4) and total shivering intensity were unaltered by this intervention. A delay (from 20 min pre-acclimation to 50 min by Week 4) and shift in the mean skin temperature to which shivering was initiated (from 27.8 ± 0.6 °C pre-acclimation to 26.3 ± 0.3 °C by Week 4) combined with changes to the EMG signature, particularly in the more active proximal muscles, partially explain such conflicting findings. Collectively, these results suggest that a contraction-stimulated fiber-type switch combined with bioenergetic changes in shivering muscles may explain the unaltered cold-induced thermogenesis and shivering intensity seen here. Investigating the underlying mechanisms involved in maintaining heat production following a cold acclimation intervention may provide interesting insight on the therapeutic potential of cold exposure.

INTRODUCTION

As endotherms, humans exposed to a compensable cold environment can remain homeothermic by producing sufficient heat to counteract the rate of heat loss. When acutely exposed to a moderate cold (2-3×RMR), a combination of shivering (Haman *et al.*, 2002; Haman *et al.*, 2004c; Haman *et al.*, 2005) and non-shivering (Wijers *et al.*, 2008; Ouellet *et al.*, 2012) means of producing heat are required to maintain this thermal balance. Chronic or repeated exposure to a cold stress can elicit various acclimation responses that modulate these thermoregulatory responses which can be either insulative [*i.e.* lower skin temperature; (Scholander *et al.*, 1958; Hong, 1973)], hypothermic [*i.e.* un-defended fall in core temperature; (Davis, 1961)] or metabolic [*i.e.* increased cold-induced heat production; (Hammel *et al.*, 1959; Elsner *et al.*, 1960; Hart *et al.*, 1962)] in nature or a combination of these [see (Young, 1996) for review].

A trademark of cold acclimation in rodents and other small mammals is the successive shift in the mechanisms of heat production being recruited, shifting from predominantly shivering to primarily brown adipose tissue (BAT)-derived thermogenesis [e.g. (Chaffee *et al.*, 1975; Wiesinger *et al.*, 1990)]. This is often accomplished without exhibiting changes in whole body heat production. Further, whether these two mechanisms of heat production are evoked separately or simultaneously by the cold stimulus depends on the acclimation status of the animal and the thermal demands of the acute cold exposure (Himms-Hagen, 2004). In humans, this relationship has remained ambiguous. Although the variability in cold-acclimation phenotypes have been described in various reviews (Young, 1996; Launay & Savourey, 2009; Makinen, 2010), very little information exists on the changes in the thermogenic processes that are recruited as a result of the acclimation process. In part, this is a result of the previously held

belief that cold-induced heat production was generated almost exclusively from shivering skeletal muscles, since BAT-mediated thermogenesis was considered insignificant or absent in adult humans. However, our more recent understanding and presumptions regarding cold-induced thermogenesis have changed substantially. In particular, three significant findings have influenced our understanding of facultative thermogenesis: (1) BAT is present in adult humans (van Marken Lichtenbelt *et al.*, 2009; Virtanen *et al.*, 2009) and cold exposure stimulates BAT-mediated thermogenesis (Orava *et al.*, 2011; Ouellet *et al.*, 2012); (2) skeletal muscle-mediated thermogenesis can come in both an ATPase and uncoupling form of thermogenesis (Wijers *et al.*, 2008) and; (3) skeletal muscle-mediated thermogenesis can be influenced by the recruitment of distinct muscle fibers (Haman *et al.*, 2004b) or different metabolic pathways within the same muscle fibers (Haman *et al.*, 2004a; Blondin *et al.*, 2011). In large mammals or birds where BAT represents a smaller proportion of total body weight or is absent, skeletal muscle-derived thermogenesis in the form of shivering or non-shivering thermogenesis is the predominant source of heat production (Schaeffer *et al.*, 2005; Teulier *et al.*, 2010). Consequently, cold-acclimation in these models and human cold acclimatization studies (*i.e.* resulting from living or working in a cold environment) tend to demonstrate structural and metabolic alterations in skeletal muscle which resemble the training effects of endurance exercise, in particular changes in metabolic efficiency and interconversion of muscle fibers (Duchamp *et al.*, 1992; Bae *et al.*, 2003; Schaeffer *et al.*, 2003). More importantly, whether repeated cold exposure stimulates changes in BAT, skeletal muscle or both, the physiological capacity of these structural modifications may only manifest under conditions where it is required, namely at temperatures below the cold-acclimation temperature (Himms-Hagen, 2004).

The goals of this investigation were: (1) to establish the temporal changes in the thermoregulatory responses resulting from daily cold exposure, particularly whole body heat production and shivering intensity; (2) to determine whether the electromyographic (EMG) pattern of muscle recruitment or the recruitment of particular muscle groups were modulated as a result of daily cold exposure; and (3) examine the consequent effects on substrate metabolism. We have previously shown that heat production can be maintained by recruiting different metabolic pathways within the same fibers (Haman *et al.*, 2004a) and by recruiting specific subpopulations of fibers within the same muscle (Haman *et al.*, 2004b). We hypothesize that, if a training effect is apparent following the cold-acclimation, a decrease in shivering intensity would coincide with a decrease in burst shivering activity, indicative of a shift towards the recruitment of slow-oxidative muscle fibers. The aim was to investigate these changes under acute cold challenges that are colder than the acclimation temperature.

METHODS

Study participants

Eight healthy, lean men aged 23 ± 1 years with a BMI of 24.7 ± 1.0 kg/m^2 were invited to participate in a four-week cold-acclimation protocol and undergo acute cold exposure studies prior to and following the intervention. Individuals taking any medications or with a history or clinical evidence of a medical condition known to affect glycemia, lipid levels or insulin sensitivity or had known cardiovascular disease were excluded. Participants were fully informed of the risks and methodologies applied and provided their written consent to participate in this study, in accordance with the Declaration of Helsinki. This study received ethics approval from the Office of Research Ethics and Integrity at the University of Ottawa.

Experimental Protocols

All subjects participated in three metabolic experimental sessions within a four week interval designed to assess whole body thermoregulatory responses during an acute cold exposure. Between these acute cold exposure experimental sessions, participants followed a cold acclimation protocol consisting of daily cold exposure lasting two hours, repeated five consecutive days per week for four consecutive weeks for a total of 17 acclimation sessions and three testing sessions. Participants arrived between 7.00 and 9.00 h in a fasted state and were fitted with a liquid conditioned suit (LCS; Three Piece, Allen-Vanguard, Ottawa, ON) where 10°C water was circulated for two hours. Participants were asked to maintain their current training regiment and refrain from drinking caffeinated or alcoholic beverages for the duration of the study.

Each acute cold exposure experimental session was conducted between 7.30 h and 16.00 h, following 48h without strenuous physical activity. The last evening meal ingested between 18.00 h and 20.00 h was standardized (3220 kJ or 770 kcal, 42% CHO, 28% fat and 30% protein) and subjects were asked to report to the laboratory at 7.30 h the next morning after a 12-14 h fast. Upon their arrival in the laboratory, subjects wearing only shorts were weighed and instrumented with temperature sensors and surface EMG electrodes. Participants were then fitted with the LCS, ingested a telemetric thermometry capsule to measure core temperature (Vital Sense monitor and Jonah temperature capsule, Mini Mitter Co., Inc., Bend, OR, USA) and performed a series of exercises to estimate the maximal voluntary contraction (MVC) of each of the muscles being measured for shivering activity. Subjects were then asked to empty their bladder and remain seated for 90 min at ambient temperature (~23-25°C). Following this baseline period, the LCS was perfused with 4°C water (Time = 0) using a temperature and flow controlled circulation bath. Thermal responses, muscle activity, metabolic rate and fuel utilization were measured continuously during the final 30 min of the baseline period and the subsequent 150 min of cold exposure.

Thermal responses

Core temperature (T_{core}) was measured using an ingested telemetric pill which measures the temperature in the intestine. Mean skin temperature ($\overline{T}_{skin}$) was monitored continuously using 12 autonomous wireless temperature sensors (Thermochron iButton® model DS1922H, Maxim) fixed to the skin, calculated using an area-weighted equation from 12 sites: forehead, chest, biceps, forearm, abdomen, lower and upper back, front and back calf, quadriceps, hamstrings and hand (Hardy JD, 1938). Proximal skin temperature was defined as the mean skin temperatures of the forehead, chest, abdomen and the lower and upper back. Distal skin temperature was

represented by the hand temperature. The core-mean skin temperature and core-proximal skin temperature gradients were calculated as measures of core insulation. The proximal-distal skin temperature gradient was calculated as an index of vasoconstriction. The temperatures entering and leaving the LCS were continuously measured using custom t-type thermocouples (Omega Environmental Inc. Laval, Quebec, Canada) connected at the entry and exit connectors of the LCS.

Thermogenesis and Fuel Selection

Whole body metabolic rate ($\dot{M}$) and fuel selection were quantified by indirect calorimetry (TurboFox, Sable Systems International, Las Vegas, NV). The rates of oxygen consumption ($\dot{V}O_2$) and carbon dioxide production ($\dot{V}CO_2$) were calculated using equations derived by Brown et al. (Brown *et al.*, 1984) adapted for its application with a canopy. This approach allowed for a constant measurement and subsequent correction for the dilution effect of water vapor pressure on $\dot{V}O_2$ and $\dot{V}CO_2$. A background baselining technique developed by Sable Systems International [described in (Melanson *et al.*, 2010)] was then applied to correct for analyser drift. Total protein (RP_{ox}), carbohydrate (RC_{ox}) and lipid (RF_{ox}) oxidation rates (in g/min) were calculated as described previously (Haman *et al.*, 2002; Haman *et al.*, 2004c):

$$RP_{ox}\,(g/min) = 2.9 \times UREA_{urine}\,(g/min) \quad (1)$$

$$RC_{ox}\,(g/min) = 4.59\,\dot{V}CO_2\,(l/min) - 3.23\,\dot{V}O_2\,(l/min) \quad (2)$$

$$RF_{ox}\,(g/min) = -1.70\,\dot{V}CO_2\,(l/min) + 1.70\,\dot{V}O_2\,(l/min) \quad (3)$$

where urinary urea excretion ($UREA_{urine}$) was measured in urine collected over the 120 min of the baseline period, and 150 min in the cold using a commercial urea assay kit (BioAssay Systems, Hayward, CA), and $\dot{V}CO_2$ (l/min) and $\dot{V}O_2$ (l/min) were corrected for the volumes of O_2 and CO_2 corresponding to protein oxidation (1.010 and 0.843 l/g, respectively). Energy potentials of 16.3 kJ/g (CHO), 40.8 kJ/g (lipids), and 19.7 kJ/g (proteins) were used to calculate the relative contributions of each fuel to total heat production (Elia, 1991; Péronnet & Massicotte, 1991). Shivering (ST) and non-shivering thermogenesis (NST) were determined by simultaneously measuring ($\dot{M}$) and EMG throughout cold exposure. A shivering threshold temperature (STT) was determined as the mean skin temperature at the time in which whole body EMG activity was significantly increased. The NST was then defined as the cold-induced $\dot{M}$ that is not yet accompanied by shivering activity, thus at the STT, minus the $\dot{M}$ measured during exposure to ambient temperature. The thermogenic contribution of shivering was determined as the average $\dot{M}$ of the final 30 min of cold exposure minus NST.

Muscle recruitment

Shivering EMG signals were recorded from 12 muscles: *m. trapezius superior* (TS), *m. latissimus dorsi* (LD), *m. sternocleidomastoid* (SCM)*, m. pectoralis major* (PM), *m. deltoideus* (DT)*, m. bicep brachii* (BB)*, m. tricep brachii* (TB)*, m. rectus abdominis* (RA), *m. vastus lateralis* (VL), *m.rectus femoris* (RF), *m. vastus medialis* (VM) and *m. bicep femoris (*BF). Surface electrodes (Delsys, Boston, MA) were placed over the bellies of each muscle and their exact positions were identified with an indelible skin marker to allow consistent placement between experimental sessions. Raw EMG signals were collected at 1000 Hz, filtered to remove spectral components below 20 Hz and above 500 Hz as well as 60-Hz contamination and related harmonics, and analyzed using custom-designed MATLAB algorithms (Mathworks, Natick,

MA). Shivering activity of the 12 individual muscles was monitored 10 min before and continuously throughout cold exposure. Voluntary muscle activity was minimized as much as possible throughout cold exposure by asking participants to avoid voluntary movements during recording periods.

Shivering intensity of individual muscles was determined from root-mean-square (RMS) values calculated from raw EMG signals using a 50-ms overlapping window (50%). In brief, baseline RMS values ($RMS_{baseline}$: 15 min RMS average measured prior to cold exposure) were subtracted from shivering RMS (RMS_{shiv}) values and RMS values obtained from the maximal voluntary contractions of individual muscles (RMS_{mvc}). Shivering intensity was normalized to RMS_{mvc} by using the following equation:

$$\text{Shivering Intensity (\%MVC)} = \frac{RMS_{shiv} - RMS_{baseline}}{RMS_{mvc} - RMS_{baseline}} \times 100 \quad (1)$$

Shivering activities of each muscle were summed, taking into account the relative mass of the body region they represent, to obtain an index of whole body shivering activity, as described previously (Bell *et al.*, 1992; Haman *et al.*, 2004a).

$$Shiv_{WBI} = \sum f_{UT}\, EMG_{shiv}^{UT} + f_{LT}\, EMG_{shiv}^{LT} + f_{UL}\, EMG_{shiv}^{UL} + f_{LL}\, EMG_{shiv}^{LL} \quad (2)$$

where EMG_{shiv}^{UT}, EMG_{shiv}^{LT}, EMG_{shiv}^{UL}, EMG_{shiv}^{LL} are upper trunk (UT: average of TR, LD, SCM, PM), lower trunk (LT: RA), upper limb (UL: average of VL, RF, VM, BF), lower limb (LL: average of DT, BB, TB) shivering activities. The coefficients f_{UT} (0.34), f_{LT} (0.19), f_{UL}(0.29), f_{LL} (0.085) correspond to the relative muscle masses of each body region to total muscle mass (Bell *et al.*, 1992). This whole body index represents 91% of total muscle mass and excludes

deep muscle groups, lower leg muscles and muscles found on the head, hand or feet. To compare the shivering intensity of proximal and distal muscle groups, an average shivering intensity was calculated for each (Proximal: average of TR, LD, SCM, PM, RA; Distal: average of VL, RF, VM, BF, DT, BB, TB). Shivering pattern was determined as previously described (Haman *et al.*, 2004a), where an example of EMG signal showing the two shivering patterns is illustrated. In brief, a shivering burst was defined as an EMG interval with a duration >0.2 s, an inter-burst interval >0.75 s and an amplitude higher than the intensity threshold at each recording period. Intensity threshold was determined by: (i) averaging shivering intensity (A_{EMG}) over the entire recording period, (ii) averaging the remaining values above A_{EMG} (B_{EMG}), and (iii) setting the intensity threshold at B_{EMG}. Whole body burst shivering was calculated as the average of the burst rate of individual muscles. The mean shivering intensity (in %MVC) of both continuous shivering and burst shivering were also determined.

Statistical analysis

Data are expressed as mean ± SEM. Paired Student's *t* test was used to compare between acute cold exposure experimental sessions. ANOVA for repeated measures with acclimation status, temperature and their interaction as the independent variables was used to analyze acclimation- and temperature-dependent differences in thermal responses (T_{core}, $\overline{T}_{skin}$, temperature gradients), metabolic responses ($\dot{M}$ and fuel utilization) and electromyographic activity (shivering intensity, burst rate) throughout the protocols. Bonferonni's multiple comparisons post-hoc test was used, where applicable. Spearman correlation coefficients were used to determine correlations between variables. A 2-tailed *P* value of less than 0.05 was

considered significant. All analyses were performed using SPSS for Windows (version 16.0; SPSS Inc., Chicago IL) or GraphPad Prism version 6.00 for Windows (GraphPad, San Diego, CA).

RESULTS

Insulative Responses

Changes in insulative responses are presented in Table 1 and Figure 1. Acute cold exposure, following a four-week cold acclimation, resulted in a 0.5 ± 0.2°C decrease in core temperature as early as two weeks into the protocol (Table 1). Cold-induced decreases in $\overline{T}_{skin}$, proximal skin temperature and distal skin temperature did not differ as a result of chronic cold exposure (Table 1). Similarly, the temperature gradient between the core and skin, an indicator of the thermal insulation of the core, increased during an acute cold exposure but were not influenced by daily cold exposure (Table 1). This is consistent with the significant inverse relationship observed between the cold-induced change in $\overline{T}_{skin}$ and metabolic rate in all three acute cold exposure sessions (Fig.1). The similar slopes of the regression lines suggest a similar thermal insulation or thermal sensitivity between experimental sessions (-0.55 ± 0.20 $kJ \cdot min^{-1} \cdot °C^{-1}$ during pre-acclimation compared to -0.58 ± 0.18 $kJ \cdot min^{-1} \cdot °C^{-1}$ and -0.77 ± 0.24 $kJ \cdot min^{-1} \cdot °C^{-1}$ following week 2 and week 4, respectively; $P = 0.74$). The proximal-distal skin temperature gradient also increased during cold exposure, but did not change over the course of the acclimation protocol (Table 1). The temperature gradient between the water entering and leaving the cooling garment, an indicator of the transfer of heat from the cold-exposed participant to the cold water circulating in the suit, were the same between acute cold exposures (between 7.0 ± 0.2 °C and 6.8 ± 0.3°C).

Table 1. Temperature responses averaged over the final 30 min of the baseline and cold exposure periods prior to, during and following a four-week cold acclimation.

	Pre-acclimation		Week 2		Week 4	
	Baseline	**Cold**	**Baseline**	**Cold**	**Baseline**	**Cold**
Core temperature (°C)	36.9 ± 0.1	36.7 ± 0.1	36.9 ± 0.1	36.4 ± 0.2[#]	37.0 ± 0.1	36.5 ± 0.1[#]
Skin temperature (°C)	33.0 ± 0.2	25.1 ± 0.6**	32.8 ± 0.3	24.7 ± 0.4**	33.1 ± 0.2	24.4 ± 0.4**
Proximal skin temperature (°C)	34.2 ± 0.2	28.4 ± 0.9**	33.7 ± 0.2	28.5 ± 0.6**	34.2 ± 0.2	28.6 ± 0.6**
Distal skin temperature (°C)	28.6 ± 1.0	21.2 ± 0.4**	28.9 ± 1.0	21.4 ± 0.6**	28.3 ± 1.0	21.1 ± 0.7**
Gradient core-mean skin temperature (°C)	3.9 ± 0.2	11.6 ± 0.7**	4.1 ± 0.3	11.6 ± 0.4**	3.9 ± 0.3	12.1 ± 0.5**
Gradient core-proximal skin temperature (°C)	2.7 ± 0.2	8.4 ± 0.9**	3.2 ± 0.2	7.9 ± 0.6**	2.8 ± 0.2	7.9 ± 0.6**
Gradient proximal-distal skin temperature (°C)	5.6 ± 0.9	7.1 ± 0.8*	4.8 ± 1.1	7.2 ± 1.1*	6.0 ± 1.1	7.5 ± 0.8*
Gradient water entering-leaving cooling garment (°C)	-	7.0 ± 0.2	-	6.6 ± 0.2	-	6.8 ± 0.3
Shivering skin temperature threshold (°C)	-	27.8 ± 0.6	-	26.1 ± 0.3[$]	-	26.3 ± 0.3[$]

Values are means ± SE (n = 9 for pre-acclimation and Week 4 and n = 8 for Week 2).

* P <0.01, significantly different than Baseline; **, P <0.0001

[#] P < 0.01, significantly different than pre-acclimation (temperature x acclimation interaction)

[$] P < 0.05, significantly different than pre-acclimation

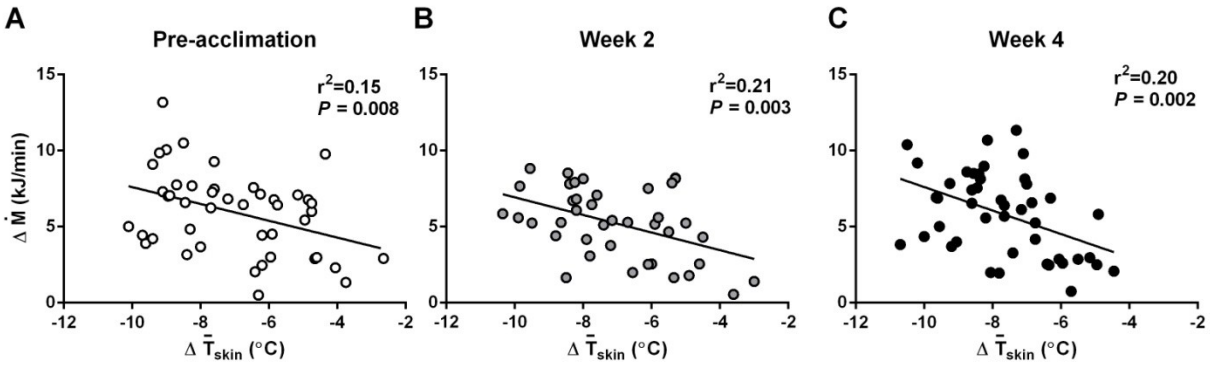

Figure 1. Relationship between changes in metabolic rate ($\dot{M}$) and changes in mean skin temperature ($\overline{T}_{skin}$) in men exposed to 4 °C for 150 min prior to (A), during (B) and following (C) a four-week cold acclimation. Values are presented for all subjects (n = 9 for pre-acclimation and Week 4 and n = 8 for Week 2) and were averaged at 5 sampling intervals during cold exposure (time = 30, 60, 90, 120 and 150 min).

Shivering thermogenesis

The relationship between $\dot{M}$, $\overline{T}_{skin}$ and shivering intensity during an acute cold exposure in individuals not acclimated to the cold, acclimated for two weeks and acclimated for four weeks are presented in Fig. 2. The shivering threshold was defined as the point in which a statistically significant difference in shivering intensity was calculated. The shivering threshold during the acute cold exposure was at 20 min during the pre-acclimation session (Fig.2A), at 60 min following two weeks of daily cold exposure (Fig. 2B) and at 50 min following four weeks of cold acclimation (Fig. 2C). This represented a shivering mean skin temperature threshold of 28.7 ± 0.5 °C during the pre-acclimation acute cold exposure, which was significantly warmer than following two and four weeks of acclimation (26.1 ± 0.3 °C and 26.3 ± 0.3 °C, respectively; Fig. 2 and Table 1). Given the differences in shivering onset, overall shivering intensity was presented as an area under the curve (Fig. 3). Shivering intensity, using a weighted mean of 12 muscles, was not significantly different over the course of the four week cold-acclimation (Fig. 3A). Proximal muscles were the most active muscles during an acute cold exposure, regardless

of the acclimation status, but their intensity did not change over the course of the four weeks. This shivering pattern transiently changed over the course of the four weeks, such that the total number of bursts decreased significantly by 20% between the pre-acclimation cold exposure and two weeks into cold acclimation (from 574 ± 28 bursts to 478 ± 43 bursts following two weeks of daily cold exposure; $P = 0.04$), before returning to pre-acclimation levels following four weeks of daily cold exposure (Fig. 3B). To examine whether the shivering pattern was altered between muscle groups, the total number of bursts were compared between proximal and distal skeletal muscles. There was an acclimation by muscle interaction ($P < 0.001$), whereby the total number of bursts in proximal muscles fell progressively over the course of the cold acclimation (Week 4 was significantly lower than Week 2 and Pre-acclimation), but not in distal skeletal muscles. To examine whether there was a shift in the contribution of the shivering intensity between the two types of shivering patterns over the course of the four week acclimation, continuous shivering intensity and burst shivering intensity were each calculated. Both continuous shivering intensity (Fig. 3C) and burst shivering intensity (Fig. 3D) did not change over the course of the cold acclimation, nor was an interaction between the two determined. Continuous shivering intensity of proximal muscles was significantly higher than distal muscles ($P = 0.02$; Fig. 3C), while burst shivering intensity was not significantly different between muscle groups ($P = 0.15$; Fig. 3D).

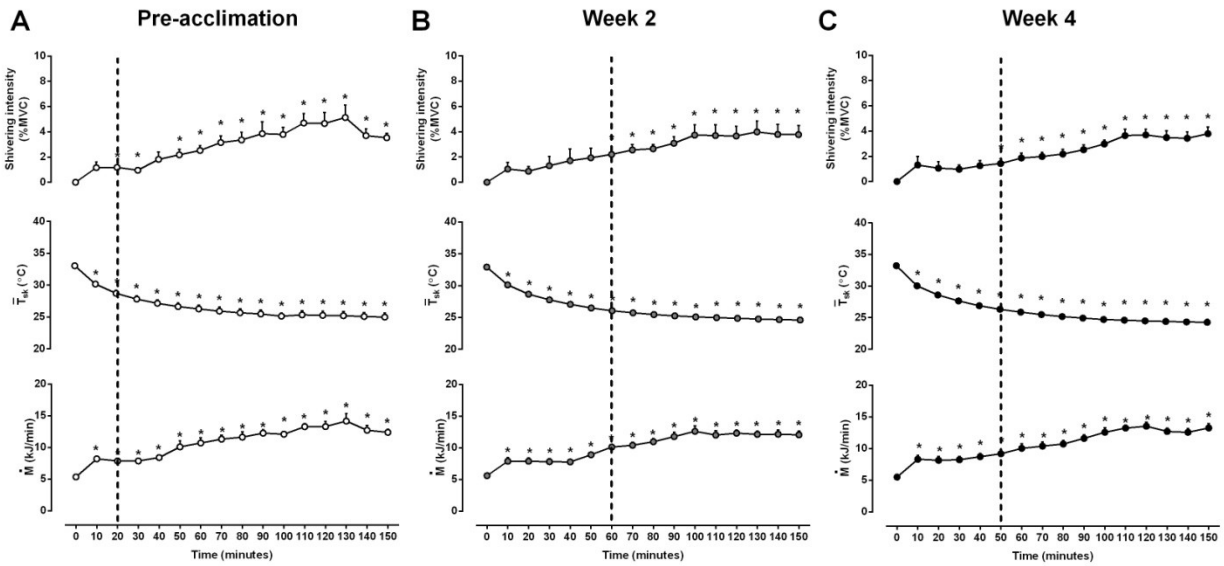

Figure 2. Changes in shivering intensity, mean skin temperature ($\overline{T}_{skin}$) and metabolic rate ($\dot{M}$) over time in men exposed to 4°C for 150 min prior to (A), during (B) and following (C) a four-week cold acclimation. Dashed line represents shivering skin temperature threshold. Values are means ± SE (n = 9 for pre-acclimation and Week 4 and n = 8 for Week 2).
* Significantly different from baseline values before cold exposure, $P \leq 0.05$.

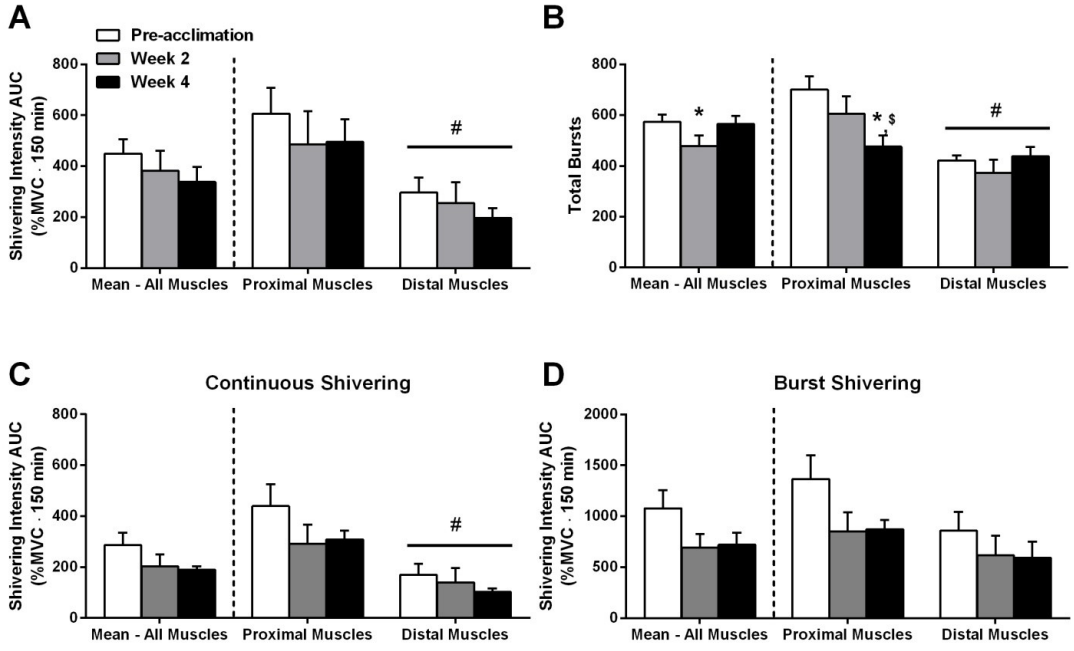

Figure 3. Overall shivering intensity (A), burst shivering (B) and continuous (C) and burst shivering intensity (D) of whole body, proximal and distal muscle groups in men exposed to 4 °C for 150 min prior to (Pre-acclimation), during (Week 2) and following (Week 4) a four-week cold acclimation. Values are means ± SE (n = 9 for pre-acclimation and Week 4 and n = 8 for Week 2). * Significantly different from pre-acclimation, $P \leq 0.05$; $ Significantly different from Week 2, $P \leq 0.05$; # Significantly different from Proximal muscles, $P \leq 0.05$.

Examining the thermogenic rate at the shivering threshold during the pre-acclimation, Week 2 and Week 4 acute cold exposures, the capacity for cold-induced non-shivering thermogenesis (NST) was estimated to be significantly greater following two weeks of daily cold exposure compared to pre-acclimation values (2.5±0.4 kJ/min compared to 4.5 ± 0.4 kJ/min; P = 0.005) but were not statistically different following four weeks (Fig. 4).

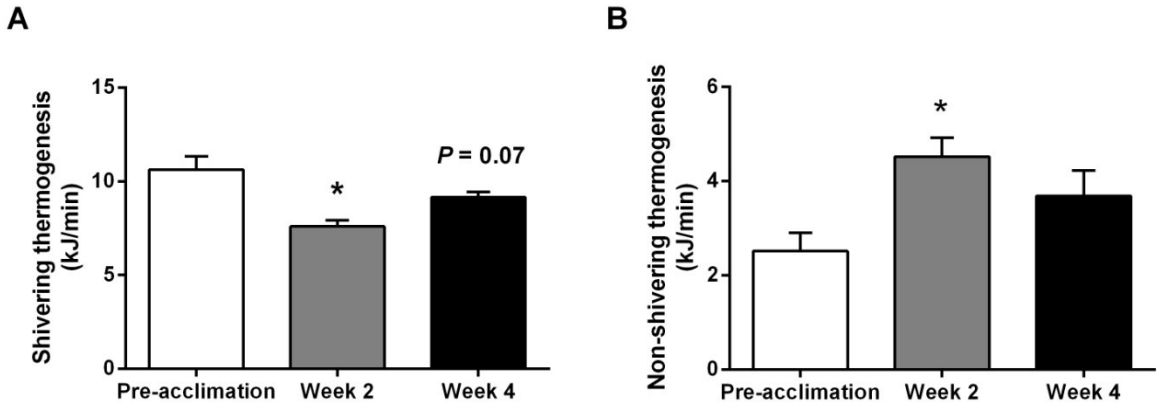

Figure 4. Shivering thermogenesis (A) and Non-shivering thermogenesis (B) of men exposed to 4°C for 150 min prior to (Pre-acclimation), during (Week 2) and following (Week 4) a four-week cold acclimation. Values are means ± SE (n = 9 for pre-acclimation and Week 4 and n = 8 for Week 2). * Significantly different from pre-acclimation, $P \leq 0.05$.

A strong direct correlation between shivering intensity and the cold-induced metabolic rate ($\Delta \dot{M}$) was observed in the pre-acclimation condition (r = 0.68, $P < 0.0001$), during Week 2 (r = 0.81, $P < 0.0001$) and during Week 4 (r = 0.85, $P < 0.0001$)(Figure 5). The slope of the regression lines were significantly different between the pre-acclimation condition and Week 4 (P = 0.001) and between Week 2 and Week 4 (P = 0.01), but not between pre-acclimation and Week 2 (P = 0.23). These differences in the slope of the regression lines infer changes in the coupled form of shivering thermogenesis.

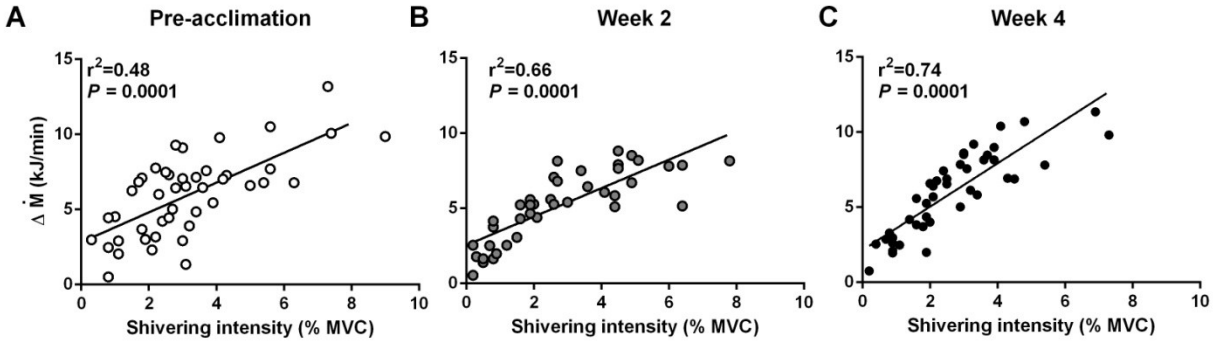

Figure 5. Relationship between changes in metabolic rate ($\dot{M}$) and shivering intensity in men exposed to 4 °C for 150 min prior to (A), during (B) and following (C) a four-week cold acclimation. Values are presented for all subjects (n = 9 for pre-acclimation and Week 4 and n = 8 for Week 2) and were averaged at 5 sampling intervals during cold exposure (time = 30, 60, 90, 120 and 150 min).

Metabolic Rate and Fuel Selection

Changes in metabolic rate, absolute rates of oxidative fuel selection and the relative contribution of these oxidized fuels to the metabolic rate are presented in Table 2. In response to an acute cold exposure, the metabolic rate increased between 2.2 and 2.4-times above levels observed at ambient conditions. The absolute rate of carbohydrate oxidation (RG_{ox}) increased throughout the acute cold exposure, with the cold-induced rate being significantly different between week 2 and week 4 but not compared to the pre-acclimation rate. The rate of lipid oxidation (RF_{ox}) increased 2.5-fold in response to an acute cold exposure in the pre-acclimation condition and after 4 weeks (from 82 ± 7 during ambient exposure to 203 ± 12 $mg \cdot min^{-1}$ during cold exposure in pre-acclimation and from 82 ± 9 to 204 ± 22 $mg \cdot min^{-1}$ after four weeks) and 3-fold after 2 weeks of cold acclimation (from 65 ± 6 to 201 ± 16 $mg \cdot min^{-1}$). A significant temperature by acclimation interaction was detected for the rate of protein oxidation (RP_{ox}) indicating that RP_{ox} increased during acute cold exposure pre-acclimation (from 65 ± 9 to 83 ±

10 mg·min^{-1}) and following two weeks of daily cold exposure (from 47 ± 10 to 75 ± 10 mg·min^{-1}), but not following four weeks of exposure (from 70 ± 10 to 70 ± 7 mg·min^{-1}).

A significant temperature by acclimation interaction was detected for the relative contribution of carbohydrate utilization to total metabolic heat production (%$\dot{M}$), such that it decreased during an acute cold exposure following two weeks of daily cold exposure, compared to the pre-acclimation session and following four weeks of cold acclimation ($P < 0.05$; Table 2). Consequently, the relative contribution of lipid oxidation to total metabolic heat production increased following two weeks of cold exposure compared to pre-acclimation and compared to four weeks of cold-acclimation ($P < 0.05$). The relative contribution of protein oxidation to total metabolic heat production decreased in response to cold exposure in the pre-acclimation condition and after four weeks of daily cold exposure, but was unaltered in Week 2 of cold acclimation ($P < 0.05$).

Table 2. Absolute oxidation of substrates and their relative contribution to the metabolic rate averaged over the final 30 min of the baseline and cold exposure periods prior to, during and following a four-week cold acclimation.

	Pre-acclimation		Week 2		Week 4	
	Baseline	**Cold**	**Baseline**	**Cold**	**Baseline**	**Cold**
$\dot{M}$ (kJ/min)	5.4 ± 0.2	13.2 ± 0.7**	5.6 ±0.2	12.2 ± 0.5**	5.5 ± 0.2	13.0 ± 0.6**
RG_{ox}						
mg/min	58 ± 22	196 ± 46*	129 ± 14	163 ± 28*	52 ± 19	197 ± 38*†
% $\dot{M}$	16.8 ± 5.8	23.1 ± 4.0	37.9 ± 5.1	20.8 ± 3.3#	15.3 ± 5.7	24.8 ±5.2†
RF_{ox}						
mg/min	82 ± 7	203 ± 12**	65 ± 6	201 ± 16**	82 ± 9	204 ± 22**
% $\dot{M}$	61.1 ± 4.7	63.8 ± 3.7	46.3 ± 3.3	64.9 ± 4.0#	60.1 ± 6.4	62.6 ± 5.4†
RP_{ox}						
mg/min	62 ± 8	83 ± 10	47 ± 10	75 ± 10	70 ± 10	70 ± 7#†
% $\dot{M}$	22.2 ± 3.2	13.1 ± 1.9*	15.8 ± 2.8	14.3 ± 1.7#	24.6 ± 3.4	12.6 ± 1.7*†

Values are means ± SE (n = 9 for pre-acclimation and Week 4 and n = 8 for Week 2).

* $P < 0.005$, significantly different than Baseline; **, $P < 0.0001$

# $P < 0.05$, significantly different than pre-acclimation (temperature x acclimation interaction),

† $P < 0.05$, significantly different than week 2 (temperature x acclimation interaction),

DISCUSSION

This study is the first to simultaneously quantify whole body metabolic heat production and electromyographically-determined shivering intensity and pattern of muscle fiber recruitment during an acute cold exposure, following a four week cold acclimation intervention. It was especially important to characterize these changes during acute thermal stress that is colder than the acclimation temperature to ensure that the recruited thermogenic processes are adequately stimulated. Our results showed that the cold-acclimation protocol applied elicited an hypothermic form of acclimation, such that a greater uncompensated drop in T_{core} was presented following four weeks of daily cold exposure (Table 1). Although the metabolic heat production and whole body shivering intensity induced by an acute cold exposure were the same throughout the acclimation protocol, the pattern of muscle recruitment changed significantly. This change in shivering pattern appeared to be driven by changes in the fibre recruitment in proximal muscle groups in particular (Figure 3). Further, there was indirect evidence suggestive of bioenergetic changes in shivering muscles towards a greater coupling between the oxidation of substrates and ATP synthesis to support contractions (improved coupling of oxidative phosphorylation).

Hypothermic form of acclimation

The hypothermic acclimation pattern demonstrated here is characterized by a fall in core temperature (Table 1), due to a blunted metabolic response to the same skin temperature or rate of heat loss (Figure 1). This acclimation pattern is consistent with the adjustments reported in a number of other experimentally-induced cold acclimation studies using cold air exposure for a longer daily exposure [7.5h/day for 17 days and 8 h/day for 31 days; (Keatinge WR, 1960; Davis, 1961)]. This form of acclimation may simply be an unavoidable consequence of

conducting such studies during periods when participants are considered least acclimatized to the cold, in late summer. Under such conditions, the influence of the cold stimulus combined with the heat stress during the day seems to elicit similar cold-acclimation patterns as that observed in primitive people living in temperate weather who experience cold nights and hot days (Scholander *et al.*, 1958). In addition, the undefended fall in core temperature also lends further support to the thermoregulatory model previously proposed, suggesting that shivering is modulated primarily by the stimulation of cutaneous thermal sensory receptors, which respond to skin cooling, rather than stimulation of visceral thermal receptors, which respond to core cooling (Tanaka *et al.*, 2006). Rather, some have suggested that core temperature changes act more through the feedback mechanisms of thermoregulation (Nakamura, 2011), with the present results suggesting a blunting or inhibition of this signaling pathway as a result of daily cold exposure.

Modulating the heat producing mechanisms

Despite the extensive list of studies published regarding the various cold-acclimation patterns in humans, our understanding of the changes to the thermogenic mechanisms recruited remains limited. To our knowledge, the present study is only one of three studies to date to have provided quantitative information on shivering activity resulting from daily cold exposure (Davis, 1961; Blondin *et al.*, 2014). Of those, only one has simultaneously quantified both shivering and BAT-derived cold-induced thermogenesis (Blondin *et al.*, 2014). In that investigation, cold-induced shivering activity and BAT oxidative metabolism and glucose uptake, using PET with ^{11}C-acetate and ^{18}F-fluorodeoxyglucose (^{18}FDG), were measured concurrently in a sub-group of participants from the present investigation exposed to a mild cold (LCS perfused with 17-18 °C water for 3h). Although BAT volume increased by 45% and its

total oxidative capacity increased 2.2-fold in these participants, shivering remained present albeit limited to ~2 % MVC pre and post-acclimation despite whole body heat production also remaining the same in both conditions (1.9×RMR). The use of PET imaging also bears some inherent limitations such that shivering must be kept to a minimum to ensure image quality. Consequently, the acute cold exposures were restricted to an environmental temperature warmer than the acclimation temperature (17-18 °C *vs.* 10 °C, respectively). Interestingly, the majority of cold acclimation studies conducted to date have used experimental protocols where both the acclimation and acute cold exposure experimental sessions are performed at the same environmental temperature [see (Young, 1996) for review]. This limits the extent to which the acclimation-induced changes to the thermogenic mechanisms need to fully manifest themselves and has restricted the full characterization of the thermogenic responses resulting from cold-acclimation. The present study, provides the first attempt at investigating the effects of exposing cold-acclimated men to environmental conditions colder than the temperature to which they were acclimated. These participants maintained their total heat production (1629 ± 46 kJ pre-acclimation *vs.* 1595 ± 68 kJ in Week 4) but presented a delay (from 20 min pre-acclimation to 50 min by Week 4; Figure 2) and shift in the $\overline{T}_{skin}$ to which shivering was initiated (from 27.8 ± 0.6 °C pre-acclimation to 26.3 ± 0.3 °C by Week 4). Despite the same total heat production, the thermogenic contribution of shivering transiently decreased while that of non-shivering mechanisms of heat production increased (Figure 2). Total shivering activity (449 ± 56 %MVC · 150 min pre-acclimation *vs.* 338 ± 59 %MVC · 150 min in Week 4), as measured with EMG, remained the same throughout the four-week acclimation (Figure 3). To determine whether alterations to the shivering pattern could explain these conflicting findings, we also investigated

the recruitment of particular muscle groups and the recruitment of fuel-specific muscle fiber populations.

Changing shivering pattern rather than intensity through acclimation

When examining an EMG recording of shivering muscles, two distinct, superimposed patterns emerge: (1) thermoregulatory muscle tone or continuous, low-intensity shivering (associated with the recruitment of low-threshold type I motor units) and high-intensity burst shivering (associated with the recruitment of high-threshold type II motor units) (Petajan & Williams, 1972; Israel & Pozos, 1989; Meigal, 2002; Haman *et al.*, 2004a). Cold-induced thermogenesis in humans can be maintained despite differences in the muscle fibre recruitment (Haman *et al.*, 2004b) or differences in the recruitment of different metabolic pathways within the same muscle fibres (Haman *et al.*, 2004a; Blondin *et al.*, 2011). These differences in muscle fiber recruitment and recruitment of specific metabolic pathways also influence whole body fuel selection which may subsequently impact the thermogenic contribution of shivering. We hypothesized that the shivering pattern could explain the apparent contradiction between the lack of change in the whole body shivering intensity, yet transient difference in the thermogenic contribution of shivering. Indeed, the total number of bursts throughout the acute cold exposure, indicative of the recruitment of fast type II fibers, was lowest following Week 2 (Figure 3). Further, a strong direct association between total bursts and shivering thermogenesis was apparent ($r = 0.44$, $P = 0.02$), indicating that the thermogenic contribution of shivering was influenced by muscle fibre recruitment. There are a number of plausible explanations for this transient relationship, including either: 1) a transient shift in the muscle fiber recruitment pattern over the course of the four-week acclimation; 2) a shift in muscle fiber composition (*i.e.* muscle fiber-type switching) and subsequent preferential recruitment of these fibers or; 3) an initial shift

in fiber type composition followed by a later shift in the regulation of pathways being recruited within these muscle fibers. The present findings confirm that the recruitment of distinct fibre populations was indeed modulated throughout the cold acclimation, particularly in proximal muscle groups (Figure 3). However, it remains unclear whether this shift in fiber recruitment was a result of a change in recruitment pattern *per se* or a reflection of a change in fiber distribution and subsequent recruitment. A study examining the morphological characteristics of the *m. vastus lateralis* in cold-acclimatized Korean women breath-hold divers compared to non-acclimatized non-divers has demonstrated a greater proportion of type IIx muscle fibers and lower proportion of type IIa muscle fibers in the cold-acclimatized divers compared to their non-acclimatized peers (Bae *et al.*, 2003). This suggests that such a cold-acclimation induced muscle fiber-type switching is plausible, but with the degree of cold stress likely dictating the direction of the switch. For instance, the adaptation of muscle fibers appears mediated by the pattern of motor neuron firing, such that tonic motor neuron activity stimulates a slow oxidative phenotype (upregulation of type I and IIa-specific gene expression) whereas interspersed bursts of high amplitude firing promotes a fast glycolytic phenotype (Chin *et al.*, 1998). Consequently, the fiber recruitment pattern (continuous *vs.* burst shivering) and amplitude of the respective shivering components seen here would lead to the suggestion that the cold-acclimation protocol applied in this investigation could evoke changes towards a slow-fiber-specific phenotype to support an increase in intramuscular triglyceride utilization and preservation of glycogen reserves. Muscle biopsy experiments are required to confirm that such cold-acclimation-induced phenotypic changes to shivering skeletal muscle are indeed occurring. However, judging by the transient fall in burst shivering combined with a relative decrease in burst shivering intensity, there are many indications of the presence of this adaptation.

Fueling shivering thermogenesis

Although cold-induced fuel selection was not modified as a result of this four-week cold acclimation, there are indications of changes in muscle bioenergetics. The relationship between the EMG shivering intensity, used as a surrogate of contraction-mediated ATP utilization, and whole body metabolic heat production was examined. We showed greater coupling between contracting shivering muscles and heat production as a result of daily cold exposure, indicative of changes in the coupling of oxidative phosphorylation (Figure 5). During exercise, bioenergetic efficiency or contraction-coupling efficiency is defined as the external work produced for a given amount of energy expended (Whipp & Wasserman, 1969). However, when examining the relationship between shivering evoked through cold exposure and its by-product, metabolic heat production, we can consider metabolic heat production as analogous to external work and heat produced from exercise and shivering intensity analagous to ATP turnover. A recent investigation demonstrated a cold-induced mitochondrial uncoupling in skeletal muscle of un-acclimatized cold-exposed men (Wijers *et al.*, 2008). In addition, endurance trained individuals exhibit contraction-induced mitochondrial adaptations that include a reduction in mitochondrial uncoupling compared to untrained inviduals (Fernstrom *et al.*, 2004), which may be related to the enhanced capacity to oxidize fatty acids (Noland *et al.*, 2003). If a similar endurance training phenotype develops through daily cold exposure, a similar improvement in mitochondrial coupling would be expected. To date, only a single study has examined the effects of a brief cold-acclimation on skeletal muscle bioenergetics and showed no change in mitochondrial uncoupling (van der Lans *et al.*, 2013). However, the shorter acclimation period (10 days *vs.* 20 days in the present study) combined with limitations in the skeletal muscle respiration experiments in this study hinder the possibility to clearly determine the cold-induced changes in

mitochondrial uncoupling resulting from daily cold exposure. Whether such bioenergetic changes are evoked through chronic cold exposure requires further investigation, but the data reported here lends strong support towards such a change and suggests that it may be significant enough to detect through the simultaneous measurement of whole body energy expenditure and EMG-derived shivering activity.

Conclusion

In this study we characterized the temporal changes in the thermoregulatory responses resulting from daily cold exposure. In particular, we examined the impact of cold acclimation on the facultative mechanisms of heat production with a focus on skeletal muscle thermogenesis. Here, we demonstrate that the cold-acclimation protocol applied elicited an hypothermic form of acclimation, such that a greater uncompensated drop in T_{core} was presented following four weeks of daily cold exposure. More importantly, there were no changes in either the cold-indtuced thermogenesis or shivering intensity, as measured by EMG throughout the cold acclimation. This could be explained by adjustments to the pattern of muscle fiber recruitment, which were most influenced in the more active proximal muscle groups. The whole-body methodologies applied here provided valuable insight into the possible phenotypic changes that are occurring as a result of a repeated thermal stimulation Further examination of the morphological and bioenergetic adjustments in skeletal muscle that are elicited from intermittent cold exposure are clearly warranted in order to establish a more comprehensive picture of the metabolic adaptations occurring from cold acclimation. These studies should ideally combine the application of methodologies that can simultaneously quantify organ-specific metabolism and the impact on whole-body energy expenditure.

ACKNOWLEDGEMENTS

This work was supported by a grant from the Natural Sciences and Engineering Research Council of Canada (NSERC Canada) to FH. DPB is the recipient of the NSERC Postgraduate Scholarship. We also thank the subjects of this study for their collaboration, Olivier Mantha-Landry for his assistance and Allen-Vanguard Inc. (Kevin Semeniuk) for providing the liquid-conditioned suits.

REFERENCES

Bae KA, An NY, Kwon YW, Kim C, Yoon CS, Park SC & Kim CK. (2003). Muscle fibre size and capillarity in Korean diving women. *Acta Physiol Scand* **179,** 167-172.

Bell DG, Tikuisis P & Jacobs I. (1992). Relative intensity of muscular contraction during shivering. *J Appl Physiol* **72,** 2336-2342.

Blondin DP, Labbé SM, Tingelstad HC, Noll C, Kunach M, Phoenix S, Guérin B, Turcotte ÉE, Carpentier AC, Richard D & Haman F. (2014). Increased Brown Adipose Tissue Oxidative Capacity in Cold-Acclimated Humans. *J Clin Endocrinol Metab* **99,** E438-E446.

Blondin DP, Maneshi A, Imbeault MA & Haman F. (2011). Effects of the menstrual cycle on muscle recruitment and oxidative fuel selection during cold exposure. *J Appl Physiol* **111,** 1014-1020.

Brown D, Cole TJ, Dauncey MJ, Marrs RW & Murgatroyd PR. (1984). Analysis of gaseous exchange in open-circuit indirect calorimetry. *Med Biol Eng Comput* **22,** 333-338.

Chaffee RR, Allen JR, Arine RM, Fineg AJ, Rochelle RH & Rosander J. (1975). Studies on thermogenesis in brown adipose tissue in temperature-acclimated Macaca mulatta. *Comp Biochem Physiol A Comp Physiol* **50,** 303-306.

Chin ER, Olson EN, Richardson JA, Yang Q, Humphries C, Shelton JM, Wu H, Zhu W, Bassel-Duby R & Williams RS. (1998). A calcineurin-dependent transcriptional pathway controls skeletal muscle fiber type. *Genes Dev* **12,** 2499-2509.

Davis TRA. (1961). Chamber cold acclimatization in man. *J Appl Physiol* **16,** 1011-1015.

Duchamp C, Cohen-Adad F, Rouanet JL & Barre H. (1992). Histochemical arguments for muscular non-shivering thermogenesis in muscovy ducklings. *J Physiol* **457,** 27-45.

Elia M. (1991). Energy equivalents of CO2 and their importance in assessing energy expenditure when using tracer techniques. *Am J Physiol Endocrinol Metab* **260,** E75-E88.

Elsner RW, Andersen KL & Hermansen L. (1960). Thermal and metabolic responses of Arctic Indians to moderate cold exposure at the end of winter. *J Appl Physiol* **15**.

Fernstrom M, Tonkonogi M & Sahlin K. (2004). Effects of acute and chronic endurance exercise on mitochondrial uncoupling in human skeletal muscle. *J Physiol* **554,** 755-763.

Haman F, Legault SR, Rakobowchuk M, Ducharme MB & Weber J-M. (2004a). Effects of carbohydrate availability on sustained shivering II: relating muscle recruitment to fuel selection. *J Appl Physiol* **96,** 41-49.

Haman F, Legault SR & Weber J-M. (2004b). Fuel selection during intense shivering in humans: EMG pattern reflects carbohydrate oxidation. *J Physiol* **556,** 305-313.

Haman F, Péronnet F, Kenny GP, Doucet E, Massicotte D, Lavoie C & Weber J-M. (2004c). Effects of carbohydrate availability on sustained shivering I: oxidation of plasma glucose, muscle glycogen and proteins. *J Appl Physiol* **96,** 32-40.

Haman F, Péronnet F, Kenny GP, Massicotte D, Lavoie C, Scott C & Weber J-M. (2002). Effect of cold exposure on fuel utilization in humans: plasma glucose, muscle glycogen, and lipids. *J Appl Physiol* **93,** 77-84.

Haman F, Péronnet F, Kenny GP, Massicotte D, Lavoie C & Weber J-M. (2005). Partitioning oxidative fuels during cold exposure in humans: muscle glycogen becomes dominant as shivering intensifies. *J Physiol* **566,** 247-256.

Hammel HT, Elsner RW, Le Messurier DH, Andersen HT & Milan FA. (1959). Thermal and metabolic responses of the Australian aborigine exposed to moderate cold in summer. *J Appl Physiol* **14,** 605-615.

Hardy JD, Dubois EF. (1938). The technic of measuring radiation and convection. *Journal of Nutrition* **15,** 461-475.

Hart JS, Sabean HB, Hildes JA, Depocas F, Hammel HT, Andersen KL, Irving L & Foy G. (1962). Thermal and metabolic responses of coastal Eskimos during a cold night. *J Appl Physiol* **17,** 953-960.

Himms-Hagen J. (2004). Exercise in a pill: feasibility of energy expenditure targets. *Curr Drug Targes CNS Neurol Disord* **3,** 389-409.

Hong SK. (1973). Pattern of cold adaptation in women divers of Korea (ama). *Fed Proc* **32,** 1614-1622.

Israel DJ & Pozos RS. (1989). Synchronized slow-amplitude modulations in the electromyograms of shivering muscles. *J Appl Physiol* **66,** 2358-2363.

Keatinge WR, Evans M. (1960). Effect of food, alcohol and hyoscine on body-temperature and reflex responses of men immersed in cold water. *Lancet* **2,** 176-178.

Launay JC & Savourey G. (2009). Cold adaptations. *Ind Health* **47,** 221-227.

Makinen TM. (2010). Different types of cold adaptation in humans. *Front Biosci (Schol Ed)* **2,** 1047-1067.

Meigal A. (2002). Gross and fine neuromuscular performance at cold shivering. *Int J Circumpolar Health* **61,** 163-172.

Melanson EL, Ingebrigtsen JP, Bergouignan A, Ohkawara K, Kohrt WM & Lighton JR. (2010). A new approach for flow-through respirometry measurements in humans. *Am J Physiol Regul Integr Comp Physiol* **298,** R1571-1579.

Nakamura K. (2011). Central circuitries for body temperature regulation and fever. *Am J Physiol Regul Integr Comp Physiol* **301,** R1207-1228.

Noland RC, Hickner RC, Jimenez-Linan M, Vidal-Puig A, Zheng D, Dohm GL & Cortright RN. (2003). Acute endurance exercise increases skeletal muscle uncoupling protein-3 gene expression in untrained but not trained humans. *Metabolism* **52,** 152-158.

Orava J, Nuutila P, Lidell ME, Oikonen V, Noponen T, Viljanen T, Scheinin M, Taittonen M, Niemi T, Enerback S & Virtanen KA. (2011). Different metabolic responses of human brown adipose tissue to activation by cold and insulin. *Cell Metab* **14,** 272-279.

Ouellet V, Labbe SM, Blondin DP, Phoenix S, Guerin B, Haman F, Turcotte EE, Richard D & Carpentier AC. (2012). Brown adipose tissue oxidative metabolism contributes to energy expenditure during acute cold exposure in humans. *J Clin invest* **122,** 545-552.

Péronnet F & Massicotte D. (1991). Table of nonprotein respiratory quotient: an update. *Can J Sport Sci* **16,** 23-29.

Petajan JH & Williams DD. (1972). Behavior of single motor units during pre-shivering tone and shivering tremor. *Am J Phys Med* **51,** 16-22.

Schaeffer PJ, Villarin JJ & Lindstedt SL. (2003). Chronic cold exposure increases skeletal muscle oxidative structure and function in Monodelphis domestica, a marsupial lacking brown adipose tissue. *Physiol Biochem Zool* **76,** 877-887.

Schaeffer PJ, Villarin JJ, Pierotti DJ, Kelly DP & Lindstedt SL. (2005). Cost of transport is increased after cold exposure in Monodelphis domestica: training for inefficiency. *J Exp Biol* **208,** 3159-3167.

Scholander PF, Hammel HT, Hart JS, Le Messurier DH & Steen J. (1958). Cold Adaptation in Australian aborigine. *J Appl Physiol* **13,** 211-218.

Tanaka M, Owens NC, Nagashima K, Kanosue K & McAllen RM. (2006). Reflex activation of rat fusimotor neurons by body surface cooling, and its dependence on the medullary raphe. *J Physiol* **572,** 569-583.

Teulier L, Rouanet JL, Letexier D, Romestaing C, Belouze M, Rey B, Duchamp C & Roussel D. (2010). Cold-acclimation-induced non-shivering thermogenesis in birds is associated with upregulation of avian UCP but not with innate uncoupling or altered ATP efficiency. *J Exp Biol* **213,** 2476-2482.

van der Lans AAJJ, Hoeks J, Brans B, Vijgen GHEJ, Visser MGW, Vosselman MJ, Hansen J, Jörgensen JA, Wu J, Mottaghy FM, Schrauwen P & van Marken Lichtenbelt WD. (2013). Cold acclimation recruits human brown fat and increases nonshivering thermogenesis. *The Journal of Clinical Investigation* **123,** 0-0.

van Marken Lichtenbelt WD, Vanhommerig JW, Smulders NM, Drossaerts JM, Kemerink GJ, Bouvy ND, Schrauwen P & Teule GJ. (2009). Cold-activated brown adipose tissue in health men. *N Engl J Med* **360,** 1500-1508.

Virtanen KA, Lidell ME, Orava J, Heglind M, Westergren R, Niemi T, Taittonen M, Laine J, Savisto NJ, Enerbäck S & Nuutila P. (2009). Functional brown adipose tissue in healthy adults. *N Engl J Med* **360,** 1518-1525.

Whipp BJ & Wasserman K. (1969). Efficiency of muscular work. *J Appl Physiol* **26,** 644-648.

Wiesinger H, Klaus S, Heldmaier G, Champigny O & Ricquier D. (1990). Increased nonshivering thermogenesis, brown fat cytochrome-c oxidase activity, GDP binding, and uncoupling protein mRNA levels after short daily cold exposure of Phodopus sungorus. *Can J Physiol Pharmacol* **68,** 195-200.

Wijers SL, Schrauwen P, Saris WH & van Marken Lichtenbelt WD. (2008). van Marken Lichtenbelt WD, Vanhommerig JW, Smulders NM, Drossaerts JM, Kemerink GJ, Bouvy ND, Schrauwen P, Teule GJ. *PLoS One* **3,** e1777.

Young AJ. (1996). Homeostatic responses to prolonged cold exposure: human cold acclimatization. In *Handbook of Physiology, Section 4: Environmental Physiology* ed. Fregly MJ & Blatteis CM, pp. 419-438. Oxford University Press, New York.

4. DISCUSSION AND CONCLUSION

Upon starting this doctoral thesis, there were early indications that BAT in adult humans was more prevalent and more physiologically relevant, particularly in cold-induced thermogenesis, than had been estimated previously. We were entering what some considered the "second era of BAT targeting" (Dulloo, 2013). The first era of BAT investigations began in the 1970's where the role of BAT in cold-induced and diet-induced thermogenesis were first identified in rodents (Rothwell & Stock, 1979; Trayhurn *et al.*, 1982; Landsberg *et al.*, 1984) and similarities observed in humans. However, mounting evidence against the relevance of this tissue or the means in which it could be safely pharmaceutically stimulated in humans, lead to a gradual decline in these investigations in humans. Although, radiologists had regularly documented non-tumor related, symmetrical uptake of ^{18}FDG in the supraclavicular region in the early 1990's, which they named USA-fat (short for "Uptake localizing to the Supraclavicular Area - fat" (Hany *et al.*, 2002; Cohade *et al.*, 2003; Yeung *et al.*, 2003; Abouzied *et al.*, 2005). It took several years for the field of nuclear medicine to recognize this uptake as representing BAT, since this tissue was considered to be absent in adult humans, and to acknowledge that cold stimulation was the likely culprit leading to the false-positives this tissue was often creating in the identification of neoplastic pathologies. It was only upon the release of the three seminal papers published in the New England Journal of Medicine in 2009 (Cypess *et al.*, 2009; van Marken Lichtenbelt *et al.*, 2009; Virtanen *et al.*, 2009) that the characterization of BAT metabolism was re-established, thus triggering the start of the second era in BAT research. With BAT considered a vestigial thermoregulatory organ and our laboratory being one of the only groups in the world studying whole body energy metabolism in cold-exposed humans, we were ideally positioned to investigate the thermoregulatory potential of BAT both in non-acclimatized and acclimatized conditions and its incidental effect on the regulation of circulating substrates.

We were most interested in understanding the effect this tissue could have on whole body heat production, fuel selection and in particular shivering thermogenesis. This was attempted by first characterizing the metabolism of BAT under mild cold conditions, investigating the interaction between BAT and skeletal muscle in the context of both thermoregulation and metaboregulation and finally by comparing the plasticity of these two highly thermogenic tissues following a cold-acclimation intervention. What we found was that, indeed, BAT is thermogenically relevant in adult humans and under mild cold conditions its thermogenic contribution compared to shivering muscles varies tremendously between individuals. Further, both BAT and skeletal muscle demonstrated tremendous plasticity as a result of daily cold exposure. However, what was also clear is that both the contribution of BAT thermogenesis to whole body heat production and the ability to clear circulating substrates is quite limited when compared to skeletal muscle. Combined, the findings from this thesis provided indications that BAT may play a more local thermoregulatory role and perhaps clear circulating substrates sufficiently to manage small amounts of substrates in circulation, but unlikely to be sufficiently potent to reverse the effects of diabetes and obesity, where excessive levels of substrates are present.

4.1. BAT metabolism in adult humans

The objective of the first study in this thesis was to determine whether BAT is metabolically active and contributes to cold-induced thermogenesis in humans. More specifically, we aimed to quantify BAT oxidative metabolism as well as glucose and fatty acid uptake during a mild cold exposure using PET with ^{11}C-acetate, ^{18}FDG and ^{18}FTHA. Previous investigations demonstrated that cold-induced glucose uptake was increased in paracervical and supraclavicular UCP-1-positive fat depots, with multilocular intracellular lipid droplets (van Marken Lichtenbelt *et al.*, 2009; Virtanen *et al.*, 2009). However, these findings were consistent

with what had long been known about BAT (Huttunen *et al.*, 1981) and provided no further information regarding the functionality and metabolism of this tissue. Further, the thermal challenges in which participants were exposed to were highly variable, either deliberately (van Marken Lichtenbelt *et al.*, 2009) or inadvertently as a result of applying unconventional cooling methodologies (Virtanen *et al.*, 2009). This was evident by the significant relationship between metabolic rate and BAT glucose uptake reported (van Marken Lichtenbelt *et al.*, 2009). The results from our study provided the first estimates of the oxidative capacity of BAT *in vivo* in adult humans. We found that by reducing skin temperature by ~4.0 °C, evoking a 1.8-fold increase in energy expenditure, resulted in a significant cold-induced activation of BAT oxidative metabolism. Although BAT increased its glucose and NEFA uptake during cold exposure, the rate of their utilization was trivial, accounting for only 1.3% and 0.25% of plasma glucose and NEFA turnover, respectively. Combined with the rapid increase in BAT radio-density during cold exposure, this suggested that the oxidative metabolism of this tissue was supported primarily through intracellular triglyceride utilization. These findings represent the acute metabolism of BAT, during a three hour cold challenge. However, it is unclear what the contribution or metabolic fate of circulating glucose and NEFA might be under more chronic or intense stimulation, where intracellular triglycerides may become depleted, or what the metabolic fate of these substrates might be once the cold exposure is terminated. The full characterization of the transmembrane glucose and fatty acid transport proteins found in BAT (e.g. GLUT4 or CD36) and their latency periods have never been investigated and it is unclear what role these transporters might have on the clearance of circulating substrates and for how long.

A final interesting finding from this study was that, in contrast to previous investigations, there was no significant relationship between the volume of metabolically active BAT and cold-induced energy expenditure. Rather, a significant inverse relationship between BAT volume of activity and the shivering intensity, expressed as a percentage of a maximal voluntary contraction (Spearman r = -0.89), was identified. This demonstrated that under well-controlled mild cold exposure, heat production can be maintained by recruiting a combination of shivering and BAT thermogenesis, with the proportions of each varying from individual-to-individual. This relationship lead us to further investigate the relationship between BAT and shivering muscles, both in the context of thermoregulation as well as clearing circulating substrates. If BAT is to be targeted as an adjunct therapeutic strategy for the treatment of obesity and diabetes, and mild cold exposure provides the safest and most effective method of stimulating BAT, a greater understanding of not only its potential, but the impact of other facultative mechanisms recruited during cold exposure is warranted.

4.2. BAT - skeletal muscle interaction

There have been a number of promising investigations in rodents demonstrating the effectiveness of BAT in regulating: (1) triglyceride clearance (Bartelt *et al.*, 2011); (2) glucose homeostasis and insulin sensitivity (Stanford *et al.*, 2013) and (3) energy balance by dissipating excess energy during cold exposure or excess feeding (Rothwell & Stock, 1979; Feldmann *et al.*, 2009). What has also been evident is the interaction or communication between BAT and other organs such as the liver (Fisher *et al.*, 2012), white adipose tissue (Wu *et al.*, 2012; Rosenwald *et al.*, 2013), the heart (Bordicchia *et al.*, 2012) and skeletal muscle (Bostrom *et al.*, 2012; Yin *et al.*, 2013). However, confirmation of these relationships in humans has remained largely

ambiguous and indications suggest that interpretations of the limited findings may be biased by the results observed in rodents. The general aim of the second manuscript was to examine the relationship of BAT metabolism on whole body thermogenesis and substrate handling and characterize the interaction between BAT and skeletal muscle during a mild cold exposure. More specifically, our objectives were to examine the relationship between whole body sympathetically-induced lipolysis and BAT metabolism, characterize the thermoregulatory and metaboregulatory relationship between BAT activity and skeletal muscle metabolism and map the muscle activation pattern using the complementary techniques of surface EMG and PET/CT under mild cold conditions.

In prediabetic and diabetic individuals catecholamine-mediated lipolysis of intracellular TG in WAT is impaired, which appears to be associated with excess adiposity (Grenier-Larouche *et al.*, 2012). With BAT thermogenesis both stimulated and fueled by sympathetic nervous system-mediated lipolysis of intracellular TG into fatty acids (Cannon & Nedergaard, 2004), the consequence of a similar lipolytic dysfunction in brown adipocytes would likely result in a blunted or inhibited BAT thermogenic activity and thus solicit a greater heat production from shivering skeletal muscles. Until now, the relationship between catecholamine-mediated lipolysis of intracellular TG in WAT and sympathetically-induced BAT activation in humans has remained unclear. We showed that catecholamine-mediated WAT lipolysis, as measured by the cold-induced change in NEFA appearance rate, was strongly associated with the volume of metabolically active BAT, total BAT oxidative metabolism and BAT glucose uptake. This strong association suggests that perhaps the impaired catecholamine-mediated lipolysis of intracellular TG may be generalized to all adipose tissue and may explain the absence or impaired function of cold-induced BAT activity in individuals who are morbidly obese or diabetic (Vijgen *et al.*,

2011; Orava *et al.*, 2013), as previously suggested (Grenier-Larouche *et al.*, 2012). The consequence of a similar lipolytic dysfunction in brown adipocytes would likely result in a greater contribution to heat production from shivering skeletal muscles, which do not appear to be influenced by the catecholamine-mediated lipolysis.

To begin teasing out the interaction between BAT metabolism and shivering activity as well as their effect on whole body energy metabolism, we examined the association between shivering intensity and the volume of metabolically active BAT as well as its oxidative capacity. In contrast to the association identified in our first manuscript (Ouellet *et al.*, 2012), no discernible relationship was found between shivering intensity and BAT metabolic activity. This, in part, may be explained by either a limitation in the study design such that a greater variability in both BAT oxidative capacity and shivering intensity would be expected at a colder thermal challenge, or simply resulting from an apparent dichotomy in the presence of BAT. While 100% of our participants, to date, have shown a presence of metabolically active BAT, a dichotomous trend has begun appearing whereby some individuals demonstrate a large volume of BAT activity (>200 mL) whereas others demonstrate a small volume of BAT activity (<100 mL). This trend appears to be consistent with what has also been presented in the literature to date (Muzik *et al.*, 2013), where in some instances groups have been incorrectly defined as BAT-negative (a misnomer, incorrectly suggesting an absence of BAT) or BAT-positive (Saito *et al.*, 2009). These individuals categorized as BAT-negative do in fact demonstrate a presence of BAT, as defined using the currently accepted criteria (radio-density between -30 and -150 Hounsfield units and ^{18}FDG uptake of more than 1.5 SUV unit, representing a value 4-6 times greater than WAT). Interestingly, no relationship was observed between the cold-induced changes in whole body oxygen consumption and either BAT volume of activity, BAT oxidative metabolism or

shivering intensity. In brief, this suggests that core temperature is defended by indiscriminately recruiting the necessary thermoeffectors to produce heat. Although the temperature thresholds to activate each cold-defence thermoeffector may differ, no more heat will be produced than what is necessary. This is in stark contrast to the strong associations regularly presented in the literature demonstrating a relationship between cold-induced thermogenesis and BAT glucose uptake (van Marken Lichtenbelt *et al.*, 2009; Yoneshiro *et al.*, 2011; Chen *et al.*, 2013; Yoneshiro *et al.*, 2013) or BAT perfusion (Orava *et al.*, 2011; Muzik *et al.*, 2013). Aside from the single study whereby the cooling protocol is deliberately adjusted for each participant (van Marken Lichtenbelt *et al.*, 2009), the results of these other studies either defy the laws of thermodynamics or, more likely, the cold challenge is uncontrolled and not equivalent between individuals. If faced with a similar thermal challenge, energy expenditure would be expected to increase in all individuals, not just those presenting larger volumes of BAT since the thermogenic cold-defence effectors are both stimulated by changes in skin temperature [see review from Morrison (2011)].

Expanding our investigation of the metabolic interaction between BAT and shivering muscles, we then aimed to examine their respective roles in regulating circulating substrates. Although it should come as no surprise, glucose uptake and plasma glucose turnover were both more than one order of magnitude greater in skeletal muscle compared to BAT in cold-exposed humans. With BAT mass representing ~1% of total body weight in adult humans compared to the ~42% represented by skeletal muscle (Rolfe & Brown, 1997) combined with the generalized muscle recruitment inherent in shivering, the overall potential for skeletal muscle to clear circulating substrates during cold exposure *via* contraction-mediated pathways is significantly greater. Particular muscles were preferentially recruited to produce heat during cold exposure,

which would incidentally lead to circulating substrates being channeled preferentially towards these same muscles. Indeed, whether examining individual muscles or grouping them according to their anatomical location, it was clear that under mild cold conditions deep, centrally-located muscles were preferentially recruited and thus clearing plasma glucose to a greater extent than superficial, peripherally-located muscles. This was consistent with previous observations made using surface EMG (Bell *et al.*, 1992), but also highlighted some of the limitations presented with the use of surface EMG under such thermal conditions. As the method implies, surface EMG only provides accurate estimates of muscle activity in muscles located superficially. Although, electromyographic signals from deep muscles may be picked up in the process, it is impossible to determine their contribution to shivering using this technique. As will be discussed in **4.4. Future prospectives and final conclusions**, the recruitment of centrally-located muscles may have important adaptive consequences which may shed some light on the interaction between BAT and skeletal muscle.

4.3. Cold acclimation

To investigate the plasticity of both BAT and skeletal muscle, participants underwent a four week cold acclimation intervention. The goal was to fill many of the large gaps in the cold acclimation literature as it pertains to energy metabolism. Despite the large number of cold acclimation and *acclimatization* studies previously conducted, a number of key variables had never been explicitly examined. First, only a single cold *acclimatization* or acclimation study has ever documented differences in BAT mass/volume as a result of repeated cold exposure in humans (Huttunen *et al.*, 1981). Since this necropsy study simply examined the volume and histobiochemical activity of mitochondrial enzymes from excised BAT, it was never clear what

the functionality of this tissue could be *in vivo* under an acute cold challenge. Inferences made from the remaining cold acclimation studies stemmed from the apparent association between oxygen consumption or energy expenditure and shivering activity, whereby a decrease in cold-induced thermogenesis was commonly associated with a decrease in shivering and thus a greater thermogenic contribution of non-shivering thermogenesis. This, despite the former only having ever been directly measured in a single study (Davis, 1961). In addition, experimental, acute cold exposures have only ever been performed under thermal conditions that were either the same or warmer than the acclimation temperature. Consequently, any phenotypic changes would likely not be fully evoked due to the limited thermal challenge relative to the acclimation thermal stresses. In light of these significant gaps in the literature, our goal was to examine the effects of a four week cold acclimation at 10°C on BAT volume and oxidative capacity *in vivo* as well as quantify the subsequent effect on shivering muscles under a mild (17-18°C) and moderate cold challenge (4°C).

4.3.1. Effects of a mild cold exposure (warmer than acclimation temperature). Evidence from animal models (Cannon & Nedergaard, 2004) and indirect-support from human studies (Huttunen *et al.*, 1981; Vijgen *et al.*, 2012) have suggested an inherent plasticity to BAT, presenting signs of increased recruitment. The differentiation of both types of brown adipocytes (classical and beige/brite) (Wu *et al.*, 2012; Schulz *et al.*, 2013; Yin *et al.*, 2013) and its activation (van Marken Lichtenbelt *et al.*, 2009; Virtanen *et al.*, 2009; Ouellet *et al.*, 2012) appear to be largely mediated by a sympathetic input. To date, the most potent and effective sympathetic stimulator of BAT differentiation and activation in humans has been cold exposure, as most sympathomimetics applied *in vivo* have shown little to no effect on BAT activation (Cypess *et al.*, 2012; Vosselman *et al.*, 2012; Carey *et al.*, 2013). The third study of this thesis

showed that, indeed, repeated sympathetic input from daily cold exposure can increase the volume of metabolically active BAT by 45%, but more importantly, increase its oxidative capacity 2.2-fold. This was paralleled by an increase in fractional and net glucose uptake by BAT. Two recent investigations that were published just prior to submitting this manuscript for peer review, documented similar changes in volume of BAT activity (van der Lans *et al.*, 2013) and glucose uptake [as measured by mean SUV; (Yoneshiro *et al.*, 2013)]. The former also attempted to estimate non-shivering thermogenesis based on the assumption that 10% of total BAT metabolism in rats is derived from glucose uptake (Ma & Foster, 1986). What we clearly showed is that glucose uptake, using PET with ^{18}FDG, is highly dependent on the TG content of the tissue and that the uptake of this tracer can only reliably be used, at best, to estimate BAT volume of activity. It is only by using PET with ^{11}C-acetate that we could precisely quantify the changes in the oxidative capacity of the tissue as a result of cold acclimation, providing the first estimates of the functional changes to BAT in humans. Interestingly, the significant changes on BAT oxidative metabolism had no effect on shivering intensity, measured either by surface EMG or the net uptake of ^{18}FDG in skeletal muscle (presented as a shivering index). We, as well as reviewers, found these results quite perplexing. There are a number of plausible explanations for such findings, but focus on the following. First, it is possible that the acute cold challenge was insufficient to produce a significant decrease in shivering, since shivering was already limited to ~2.0 % MVC. We suggested that perhaps a colder thermal stress might have provided the necessary stimulus to reduce muscle activity, but is not possible using nuclear imaging techniques as the additional movement would impact the fusion of PET/CT images and the results from dynamic PET acquisition. With the final study in this thesis, whereby participants were exposed to a temperature colder than the acclimation temperature, we expected to see the

effect of the cold acclimation fully manifested. However, as will be discussed in the next section, this was not the case. Second, EMG activity is limited to largely superficial muscles. It is possible that deeper muscles are preferentially recruited and influenced more significantly by the increase in BAT oxidative capacity. To investigate this hypothesis, we examined both the biodistribution of ^{18}FDG in skeletal muscles as well as the oxidative metabolism index (K_{mono}, using ^{11}C-acetate) of the muscles observable in the 18 cm PET dynamic field of view. Both outcomes suggested decreases in some muscles, such as pectoralis major and sternocleidomastoid, but on the whole, muscle recruitment remained relatively unchanged as a result of cold-acclimation. Finally, EMG activity provides some insight on the muscle fiber recruitment, which can impact muscle fuel selection (Haman *et al.*, 2004a; Haman *et al.*, 2004b; Haman *et al.*, 2005). However, detecting possible changes in bioenergetic efficiency is not possible with this technique, but is an adaptation which may have occurred in this study (see **Appendix D**, for changes in fiber type and muscle bioenegetics). A possible training effect in skeletal muscle, resulting from daily muscle activity, would be a decrease in mitochondrial uncoupling. Such changes in muscle bioenergetics would essentially shift the non-shivering components of whole body thermogenesis from skeletal muscle to BAT. Although this study provided valuable insight on the phenotypic changes to BAT, many questions remained regarding its full thermogenic potential. This lead us to further investigate its role under a colder thermal challenge.

4.3.2. Effects of a moderate cold exposure (colder than acclimation temperature). Understanding the full thermogenic capacity of BAT requires that it be thermally challenged. In our previous study, the experimental design was limited by the degree of cold stimuli that could

be applied to ensure that adequate PET images could be obtained. Ultimately, the goal was to determine the extent that BAT increased in volume and whether its oxidative machinery had also changed through daily cold exposure. Since BAT volume is determined by the volume of ^{18}FDG uptake in the supraclavicular BAT depot, it need only to be metabolically active to take up the threshold levels of ^{18}FDG required to delimit its volume and distinguish the tissue from WAT. However, we expected that in order to examine the thermogenic potential of BAT both shivering and BAT activity would need to be stimulated simultaneously. We anticipated that exposure to 18°C, as in the previous study, would be insufficient and that a thermal stress colder than the acclimation temperature would be required to ensure that both thermogenic cold-defence effectors could contribute to the cold-induced rise in energy expenditure. This portion of the study not only allowed us to determine the effect of changes to BAT metabolism on shivering activity and whole body energy expenditure, but also allowed us to estimate the time-course of these changes. In addition, muscle biopsies were collected (not reported in manuscript, but presented in **Appendix D**), to examine the phenotypic changes in skeletal muscle as a result of daily cold exposure. We hypothesized that since the adaptation of muscle fibers appears mediated by the pattern of motor neuron firing, such that tonic motor neuron activity stimulates a slow oxidative phenotype (upregulation of type I and IIa-specific gene expression) whereas interspersed bursts of high amplitude firing promotes a fast glycolytic phenotype (Chin *et al.*, 1998), the fiber recruitment pattern (continuous *vs.* burst shivering) and amplitude of the respective shivering components traditionally observed in our acute cold exposure studies (Haman *et al.*, 2004a) would evoke changes towards a slow-fiber-specific phenotype. Interestingly, even at these thermal conditions, changes in BAT oxidative capacity were insufficient to induce a reduction in shivering intensity. Rather, we observed a delay and shift in

the mean skin temperature threshold for the onset of shivering. We estimated that the thermogenic contribution of shivering and non-shivering thermogenesis (*e.g.* mitochondrial uncoupling in BAT and skeletal muscle) was transiently modulated following two weeks of daily exposure, before returning to pre-acclimation levels after four weeks. Since BAT oxidative metabolism had increased significantly over the four weeks (see **4.3.1. Effects of a mild cold exposure**) and the cold-induced rise in mitochondrial uncoupling was abolished within that same time period, it is possible that the second week represents a disproportionate shift in the phenotypic changes between these two tissues. In other words, perhaps the changes in contraction-stimulated fiber-type switch combined with bioenergetic changes in shivering muscles occurred at different rates than the recruitment and changes in the oxidative machinery in BAT and that by the fourth week of acclimation these changes had stabilized. Since PET scans and muscle biopsies were only taken pre and post-acclimation, it is not possible to verify this hypothesis. Changes in the EMG signature over the four weeks suggest that significant adjustments are occurring by the second week. This may reflect either a change in the recruitment pattern of existing fibers, with a decrease in total bursts representing a shift towards recruitment of type I muscle fibers and/or a shift in fiber composition within the same activated muscles. The shift in EMG signature appeared to be greatest in proximal muscles which may simply be a reflection of the preferential recruitment of these muscles.

What this study nicely demonstrated was the extent to which redundant mechanisms are recruited to defend our core temperature. Although significant adjustments were made to the BAT and skeletal muscle phenotype in our cold-acclimated participants, ultimately cold-defence effectors were recruited to the extent necessary to maintain a constant heat production. Further, the undefended fall in core temperature observed by the fourth week of cold acclimation not only

reinforced the feedback role of visceral thermal receptors, but also demonstrated how the acclimation profile can differ based on the extended environmental conditions. For example, since this cold acclimation study was largely performed at the end of the summer, the influence of the cold stimulus combined with the heat stress during the day seemed to elicit similar cold-acclimation patterns as that observed in primitive people living in temperate weather who experience cold nights and hot days (Scholander *et al.*, 1958). Such an acclimation pattern, differs from those who experience cold days and cold nights, such as aboriginals from Central Australia (Hammel *et al.*, 1959) and North American Inuit (Elsner *et al.*, 1960; Hart *et al.*, 1962).

4.4. Future prospectives and final conclusions

Collectively, the results from the four manuscripts presented in this thesis have begun filling some of the significant gaps in the literature pertaining to energy metabolism in the cold. It has shifted not only our perspective and understanding regarding cold-induced energy metabolism and the coordination of various thermogenic organs, but in the process has ultimately humbled our future interpretations. Prior to our first study, the cold-induced energy metabolism narrative read almost exclusively as the relationship between shivering muscles and their effect on whole body heat production and fuel selection [see review from Haman, (2006)]. This is understandable given that BAT was considered thermogenically irrelevant in humans beyond infancy. While the results from the studies presented in this thesis suggest that from a whole-body perspective this may not be entirely false, there are still important indications that BAT plays an ancillary role to skeletal muscle during mild to moderate cold exposure and that communication between muscle and BAT may have important and relevant implications. For example, the supraclavicular and paraspinal localization of BAT (see **Figure 1.**) suggest that it likely plays a significant role in local heat production for the purpose of heating blood heading

towards the brain and ensuring adequate conductivity of neurons in the spinal cord to support central and peripheral nervous system function. There are three indications, that we are aware of, that demonstrate a possible link between skeletal muscle and BAT function which we hypothesize serves a well adapted function of alleviating or supporting the thermoregulatory responsibility of skeletal muscle.

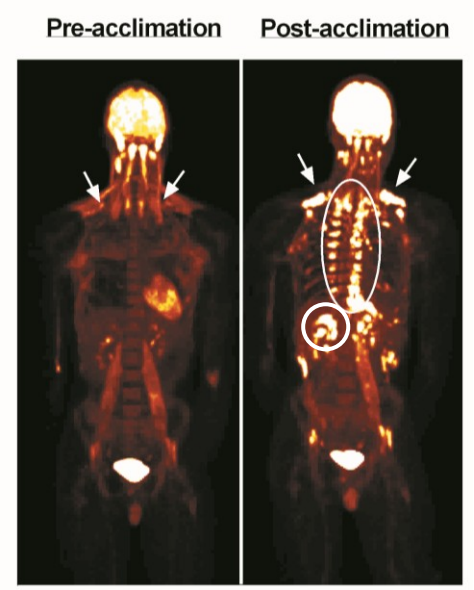

Figure 1. BAT anatomical localization.

First, since a rise in core temperature has been shown to have an inhibitory effect on the fusimotor response to skin cooling (Tanaka *et al.*, 2006), it is possible that individuals demonstrating a greater volume of BAT, which are more likely to have substantial paraspinal BAT depots (Ouellet *et al.*, 2011), may be locally heating the spinal nuclei involved in the stimulation of fusimotor fibers, thus as a consequence blunting the shivering response. This would explain the dichotomous distribution in the volume of metabolically active BAT and the shivering response. The second indication stems from the discovery of a WAT-browning myokine, irisin, that is released from skeletal muscle during endurance exercise (Bostrom *et al.*, 2012) which suggests that the signal being relayed is that there is a greater persistent need for motor movements. Consequently, skeletal muscle must necessarily shift the responsibility of

passive heating to BAT in view of this greater voluntary motor demand. Similarly, the third indication stems from the identification of a microRNA, microRNA-133, which regulates the determination of skeletal muscle stem cells/satellite cells towards either a myogenic- or BAT-specific fate (Yin *et al.*, 2013). Following 1 week of cold exposure, *miR*-133 in mice is downregulated which induces satellite cells to differentiate into brown adipocytes. Interestingly, the greatest shift towards a BAT-specific fate was observed in satellite cells derived from intercostal and paraspinal muscles. If the muscle recruitment pattern of shivering mice are similar to adult humans, these paraspinal muscles would likely be the most active during cold exposure.

Much work remains to be done if we are to fully understand the role of BAT on whole body energy expenditure and substrate handling, particularly if it is being considered as an adjunct therapeutic target to counteract the effects of obesity and diabetes. Although significant progress has been made in characterizing its developmental origin (Sharp *et al.*, 2012; Wu *et al.*, 2012), function (Ouellet *et al.*, 2012; Vosselman *et al.*, 2013) and distribution (Ouellet *et al.*, 2011; Cypess *et al.*, 2013). Greater caution in the design of future studies is necessary if we are to fully characterize the function of this tissue. Currently, we are experiencing challenges in interpreting the findings of *in vivo* studies in humans, due to poor cold exposure designs or the inappropriate use of PET tracers and the subsequent interpretation of the PET data. For example, the consensus regarding the prevalence and activity of BAT in obese and diabetic individuals is that this tissue is inactive or defective in these populations (Saito *et al.*, 2009; Ouellet *et al.*, 2011; Vijgen *et al.*, 2011; Orava *et al.*, 2013). However, given that the TG pool in the BAT depots are likely full in these populations and that ^{18}FDG is highly influenced by TG content (see Article III), it is highly likely that the presence and metabolic activity of this tissue is being

disproportionally under-estimated in these populations, simply through the use of an inappropriate radio-tracer. Since such findings tend to fit with rodent models, a confirmation bias is swaying the interpretation of the results. Consequently in studies examining BAT metabolism in obese and diabetic individuals, tracers that are not influenced by the energy status of the tissue or the substrates being used within it, such as ^{11}C-acetate or ^{15}O, should be favoured. In addition, clarifying the possible relationship between WAT and BAT lipolysis will be critical in understanding the pathogenesis of metabolic diseases such as obesity and diabetes. Finally, the role of BAT in post-prandial metabolism also requires further clarification, since BAT appears to play a substantial role in handling excessive energy substrates, particularly in clearing meal-derived TG (Bartelt *et al.*, 2011).

5. CONTRIBUTION OF AUTHORS AND CO-AUTHORS

Thesis article #1:

All authors contributed to the conception and design of the experiments. Data collection, analysis and interpretation of data were performed by SM Labbé and DP Blondin. All authors contributed to the drafting and critical revising of the manuscript. All authors have approved the final version of the manuscript. Experiments were performed at the University of Sherbrooke.

Thesis article #2:

All authors contributed to the conception and design of the experiments. Data collection, analysis and interpretation of data were performed by DP Blondin. All authors contributed to the drafting and critical revising of the manuscript. All authors have approved the final version of the manuscript. Experiments were performed at the University of Sherbrooke.

Thesis article #3:

All authors contributed to the conception and design of the experiments. Data collection, analysis and interpretation of data were performed by DP Blondin. All authors contributed to the drafting and critical revising of the manuscript. All authors have approved the final version of the manuscript. Experiments were performed at the University of Sherbrooke.

Thesis article #4:

All authors contributed to the conception and design of the experiments. Data collection, analysis and interpretation of data were performed by DP Blondin. All authors contributed to the drafting and critical revising of the manuscript. All authors have approved the final version of the manuscript. Experiments were performed at the University of Sherbrooke.

6. REFERENCES

REFERENCE LIST

Abouzied MM, Crawford ES & Nabi HA. (2005). 18F-FDG imaging: pitfalls and artifacts. *J Nucl Med Technol* **33,** 145-155; quiz 162-143.

Aherne W & Hull D. (1966). Brown adipose tissue and heat production in the newborn infant. *J Pathol Bacteriol* **91,** 223-234.

Armbrecht JJ, Buxton DB, Brunken RC, Phelps ME & Schelbert HR. (1989). Regional myocardial oxygen consumption determined noninvasively in humans with [1-11C]acetate and dynamic positron tomography. *Circulation* **80,** 863-872.

Au-Yong IT, Thorn N, Ganatra R, Perkins AC & Symonds ME. (2009). Brown adipose tissue and seasonal variation in humans. *Diabetes* **58,** 2583-2587.

Baba S, Jacene HA, Engles JM, Honda H & Wahl RL. (2010). CT Hounsfield units of brown adipose tissue increase with activation: preclinical and clinical studies. *J Nucl Med* **51,** 246-250.

Bae KA, An NY, Kwon YW, Kim C, Yoon CS, Park SC & Kim CK. (2003). Muscle fibre size and capillarity in Korean diving women. *Acta Physiol Scand* **179,** 167-172.

Bartelt A, Bruns OT, Reimer R, Hohenberg H, Ittrich H, Peldschus K, Kaul MG, Tromsdorf UI, Weller H, Waurisch C, Eychmuller A, Gordts PL, Rinninger F, Bruegelmann K, Freund B, Nielsen P, Merkel M & Heeren J. (2011). Brown adipose tissue activity controls triglyceride clearance. *Nat Med* **17,** 200-205.

Bell DG, Tikuisis P & Jacobs I. (1992). Relative intensity of muscular contraction during shivering. *J Appl Physiol* **72,** 2336-2342.

Bittel JH. (1987). Heat debt as an index for cold adaptation in men. *J Appl Physiol* **62,** 1627-1634.

Blondin DP, Dépault I, Imbeault P, Péronnet F, Imbeault M-A & Haman F. (2010). Effects of two glucose ingestion rates on substrate utilization during moderate-intensity shivering. *Eur J Appl Physiol* **108,** 289-300.

Blondin DP, Labbé SM, Tingelstad HC, Noll C, Kunach M, Phoenix S, Guérin B, Turcotte ÉE, Carpentier AC, Richard D & Haman F. (2014). Increased Brown Adipose Tissue Oxidative Capacity in Cold-Acclimated Humans. *J Clin Endocrinol Metab* **99,** E438-E446.

Blondin DP, Maneshi A, Imbeault MA & Haman F. (2011). Effects of the menstrual cycle on muscle recruitment and oxidative fuel selection during cold exposure. *J Appl Physiol* **111,** 1014-1020.

Bordicchia M, Liu D, Amri EZ, Ailhaud G, Dessi-Fulgheri P, Zhang C, Takahashi N, Sarzani R & Collins S. (2012). Cardiac natriuretic peptides act via p38 MAPK to induce the brown fat thermogenic program in mouse and human adipocytes. *J Clin invest* **122,** 1022-1036.

Bostrom P, Wu J, Jedrychowski MP, Korde A, Ye L, Lo JC, Rasbach KA, Bostrom EA, Choi JH, Long JZ, Kajimura S, Zingaretti MC, Vind BF, Tu H, Cinti S, Hojlund K, Gygi SP & Spiegelman BM. (2012). A PGC1-alpha-dependent myokine that drives brown-fat-like development of white fat and thermogenesis. *Nature* **481,** 463-468.

Brito NA, Brito MN & Bartness TJ. (2008). Differential sympathetic drive to adipose tissues after food deprivation, cold exposure or glucoprivation. *Am J Physiol Regul Integr Comp Physiol* **294,** R1445-1452.

Brown D, Cole TJ, Dauncey MJ, Marrs RW & Murgatroyd PR. (1984). Analysis of gaseous exchange in open-circuit indirect calorimetry. *Med Biol Eng Comput* **22,** 333-338.

Brown M, Marshall DR, Sobel BE & Bergmann SR. (1987). Delineation of myocardial oxygen utilization with carbon-11-labeled acetate. *Circulation* **76,** 687-696.

Brown MA, Myears DW & Bergmann SR. (1989). Validity of estimates of myocardial oxidative metabolism with carbon-11 acetate and positron emission tomography despite altered patterns of substrate utilization. *J Nucl Med* **30,** 187-193.

Buck A, Wolpers HG, Hutchins GD, Savas V, Mangner TJ, Nguyen N & Schwaiger M. (1991). Effect of carbon-11-acetate recirculation on estimates of myocardial oxygen consumption by PET. *J Nucl Med* **32,** 1950-1957.

Buxton DB, Schwaiger M, Nguyen A, Phelps ME & Schelbert HR. (1988). Radiolabeled acetate as a tracer of myocardial tricarboxylic acid cycle flux. *Circ Res* **63,** 628-634.

Campero M, Serra J, Bostock H & Ochoa JL. (2001). Slowly conducting afferents activated by innocuous low temperature in human skin. *J Physiol* **535,** 855-865.

Cannon B & Nedergaard J. (2004). Brown adipose tissue: function and physiological significance. *Physiol Rev* **84,** 277-359.

Cannon B & Nedergaard J. (2010). Metabolic consequences of the presence or absence of the thermogenic capacity of brown adipose tissue in mice (and probably in humans). *Int J Obes (Lond)* **34 Suppl 1,** S7-16.

Carey AL, Formosa MF, Van Every B, Bertovic D, Eikelis N, Lambert GW, Kalff V, Duffy SJ, Cherk MH & Kingwell BA. (2013). Ephedrine activates brown adipose tissue in lean but not obese humans. *Diabetologia* **56,** 147-155.

Carpentier A, Patterson BW, Uffelman KD, Giacca A, Vranic M, Cattral MS & Lewis GF. (2001). The effect of systemic versus portal insulin delivery in pancreas transplantation on insulin action and VLDL metabolism. *Diabetes* **50,** 1402-1413.

Carpentier AC, Frisch F, Brassard P, Lavoie F, Bourbonnais A, Cyr D, Giguere R & Baillargeon JP. (2007). Mechanism of insulin-stimulated clearance of plasma nonesterified fatty acids in humans. *Am J Physiol Endocrinol Metab* **292,** E693-701.

Carpentier AC, Frisch F, Cyr D, Genereux P, Patterson BW, Giguere R & Baillargeon JP. (2005). On the suppression of plasma nonesterified fatty acids by insulin during enhanced intravascular lipolysis in humans. *Am J Physiol Endocrinol Metab* **289,** E849-856.

Carpentier AC, Labbé SM, Grenier-Larouche T & Noll C. (2011). Abnormal dietary fatty acid metabolic partitioning in insulin resistance and Type 2 diabetes. *Clinical Lipidology* **6,** 703-716.

Casey KL, Minoshima S, Morrow TJ & Koeppe RA. (1996). Comparison of human cerebral activation pattern during cutaneous warmth, heat pain, and deep cold pain. *J Neurophysiol* **76,** 571-581.

Castellani JW, Sawka MN, DeGroot DW & Young AJ. (2010). Cold thermoregulatory responses following exertional fatigue. *Front Biosci* **Jun 1,** 854-865.

Chaffee RR, Allen JR, Arine RM, Fineg AJ, Rochelle RH & Rosander J. (1975). Studies on thermogenesis in brown adipose tissue in temperature-acclimated Macaca mulatta. *Comp Biochem Physiol A Comp Physiol* **50,** 303-306.

Chaffee RR & Roberts JC. (1971). Temperature acclimation in birds and mammals. *Annu Rev Physiol* **33,** 155-202.

Chen KY, Brychta RJ, Linderman JD, Smith S, Courville A, Dieckmann W, Herscovitch P, Millo CM, Remaley A, Lee P & Celi FS. (2013). Brown fat activation mediates cold-induced thermogenesis in adult humans in response to a mild decrease in ambient temperature. *J Clin Endocrinol Metab* **98,** E1218-1223.

Chin ER, Olson EN, Richardson JA, Yang Q, Humphries C, Shelton JM, Wu H, Zhu W, Bassel-Duby R & Williams RS. (1998). A calcineurin-dependent transcriptional pathway controls skeletal muscle fiber type. *Genes Dev* **12,** 2499-2509.

Ci X, Frisch F, Lavoie F, Germain P, Lecomte R, van Lier JE, Benard F & Carpentier AC. (2006). The effect of insulin on the intracellular distribution of 14(R,S)-[18F]Fluoro-6-thia-heptadecanoic acid in rats. *Mol Imaging Biol* **8,** 237-244.

Cohade C, Mourtzikos KA & Wahl RL. (2003). "USA-Fat": prevalence is related to ambient outdoor temperature-evaluation with 18F-FDG PET/CT. *J Nucl Med* **44,** 1267-1270.

Commission IT. (2001). Glossary of terms for thermal physiology. Second edition. Revised by The Commission for Thermal Physiology of the International Union of Physiological Sciences (IUPS Thermal Commission). *Japanese Journal of Physiology* **51,** 245-280.

Craig AD, Chen K, Bandy D & Reiman EM. (2000). Thermosensory activation of insular cortex. *Nat Neurosci* **3,** 184-190.

Croteau E, Lavallée E, Labbe SM, Hubert L, Pifferi F, Rousseau JA, Cunnane SC, Carpentier AC, Lecomte R & Bénard F. (2010). Image-derived input function in dynamic human PET/CT: methodology and validation with 11C-acetate and 18F-fluorothioheptadecanoic acid in muscle and 18F-fluorodeoxyglucose in brain. *Eur J Nucl Med Mol Imaging* **37,** 1539-1550.

Cypess AM, Chen YC, Sze C, Wang K, English J, Chan O, Holman AR, Tal I, Palmer MR, Kolodny GM & Kahn CR. (2012). Cold but not sympathomimetics activates human brown adipose tissue in vivo. *Proc Natl Acad Sci U S A* **109,** 10001-10005.

Cypess AM, Lehman S, Williams G, Tal I, Rodman D, Goldfine AB, Kuo FC, Palmer EL, Tseng YH, Doria A, Kolodny GM & Kahn CR. (2009). Identification and importance of brown adipose tissue in adult humans. *N Engl J Med* **360,** 1509-1517.

Cypess AM, White AP, Vernochet C, Schulz TJ, Xue R, Sass CA, Huang TL, Roberts-Toler C, Weiner LS, Sze C, Chacko AT, Deschamps LN, Herder LM, Truchan N, Glasgow AL, Holman AR, Gavrila A, Hasselgren PO, Mori MA, Molla M & Tseng YH. (2013). Anatomical localization, gene expression profiling and functional characterization of adult human neck brown fat. *Nat Med* **19,** 635-639.

Darian-Smith I, Johnson KO & Dykes R. (1973). "Cold" fiber population innervating palmar and digital skin of the monkey: responses to cooling pulses. *J Neurophysiol* **36,** 325-346.

Davidson AG & Buford JA. (2004). Motor outputs from the primate reticular formation to shoulder muscles as revealed by stimulus-triggered averaging. *J Neurophysiol* **92,** 83-95.

Davis KD, Kwan CL, Crawley AP & Mikulis DJ. (1998). Functional MRI study of thalamic and cortical activations evoked by cutaneous heat, cold, and tactile stimuli. *J Neurophysiol* **80,** 1533-1546.

Davis TRA. (1961). Chamber cold acclimatization in man. *J Appl Physiol* **16,** 1011-1015.

DeGrado TR, Coenen HH & Stocklin G. (1991). 14(R,S)-[18F]fluoro-6-thia-heptadecanoic acid (FTHA): evaluation in mouse of a new probe of myocardial utilization of long chain fatty acids. *J Nucl Med* **32,** 1888-1896.

DeGrado TR, Wang S, Holden JE, Nickles RJ, Taylor M & Stone CK. (2000). Synthesis and preliminary evaluation of (18)F-labeled 4-thia palmitate as a PET tracer of myocardial fatty acid oxidation. *Nucl Med Biol* **27,** 221-231.

Dubois D & Dubois EF. (1916). A formula to estimate the approximate surface area if height and weight be known. *Arch Inter Med* **17,** 863-871.

Duchamp C, Cohen-Adad F, Rouanet JL & Barre H. (1992). Histochemical arguments for muscular non-shivering thermogenesis in muscovy ducklings. *J Physiol* **457,** 27-45.

Dulloo AG. (2013). Translational issues in targeting brown adipose tissue thermogenesis for human obesity management. *Ann N Y Acad Sci* **1302,** 1-10.

Egan GF, Johnson J, Farrell M, McAllen R, Zamarripa F, McKinley MJ, Lancaster J, Denton D & Fox PT. (2005). Cortical, thalamic, and hypothalamic responses to cooling and warming the skin in awake humans: a positron-emission tomography study. *Proc Natl Acad Sci U S A* **102,** 5262-5267.

Elia M. (1991). Energy equivalents of CO2 and their importance in assessing energy expenditure when using tracer techniques. *Am J Physiol Endocrinol Metab* **260,** E75-E88.

Elsner RW, Andersen KL & Hermansen L. (1960). Thermal and metabolic responses of Arctic Indians to moderate cold exposure at the end of winter. *J Appl Physiol* **15**.

Enerback S. (2010). Brown adipose tissue in humans. *Int J Obes (Lond)* **34 Suppl 1,** S43-46.

Eyolfson DA, Tikuisis P, Xu X, Weseen G & Giesbrecht GG. (2001). Measurement and prediction of peak shivering intensity in humans. *Eur J Appl Physiol* **84,** 100-106.

Feldmann HM, Golozoubova V, Cannon B & Nedergaard J. (2009). UCP1 ablation induces obesity and abolishes diet-induced thermogenesis in mice exempt from thermal stress by living at thermoneutrality. *Cell Metab* **9,** 203-209.

Fernstrom M, Tonkonogi M & Sahlin K. (2004). Effects of acute and chronic endurance exercise on mitochondrial uncoupling in human skeletal muscle. *J Physiol* **554,** 755-763.

Fisher FM, Kleiner S, Douris N, Fox EC, Mepani RJ, Verdeguer F, Wu J, Kharitonenkov A, Flier JS, Maratos-Flier E & Spiegelman BM. (2012). FGF21 regulates PGC-1alpha and browning of white adipose tissues in adaptive thermogenesis. *Genes Dev* **26,** 271-281.

Foster DO & Frydman ML. (1979). Tissue distribution of cold-induced thermogenesis in conscious warm- or cold-acclimated rats reevaluated from changes in tissue blood flow: the dominant role of brown adipose tissue in the replacement of shivering by nonshivering thermogenesis. *Can J Physiol Pharmacol* **57,** 257-270.

Frontini A, Vitali A, Perugini J, Murano I, Romiti C, Ricquier D, Guerrieri M & Cinti S. (2013). White-to-brown transdifferentiation of omental adipocytes in patients affected by pheochromocytoma. *Biochim Biophys Acta* **1831,** 950-959.

Garcia CA, Van Nostrand D, Atkins F, Acio E, Butler C, Esposito G, Kulkarni K & Majd M. (2006). Reduction of brown fat 2-deoxy-2-[F-18]fluoro-D-glucose uptake by controlling

environmental temperature prior to positron emission tomography scan. *Mol Imaging Biol* **8,** 24-29.

Glatz JFC, Luiken JFP & Bonen A. (2010). Membrane Fatty Acid Transporters as Regulators of Lipid Metabolism: Implications for Metabolic Disease. *Physiol Rev* **90,** 367-417.

Golden FS & Tipton MJ. (1988). Human adaptation to repeated cold immersions. *J Physiol* **396,** 349-363.

Grenier-Larouche T, Labbe SM, Noll C, Richard D & Carpentier AC. (2012). Metabolic inflexibility of white and brown adipose tissues in abnormal fatty acid partitioning of type 2 diabetes. *Int J Obes Supp* **2,** S37-S42.

Haman F. (2006). Shivering in the cold: from mechanisms of fuel selection to survival. *Journal of Applied Physiology* **100,** 1702-1708.

Haman F, Blondin DP, Imbeault M-A & Maneshi A. (2010). Metabolic Requirements of Shivering Humans. *Front Biosci* **15,** 1155-1168.

Haman F, Legault SR, Rakobowchuk M, Ducharme MB & Weber J-M. (2004a). Effects of carbohydrate availability on sustained shivering II: relating muscle recruitment to fuel selection. *J Appl Physiol* **96,** 41-49.

Haman F, Legault SR & Weber J-M. (2004b). Fuel selection during intense shivering in humans: EMG pattern reflects carbohydrate oxidation. *J Physiol* **556,** 305-313.

Haman F, Péronnet F, Kenny GP, Doucet E, Massicotte D, Lavoie C & Weber J-M. (2004c). Effects of carbohydrate availability on sustained shivering I: oxidation of plasma glucose, muscle glycogen and proteins. *J Appl Physiol* **96,** 32-40.

Haman F, Péronnet F, Kenny GP, Massicotte D, Lavoie C, Scott C & Weber J-M. (2002). Effect of cold exposure on fuel utilization in humans: plasma glucose, muscle glycogen, and lipids. *J Appl Physiol* **93,** 77-84.

Haman F, Péronnet F, Kenny GP, Massicotte D, Lavoie C & Weber J-M. (2005). Partitioning oxidative fuels during cold exposure in humans: muscle glycogen becomes dominant as shivering intensifies. *J Physiol* **566,** 247-256.

Haman F, Scott CG & Kenny GP. (2007). Fueling shivering thermogenesis during passive hypothermic recovery. *J Appl Physiol* **103,** 1346-1351.

Hammel HT, Elsner RW, Le Messurier DH, Andersen HT & Milan FA. (1959). Thermal and metabolic responses of the Australian aborigine exposed to moderate cold in summer. *J Appl Physiol* **14,** 605-615.

Hany TF, Gharehpapagh E, Kamel EM, Buck A, Himms-Hagen J & von Schulthess GK. (2002). Brown adipose tissue: a factor to consider in symmetrical tracer uptake in the neck and upper chest region. *Eur J Nucl Med Mol Imaging* **29,** 1393-1398.

Hardy JD, Dubois EF. (1938). The technic of measuring radiation and convection. *Journal of Nutrition* **15,** 461-475.

Hardy JD & Dubois EF. (1937). Regulation of Heat Loss from the Human Body. *Proc Natl Acad Sci U S A* **23,** 624-631.

Hardy JD & Dubois EF. (1938). The technic of measuring radiation and convection. *J Nutr* **15,** 461-475.

Hart JS, Sabean HB, Hildes JA, Depocas F, Hammel HT, Andersen KL, Irving L & Foy G. (1962). Thermal and metabolic responses of coastal Eskimos during a cold night. *J Appl Physiol* **17,** 953-960.

Heaton JM. (1972). The distribution of brown adipose tissue in the human. *J Anat* **112,** 35-39.

Hesslink RLJ, D'Alesandro MM, Armstrong DWr & Reed HL. (1992). Human cold air habituation is independent of thyroxine and thyrotropin. *J Appl Physiol* **72,** 2134-2139.

Hilliges M, Wang L & Johansson O. (1995). Ultrastructural evidence for nerve fibers within all vital layers of the human epidermis. *J Invest Dermatol* **104,** 134-137.

Himms-Hagen J. (2004). Exercise in a pill: feasibility of energy expenditure targets. *Curr Drug Targes CNS Neurol Disord* **3,** 389-409.

Hohtola E. (2004). Shivering thermogenesis in birds and mammals. In *Life in the Cold: Evolution, Mechanisms, Adaptations, and Application*, ed. Barnes BM & Carey HV, pp.

241-252. Institute of Arctic Biology, University of Alaska Fairbanks, Fairbanks, Alaska, USA.

Hong SK. (1973). Pattern of cold adaptation in women divers of Korea (ama). *Fed Proc* **32,** 1614-1622.

Horowitz JF, Coppack SW, Paramore D, Cryer PE, Zhao G & Klein S. (1999). Effect of short-term fasting on lipid kinetics in lean and obese women. *Am J Physiol* **276,** E278-284.

Hussain R, Kudo T, Tsujikawa T, Kobayashi M, Fujibayashi Y & Okazawa H. (2009). Validation of the calculation of the clearance rate constant (k(mono)) of [(11)C]acetate using parametric k(mono) image for myocardial oxidative metabolism. *Nucl Med Biol* **36,** 877-882.

Huttunen P, Hirvonen J & Kinnula V. (1981). The occurrence of brown adipose tissue in outdoor workers. *Eur J Appl Physiol Occup Physiol* **46,** 339-345.

Imbeault M-A, Mantha OL & Haman F. (2013). Shivering modulation in humans: Effects of rapid changes in environmental temperature. *Journal of Thermal Biology* **38,** 582-587.

Israel DJ & Pozos RS. (1989). Synchronized slow-amplitude modulations in the electromyograms of shivering muscles. *J Appl Physiol* **66,** 2358-2363.

Janský L, Janáková H, Ulicný B, Srámek P, Hosek V, Heller J & Parízková J. (1996). Changes in thermal homeostasis in humans due to repeated cold water immersions. *432* **3**.

Jespersen NZ, Larsen TJ, Peijs L, Daugaard S, Homoe P, Loft A, de Jong J, Mathur N, Cannon B, Nedergaard J, Pedersen BK, Moller K & Scheele C. (2013). A classical brown adipose tissue mRNA signature partly overlaps with brite in the supraclavicular region of adult humans. *Cell Metab* **17,** 798-805.

Jocken JW, Goossens GH, van Hees AM, Frayn KN, van Baak M, Stegen J, Pakbiers MT, Saris WH & Blaak EE. (2008). Effect of beta-adrenergic stimulation on whole-body and abdominal subcutaneous adipose tissue lipolysis in lean and obese men. *Diabetologia* **51,** 320-327.

Kanosue K, Sadato N, Okada T, Yoda T, Nakai S, Yoshida K, Hosono T, Nagashima K, Yagishita T, Inoue O, Kobayashi K & Yonekura Y. (2002). Brain activation during

whole body cooling in humans studied with functional magnetic resonance imaging. *Neurosci Lett* **329,** 157-160.

Keatinge WR, Evans M. (1960). Effect of food, alcohol and hyoscine on body-temperature and reflex responses of men immersed in cold water. *Lancet* **2,** 176-178.

Kelley DE, Mokan M, Simoneau JA & Mandarino LJ. (1993). Interaction between glucose and free fatty acid metabolism in human skeletal muscle. *J Clin invest* **92,** 91-98.

Kelley DE, Williams KV, Price JC & Goodpaster B. (1999). Determination of the lumped constant for [18F] fluorodeoxyglucose in human skeletal muscle. *J Nucl Med* **40,** 1798-1804.

Kim S, Krynyckyi BR, Machac J & Kim CK. (2008). Temporal relation between temperature change and FDG uptake in brown adipose tissue. *Eur J Nucl Med Mol Imaging* **35,** 984-989.

Klein LJ, Visser FC, Knaapen P, Peters JH, Teule GJ, Visser CA & Lammertsma AA. (2001). Carbon-11 acetate as a tracer of myocardial oxygen consumption. *Eur J Nucl Med* **28,** 651-668.

Labbe SM, Croteau E, Grenier-Larouche T, Frisch F, Ouellet R, Langlois R, Guerin B, Turcotte EE & Carpentier AC. (2011). Normal postprandial nonesterified fatty acid uptake in muscles despite increased circulating fatty acids in type 2 diabetes. *Diabetes* **60,** 408-415.

Labbe SM, Grenier-Larouche T, Noll C, Phoenix S, Guerin B, Turcotte EE & Carpentier AC. (2012). Increased myocardial uptake of dietary fatty acids linked to cardiac dysfunction in glucose-intolerant humans. *Diabetes* **61,** 2701-2710.

Landsberg L, Saville ME & Young JB. (1984). Sympathoadrenal system and regulation of thermogenesis. *Am J Physiol* **247,** E181-189.

Lapp MC & Gee GK. (1967). Human acclimatization to cold water immersion. *Arch Environ Health* **15,** 568-579.

Launay JC & Savourey G. (2009). Cold adaptations. *Ind Health* **47,** 221-227.

Lean ME. (1989). Brown adipose tissue in humans. *Proc Nutr Soc* **48,** 243-256.

Lean ME, James WP, Jennings G & Trayhurn P. (1986). Brown adipose tissue in patients with phaeochromocytoma. *Int J Obes* **10,** 219-227.

Lee P, Linderman JD, Smith S, Brychta RJ, Wang J, Idelson C, Perron RM, Werner CD, Phan GQ, Kammula US, Kebebew E, Pacak K, Chen KY & Celi FS. (2014). Irisin and FGF21 Are Cold-Induced Endocrine Activators of Brown Fat Function in Humans. *Cell Metab* **19,** 302-309.

Lee P, Swarbrick MM, Zhao JT & Ho KK. (2011). Inducible brown adipogenesis of supraclavicular fat in adult humans. *Endocrinology* **152,** 3597-3602.

Leibel RL & Hirsch J. (1987). Site- and sex-related differences in adrenoreceptor status of human adipose tissue. *J Clin Endocrinol Metab* **64,** 1205-1210.

Lewis GF, Carpentier A, Adeli K & Giacca A. (2002). Disordered fat storage and mobilization in the pathogenesis of insulin resistance and type 2 diabetes. *Endocrine reviews* **23,** 201-229.

Ma SW & Foster DO. (1986). Uptake of glucose and release of fatty acids and glycerol by rat brown adipose tissue in vivo. *Can J Physiol Pharmacol* **64,** 609-614.

Mailloux RJ, Seifert EL, Bouillaud F, Aguer C, Collins S & Harper ME. (2011). Glutathionylation acts as a control switch for uncoupling proteins UCP2 and UCP3. *J Biol Chem* **286,** 21865-21875.

Makinen TM. (2010). Different types of cold adaptation in humans. *Front Biosci (Schol Ed)* **2,** 1047-1067.

Martineau L & Jacobs I. (1989). Muscle glycogen availability and temperature regulation in humans. *J Appl Physiol* **66,** 72-78.

Mauriege P, Despres JP, Prud'homme D, Pouliot MC, Marcotte M, Tremblay A & Bouchard C. (1991). Regional variation in adipose tissue lipolysis in lean and obese men. *Journal of lipid research* **32,** 1625-1633.

Mauriege P, Galitzky J, Berlan M & Lafontan M. (1987). Heterogeneous distribution of beta and alpha-2 adrenoceptor binding sites in human fat cells from various fat deposits: functional consequences. *European journal of clinical investigation* **17,** 156-165.

McAllen RM, Farrell M, Johnson JM, Trevaks D, Cole L, McKinley MJ, Jackson G, Denton DA & Egan GF. (2006). Human medullary responses to cooling and rewarming the skin: a functional MRI study. *Proc Natl Acad Sci U S A* **103,** 809-813.

McAllen RM, Tanaka M, Ootsuka Y & McKinley MJ. (2010). Multiple thermoregulatory effectors with independent central controls. *Eur J Appl Physiol* **109,** 27-33.

Meigal A. (2002). Gross and fine neuromuscular performance at cold shivering. *Int J Circumpolar Health* **61,** 163-172.

Meigal AY, Lupandin YV & Hanninen O. (1996). Head and body positions affect thermoregulatory tonus in deltoid muscles. *J Appl Physiol* **80,** 1397-1400.

Meigal AY, Oksa J, Hohtola E, Lupandin YV & Rintamaki H. (1998). Influence of cold shivering on fine motor control in the upper limb. *Acta Physiol Scand* **163,** 41-47.

Melanson EL, Ingebrigtsen JP, Bergouignan A, Ohkawara K, Kohrt WM & Lighton JR. (2010). A new approach for flow-through respirometry measurements in humans. *Am J Physiol Regul Integr Comp Physiol* **298,** R1571-1579.

Menard SL, Croteau E, Sarrhini O, Gelinas R, Brassard P, Ouellet R, Bentourkia M, van Lier JE, Des Rosiers C, Lecomte R & Carpentier AC. (2010). Abnormal in vivo myocardial energy substrate uptake in diet-induced type 2 diabetic cardiomyopathy in rats. *Am J Physiol Endocrinol Metab* **298,** E1049-1057.

Morrison SF. (2011). 2010 Carl Ludwig Distinguished Lectureship of the APS Neural Control and Autonomic Regulation Section: Central neural pathways for thermoregulatory cold defense. *J Appl Physiol* **110,** 1137-1149.

Muzik O, Mangner TJ & Granneman JG. (2012). Assessment of oxidative metabolism in brown fat using PET imaging. *Front Endocrinol* **3,** 15.

Muzik O, Mangner TJ, Leonard WR, Kumar A, Janisse J & Granneman JG. (2013). 15O PET measurement of blood flow and oxygen consumption in cold-activated human brown fat. *J Nucl Med* **54,** 523-531.

Nakamura K. (2011). Central circuitries for body temperature regulation and fever. *Am J Physiol Regul Integr Comp Physiol* **301,** R1207-1228.

Nakamura K & Morrison SF. (2008). A thermosensory pathway that controls body temperature. *Nat Neurosci* **11,** 62-71.

Nedergaard J & Cannon B. (2013). UCP1 mRNA does not produce heat. *Biochim Biophys Acta* **1831,** 943-949.

Ng CK, Huang SC, Schelbert HR & Buxton DB. (1994). Validation of a model for [1-11C]acetate as a tracer of cardiac oxidative metabolism. *Am J Physiol* **266,** H1304-1315.

Noland RC, Hickner RC, Jimenez-Linan M, Vidal-Puig A, Zheng D, Dohm GL & Cortright RN. (2003). Acute endurance exercise increases skeletal muscle uncoupling protein-3 gene expression in untrained but not trained humans. *Metabolism* **52,** 152-158.

Orava J, Nuutila P, Lidell ME, Oikonen V, Noponen T, Viljanen T, Scheinin M, Taittonen M, Niemi T, Enerback S & Virtanen KA. (2011). Different metabolic responses of human brown adipose tissue to activation by cold and insulin. *Cell Metab* **14,** 272-279.

Orava J, Nuutila P, Noponen T, Parkkola R, Viljanen T, Enerbäck S, Rissanen A, Pietiläinen KH & Virtanen KA. (2013). Blunted metabolic responses to cold and insulin stimulation in brown adipose tissue of obese humans. *Obesity* **21,** 2279-2287.

Ouellet V, Labbe SM, Blondin DP, Phoenix S, Guerin B, Haman F, Turcotte EE, Richard D & Carpentier AC. (2012). Brown adipose tissue oxidative metabolism contributes to energy expenditure during acute cold exposure in humans. *J Clin invest* **122,** 545-552.

Ouellet V, Routhier-Labadie A, Bellemare W, Lakhal-Chaieb L, Turcotte E, Carpentier AC & Richard D. (2011). Outdoor Temperature, Age, Sex, Body Mass Index, and Diabetic Status Determine the Prevalence, Mass, and Glucose-Uptake Activity of 18F-FDG-Detected BAT in Humans. *J Clin Endocrinol Metab* **96,** 192-199.

Palmes ED & Park CR. (1947). Thermocouples for the measurement of the surface temperature of the skin. *Fed Proc* **6,** 175.

Patlak CS, Blasberg RG & Fenstermacher JD. (1983). Graphical evaluation of blood-to-brain transfer constants from multiple-time uptake data. *J Cereb Blood Flow Metab* **3,** 1-7.

Perkins JF, Jr. (1945). The role of the proprioceptors in shivering. *Am J Physiol* **145,** 264-271.

Péronnet F & Massicotte D. (1991). Table of nonprotein respiratory quotient: an update. *Can J Sport Sci* **16,** 23-29.

Petajan JH & Williams DD. (1972). Behavior of single motor units during pre-shivering tone and shivering tremor. *Am J Phys Med* **51,** 16-22.

Petrovic N, Walden TB, Shabalina IG, Timmons JA, Cannon B & Nedergaard J. (2010). Chronic peroxisome proliferator-activated receptor gamma (PPARgamma) activation of epididymally derived white adipocyte cultures reveals a population of thermogenically competent, UCP1-containing adipocytes molecularly distinct from classic brown adipocytes. *J Biol Chem* **285,** 7153-7164.

Phelps ME. (2000). Positron emission tomography provides molecular imaging of biological processes. *Proc Natl Acad Sci U S A* **97,** 9226-9233.

Pike VW, Eakins MN, Allan RM & Selwyn AP. (1982). Preparation of [1-11C]acetate--an agent for the study of myocardial metabolism by positron emission tomography. *Int J Appl Radiat Isot* **33,** 505-512.

Poyart CF, Bursaux E & Freminet A. (1975). The bone CO2 compartment: evidence for a bicarbonate pool. *Respir Physiol* **25,** 89-99.

Reynisdottir S, Ellerfeldt K, Wahrenberg H, Lithell H & Arner P. (1994). Multiple lipolysis defects in the insulin resistance (metabolic) syndrome. *J Clin Invest* **93,** 2590-2599.

Richard D, Carpentier AC, Dore G, Ouellet V & Picard F. (2010). Determinants of brown adipocyte development and thermogenesis. *Int J Obes (Lond)* **34 Suppl 2,** S59-66.

Richard D & Picard F. (2011). Brown fat biology and thermogenesis. *Front Biosci (Landmark Ed)* **16,** 1233-1260.

Ricquier D, Nechad M & Mory G. (1982). Ultrastructural and biochemical characterization of human brown adipose tissue in pheochromocytoma. *J Clin Endocrinol Metab* **54,** 803-807.

Riddle CN, Edgley SA & Baker SN. (2009). Direct and indirect connections with upper limb motoneurons from the primate reticulospinal tract. *J Neurosci* **29,** 4993-4999.

Rolfe DFS & Brown GC. (1997). Cellular energy utilization and molecular origin of standard metabolic rate in mammals. *Physiol Rev* **77,** 731-758.

Rosenwald M, Perdikari A, Rulicke T & Wolfrum C. (2013). Bi-directional interconversion of brite and white adipocytes. *Nat Cell Biol* **15,** 659-667.

Rothwell NJ & Stock MJ. (1979). A role for brown adipose tissue in diet-induced thermogenesis. *Nature* **281,** 31-35.

Rothwell NJ & Stock MJ. (1983). Luxuskonsumption, diet-induced thermogenesis and brown fat: the case in favour. *Clin Sci (Lond)* **64,** 19-23.

Saito M, Okamatsu-Ogura Y, Matsushita M, Watanabe K, Yoneshiro T, Nio-Kobayashi J, Iwanaga T, Miyagawa M, Kameya T, Nakada K, Kawai Y & Tsujisaki M. (2009). High incidence of metabolically active brown adipose tissue in healthy adult humans: effects of cold exposure and adiposity. *Diabetes* **58,** 1526-1531.

Sallis JF, Haskell WL, Wood PD, Fortmann SP, Rogers T, Blair SN & Paffenbarger RSJ. (1985). Physical activity assessment methodology in the Five-City Project. *Am J Epidemiol* **121,** 91-106.

Schaeffer PJ, Villarin JJ & Lindstedt SL. (2003). Chronic cold exposure increases skeletal muscle oxidative structure and function in Monodelphis domestica, a marsupial lacking brown adipose tissue. *Physiol Biochem Zool* **76,** 877-887.

Schaeffer PJ, Villarin JJ, Pierotti DJ, Kelly DP & Lindstedt SL. (2005). Cost of transport is increased after cold exposure in Monodelphis domestica: training for inefficiency. *J Exp Biol* **208,** 3159-3167.

Schepers RJ & Ringkamp M. (2010). Thermoreceptors and thermosensitive afferents. *Neurosci Biobehav Rev* **34,** 177-184.

Scholander PF, Hammel HT, Hart JS, Le Messurier DH & Steen J. (1958). Cold Adaptation in Australian aborigine. *J Appl Physiol* **13,** 211-218.

Schulz TJ, Huang P, Huang TL, Xue R, McDougall LE, Townsend KL, Cypess AM, Mishina Y, Gussoni E & Tseng YH. (2013). Brown-fat paucity due to impaired BMP signalling induces compensatory browning of white fat. *Nature* **495,** 379-383.

Seale P, Bjork B, Yang W, Kajimura S, Chin S, Kuang S, Scime A, Devarakonda S, Conroe HM, Erdjument-Bromage H, Tempst P, Rudnicki MA, Beier DR & Spiegelman BM. (2008). PRDM16 controls a brown fat/skeletal muscle switch. *Nature* **454,** 961-967.

Sell H, Deshaies Y & Richard D. (2004). The brown adipocyte: update on its metabolic role. *Int J Biochem Cell Biol* **36,** 2098-2104.

Shapovalov AI. (1972). Extrapyramidal monosynaptic and disynaptic control of mammalian alpha-motoneurons. *Brain Res* **40,** 105-115.

Sharp LZ, Shinoda K, Ohno H, Scheel DW, Tomoda E, Ruiz L, Hu H, Wang L, Pavlova Z, Gilsanz V & Kajimura S. (2012). Human BAT possesses molecular signatures that resemble beige/brite cells. *PLoS One* **7,** e49452.

Sidossis LS, Coggan AR, Gastaldelli A & Wolfe RR. (1995). Pathway of free fatty acid oxidation in human subjects. Implications for tracer studies. *J Clin invest* **95,** 278-284.

Silva JE. (2006). Thermogenic mechanisms and their hormonal regulation. *Physiol Rev* **86,** 435-464.

St-Onge M, Mignault D, Allison DB & Rabasa-Lhoret R. (2007). Evaluation of a portable device to measure daily energy expenditure in free-living adults. *Am J Clin Nutr* **85,** 742-749.

Stanford KI, Middelbeek RJ, Townsend KL, An D, Nygaard EB, Hitchcox KM, Markan KR, Nakano K, Hirshman MF, Tseng YH & Goodyear LJ. (2013). Brown adipose tissue regulates glucose homeostasis and insulin sensitivity. *J Clin invest* **123,** 215-223.

Steegman AT, Cerny FJ & Holliday TW. (2002). Neandertal cold adaptation: physiological and energetic factors. *Am J Hum Biol* **14,** 566-583.

Steele R. (1959). Influences of glucose loading and of injected insulin on hepatic glucose output. *Ann N Y Acad Sci* **82,** 420-430.

Stocks JM, Patterson MJ, Hyde DE, Mittleman KD & Taylor NA. (2001). Metabolic habituation following repeated resting cold-water immersion is not apparent during low-intensity cold-water exercise. *J Physiol Anthropol Appl Human Sci* **20,** 263-267.

Takala TO, Nuutila P, Pulkki K, Oikonen V, Gronroos T, Savunen T, Vahasilta T, Luotolahti M, Kallajoki M, Bergman J, Forsback S & Knuuti J. (2002). 14(R,S)-[18F]Fluoro-6-thia-heptadecanoic acid as a tracer of free fatty acid uptake and oxidation in myocardium and skeletal muscle. *Eur J Nucl Med Mol Imaging* **29,** 1617-1622.

Tanaka M, Owens NC, Nagashima K, Kanosue K & McAllen RM. (2006). Reflex activation of rat fusimotor neurons by body surface cooling, and its dependence on the medullary raphe. *J Physiol* **572,** 569-583.

Teulier L, Rouanet JL, Letexier D, Romestaing C, Belouze M, Rey B, Duchamp C & Roussel D. (2010). Cold-acclimation-induced non-shivering thermogenesis in birds is associated with upregulation of avian UCP but not with innate uncoupling or altered ATP efficiency. *J Exp Biol* **213,** 2476-2482.

Trayhurn P, Ashwell M, Jennings G, Richard D & Stirling DM. (1987). Effect of warm or cold exposure on GDP binding and uncoupling protein in rat brown fat. *Am J Physiol* **252,** E237-243.

Trayhurn P, Jones PM, McGuckin MM & Goodbody AE. (1982). Effects of overfeeding on energy balance and brown fat thermogenesis in obese (ob/ob) mice. *Nature* **295,** 323-325.

Turkington TG. (2001). Introduction to PET instrumentation. *J Nucl Med Technol* **29,** 4-11.

van den Hoff J, Burchert W, Borner AR, Fricke H, Kuhnel G, Meyer GJ, Otto D, Weckesser E, Wolpers HG & Knapp WH. (2001). [1-(11)C]Acetate as a quantitative perfusion tracer in myocardial PET. *J Nucl Med* **42,** 1174-1182.

van der Lans AAJJ, Hoeks J, Brans B, Vijgen GHEJ, Visser MGW, Vosselman MJ, Hansen J, Jörgensen JA, Wu J, Mottaghy FM, Schrauwen P & van Marken Lichtenbelt WD. (2013). Cold acclimation recruits human brown fat and increases nonshivering thermogenesis. *The Journal of Clinical Investigation* **123,** 0-0.

van Marken Lichtenbelt WD, Vanhommerig JW, Smulders NM, Drossaerts JM, Kemerink GJ, Bouvy ND, Schrauwen P & Teule GJ. (2009). Cold-activated brown adipose tissue in health men. *N Engl J Med* **360,** 1500-1508.

Vijgen GH, Bouvy ND, Teule GJ, Brans B, Hoeks J, Schrauwen P & van Marken Lichtenbelt WD. (2012). Increase in brown adipose tissue activity after weight loss in morbidly obese subjects. *J Clin Endocrinol Metab* **97,** E1229-1233.

Vijgen GH, Bouvy ND, Teule GJ, Brans B, Schrauwen P & van Marken Lichtenbelt WD. (2011). Brown adipose tissue in morbidly obese subjects. *PLoS One* **6,** e17247.

Villarroya F & Vidal-Puig A. (2013). Beyond the sympathetic tone: the new brown fat activators. *Cell Metab* **17,** 638-643.

Virtanen KA, Lidell ME, Orava J, Heglind M, Westergren R, Niemi T, Taittonen M, Laine J, Savisto NJ, Enerbäck S & Nuutila P. (2009). Functional brown adipose tissue in healthy adults. *N Engl J Med* **360,** 1518-1525.

Vosselman MJ, Brans B, van der Lans AA, Wierts R, van Baak MA, Mottaghy FM, Schrauwen P & van Marken Lichtenbelt WD. (2013). Brown adipose tissue activity after a high-calorie meal in humans. *Am J Clin Nutr* **98,** 57-64.

Vosselman MJ, van der Lans AA, Brans B, Wierts R, van Baak MA, Schrauwen P & van Marken Lichtenbelt WD. (2012). Systemic beta-adrenergic stimulation of thermogenesis is not accompanied by brown adipose tissue activity in humans. *Diabetes* **61,** 3106-3113.

Wahrenberg H, Lonnqvist F & Arner P. (1989). Mechanisms underlying regional differences in lipolysis in human adipose tissue. *J Clin Invest* **84,** 458-467.

Wang L, Hilliges M, Jernberg T, Wiegleb-Edstrom D & Johansson O. (1990). Protein gene product 9.5-immunoreactive nerve fibres and cells in human skin. *Cell Tissue Res* **261,** 25-33.

Wasserman DH, Kang L, Ayala JE, Fueger PT & Lee-Young RS. (2011). The physiological regulation of glucose flux into muscle in vivo. *J Exp Biol* **214,** 254-262.

Wells JC & Stock JT. (2007). The biology of the colonizing ape. *Am J Phys Anthropol* **Suppl 45,** 191-222.

Whipp BJ & Wasserman K. (1969). Efficiency of muscular work. *J Appl Physiol* **26,** 644-648.

Wiesinger H, Klaus S, Heldmaier G, Champigny O & Ricquier D. (1990). Increased nonshivering thermogenesis, brown fat cytochrome-c oxidase activity, GDP binding, and uncoupling protein mRNA levels after short daily cold exposure of Phodopus sungorus. *Can J Physiol Pharmacol* **68,** 195-200.

Wijers SL, Schrauwen P, Saris WH & van Marken Lichtenbelt WD. (2008). van Marken Lichtenbelt WD, Vanhommerig JW, Smulders NM, Drossaerts JM, Kemerink GJ, Bouvy ND, Schrauwen P, Teule GJ. *PLoS One* **3,** e1777.

Wolfe RR & Chinkes DL. (2005). *Isotope tracers in metabolic research : principles and practice of kinetic analysis*. Wiley-Liss, Hoboken, NJ.

Wu J, Bostrom P, Sparks LM, Ye L, Choi JH, Giang AH, Khandekar M, Virtanen KA, Nuutila P, Schaart G, Huang K, Tu H, van Marken Lichtenbelt WD, Hoeks J, Enerback S, Schrauwen P & Spiegelman BM. (2012). Beige adipocytes are a distinct type of thermogenic fat cell in mouse and human. *Cell* **150,** 366-376.

Wyss MT, Weber B, Treyer V, Heer S, Pellerin L, Magistretti PJ & Buck A. (2009). Stimulation-induced increases of astrocytic oxidative metabolism in rats and humans investigated with 1-11C-acetate. *J Cereb Blood Flow Metab* **29,** 44-56.

Yeung HW, Grewal RK, Gonen M, Schoder H & Larson SM. (2003). Patterns of (18)F-FDG uptake in adipose tissue and muscle: a potential source of false-positives for PET. *J Nucl Med* **44,** 1789-1796.

Yin H, Pasut A, Soleimani VD, Bentzinger CF, Antoun G, Thorn S, Seale P, Fernando P, van Ijcken W, Grosveld F, Dekemp RA, Boushel R, Harper ME & Rudnicki MA. (2013). MicroRNA-133 controls brown adipose determination in skeletal muscle satellite cells by targeting Prdm16. *Cell Metab* **17,** 210-224.

Yoneshiro T, Aita S, Matsushita M, Kameya T, Nakada K, Kawai Y & Saito M. (2011). Brown adipose tissue, whole-body energy expenditure, and thermogenesis in healthy adult men. *Obesity (Silver Spring)* **19,** 13-16.

Yoneshiro T, Aita S, Matsushita M, Kayahara T, Kameya T, Kawai Y, Iwanaga T & Saito M. (2013). Recruited brown adipose tissue as an antiobesity agent in humans. *J Clin Invest* **123,** 3404-3408.

Young AJ. (1996). Homeostatic responses to prolonged cold exposure: human cold acclimatization. In *Handbook of Physiology, Section 4: Environmental Physiology* ed. Fregly MJ & Blatteis CM, pp. 419-438. Oxford University Press, New York.

Young AJ, Muza SR, Sawka MN, Gonzalez RR & Pandolf KB. (1986). Human thermoregulatory responses to cold air are altered by repeated cold water immersion. *J Appl Physiol* **60,** 1542-1548.

Young AJ, Sawka MN, Neufer PD, Muza SR, Askew EW & Pandolf KB. (1989). Thermoregulation during cold water immersion is unimpaired by low muscle glycogen levels. *Journal of Applied Physiology* **66,** 1809-1816.

Zingaretti MC, Crosta F, Vitali A, Guerrieri M, Frontini A, Cannon B, Nedergaard J & Cinti S. (2009). The presence of UCP1 demonstrates that metabolically active adipose tissue in the neck of adult humans truly represents brown adipose tissue. *FASEB J* **23,** 3113-3120.

7. APPENDICES

APPENDIX A:

Ethics approval notices for thesis research projects

Centre hospitalier universitaire de Sherbrooke
Centre de recherche clinique Étienne-Le Bel

CHUS Centre hospitalier universitaire de Sherbrooke

Avec vous, pour la Vie

Le 12 juillet 2012

Dr André Carpentier
Endocrinologie
CHUS - Fleurimont

OBJET: Projet # 09-059-A2
Métabolisme énergétique de la graisse brune suite à un programme d'acclimatation au froid modéré.

Dr Carpentier ,

Nous aimerions, par la présente, vous aviser que votre protocole de recherche cité en rubrique a été approuvé par le Comité d'éthique de la recherche en santé chez l'humain du CHUS.

Puisque les conditions requises à la réalisation de ce projet de recherche sont réunies, il nous fait plaisir de vous autoriser à le débuter.

Nous désirons également vous faire part qu'à titre de partie contractante, nous conserverons un original du contrat (ou entente financière) et de ses annexes, signé par toutes les parties. Pour faire ouvrir une unité administrative en lien avec ce projet, bien vouloir contacter Mme Anie Normandin au poste 23548, ou par courriel à l'adresse suivante: anormandin.chus@ssss.gouv.qc.ca.

Vous souhaitant tout le succès escompté dans le déroulement de cette étude, je vous prie de croire à l'expression de mes sentiments les plus distingués.

Serge Marchand, Ph.D.
Directeur scientifique
Centre de recherche clinique Étienne-Le Bel
/hl

cc:

File Number: H06-11-08 **Date (mm/dd/yyyy):** 05/17/2013

3/03

Université d'Ottawa University of Ottawa
Bureau d'éthique et d'intégrité de la recherche Office of Research Ethics and Integrity

Ethics Approval Notice

Health Sciences and Science REB

ote

Principal Investigator / Supervisor / Co-investigator(s) / Student(s)

First Name	Last Name	Affiliation	Role
François	Haman	Health Sciences / Human Kinetics	Supervisor
Céline	Aguer	Medicine / Medicine	Co-investigator
Hans Christian	Tingelstad	Health Sciences / Human Kinetics	Co-investigator
Denis	Blondin	Health Sciences / Human Kinetics	Student Researcher
André	Carpentier	Others / Others	Other Collaborator
Denis	Richard	Others / Others	Other Collaborator
Eric	Turcotte	Others / Others	Other Collaborator

File Number: H06-11-08

Type of Project: PhD Thesis

Title: Thermogenesis and Fuel Selection during Cold Exposure: Effects of Cold Acclimation

	Expiry Date (mm/dd/yyyy)	Approval Type
07/11/2013	07/10/2014	Ia

(Ia: Approval, Ib: Approval for initial stage only)

Special Conditions / Comments:
N/A

550, rue Cumberland, pièce 154 550 Cumberland Street, room 154
Ottawa (Ontario) K1N 6N5 Canada Ottawa, Ontario K1N 6N5 Canada
(613) 562-5387 • Téléc./Fax (613) 562-5338
http://www.research.uottawa.ca/ethics/index.html
http://www.recherche.uottawa.ca/deontologie/index.html

Hôpital **Montfort** Hospital
Comité d'éthique de la recherche

713, chemin Montréal Road
Ottawa, Ontario K1K 0T2
www.hopitalmontfort.com

613-746-4621 (tél/tel)
613-748-4914 (téléc/fax)
montfort@montfort.on.ca

Avis d'approbation déontologique
Comité d'éthique de la recherche de l'Hôpital Montfort

Le 7 septembre 2012

Chercheur principal :

Titre du projet : « Thermogenèse et le métabolisme énergétique lors d'une exposition au froid : l'effet d'une acclimatation au froid »

Numéro du dossier : DP-09-05-12

Date d'approbation : 2012-09-07

Date d'expiration : 2013-09-07

Commentaires ou restrictions : Veuillez ajouter le bureau d'éthique de l'Hôpital Montfort dans la liste des CÉR dans les sections suivantes :

- Arrêt du projet de recherche p. 8
- Confidentialité p.9
- Personnes-ressources p. 10
- Surveillance des aspects éthiques p. 10

Bureau d'éthique de la recherche de l'Hôpital Montfort
713, chemin Montréal
Salle 2D133
Ottawa (Ontario)
K1K 0T2
Tél. : 613-736-3621 poste 6058
Téléc. : 613-48-4922
Courriel : ethiquerecherche@montfort.on.ca

En concordance avec l'énoncé des trois conseils et les lois et règlements applicables en Ontario, je confirme que le Comité d'éthique de la recherche (CÉR) de l'Hôpital Montfort a étudié et approuvé votre demande d'approbation déontologique pour une période d'un an.

Le protocole de l'étude ne peut être modifié sans une approbation préalable du CÉR sauf s'il est question de la sécurité immédiate des participants ou de logistique administrative comme un changement de numéro de téléphone. Vous devez aviser le CÉR immédiatement de tout changement, événement indésirable ou nouvelle information pouvant augmenter le risque de l'étude, modifier le cours de l'étude ou atteindre la sécurité des participants. Les modifications au projet et aux outils de recrutements doivent être soumises au CÉR.

Veuillez nous acheminer avant la date d'échéance de cet avis d'approbation, un rapport final afin de fermer le dossier ou de faire une demande de renouvellement de l'étude.

Cordialement,

Lynn Casimiro, Pht., Ph. D.
Présidente du Comité d'éthique de la recherche - Hôpital Montfort

INSTITUT UNIVERSITAIRE
DE CARDIOLOGIE
ET DE PNEUMOLOGIE
DE QUÉBEC

APPROBATION DU COMITÉ D'ÉTHIQUE DE LA RECHERCHE DE L'IUCPQ

Titre:
Métabolisme énergétique de la graisse brune chez l'humain suite à une acclimatation au froid. GB1.
Protocole:
version datée du 27 novembre 2009
Chercheurs principaux:
Richard,Denis; Haman François, u. Ottawa; Carpentier André, U. Sherbrooke; Trottier Mikael, Guimond Jean, Tessier Michel, IUCPQ
Chercheurs secondaires:
Numéro:
20793

En date du 30 janvier 2012, le chercheur principal de l'étude dans notre centre nous soumet pour approbation le protocole précité.

Les lettres d'approbation suivantes sont soumises :

- Lettre d'approbation du Comité d'éthique de la recherche en santé chez l'humain du Centre Hospitalier Universitaire de Sherbrooke, lettre datée du 20 juillet 2009.
- Lettre d'approbation du Comité d'éthique de l'Université d'Ottawa, approbation valable du 11 août 2011 au 10 août 2012.
- Lettre d'approbation du Comité de révision scientifique, axe obésité et autres composantes de l'Institut universitaire de cardiologie et de pneumologie de Québec (IUCPQ), lettre datée du 25 janvier 2012.

Les documents suivants ont été présentés au Comité d'éthique de la recherche de l'IUCPQ :

- Protocole, version datée du 27 novembre 2009;
- Formulaire d'information et de consentement, version datée du 21 février 2012. (ce document a été d'éthique de l'Université d'Ottawa le 21 février 2012 et déposé au Comité d'éthique PQ le 22 février 2012).
- Formulaire HL-4610 (document de régie interne).

Comité d'éthique de la recherche de l'Institut universitaire de cardiologie et de pneumologie de Québec (IUCPQ)
22 février 2012
Ce comité d'éthique de la recherche fonctionne selon les règles établies par
Les Bonnes Pratiques Cliniques : Directives Consolidées (Directive tripartite harmonisée CIH)

2725, CHEMIN SAINTE-FOY, QUÉBEC (QUÉBEC) G1V 4G5 CANADA
TÉLÉPHONE 418 656-8711
IUCPQ.qc.ca

APPENDIX B:

Final version of invited review article from Comprehensive Physiology

Comprehensive Physiology

Maintaining thermogenesis in cold exposed humans: relying on multiple metabolic pathways

Journal:	*Comprehensive Physiology*
Manuscript ID:	CPHY-13-0043.R2
Wiley - Manuscript type:	Overview Article
Date Submitted by the Author:	n/a
Complete List of Authors:	Blondin, Denis; Université de Sherbrooke, Department of Medicine Tingelstad, Hans; University of Ottawa, Faculty of Health Sciences Mantha, Olivier; University of Ottawa, Faculty of Health Sciences Gosselin, Chantal; University of Ottawa, Faculty of Health Sciences Haman, Francois; University of Ottawa, Faculty of Health Sciences
Keywords:	metabolism < Endocrinology and Metabolism, energy < Endocrinology and Metabolism, thermogenesis < Endocrinology and Metabolism
Abstract:	In cold exposed humans, increasing thermogenic rate is essential to prevent decreases in core temperature. This review describes the metabolic requirements of thermogenic pathways, mainly shivering thermogenesis, the largest contributor of heat. Research has shown that thermogenesis is sustained from a combination of carbohydrates (CHO), lipids and proteins. The mixture of fuels is influenced by shivering intensity and pattern as well as by modifications in energy reserves and nutritional status. To date, there are no indications that differences in the types of fuel being used can alter shivering and overall heat production. We also bring forth the potential contribution of nonshivering thermogenesis in adult humans via the activation of brown adipose tissue (BAT) and explore some means to stimulate the activity of this highly thermogenic tissue. Clearly, the potential role of BAT, especially in young lean adults, can no longer be ignored. However, much work remains to clearly identify the quantitative nature of this tissue's contribution to total thermogenic rate and influence on shivering thermogenesis. Identifying ways to potentiate the effects of BAT via cold acclimation and/or the ingestion of compounds that stimulate the thermogenic process may have important implications in cold endurance and survival.

Maintaining thermogenesis in cold exposed humans: relying on multiple metabolic pathways

Denis P. Blondin[1], Hans Christian Tingelstad[2], Olivier Mantha[2],

Chantal Gosselin[2] and François Haman[2]

[1] Department of Medicine, Université de Sherbrooke, Sherbrooke, Québec, Canada, J1H 5N4

[2] Faculty of Health Sciences, University of Ottawa, Ottawa, Ontario, Canada K1N 6N5

***Running Head*: Cold-induced thermogenesis in humans**

Abstract

In cold exposed humans, increasing thermogenic rate is essential to prevent decreases in core temperature. This review describes the metabolic requirements of thermogenic pathways, mainly shivering thermogenesis, the largest contributor of heat. Research has shown that thermogenesis is sustained from a combination of carbohydrates (CHO), lipids and proteins. The mixture of fuels is influenced by shivering intensity and pattern as well as by modifications in energy reserves and nutritional status. To date, there are no indications that differences in the types of fuel being used can alter shivering and overall heat production. We also bring forth the potential contribution of nonshivering thermogenesis in adult humans via the activation of brown adipose tissue (BAT) and explore some means to stimulate the activity of this highly thermogenic tissue. Clearly, the potential role of BAT, especially in young lean adults, can no longer be ignored. However, much work remains to clearly identify the quantitative nature of this tissue's contribution to total thermogenic rate and influence on shivering thermogenesis. Identifying ways to potentiate the effects of BAT via cold acclimation and/or the ingestion of compounds that stimulate the thermogenic process may have important implications in cold endurance and survival.

Key words: shivering thermogenesis, energy metabolism, lipid oxidation, carbohydrate oxidation, muscle glycogen, electromyography (EMG), muscle recruitment, fuel selection mechanisms

Introduction

Human bodies are particularly efficient at dissipating heat in warm climates but have a reduced capacity to preserve it in cold environments. In fact, preventing significant decreases of core temperature are virtually impossible without proper behavioral strategies to assist in the reduction of heat loss (e.g. building shelters, wearing clothing, mastering fire)(138). When exposure to cold temperatures is inevitable, humans must rely on the concerted activation of physiological processes that increase heat production and lower heat loss. This review focuses specifically on the processes of thermogenesis in cold exposed adults. It describes the thermogenic pathways activated to compensate for increases in heat loss and presents the metabolic fuels required to sustain these pathways under various nutritional conditions and cold exposure intensities. While the main emphasis is on shivering thermogenesis (ST) - *by far the greatest contributor heat in adult humans* - this review also brings forth the potential contribution of non-shivering thermogenesis (NST) *via* the activation of brown adipose tissue (BAT). Clearly, the role of this highly thermogenic tissue cannot be overlooked as it is now known to be present and metabolically active in adult humans (29, 90, 128, 132, 145). In this context, we explore the metabolic importance of BAT in adults and suggest means for increasing its activity to increase overall thermogenesis and/or reduce skeletal muscle activity during ST.

Heat production in cold exposed humans

Heat production or thermogenesis is a by-product of the combustion of substrates and other exothermic biochemical reactions occurring within cells throughout the body. Under thermoneutral conditions, metabolic activity of various human tissues provides a combined heat production of ~5 kJ of heat per kilogram per hour. As ambient temperature progressively decreases, metabolic and physiological processes are activated to reduce rates of heat loss and increase rates of heat production. The main purpose of these combined responses is to maintain an optimal core temperature of ~37°C. When exercise is not possible or advisable (e.g.

overexertion, limited food supply), combined activation of ST and of NST is essential for maintaining heat production. Before 2009, researchers in the field of thermoregulation believed that heat production in cold exposed adults was almost exclusively produced through ST while the contribution of NST was negligible (see 48 for review). This assumption was mainly related to the belief that the greatest contributor to total NST, the highly thermogenic BAT, was absent or at least metabolically inactive past the first year of life (59). In contrast, others researchers held firm that BAT was present and could be a metabolically relevant tissue in humans (87). In 2009, using Positron Emission Tomography coupled with Computed Tomography (PET/CT) with the PET glucose analogue ^{18}F-fluorodeoxyglucose (^{18}F-FDG), three leading studies confirmed the presence of significant amounts of BAT in adult humans (29, 128, 132). Later, by combining ^{11}C-acetate to PET/CT methods, results showed that BAT was not only present but also contributed to cold-induced thermogenesis (90). Even though there is little doubt that ST is the greatest contributor of heat in cold humans, the potential contribution of BAT to total thermogenic rate should not be ignored especially during mild cold exposure. Some strategies that may increase the contribution of this tissue to total heat production are discussed later (*Compounds that may stimulate BAT in the cold*).

Activating thermogenic pathways

In endotherms, activation pathways for the various thermogenic processes have evolved over millions of year and share many commonalities between species. The functional model commonly applied to describe our current understanding of the central thermoregulatory circuits have been derived from the use of transsynaptic retrograde tracing techniques using pseudorabies virus, direct electrical brain stimulation or pharmocological stimulation and inhibition of neural pathways in various animal models [see (85) for review]. Only recently have functional magnetic resonance imaging (fMRI) (31, 71, 81) and PET/CT been used to map the thermoregulatory centers of the human brain (23, 34). A recent fMRI study has suggested that the anatomical locations of neurons in the medulla critically involved in stimulating the cold-

defense responses in humans are homologous to those found in rodents (81), which allows for the application of rodent models as a base of interpretation.

Although a thorough review of the autonomic control of thermoregulation is beyond the scope of this particular review and can be found elsewhere (82, 85, 86, 102), a general description of the processes in which the thermogenic pathways are stimulated will be provided (Figure 1). It is likely that much of the variability in the thermoregulatory and metabolic responses commonly observed in cold exposure studies, whether deliberate or not, can be attributed to the methodologies used to stimulate these thermogenic pathways. The thermoregulatory system consists of a sensory afferent axis, an integration centre and an efferent pathway. Cooling the skin activates the temperature-sensitive transient receptor ion channels (termed thermoTRP), expressed in free nerve endings located in the dermis and epidermis (61, 134). This stimulation, conveys thermal afferent information through the spinal cord, to the thalamus and cerebral cortex for the conscious perception and localization of changes in temperature (31, 34) as well as to the thermoregulatory centre located in the preoptic area of the hypothalamus to activate homeostatic cold-defense responses (34). Interestingly, the spinothalamocortical pathway that is involved in temperature perception does not appear to mediate the autonomous thermoregulatory responses (85). The feed-forward response resulting from skin cooling, whereby cold defense effectors are activated prior to changes in core temperature (T_{core}), ensure that thermoregulatory responses are activated before the environmental thermal challenge can elicit such an influence on T_{core}. The threshold skin temperature that triggers cutaneous vasoconstriction (CVC), BAT or shivering thermogenesis may vary depending upon the effector, with shivering, for example, demonstrating a lower threshold than BAT and CVC in rodents (86). A number of thermoTRPs have been identified, each sensitive to a relatively narrow and distinct range of temperatures but collectively detect a span of temperatures ranging from innocuous to noxious (painful) (106). In addition to being found subcutaneously, thermoTRPs are also expressed among afferent nerve fibers located in the abdomen/viscera, spinal cord and hypothalamus, with this afferent input providing feedback on the present thermal state which may potentiate responses of some but not all thermoeffectors (82)(e.g. Figure 2 demonstrates shivering as being relatively more responsive to

skin temperature). Both the peripheral and central cold-sensitive receptors exhibit a vigorous increase in nerve impulse activity upon a decrease in ambient or skin temperature followed by a steady-state continuous discharge when the temperature is held constant (18, 30), demonstrating an acute habituation effect. Both the dynamic and steady-state firing patterns can also be seen in the activation of the effector responses to an innocuous cold stimulus whereby, upon cooling, shivering electromyography increases dramatically, before stabilizing to a lower amplitude (66).

The preoptic area of the hypothalamus is recognized as the thermoregulatory center in that it integrates afferent signals and initiates autonomic thermoregulatory responses such as skin vasomotor responses, BAT stimulation and shivering during cold exposure. In ambient conditions, warm-sensitive neurons in the preoptic area are tonically active to suppress thermogenic effectors. This tonic discharge is reduced by skin cooling thereby disinhibiting thermoeffector neurons that drive these cold-defense responses. Neural output from raphé pallidus/arcuate nucleus in the medulla appears to increase as a function of decreases in skin temperature (81) in humans. Interestingly, despite the common afferent input, cold-defense thermoeffectors are controlled largely independently of one another and activated in parallel but possibly at different threshold temperatures suggesting that their interactions may simply be by-products of the afferent feedback received. For example, following the neural relay of the medullary raphé, activated sympathetic premotor neurons provide excitatory input to sympathetic preganglionic neurons in the intermediolateral nucleus to drive BAT stimulation and CVC responses, while premotor neurons in this same medullary region provide excitatory input to somatomotor neurons in the ventral horn which excite the alpha (α) and gamma (γ) motoneurons required for shivering (86, 104, 105, 115). Consequently, rather than having complementary functions, there is evidence to suggest redundancies in the thermoregulatory system. Extensive work is still required to confirm this hypothesis, as the brain mapping and functional imaging of the autonomous control of thermoregulation in humans still remains largely unexplored.

With the resurgence in BAT research in humans, much attention has recently been drawn to cold-induced NST, more specifically the role of BAT. However, in the process, skeletal

muscle thermogenesis under mild cold conditions has been overlooked as has the relationship between these two organs. Although many have reported an absence of overt shivering determined by observation or subject-led reporting (28, 128, 130, 131, 133, 145), only one study to date has simultaneously quantified both shivering and BAT activity (90). This study demonstrated a significant increase in cold-induced BAT oxidative metabolism and limited but detectable levels of shivering activity, measured by surface electromyography (sEMG), representing only ~2% of a maximal voluntary contraction (%MVC). Based on these observations, the associated rise in cold-induced thermogenesis cannot be related entirely to the activation of BAT but rather to a combination of ST and NST. In addition, cooling methods used may have unintended consequences relating to the stimulation of heat production. For example, a common cooling strategy employed to examine BAT activation involves cold air exposure (19°C) combined with intermittently putting legs of the participant on blocks of ice (103, 145) or in ice water (72, 89, 132). The unintended consequence of applying legs on blocks of ice or in ice water is the stimulation of pain sensitive receptors (nocireceptors). When stimulated these receptors, in addition to signaling a painful cold sensation, stimulates afferent fibers which normally would be sensitive to heat stimuli, which explains this hot or burning sensation. As a consequence, such an extreme cold may have inhibitory or blunting effect on the cold-evoked thermoeffectors, such as BAT stimulation (106). This could explain the high variability in BAT activation in these studies compared to the near 100% BAT activation found in studies simply applying cold air (128, 131, 133) or a liquid-perfused garment (90). Before addressing the potential effects of BAT activation on the thermogenic response, we will focus on metabolic basis of ST, by far the largest contributor of heat during cold exposure.

Sustaining shivering thermogenesis

In a lean individual weighing 72 kg, skeletal muscles represent ~40% of total body mass or ~30kg (101, 107). Not only is this tissue mass large but it is also able to increase its metabolic/thermogenic capacity far beyond that of any other tissue. During exercise, voluntary muscle contractions can increase metabolic rate by as much as 15 to 20 times. In contrast, during cold exposure, maximal heat production can only increase ~5 times above baseline values or 40%VO_2max (36). Exact physiological reasons why maximal thermogenesis is 3 to 4 times lower during shivering than during exercise is far from being well understood. Interestingly, however, this maximum seems consistent with maximal shivering intensity of avian and large mammalian species which rely almost entirely on this mode of heat production during cold exposure (9, 98). Research has also shown that high ST intensities may interfere with voluntary movements (83, 84). Perhaps, through our evolution, lower shivering intensities produced sufficient heat to increase odds of survival without compromising locomotion and/or cold survival.

Using sEMG methodologies, researchers have been able to quantify changes in shivering intensity as well as electrophysiological characteristics of shivering muscles (continuous *vs* burst shivering as discussed below)(8, 12, 50, 51, 67, 90). This work has shown that changes in shivering intensity are closely related to changes in both skin and core temperatures which are the ultimate driving force of ST (36, 120, 143). It is important to note that even without significant changes in core temperature, shivering intensity increases progressively as average skin temperature decreases (Figure 2). For example, using a liquid conditioned garment, a ~3°C decrease in average skin temperature results in an average increase of ~2% of maximal voluntary contractions (%MVC) while a ~9°C decrease in skin temperature increases shivering to ~10%MVC (44, 54, 90). Under compensable cold conditions, where rates of heat production match rates of heat dissipation, the stimulation of shivering and total thermogenic rate can occur rapidly with quick alterations in skin temperature (66).

Quantification of shivering EMG also reveals two distinct shivering patterns in individual skeletal muscles based on their differences in intensity [2-5 vs. 7-15 % of maximal voluntary

contraction (%MVC)] and rate of occurrence (8-10 vs. 0.1-0.2 Hz)(51, 67). Continuous, low-intensity shivering is related to low threshold fibers (type I, specialized for lipid use) while high-intensity bursts are associated with high-threshold fibers (type II, specialized for CHO use)(83). The origins and thermogenic importance of this dual pattern in humans are still unclear at best. In shivering birds, researchers have indicated that burst activity is attributed to variations in fiber composition where anaerobic muscles tend to burst more than aerobic ones (62, 88). However, fiber composition in avian flight and leg muscles is generally more homogeneous than what is found in humans. Human skeletal muscles are made of the different types of fibers and the presence of these various fiber types varies greatly between skeletal muscles and individuals (39, 110). In this context, it may be more difficult to clearly establish a relationship between burst activity and fiber composition.

Of particular interest, shivering intensity and burst rate are extremely consistent within the same individual even when CHO availability is modified in men (52; Discussed in Fueling shivering thermogenesis) or when measurements are made at the luteal and follicular phases of the menstrual cycle in women (13). In contrast, between individuals, large inter-individual variations in skeletal muscle and fiber recruitment exist even in morphologically similar adults (8, 13, 48, 49, 51). At the whole body level, these variations in relative contributions of high intensity bursts and continuous low-intensity shivering do not seem to affect total thermogenic rate even during mild to moderate intensity shivering (51). However, they have important consequences on metabolic fuel selection (53) as well as possibly on shivering endurance and survival in the cold (48).

Fueling Shivering Thermogenesis.

Muscle contractions during ST are sustained by the combined oxidation of carbohydrates (CHO), lipids and proteins (see 48, 137 for review). Each metabolic fuel presents distinct differences in their energy potential and in the size of their reserves. In order to maintain ATP production during ST, these substrates need to be provided to shivering muscles at appropriate times and rates from intramuscular reserves and/or from other tissues *via* circulation. Over the last decades, metabolic research in the cold has focused on understanding whether, like exercise, the depletion of CHO reserves could limit ST endurance (142). However, to date, evidence indicates that adult humans are able to sustain ST and whole-body thermogenesis using a wide variety of metabolic fuels. When one fuel source is depleted or reduced, others compensate in order to maintain ATP production and thermogenic rate. Current knowledge on the importance of CHO, lipids and proteins in the cold will be described in the following sections.

Carbohydrates

CHO account for only ~1% of total energy stores (~95% for lipids and ~4% for proteins) and have an energy potential more than half of that of lipids at 17.3 kilojoules per gram (136). This fuel is well known to limit prolonged endurance exercise but does not seem to be limiting for shivering in the cold. During shivering, in men and women with normal glycogen reserves, CHO provide ~20-80% of all the heat produced (see 48 for review) with rates of oxidation ranging from ~130 to 500 mg kg^{-1} h^{-1} from mild to moderate cold exposure (13, 54; see Figure 3). The highest rates of whole-body CHO oxidation were found during passive rewarming (55). When men were re-warmed from a T_{core} of ~34.5 to 36.5°C following a 7°C water immersion, CHO oxidation rates reached as much as ~1.5 $g \cdot min^{-1}$ and accounted for three quarters of all the heat produced. Together, these findings during cold exposure and during re-warming demonstrate that CHO are a substantial fuel source to sustain thermogenesis.

The glucose required for maintaining ATP production in shivering muscles is supplied from liver glycogen *via* the circulation and from *in situ* utilization of glycogen within muscle fibers. Both plasma glucose and muscle glycogen were reported to play significant roles for maintaining heat production during cold exposure (52-54). Research has indicated that muscle glycogen supplied at least ~75-80% of the glucose required to sustain thermogenesis whereas the contribution of plasma glucose remained constant at ~20-25% (52-54). It is important to note that the respective contributions of muscle glycogen and plasma glucose to total CHO oxidation remains the same independently of changes in glycogen availability or shivering intensity. Similar to exercise, muscle glycogen is always the greatest source of glucose for sustaining whole-body CHO oxidation and energy demands in the cold. This brings forth a very important question: are muscle glycogen reserves essential for shivering endurance or can lipids and proteins compensate for reductions in endogenous CHO availability?

In three independent studies, CHO availability was artificially altered through dietary and exercise manipulations before exposing men to either mild (2.5X RMR; 51) or moderate cold exposure (3.5X RMR; 80, 150). Results showed that at both shivering intensities modifying the size of glycogen reserves caused a large shift in fuel use from CHO dominance (up to ~80% $\dot{H}_{prod}$) to lipid dominance (up to ~80% $\dot{H}_{prod}$). Despite this large shift in substrate utilization, core and skin temperatures as well as whole body heat production were the same between treatments. This indicates that decreases and increases in CHO availability result in a respective up- or down-regulation in the use of lipids and proteins. This metabolic flexibility may not be surprising considering the relatively low metabolic rates achieved in the cold. Adding to this conclusion, Haman *et al.* (50, 52) showed that, during mild shivering, humans are able to sustain a constant thermogenic rate by oxidizing these widely different fuel mixtures without modifying sEMG shivering pattern or muscle fiber recruitment (i.e. intensity, burst *vs.* continuous shivering). Therefore, the drastic switch in fuel metabolism found as a result of glycogen depletion and loading (CHO, ~28 vs 65%; lipids, ~53 vs 23%; proteins, ~19 vs 12% $\dot{H}_{prod}$, respectively) can be maintained within the same muscle fibers. Research during exercise has shown that large

changes in fuel selection within the same fibers can be regulated by modulations in intracellular metabolites (acetyl-CoA, malonyl-CoA, Ca^{2+}, ADP, AMP, P_i and AMPK I) (68, 114). It is likely that the same mechanisms for the regulation of metabolic fuels are involved during shivering. These results emphasize the importance of proteins and lipids in compensating for large decreases in CHO availability and indicate that CHO might not be essential to sustain ATP production during ST.

In follow up experiments, Haman et al. (51) showed that, during moderate intensity shivering, fuel selection can also be modified by inter-individual variations in EMG shivering pattern. At a shivering intensity of ~3.5XRMR, fuel selection in men ranged from 33 to 78% $\dot{H}_{prod}$ for CHO and from 14 to 60% $\dot{H}_{prod}$ for lipids. EMG analysis of 8 large muscles showed that burst shivering activity also exhibited large variability amongst individuals ranging from ~2 to 8 bursts per minutes. Because burst activity was previously associated with the recruitment of glycolytic type II muscle fibers (83, 84), it was assumed that whole body CHO oxidation rate would be correlated with burst shivering activity. The relationships between inter-individual variations in bursts shivering rate and plasma glucose, muscle glycogen and whole-body CHO utilization rates are presented in Figure 4. Results show that both muscle glycogen and whole-body CHO oxidation co-vary closely with individual variations in burst activity whereas the use of plasma glucose does not. This demonstrates that individuals with higher burst rates not only oxidize more glucose at the whole body level but would deplete muscle glycogen faster than the ones that display low bursting activity at the same given shivering intensity. If this is the case, could there be an *optimal fuel mix* and an *optimal fiber recruitment* for promoting shivering endurance during prolonged cold exposure?

In a review published by Haman (48), the potential consequences of large modifications in fuel utilization on shivering endurance, induced by changes in CHO availability and inter-individual variations in muscle activity pattern, were presented. Conclusions drawn were based to a large extent on the assumption that muscle glycogen is essential for shivering during exposures lasting for longer than 2h. *If this is the case*, these calculations showed that a)

modifying the fuel mix used for shivering does not provide a survival advantage and b) cold endurance varies greatly among individuals shivering at the same relative intensity because of large differences in fiber recruitment pattern. When it comes to finding the *optimal fuel mixture* to sustain ST, time to glycogen depletion can be calculated assuming that a) individuals shivered at 200 W, b) the relative use of the different fuels remained the same until glycogen depletion, c) 80% of total muscle glycogen was available for oxidation, d) active muscle mass during shivering was 70% of 36 kg, e) mean muscle glycogen concentrations were 62, 102 and 137 mmol glucosyl units/ kg wet mass as observed in Young *et al.* (150), and f) muscle glycogen oxidation rate was 16, 21 and 30 μmol·kg body mass^{-1}·min^{-1} as observed in Haman *et al.* (52, 53) for low, normal and high glycogen reserves, respectively. These calculations of muscle glycogen depletion time suggest that humans are able to maintain a thermogenic rate of 200 W for the same amount of time (~20 h) independently of differences in the composition of fuels being used. While this could be true during low-intensity shivering, it is still unclear whether this would also be the case at higher shivering intensities. Important increases in the use of muscle glycogen reserves have been found as shivering intensifies (54). When it comes to establishing an *optimal shivering pattern* to maintain ST, time to glycogen depletion was calculated assuming that: a) the relative use of the different fuels remains the same as after 90 min of shivering, b) 80% of total muscle glycogen is available for oxidation, c) active muscle mass during shivering is 70% of 36 kg, d) mean muscle glycogen concentrations are 100 mmol glucosyl units/ kg wet mass as observed in Martineau *et al.*, (80), and e) muscle glycogen oxidation rates range between 15 and 51 μmol·kg body mass^{-1}·min^{-1} (54)]. According to these estimates, individuals with high (~8 burst·min^{-1}) and low burst shivering rates (~4 burst·min^{-1}) would shiver respectively at 300 W for ~5 h and ~25 h before depleting muscle glycogen reserves. These estimates confirm that reducing burst shivering activity rate may be a key strategy to improve shivering endurance and survival time in the cold. With this said, *if muscle glycogen is not essential,* these calculations indicate that lipids and proteins are able to compensate for varying contributions from CHO and the above estimates of cold endurance can be increased substantially.

It is important to note that prior to obtaining detailed quantifications of the partitioning of CHO reserves for energy production in the cold, Wissler (142) had proposed an elaborate model to predict shivering endurance based on empirical observations from Beckman and Reeves (1966). In his model, shivering fatigue was determined from the onset of muscle cramping observed in a group of men exposed to 24°C water. Under conditions previously describe in glycogen depleted and glycogen loaded individuals (52), the model of Wissler predicts that shivering at 200 W could be sustained for 33 to 42 h. In addition, Tikuisis *et al.* (119) later suggested that the Wissler model may underestimate true values. Our calculated shivering endurance of 20 h based on whole-body oxidation of glycogen is clearly shorter than that predicted by Wissler *et al.* (142) or Tikuisis *et al.* (119). Again, this observation suggests two possible shortcomings for our simple approach: a) glycogen may not be essential, and low-intensity shivering is sustainable solely on lipids and proteins and/or, b) a significant shift in fuel selection to spare glycogen takes place after 2 h of shivering (in fact, a progressive increase in fat oxidation was observed by Tikuisis *et al.* (119) during prolonged shivering lasting for up to 4 h). No detailed information is currently available on fuel selection for shivering in excess of 4 h, and it is still unclear whether glycogen depletion coincides with muscle fatigue. Future studies should address this interesting problem. At the moment, however, research has demonstrated that lipid and protein oxidation can compensate for any reductions in CHO availability over a period of 90-120 min at shivering intensities ranging between ~2.5 to 3.5 XRMR. Of course, longer exposure times and different shivering intensities would be needed to validate this assumption.

Lipids

Lipids are by far the largest and most energy dense of all metabolic fuel stores (136). Size of reserves and total energy potential are determined by the one's level of adiposity. An individual weighing 70kg with 10% body fat would have ~7 kg of lipids resulting in an energy content of ~285 Mj; assuming that all lipids are accessible for energy production at ~40.8 kilojoules per gram. It is well established that during exercise, lipids are the preferred fuel for endurance

exercise below ~50-60% of maximal power. In the cold, Haman *et al.* (54) showed that the relative contribution of lipids dominate below 50% of maximal shivering intensity (~20%VO2max) but that the role of this fuel is reduced progressively as shivering intensifies and more type II fibers are recruited. This reduction in the relative use of lipids is not associated with a reduction in absolute rates of oxidation. Whether at low to moderate intensity shivering during cold exposure (54) or up to maximal shivering intensity during rewarming (55), absolute rates of lipid oxidation always remains constant at an average of ~140 $mg \cdot kg^{-1} \cdot h^{-1}$ (Figure 3). This observation indicates that maximal lipid oxidation is already reached at low shivering intensities of ~2.5XRMR. Assuming a total energy content from lipids of ~285MJ, a 70kg individual with 10% body fat could shiver for ~30 days at this lipid oxidation rate before depleting lipid reserves. This highlights the tremendous capacity of lipids as an energy fuel source especially at low metabolic rates. Still, it remains unclear why lipid oxidation would plateau at a value ~3 times lower than what would be found during exercise at a similar metabolic rate (1). Even when glycogen stores are depleted or loaded prior during mild cold exposure, lipid use remains at ~140 $mg \cdot kg^{-1} \cdot h^{-1}$ when reserves were low and decreases by more than half to ~60 $mg \cdot kg^{-1} \cdot h^{-1}$ when CHO availability are high (52). Only in women was lipid oxidation rates higher ranging between ~190 and 200 $mg \cdot kg^{-1} \cdot h^{-1}$ in the luteal and follicular phases of the menstrual cycle (13). In effect, the calculated relative contributions of lipids to total heat production were much higher at both menstrual phases (~72-75% Hprod) in women than in men. While differences in fat oxidation between menstrual cycle phases have been reported at resting and during exercise with elevated concentrations of estrogen (46, 139), these differences do not appear to be consistent with cold exposure studies. Elevated estrogen levels promote lipolysis, increasing fatty acid availability resulting in increases in lipid oxidation (22, 117). However, some investigators have failed to see changes in fuel selection between menstrual cycle phases, despite observing differences in estradiol concentration (64), while others have suggested that these phase-related differences only occur at much greater exercise intensities [90% of Lactate Threshold; (151)]. Two studies during mild cold exposure showed that the large differences in these sex hormones between luteal and follicular phases do not modify thermogenic rate or substrate utilization in women (13, 41). This

may suggest that the cold-induced sympathetic stimulation is masking the effects of these sex hormones. Even though these differences emphasize further the divergence in energy metabolism between shivering and exercise, they also indicate that the important role of lipids for sustaining thermogenesis in the cold.

Lipids are oxidized as fatty acids which are obtained from the lipolysis of triacylglycerol (TAG) stores located in adipose tissue, in the liver or in muscles. In the cold, the relative contribution of each compartment is still unknown. Using stable isotope tracer methods, Vallerand *et al.* (126) and Ouellet (90) indicated that the turnover rate of circulating fatty acids and rates of lipolysis increase proportionally to the increase in metabolic rate found during mild cold exposure. This indicates that circulating fatty acids are likely being used to sustain ATP production in the cold. However, two earlier studies by Martineau and Jacobs (78, 79) identified the effects of a reduction in plasma fatty acids availability in men with normal or reduced CHO reserves immersed at 18°C for 90 min. In both studies, the reduction in circulating fatty acids was induced by an ingestion of capsules containing nicotinic acid (3.2 mg/kg as niacin) before and during cold exposure. When fatty acid concentrations were reduced in men with normal glycogen reserves, results showed that heat production remained unchanged presumably by increasing the use of intra-muscular lipids and of CHO reserves (79). Similarly, in the second study, where both plasma fatty acids and CHO reserves were reduced, changes in metabolic heat production, immersion times and rectal temperature were not different from results found in CHO loaded and normal plasma fatty acid treatments (78). This further highlights the great versatility in fuel selection for sustaining heat production in the cold.

Proteins

It was assumed for decades that involuntary muscle contractions during shivering were almost entirely fueled by CHO and lipids, while the contribution of protein oxidation remained

negligible (~10%). Consequently, as it is customary in exercise studies, few cold exposure studies corrected CHO and lipid oxidation rates to account for the contribution of proteins. However, evidence clearly shows that proteins can contribute as much as plasma glucose in the cold (~10%Hprod, 53) and that this contribution is affected by changes in shivering intensity (54) and nutritional status of individuals (52). Most importantly, no research to date has indicated that absolute rates of protein oxidation are affected by acute cold exposure. Consequently, the relative contribution to total thermogenic rate decreases proportionally with to the cold-induced increase in metabolic rate. Haman *et al.* (52) indicated that protein oxidation plays a more substantial role (~25% $\dot{H}_{prod}$) than previously anticipated in compensating for the decrease in CHO oxidation when glycogen reserves are low. In fact, failing to account for the oxidation of proteins in the total energy budget may result in a significant overestimation of CHO and lipid oxidation rates. Generally, the cold-induced increases in metabolic rate is accompanied by a proportional decrease in the relative use of this fuel (52, 54). For this reason, when protein oxidation rate is high before cold exposure, the relative importance of this fuel to total heat production remains elevated during shivering. In contrast, when it is low, its contribution tends to become minimal. For example, during low-intensity shivering (Fig. 2A), proteins provide only 10% $\dot{H}_{prod}$ (25% $\dot{H}_{prod}$ before cold exposure) when glycogen reserves are high but as much as 25% $\dot{H}_{prod}$ (40% $\dot{H}_{prod}$ before cold exposure) when glycogen reserves are low. Together these observations indicate that future shivering studies should not only normalize subjects as much as possible for differences in nutritional status (i.e. size of glycogen reserves) but also provide estimates of protein oxidation rates to allow inter-study comparisons.

Energy deficit in the cold

Little is known on the effects of energy deficits on ST. Following a 12 and 48 h fast, MacDonald *et al.* (75) showed that core temperature was lowest in a prolonged unfed state (48h fast) than following the 12h fast during five progressively reduced levels of cold stress. This

lowered core temperature was associated with an increased heat loss linked to a greater forearm blood flow in the 48h fasted group compared to the 12h fasted individuals. Interestingly, the reduction in core temperature occurred independently of a significant increase in thermogenic rate. Such increases in heat production are typically observed following 36-48 h fasts (76, 77, 135) and are attributed to substrate cycling (triglyceride-fatty acid and alanine-glucose cycling and the Cori cycle) common in the gluconeogenic phase of prolonged fasting (37). Metabolic rate generally returns to pre-fasted levels after more prolonged starvation [72-h; (135)]. Later, Young *et al.*(148) and Castellani *et al.* (24) reported that chronic energy deficits from underfeeding and strenuous military training lasting longer than 48-h (84-h to 61 days) reduce the capacity to thermoregulate in the cold. This effect is related to a reduced thermogenic rate as well as a reduction in insulative capacity from decreased lean and fat mass. The effects on thermogenic rate are restored after 48 h period of rest and refeeding but it may take as much as three months for the insulative capacity to return to pre-camp levels (148). It has been speculated that the decreased in heat production may be linked to limited substrate availability or to the decrease in glycaemia generally observed in prolonged fasted individuals [from 5.2 mmol/L in 12-h fast to 3.8 mmol/L in 60h fast; (21)]. Together these findings supports the premise that shivering endurance is affected by chronic energy deficit and its effects on CHO availability (119) and glucose concentration (47, 93). In this context, providing supplemental exogenous substrates through feeding may prove beneficial to maintain ST.

As mentioned above, it has long been speculated that the main limiting factor for survival in the cold is the depletion of muscle glycogen, leading to a reduced cold sensitivity [lowered drive to shiver (119)], or hypoglycaemia (glucose concentration <2.8 mM) leading to reduced or inhibited shivering thermogenesis (38, 47, 93). To date, no studies have successfully elicited such responses through prolonged cold exposure. However, there is little doubt that preserving the scarce endogenous glycogen reserves is of critical importance. Although it is well documented that when muscle glycogen reserves are reduced, lipid and protein oxidation compensate to maintain a constant rate of heat production (52), it is unclear whether this mechanism is sufficient to maintain heat production for a prolonged period, particularly if muscle

glycogen, this limited resource, is still strongly mobilized. This has lead researchers to suggest that sparing CHO reserves through CHO supplementation may be an important strategy in prolonging thermogenesis (53, 119).

Eating in the cold: from choice of macronutrients to thermogenic compounds

Few studies have investigated the effects of food consumption before or during cold exposure on thermoregulatory responses and the overall energy balance (11, 42, 43, 121, 123, 124). While the purpose of these respective studies varied tremendously, most of the earlier studies were directed at identifying whether ingesting CHO could increase total heat production, *via* the thermic effect of feeding, during shivering thermogenesis (42, 123, 124). Their findings unequivocally showed that ingesting CHO did not affect the thermoregulatory responses to cold exposure. Of these, only Vallerand, *et al*. (122, 124) and Blondin *et al*. (11) reported estimates of changes in CHO, lipid and protein oxidation in men during low to moderate intensity shivering (2.0 – 3.0 X RMR) following the ingestion of CHO. Vallerand *et al.* (124) showed that when cold-exposed men ingested starch jellies (712 kJ or ~45g CHO) or a high-CHO bar (712 kJ; ~30g CHO, ~4g fat and ~4 g protein), at the beginning and after 90 min of cold exposure, discernible changes in CHO and lipid utilization were only observed when ingesting the jellies. A more recent study, using a combination of stable isotopes and indirect calorimetry methodologies, showed that the relative contribution of CHO to total heat production increased by ~14% and that of lipids tended to decrease to a similar extent when glucose was ingested at a rate of 400 or 800 mg/min over 2h (11)(Figure 3). This study was also the first to partition the utilization of CHO (Figure 5). The utilization of liver-derived glucose decreased in a dose-dependent manner, thus sparing valuable endogenous CHO reserves, while muscle glycogen utilization did not differ from the control condition. Interestingly, the rate of exogenous glucose oxidation reached a peak and plateau of 195 mg/min at the lower ingestion rate; an oxidation rate that was one-third less than what has been reported during exercise eliciting a similar metabolic rate (94). This study also showed that 55-77% of the ingested glucose was not oxidized and thus was unaccounted for.

Presumably the remaining portion was either not absorbed and/or directed towards non-oxidative disposal. These findings lead to a series of studies designed to examine the various strategies to increase the rate of exogenous glucose oxidation as well as increase the quantity of ingested CHO being directed to non-oxidative disposal. For instance, we first looked to manipulate the timing of CHO ingestion, to illicit an insulinemic peak that would coincide with the shivering steady state (15). The hypothesis was that the increased insulinemia combined with the muscle contractions from shivering would increase glucose entry into the shivering muscles, *via* the combined effects of insulin- and muscle contraction -stimulated hemodynamic responses (96) and transmembrane glucose transport (99). This increased uptake would result in an increase in exogenous glucose oxidation and non-oxidative disposal. Indeed, if comparing the same quantity of glucose ingested, consuming glucose later in a cold exposure elicited a greater exogenous glucose oxidation rate (159 ± 17 $mg \cdot min^{-1}$ compared to 118 ± 17 $mg \cdot min^{-1}$). However, in the long term, the utilization rate was greater when glucose was ingested later and the reliance on endogenous CHO reserves was 20% lower compared to ingesting glucose later and 65% lower compared to simply ingesting water. Ingesting multiple transportable CHO (Glucose with Fructose) increased the rate of exogenous glucose oxidation even further (14) while also potentially increasing non-oxidative disposal as a result of the gluconeogenic properties of fructose metabolism.

The thermoregulatory differences between exercise and cold exposure could be the most significant contributing factors to the differences in exogenous substrate utilization observed between these two metabolic conditions. In addition to differences in muscle recruitment patterns mentioned earlier in this review, cold exposure stimulates vasoactive responses which serve to create an insulative shell to reduce the thermal conductance between the environment and the core (97). Veicteinas *et al.* (129) previously showed that 10-15% of the overall body tissue insulation stems from the diminished perfusion of skin and subcutaneous fat when immersed in water, at a temperature eliciting no increase in metabolic rate. The remaining proportion has been attributed to underperfused muscles. As skeletal muscles become perfused, as a result of an increase in heat production (from onset of exercise or shivering), total body insulation

progressively falls as a function of the metabolic rate elicited (17, 92) however, this elevation in perfusion is likely significantly lower than what is found during exercise of the same metabolic rate performed in ambient conditions. In addition, animal models suggest that blood flow to the small intestine during cold exposure, inducing a metabolic rate two-times that of resting metabolism, is reduced by 30-50% of that seen in a thermoneutral condition. Whether a similar response is observed in humans is unconfirmed. Differences in skeletal muscle glucose uptake, and absorption at the gut combined with the previously mentioned differences in muscle recruitment patterns suggest that these fundamental limitations are driving the divergence in exogenous substrate utilization between cold and exercise.

While CHO ingestion has received a lot of attention, far less is known on the effects of lipid and protein feeding on cold endurance. The practice of ingesting protein and/or fat during cold exposure is one that has been employed by Northern inhabitants around the world for centuries (108, 112). It is only due to the modernization of these communities that a shift in macronutrient intake has been observed. Some have questioned whether these macronutrients were consciously chosen for their thermogenic properties or simply due to availability (69). The thermogenic effect of protein ingestion has been reported to elevate the resting metabolic rate for several hours after ingestion in thermoneutral conditions (116). Whether thermic effects of feeding can contribute to total heat production during prolonged cold exposure remains controversial. Beavers and Covino (7) found that ingesting 30 g of glycine during cold exposure at -18°C for 75 min, by heavily clothed individuals, increased the metabolic rate above values observed when ingesting 30 g of glucose. This suggests that the thermic effect of ingesting glycine was additive to shivering thermogenesis. In contrast, a later study by Rochelle and Hovarth (100) showed that when semi-nude men, exposed to 7.5°C for 120 min, ingested either (1) 53.4 g of glucose, (2) 30 g of glycine with 22.1 g of glucose or (3) a 142-g steak heat production and oxygen consumption increased in parallel for all three conditions during the first 90 min. Rochelle and Hovarth (100) attributed this discrepancy to the colder stress imposed in their study compared to Beavers and Covino (7). The subsequent 30 min of cold exposure in Rochelle and Hovarth (100) provided further insight into a possible thermic effect of feeding

during cold exposure such that heat production and oxygen consumption proceeded to stabilize in the glucose and steak conditions but, according to authors, continued to increase in the glycine condition. Further, authors observed that shivering was nearly negligible in the glycine meal, and lower in the steak meal than the glucose meal despite similar rates of heat production. This could indicate that the thermic effect of food may have a supplementary effect on whole body thermogenesis rather than the additive effect originally suggested by Beavers and Covino (7). In more recent studies conducted by Vallerand *et al* (123, 124), participants ingested high-CHO energy bars containing ~30g CHO, ~4g fat, ~4 g protein and theobromine (caffeine-like substance). They observed no significant changes in thermal responses compared to a control condition when volunteers ingested water. They concluded that perhaps the thermic effect of food was masked by shivering thermogenesis when exposed to a cold condition eliciting an increase in metabolic rate of 2.5-3.5 X RMR. This further suggests that rather than adding to the heat production, the thermic effect of food may simply be supplementing shivering thermogenesis, particularly at greater cold stresses where TEF may be indistinguishable. Clearly, further investigations are needed to investigate the role of TEF in maintaining a thermal balance during compensable cold exposure.

More than just shivering: potential contribution of BAT?

The presence of BAT in humans has been recognized since the 16th century (40) but the metabolic relevance of this tissue in adults remained uncertain for centuries. Using quantifications of ^{18}FDG uptake by PET imaging, the amount of BAT present in adults was quantified *in vivo* leaving little doubt that this highly thermogenic tissue could play a role in sustaining heat production during a mild cold exposure . Initial assessments have shown that the quantity of BAT is highly variable between studies ranging from ~60-170g in three studies (12, 90, 132) and up to ~1 kg in another (127). Exact reasons for these large discrepancies between studies are unknown but could be attributed to inter-individual and/or methodological differences. In a retrospective study that included 1013 women and 959 men reported that the presence of

this tissue is influenced by gender, age, percent body fat and season (91). Metabolically, further work is required to determine whether the cold-induced stimulation of BAT can significantly alter whole-body thermogenic rate, shivering intensity and metabolic fuel selection. It is likely that this tissue would contribute most at low shivering intensities where muscle ST is at its minimum. As cold stress intensifies, heat production from the recruitment of large amounts of shivering muscles should rapidly exceed BAT thermogenic capacity (Discussed in *Sustaining shivering thermogenesis*). For this reason, most researcher in this field of physiology have attempted to cold-activate BAT at the lowest shivering intensities possible. Using a combination of fuel kinetics and metabolic tracers with PET/CT methods, it was estimated that BAT supplied ~20% of all the heat produced during a 3h cold exposure resulting in a ~1.8 increase in metabolic rate; with a 3°C decrease in mean skin temperature and no change in core temperature (12, 90). The study by Ouellet *et al*. (2012) also demonstrated that BAT volume was highly variable even in men of similar adiposity, morphology and age. We may speculate that these variations are linked to cold exposure history and/or genetic diversity. In rodents, increased BAT is associated with decreased shivering activity (87). Similarly, Ouellet et al (2012) showed that individuals with large amounts of BAT shivered less than individuals with small quantities of BAT. These important differences in the respective contribution of BAT and ST occurred without modifying thermal responses and whole body thermogenic rate. Together, these studies indicate that the potential effects of BAT activation on whole body metabolism are particularly important in young, healthy adults (90). Perhaps increasing the mass or oxidative capacity of BAT may reduce shivering sufficiently to avoid restricting motor control. In this context, it becomes important to understand whether cold acclimation or the ingestion of known thermogenic compounds could potentiate BAT activity.

Cold acclimation

Humans chronically or intermittently exposed to a cold stress exhibit modified physiological responses to a cold stimulus. Some of these responses are genotypic

characteristics that have evolved through natural selection to favour survival in a cold environment, which are either common to all endotherms or have evolved in hominids in particular. Other responses are a result of cold acclimatization or cold acclimation. The former is defined, by the IUPS Thermal Commission, as physiological changes naturally occurring as a result of the climate in which the organism is exposed to (e.g. seasonal, geographical, working conditions)(27). The latter refers to the physiological changes induced experimentally in a controlled setting (27). The distinction between these terms is not only important as a means of establishing operational definitions and consistency in their usage in the literature, but also assist in identifying what is truly an adaptive response versus a phenotypic change to an already existing physiological response. In addition, the physiological changes that have been observed in acclimatization studies can often help explain some of the physiological changes evoked through acclimation. Although the physiological adjustments commonly observed following a cold acclimatization or acclimation include the development of a thermogenic (commonly referred to as metabolic), insulative or hypothermic phenotype, or a combination thereof, this review will focus primarily on the metabolic adjustments resulting from cold acclimation. A thorough description of the various cold acclimatization or acclimation patterns are beyond the scope of this review but has been comprehensively described elsewhere (147).

A metabolic form of acclimatization or acclimation refers to an increase, relative to unacclimatized/unacclimated conditions, in cold-induced metabolic heat production which is often accompanied by higher skin temperatures but a normal core temperature. To our knowledge, such adjustments have only been found in certain populations living in cold conditions [eg.(35, 56, 58)]. Consequently, the differences in the physiological responses between this population and the control comparison group is likely attributable to genetic adaptations related to differences in physical characteristics, such as morphology and fitness, or dietary factors such as an increased consumption of proteins. To date, the results and interpretation of results from cold acclimation studies have been quite contradictory. While some have demonstrated a 17% decrease in heat production (60), others have demonstrated either a slight ~10% increase in thermogenic rate (10) or no change (149). The divergent thermogenic adjustments exhibited in response to

experimentally induced cold-acclimation may be related in part to differences in acclimation protocols; 30 min twice daily at 4.4ºC for 8 weeks (60), 90 min 5 days a week for 5 weeks in 18°C water (149) and 60-180 min for 4 to 5 days per week depending on individual tolerance in 10-15ºC water for 8 weeks (10). In these examples, the main focus was placed on changes in metabolic heat production measured from changes in whole-body rates of oxygen consumption. Consequently, the extent that ST or NST were modulated over the course of these acclimations is unclear. It is likely that changes in the respective contribution of ST and NST to total thermogenesis can occur without modifying rates of oxygen consumption. This would be consistent with the cold-acclimation pattern observed in various species of birds and mammals which decrease the contribution of ST-mediated metabolic heat production and increase that of BAT- or muscle-derived NST (6, 19, 25, 57, 95, 118) through cold acclimation.

In humans, the quantitative assessment of changes in the recruitment of thermogenic processes resulting from cold-acclimation has been limited. In one of the earlier cold-acclimation studies, Davis *et al.* (32) showed that exposing six unacclimated men to 12-14°C air, 8 hours per day for 31 consecutive days could reduce mean shivering activity to 20% of pre-acclimation values which was also accompanied by a ~20% fall in heat production. By definition this implies an increase in cold-induced NST. Necropsies performed on outdoor workers have suggested that repeated cold exposure can result in a greater BAT mass, compared to indoor workers of the same age (65), implying that perhaps the changes from this earlier study could be explained by an increase in BAT mass and activity. However, studies examining the function of this phenotypic change and the implications on whole body thermoregulation have been lacking. Recently, two studies have investigated the effects of daily cold exposure on BAT recruitment (127, 146). Both investigations confirm the findings from the earlier necropsy studies, that daily cold exposure ranging from 10 days to 6 weeks can increase the volume of BAT taking up circulating glucose. However, the functionality of this tissue and its effect on whole body metabolism has still remained ambiguous. To address this significant gap, we recently examined the functionality of these phenotypic changes in six healthy men exposed to 10°C, two hours daily for four weeks, by quantifying shivering intensity, BAT oxidative metabolism and glucose uptake using EMG coupled

with PET methodologies (12). We found that daily cold exposure not only increased the volume of metabolically active BAT by 45%, but more importantly increased its oxidative capacity 2.2-fold. This was paralleled by an increase in fractional and net glucose uptake by BAT. Interestingly, the significant changes in BAT oxidative metabolism had no effect on shivering intensity, measured either by surface EMG or the net uptake of ^{18}FDG in skeletal muscle (presented as a shivering index), despite whole body energy expenditure remaining the same. It may be that shivering was already limited to ~2.0 % MVC and that perhaps a colder thermal stress might have provided the necessary stimulus to demonstrate a reduction in shivering intensity. However, the immobilization required for accurate dynamic PET acquisition preclude the possibility of studying BAT functionality using a colder stimulus.

Intermittent cold exposure may also elicit changes to skeletal muscle phenotype, particularly muscle bioenergetics, which could suggest that the thermogenic contribution of shivering relative to non-shivering mechanisms may also change. Currently, very little is known regarding the structural and metabolic alterations that may result from repeated cold exposure, particularly with regards to changes in metabolic efficiency and properties of muscle fibers. Prolonged exposure to a mildly cold environment (82 hours at 16°C air) has been shown to result in cold-induced mitochondrial uncoupling in skeletal muscle (141), clearly demonstrating the potential for muscle-derived NST. However, a more recent study, from the same group (127), showed that a shorter cold exposure may not evoke such changes to mitochondrial uncoupling, nor does cold acclimation through daily exposure to 15-16 °C for 6 hours for 10 days. These findings are difficult to consolidate but warrant further investigation if we are to gain a greater global perspective of the thermogenic alterations that occur through cold-acclimation.

Similar to the bioenergetic changes, the properties of muscle fibers may also play a critical role in modulating the thermogenic responses to repeated cold exposure. Electrical stimulation studies have shown that the adaptation of muscle fibers appears mediated by the pattern of motor neuron firing, such that tonic motor neuron activity stimulates a slow oxidative phenotype (upregulation of type I and IIa-specific gene expression) whereas interspersed bursts

of high amplitude firing promotes a fast glycolytic phenotype (26). The fiber recruitment pattern (continuous *vs.* burst shivering) and amplitude of the respective shivering components traditionally observed during an acute cold exposure (50) should evoke changes towards a slow-fiber-specific phenotype under more chronic stimulation. The only study to date demonstrating possible temperature-induced changes in fiber composition [Korean breath-hold divers, Ama; (5)] , may be confounded by the cooling medium (water), extreme cooling (oral temperature reaching 35°C in the summer or 33°C in the winter; (63, 70), effects of hydrostatic pressure and the hypoxic conditions (63) resulting from breath-hold diving. In this study, the breath-hold divers demonstrated greater type IIx muscle fibers which was also accompanied by a reduction in fiber cross-sectional area and capillarization, compared to athletic women, all indicative of hypoxic and hemodynamic-induced alterations rather than temperature-induced.

Combined, these studies demonstrate that there remain substantial gaps in our understanding of the metabolic pathways and the subsequent fuel selection that may be modulated through chronic cold exposure. Despite a possible successive shift in mechanisms of heat production occurring through cold-acclimation, the resultant effect on whole body heat production and fuel selection is unremarkable. For example, as described in *Fueling thermogenesis,* whole-body rates of lipid oxidation increases proportionally to the rate of heat production. This whole-body lipid oxidation, in unacclimated conditions, is likely derived from the uptake and utilization of circulating fatty acids by skeletal muscle combined with the lipolysis and utilization of intramyocellular triglycerides. A successive shift in heat production towards BAT-derived thermogenesis would likely have an undetectable effect on whole body fuel selection since BAT relies predominantly on intracellular triglycerides as its primary fuel source (90), independently of acclimation status (12). In addition, conditions that favor fatty acid oxidation, such as low-intensity exercise, food deprivation (fasting or prolonged starvation) and presumably mild cold exposure , tend to also result in skeletal muscle adaptations that promote fatty acid oxidation. Examining the compounds that may stimulate BAT activity in the cold may provide further evidence to support such a hypothesis.

Compounds that may stimulate BAT in the cold

Finding strategies to acutely stimulate the activity of BAT and overall NST would provide a means to prevent excessive shivering, improve thermal comfort and increase overall cold tolerance. BAT is a particularly interesting target for pharmaceutical agents as it has substantial sympathetic nervous system (SNS) innervations (152). In addition, the SNS is known as the main stimulator of BAT during cold exposure (85). Norepinephrine (NE), released by the postganglionic neurons of the SNS, act on the β-adrenergic receptors of BAT which initiates the breakdown of intracellular triglycerides, leading to the release of fatty acids which act as both a thermogenic substrate and regulator of BAT thermogenic activity (19). BAT activation can be inhibited by injection of the nonselective β-blocker, propanolol (113), indicating that BAT activation is indeed mediated through β-adrenergic receptors. However, to date, the infusion of a non-selective β-agonist has been unsuccessful in activating BAT in humans (133) at the doses given, while compounds affecting parts of the β-adrenergic cascade, or potentiating the release of NE, could have the ability to activate BAT. It is important to note that the use of non-selective β-agonists at greater doses than previously reported may also provoke undesirable side-effects such as tachycardia, arrhythmias, increases in systolic blood pressure and circulating lipid levels which may provoke the atherosclerotic state of those in which it is targeted, overweight or obese individuals. Are there safe and effective compounds that could activate BAT activity?

Since the discovery of BAT by PET/CT in 2009, three recent studies have investigated the effects of a capsinoid (144) and ephedrine (20, 28) on BAT activity (Table 1). These studies focused exclusively on examining the effect of ingesting these compounds on BAT activity, not their effect on cold-induced BAT activity. In their study, Yoneshiro *et al*. (144) categorized their non-cold acclimatized men either as BAT negative (BAT-) or BAT positive (BAT+) using ^{18}FDG tracer uptake with PET/CT. Both groups were then given either 9 mg of capsinoids or a placebo and energy expenditure was quantified by indirect calorimetry at 27°C. When compared to placebo, results showed that whole-body energy expenditure remained unchanged in BAT-individuals whereas in the BAT+ individuals, thermogenesis increased slightly by ~15 kJ/h (or

less than ~5% increase of total heat production). The potential effects of capsinoids on BAT, both in human and in rodents, are believed to be elicited through the gastro intestinal transient receptor potential vanilloid subfamily, member 1(TRPV1) and related receptors (144) which then stimulate the SNS and ultimately BAT. However, much work is still required to confirm this pathway in humans. Currently, only indirect evidence exists suggesting that capsinoid ingestion stimulates the SNS and subsequently BAT. Nevertheless, it is also plausible that the increase in energy expenditure and BAT activation resulting from capsinoid ingestion is a secondary effect resulting from the drive to re-establish equilibrium following the initial stimulation of heat loss responses (73). Two other researchers have chosen ephedrine to stimulate BAT as it is has been used for decades in weight loss and athletic performances. Compared with other molecules, it is safe and well known to activate the SNS. In one study, ephedrine was injected intravenously at 1 mg kg^{-1} in lean men and women while in the other study, a dose of 2.5 mg kg^{-1} was given orally in lean and obese men. Using a relatively low dose, Cypess et al. (28) did not observe any changes in BAT activation. In contrast, at a higher dose, Carey et al. (20) reported a significant increase in BAT activation in lean but not in obese individuals. Early indications suggest that obese individuals may have a smaller BAT mass or less active BAT than lean individuals (131), which could explain the absence of BAT activity in the obese participants given ephedrine. Alternatively, the blunted response to catecholamine-induced lipolysis in white adipose tissue of obese insulin-resistant individuals suggest that if this catecholamine resistance is generalized to all adipose tissues, SNS-mediated intracellular lipolysis in brown adipocytes might also be blunted in this population (see 45 for further review). Although ephedrine has a stimulatory effect on BAT, its activation was shown to be much lower compared to cold exposure (20). Further, the ingestion of ephedrine comes with a number of cardiovascular risks including an increase in both systolic and diastolic blood pressure (2, 3, 20, 28) and heart rate (3, 20, 28, 74), which makes it an unsuitable pharmacological treatment strategy to stimulate BAT activation for the purpose of weight loss. Together, these findings indicate that both capsinoids and ephedrine have the potential to stimulate BAT especially in lean individuals. However, their effects on BAT, whole

body energy metabolism and muscle recruitment during cold exposure are still unclear at best, as measurements have only been made at room temperatures between 20 and 27°C.

More than 20 years ago, thermal physiologists attempted to identify molecules that may increase cold tolerance by reducing the onset of hypothermia. The general strategy was to identify compounds that could stimulate overall rates of heat production thus reducing rates of decrease in T_{core}. Methylxanthines, such as caffeine, theophylline and theobromine, were identified as the most promising of these compounds. Table 1 summarizes the effects of these three naturally-occurring methylxanthines as well as that of aminophylline, ephedrine and green tea extracts on thermal and metabolic responses in non-cold acclimatized men exposed to various types of cold exposure. It is important to note that, to date, all studies have been conducted in young, lean, non-cold acclimatized men exposed to either cold air, cold water or using a liquid conditioned garment. The initial 6 studies conducted between 1986 and 1993 were aimed at finding the methylxanthine or the mixture of methylxanthines and other compounds that would produce the greatest increase in thermogenic rate and smallest reduction in core temperature. In their study, Vallerand *et al* (122) found entirely different results between participants when theobromine (7.5 mg kg^{-1}) was ingested alone at 7°C for 3h. For this reason, Vallerand *et al*. (125) dichotomized the participants into responders and non-responders. With this approach, results showed that total heat production was 20% higher in responders compared to non-responders. However, these researchers could not assess the effects of theobromine on changes in skin and rectal temperature, based on this grouping, as baseline values were also very different between responders and non-responders. The largest effects of any compound on thermal and metabolic responses were observed when ephedrine, caffeine and theophylline were given in combination. In men exposed to 7-10°C for 3h, ingestion of these compounds in combination increased heat production by close to 20% and substantially reduced decreases in skin and rectal temperature. While these studies expose the potential effect of these molecules in stimulating thermogenesis in the cold, they provide little information on the changes in the contribution of ST and NST to this increase in thermogenic rate.

Only one study has used combined thermal, metabolic and electrophysiological methods in an attempt to identify effects of ingesting green tea extracts on thermogenic rate and on the relative contribution of ST and NST during mild cold exposure. Gosselin et al. (44) quantified the effects of ingesting a large dose of green tea extracts (1600mg of EGCG and 600mg of caffeine) given during a 3h cold exposure using a liquid condition garment circulating 15°C water. When compared to the placebo, the ingestion of green tea extracts increased whole-body heat production by 10% and reduced shivering intensity by 20%. These changes occurred without modifying core and mean skin temperature, fuel selection or relative contribution of individual muscles to total shivering. These results revealed that cold-induced NST and whole-body heat production are up-regulated by the ingestion of green tea extracts. However, this analysis does not provide the exact sites responsible for the increase in NST and therefore, it is unclear whether BAT was the main NST site activated. In green tea extracts, the two most abundant and physiologically active components are caffeine and catechin polyphenols, with epigallocatechin gallate (EGCG) being the most potent and active of these polyphenols (140). The thermogenic effect of catechins stems from the inhibition of catechol-O-methyltransferase (COMT), the enzyme that degrades NE in the synaptic cleft (16). This results in prolonging the action of NE on target tissues such as BAT (33, 109). Combined, caffeine works to potentiate the effect of EGCG since their respective actions act at different steps in the cascade. Even though BAT would be stimulated by this enhanced release in NE, many other thermogenic processes may also contribute to total NST such as uncoupled mitochondrial oxidative phosphorylation in skeletal muscle (141), stimulation of futile cycles, such as the TAG/NEFA cycle (126) and dysregulation of Ca^{2+} handling in skeletal muscle (4, 111). Direct measurements of changes in BAT activity would be needed to determine whether this tissue is the primary NST site being stimulated when green tea extracts are ingested. Hopefully, in the future, the various measurement methods used by the studies in Table 1 can be combined in order to obtain a better insight on the effects of potentially thermogenic compounds on cold tolerance and energy metabolism.

What these studies demonstrate is that ingesting these thermogenic compounds may play a role in increasing the recruitment of BAT or potentiating BAT activity once it is stimulated.

However, their ingestion alone appear insufficient in activating BAT under thermoneutral conditions and still require a cold stimulus in order to have their potentiating effect on thermogenesis or lipid utilization. This is in contrast to the likely effect these compounds may have on muscle NST which may be stimulated even under thermoneutral conditions as it does not require an activator, such as cold exposure, in order for the tissue to be recruited or stimulated.

Conclusion

This review shows that the contribution of CHO, lipids and proteins to total heat production is influenced by changes in shivering intensity and pattern as well as modifications in energy reserves and nutritional status. Lipids are generally preferred during low intensity shivering while the role of CHO becomes more important as shivering intensity increases. Muscle glycogen is the most important source of glucose representing as much as ~80% of all the CHO oxidized in the cold under all conditions presented here. However, when CHO reserves are reduced, lipids and proteins increase their oxidation rate to maintain heat production. Consumption of glucose and fructose in combination may help reduce the oxidation of glucose derived from muscle glycogen by increasing the use of plasma glucose. Even though energy deficit is known to reduce cold tolerance, much work remains to fully understand the effects of specific macronutrients on shivering endurance during cold exposure. In addition to shivering, it is now clear that the highly thermogenic brown adipose tissue could contribute substantially to total thermogenic rate in young adults. However, the quantitative nature of this contribution is unclear at best. Finding means to potentiate this effect through cold acclimation and/or the ingestion of compounds that stimulate the thermogenic process (i.e. green tea extracts) may have important implications in cold endurance and survival.

References

1. **Achten J, Gleeson M, and Jeukendrup AE.** Determination of the exercise intensity that elicits maximal fat oxidation. *Med Sci Sports Exerc* 34: 92-97, 2002.
2. **Astrup A, Bulow J, Madsen J, and Christensen NJ.** Contribution of BAT and skeletal muscle to thermogenesis induced by ephedrine in man. *Am J Physiol* 248: E507-515, 1985.
3. **Astrup A, Toubro S, Cannon S, Hein P, and Madsen J.** Thermogenic synergism between ephedrine and caffeine in healthy volunteers: a double-blind, placebo-controlled study. *Metabolism* 40: 323-329, 1991.
4. **Aydin J, Shabalina IG, Place N, Reiken S, Zhang SJ, Bellinger AM, Nedergaard J, Cannon B, Marks AR, Bruton JD, and Westerblad H.** Nonshivering thermogenesis protects against defective calcium handling in muscle. *FASEB J* 22: 3919-3924, 2008.
5. **Bae KA, An NY, Kwon YW, Kim C, Yoon CS, Park SC, and Kim CK.** Muscle fibre size and capillarity in Korean diving women. *Acta Physiol Scand* 179: 167-172, 2003.
6. **Barre H, Geloen A, Chatonnet J, Dittmar A, and Rouanet JL.** Potentiated muscular thermogenesis in cold-acclimated muscovy duckling. *Am J Physiol* 249: R533-538, 1985.
7. **Beavers WR and Covino BG.** Effects of oral glycine during cold exposure in man. *J Appl Physiol* 14: 390-392, 1959.
8. **Bell DG, Tikuisis P, and Jacobs I.** Relative intensity of muscular contraction during shivering. *J Appl Physiol* 72: 2336-2342, 1992.
9. **Bishop CM.** The maximum oxygen consumption and aerobic scope of birds and mammals: getting to the heart of the matter. *Proc Biol Sci* 266: 2275-2281, 1999.
10. **Bittel JH.** Heat debt as an index for cold adaptation in men. *J Appl Physiol* 62: 1627-1634, 1987.
11. **Blondin DP, Dépault I, Imbeault P, Péronnet F, Imbeault M-A, and Haman F.** Effects of two glucose ingestion rates on substrate utilization during moderate-intensity shivering. *Eur J Appl Physiol* 108: 289-300, 2010.
12. **Blondin DP, Labbé SM, Tingelstad HC, Noll C, Kunach M, Phoenix S, Guérin B, Turcotte ÉE, Carpentier AC, Richard D, and Haman F.** Increased Brown Adipose Tissue Oxidative Capacity in Cold-Acclimated Humans. *J Clin Endocrinol Metab* 99: E438-E446, 2014.
13. **Blondin DP, Maneshi A, Imbeault MA, and Haman F.** Effects of the menstrual cycle on muscle recruitment and oxidative fuel selection during cold exposure. *J Appl Physiol* 111: 1014-1020, 2011.
14. **Blondin DP, Peronnet F, and Haman F.** Coingesting glucose and fructose in the cold potentiates exogenous CHO oxidation. *Med Sci Sports Exerc* 44: 1706-1714, 2012.
15. **Blondin DP, Peronnet F, and Haman F.** Effects of ingesting [13C]glucose early or late into cold exposure on substrate utilization. *J Appl Physiol* 109: 654-662, 2010.

16. **Borchardt RT and Huber JA.** Catechol O-methyltransferase. 5. Structure-activity relationships for inhibition by flavonoids. *Journal of medicinal chemistry* 18: 120-122, 1975.
17. **Burton A and Bazett J.** A study of the average temperature of the tissues, of exchanges of heat, and vasomotor responses in man by means of a bath calorimeter. *Am J Physiol* 117: 36, 1936.
18. **Campero M, Serra J, Bostock H, and Ochoa JL.** Slowly conducting afferents activated by innocuous low temperature in human skin. *J Physiol* 535: 855-865, 2001.
19. **Cannon B and Nedergaard J.** Brown adipose tissue: function and physiological significance. *Physiol Rev* 84: 277-359, 2004.
20. **Carey AL, Formosa MF, Van Every B, Bertovic D, Eikelis N, Lambert GW, Kalff V, Duffy SJ, Cherk MH, and Kingwell BA.** Ephedrine activates brown adipose tissue in lean but not obese humans. *Diabetologia* 56: 147-155, 2013.
21. **Carlson M, Snead W, and Campbell P.** Fuel and energy metabolism in fasting humans. *Am J Clin Nutr* 60: 29-36, 1994.
22. **Casazza GA, Jacobs KA, Suh SH, Miller BF, Horning MA, and Brooks GA.** Menstrual cycle phase and oral contraceptive effects on triglyceride mobilization during exercise. *J Appl Physiol* 97: 302-309, 2004.
23. **Casey KL, Minoshima S, Morrow TJ, and Koeppe RA.** Comparison of human cerebral activation pattern during cutaneous warmth, heat pain, and deep cold pain. *J Neurophysiol* 76: 571-581, 1996.
24. **Castellani JW, Stulz DA, Degroot DW, Blanchard LA, Cadarette BS, Nindl BC, and Montain SJ.** Eighty-four hours of sustained operations alter thermoregulation during cold exposure. *Med Sci Sports Exerc* 35: 175-181, 2003.
25. **Chaffee RR, Roberts JC, Conaway CH, and Sorenson MW.** Comparative effects of temperature exposure on mass and oxidative enzyme activity of brown fat in insectivores, tupaiads and primates. *Lipids* 5: 23-29, 1970.
26. **Chin ER, Olson EN, Richardson JA, Yang Q, Humphries C, Shelton JM, Wu H, Zhu W, Bassel-Duby R, and Williams RS.** A calcineurin-dependent transcriptional pathway controls skeletal muscle fiber type. *Genes Dev* 12: 2499-2509, 1998.
27. **Commission IT.** Glossary of terms for thermal physiology. Second edition. Revised by The Commission for Thermal Physiology of the International Union of Physiological Sciences (IUPS Thermal Commission). *Japanese Journal of Physiology* 51: 245-280, 2001.
28. **Cypess AM, Chen YC, Sze C, Wang K, English J, Chan O, Holman AR, Tal I, Palmer MR, Kolodny GM, and Kahn CR.** Cold but not sympathomimetics activates human brown adipose tissue in vivo. *Proc Natl Acad Sci U S A* 109: 10001-10005, 2012.
29. **Cypess AM, Lehman S, Williams G, Tal I, Rodman D, Goldfine AB, Kuo FC, Palmer EL, Tseng YH, Doria A, Kolodny GM, and Kahn CR.** Identification and importance of brown adipose tissue in adult humans. *N Engl J Med* 360: 1509-1517, 2009.
30. **Darian-Smith I, Johnson KO, and Dykes R.** "Cold" fiber population innervating palmar and digital skin of the monkey: responses to cooling pulses. *J Neurophysiol* 36: 325-346, 1973.

31. **Davis KD, Kwan CL, Crawley AP, and Mikulis DJ.** Functional MRI study of thalamic and cortical activations evoked by cutaneous heat, cold, and tactile stimuli. *J Neurophysiol* 80: 1533-1546, 1998.
32. **Davis TRA.** Chamber cold acclimatization in man. *J Appl Physiol* 16: 1011-1015, 1961.
33. **Dulloo AG, Seydoux J, Girardier L, Chantre P, and Vandermander J.** Green tea and thermogenesis: interactions between catechin-polyphenols, caffeine and sympathetic activity. *International journal of obesity and related metabolic disorders : journal of the International Association for the Study of Obesity* 24: 252-258, 2000.
34. **Egan GF, Johnson J, Farrell M, McAllen R, Zamarripa F, McKinley MJ, Lancaster J, Denton D, and Fox PT.** Cortical, thalamic, and hypothalamic responses to cooling and warming the skin in awake humans: a positron-emission tomography study. *Proc Natl Acad Sci U S A* 102: 5262-5267, 2005.
35. **Elsner RW, Andersen KL, and Hermansen L.** Thermal and metabolic responses of Arctic Indians to moderate cold exposure at the end of winter. *J Appl Physiol* 15, 1960.
36. **Eyolfson DA, Tikuisis P, Xu X, Weseen G, and Giesbrecht GG.** Measurement and prediction of peak shivering intensity in humans. *Eur J Appl Physiol* 84: 100-106, 2001.
37. **Frayn KN.** *Metabolic regulation : a human perspective*. Malden, MA: Blackwell, 2003.
38. **Gale EA, Bennett T, Green JH, and MacDonald IA.** Hypoglycaemia, hypothermia and shivering in man. *Clin Sci (Lond)* 61: 463-469, 1981.
39. **Gardiner P.** *Neuromuscular aspects of physical activity*. Windsor, ON, Canada: Human Kinetics, 2001.
40. **Gessner K.** Conradi Gesneri medici Trigurine Historae Animalium: Lib. I De Quadredibus viviparis. . 1551.
41. **Glickman-Weiss E, Caine N, Cheatham CC, Blegen M, Scharschmidt T, and Marcinkiewicz J.** The effects of gender and menstrual phase on carbohydrate utilization during acute cold exposure. *Wilderness Env Med* 11: 5-11, 2000.
42. **Glickman-Weiss EL, Nelson AG, Hearon CM, Vasanthakumar SR, and Stringer BT.** Does feeding regime affect physiologic and thermal responses during exposure to 8, 20, and 27°C? *Eur J Appl Physiol* 67: 30-34, 1993.
43. **Glickman-Weiss EL, Nelson AG, Hearon CM, Windhauser M, and Heltz D.** The thermogenic effect of carbohydrate feeding during exposure to 8, 12 and 27°C. *Eur J Appl Physiol* 68: 291-297, 1994.
44. **Gosselin C and Haman F.** Effects of green tea extracts on non-shivering thermogenesis during mild cold exposure in young men. *Br J Nutr* 110: 282-288, 2013.
45. **Grenier-Larouche T, Labbe SM, Noll C, Richard D, and Carpentier AC.** Metabolic inflexibility of white and brown adipose tissues in abnormal fatty acid partitioning of type 2 diabetes. *Int J Obes Supp* 2: S37-S42, 2012.
46. **Hackney AC, McCracken-Compton MA, and Ainsworth B.** Substrate responses to submaximal exercise in the midfollicular and midluteal phases of the menstrual cycle. . *Int J Sport Nutr* 4: 299-308, 1994.

47. **Haight JS and Keatinge WR.** Failure of thermoregulation in the cold during hypoglycaemia induced by exercise and ethanol. *J Physiol* 229: 87-97, 1973.
48. **Haman F.** Shivering in the cold: from mechanisms of fuel selection to survival. *J Appl Physiol* 100: 1702-1708, 2006.
49. **Haman F, Blondin DP, Imbeault MA, and Maneshi A.** Metabolic requirements of shivering humans. *Front Biosci (Schol Ed)* 2: 1155-1168, 2010.
50. **Haman F, Legault SR, Rakobowchuk M, Ducharme MB, and Weber J-M.** Effects of carbohydrate availability on sustained shivering II: relating muscle recruitment to fuel selection. *J Appl Physiol* 96: 41-49, 2004.
51. **Haman F, Legault SR, and Weber JM.** Fuel selection during intense shivering in humans: EMG pattern reflects carbohydrate oxidation. *J Physiol* 556: 305-313, 2004.
52. **Haman F, Peronnet F, Kenny GP, Doucet E, Massicotte D, Lavoie C, and Weber JM.** Effects of carbohydrate availability on sustained shivering I. Oxidation of plasma glucose, muscle glycogen, and proteins. *J Appl Physiol* 96: 32-40, 2004.
53. **Haman F, Péronnet F, Kenny GP, Massicotte D, Lavoie C, Scott C, and Weber J-M.** Effect of cold exposure on fuel utilization in humans: plasma glucose, muscle glycogen, and lipids. *J Appl Physiol* 93: 77-84, 2002.
54. **Haman F, Péronnet F, Kenny GP, Massicotte D, Lavoie C, and Weber J-M.** Partitioning oxidative fuels during cold exposure in humans: muscle glycogen becomes dominant as shivering intensifies. *J Physiol* 566: 247-256, 2005.
55. **Haman F, Scott CG, and Kenny GP.** Fueling shivering thermogenesis during passive hypothermic recovery. *J Appl Physiol* 103: 1346-1351, 2007.
56. **Hammel HT, Elsner RW, Le Messurier DH, Andersen HT, and Milan FA.** Thermal and metabolic responses of the Australian aborigine exposed to moderate cold in summer. *J Appl Physiol* 14: 605-615, 1959.
57. **Hart JS, Heroux O, and Depocas F.** Cold acclimation and the electromyogram of unanesthetized rats. *J Appl Physiol* 9: 404-408, 1956.
58. **Hart JS, Sabean HB, Hildes JA, Depocas F, Hammel HT, Andersen KL, Irving L, and Foy G.** Thermal and metabolic responses of coastal Eskimos during a cold night. *J Appl Physiol* 17: 953-960, 1962.
59. **Heaton JM.** The distribution of brown adipose tissue in the human. *J Anat* 112: 35-39, 1972.
60. **Hesslink RLJ, D'Alesandro MM, Armstrong DWr, and Reed HL.** Human cold air habituation is independent of thyroxine and thyrotropin. *J Appl Physiol* 72: 2134-2139, 1992.
61. **Hilliges M, Wang L, and Johansson O.** Ultrastructural evidence for nerve fibers within all vital layers of the human epidermis. *J Invest Dermatol* 104: 134-137, 1995.
62. **Hohtola E, Henderson RP, and Rashotte ME.** Shivering thermogenesis in the pigeon: the effects of activity, diurnal factors, and feeding state. *Am J Physiol* 275: R1553-1562, 1998.
63. **Hong SK, Rahn H, Kang DH, Song SH, and Kang BS.** Diving pattern, lung volumes, and alveolar gas of the Korean diving woman (ama). *J Appl Physiol* 18: 457-465, 1963.
64. **Horton TJ, Miller EK, Glueck D, and Tench K.** No effect of menstrual cycle phase on glucose kinetics and fuel oxidation during moderate-intensity exercise. *Am J Physiol Endocrinol Metab* 282: E752-E762, 2002.

65. **Huttunen P, Hirvonen J, and Kinnula V.** The occurrence of brown adipose tissue in outdoor workers. *Eur J Appl Physiol Occup Physiol* 46: 339-345, 1981.
66. **Imbeault M-A, Mantha OL, and Haman F.** Shivering modulation in humans: Effects of rapid changes in environmental temperature. *Journal of Thermal Biology* 38: 582-587, 2013.
67. **Israel DJ and Pozos RS.** Synchronized slow-amplitude modulations in the electromyograms of shivering muscles. *J Appl Physiol* 66: 2358-2363, 1989.
68. **Jeukendrup AE.** Regulation of fat metabolism in skeletal muscle. *Ann NY Acad Sci* 967: 217-235, 2002.
69. **Jones P and Lee I.** Macronutrient requirements for work in cold environments. In: *Nutrional Needs in Cold and In High-Altitude Environments: Applications for Military Personnel in Field Operations*, edited by Marriott B and Carlson S. Washington, D.C.: National Academy Press, 1996, p. 189-202.
70. **Kang BS, Song SH, Suh CS, and Hong SK.** Changes in body temperature and basal metabolic rate of the ama. *J Appl Physiol* 18: 483-488, 1963.
71. **Kanosue K, Sadato N, Okada T, Yoda T, Nakai S, Yoshida K, Hosono T, Nagashima K, Yagishita T, Inoue O, Kobayashi K, and Yonekura Y.** Brain activation during whole body cooling in humans studied with functional magnetic resonance imaging. *Neurosci Lett* 329: 157-160, 2002.
72. **Klein LJ, Visser FC, Knaapen P, Peters JH, Teule GJ, Visser CA, and Lammertsma AA.** Carbon-11 acetate as a tracer of myocardial oxygen consumption. *Eur J Nucl Med* 28: 651-668, 2001.
73. **Kobayashi A, Osaka T, Namba Y, Inoue S, Lee TH, and Kimura S.** Capsaicin activates heat loss and heat production simultaneously and independently in rats. *Am J Physiol* 275: R92-98, 1998.
74. **Kowalczyk M, Antkowiak B, Antkowiak O, Brytan M, Zdanowski R, Klos A, and Frankiewicz-Jozko A.** Ephedrine-caffeine mixture in wet-cold stress. *Pharmacological reports : PR* 58: 364-372, 2006.
75. **Macdonald I, Bennett T, and Sainsbury R.** The effect of a 48h fast on the thermoregulatory responses to graded cooling in man. *Clin Sci* 67: 445-452, 1984.
76. **Mansell P, Fellows I, and Macdonald I.** Enhanced thermogenic response to epinephrine after 48-h starvation in humans. *Am J Physiol Regul Integr Comp Physiol* 258: 87-93, 1990.
77. **Mansell P and Macdonald I.** Effects of underfeeding and of starvation on thermoregulatory responses to cooling in women. *Clin Sci* 77: 245-252, 1989.
78. **Martineau L and Jacobs I.** Effects of muscle glycogen and plasma FFA availability on human metabolism responses in cold water. *J Appl Physiol* 71: 1331-1339, 1991.
79. **Martineau L and Jacobs I.** Free fatty acid availability and temperature regulation in cold water. *J Appl Physiol* 67: 2466-2472, 1989.
80. **Martineau L and Jacobs I.** Muscle glycogen availability and temperature regulation in humans. *J Appl Physiol* 66: 72-78, 1989.
81. **McAllen RM, Farrell M, Johnson JM, Trevaks D, Cole L, McKinley MJ, Jackson G, Denton DA, and Egan GF.** Human medullary responses to cooling and rewarming the skin: a functional MRI study. *Proc Natl Acad Sci U S A* 103: 809-813, 2006.

82. **McAllen RM, Tanaka M, Ootsuka Y, and McKinley MJ.** Multiple thermoregulatory effectors with independent central controls. *Eur J Appl Physiol* 109: 27-33, 2010.
83. **Meigal A.** Gross and fine neuromuscular performance at cold shivering. *Int J Circumpolar Health* 61: 163-172, 2002.
84. **Meigal A, Lupandin V, and Kuzmina GI.** Electromyographic patterns of thermoregulatory activity of motor units in the course of body cooling. *Fiziol Cheloveka* 19: 106-114 (in Russian), 1993.
85. **Morrison SF.** 2010 Carl Ludwig Distinguished Lectureship of the APS Neural Control and Autonomic Regulation Section: Central neural pathways for thermoregulatory cold defense. *J Appl Physiol* 110: 1137-1149, 2011.
86. **Nakamura K.** Central circuitries for body temperature regulation and fever. *Am J Physiol Regul Integr Comp Physiol* 301: R1207-1228, 2011.
87. **Nedergaard J, Bengtsson T, and Cannon B.** Unexpected evidence for active brown adipose tissue in adult humans. *Am J Physiol Endocrinol Metab* 293: E444-452, 2007.
88. **Olson JM.** The ontogeny of shivering thermogenesis in the red-winged blackbird (*agelaius phoeniceus*). *J Exp Biol* 191: 59-88, 1994.
89. **Orava J, Nuutila P, Noponen T, Parkkola R, Viljanen T, Enerback S, Rissanen A, Pietilainen KH, and Virtanen KA.** Blunted Metabolic Responses to Cold and Insulin Stimulation in Brown Adipose Tissue of Obese Humans. *Obesity (Silver Spring)*, 2013.
90. **Ouellet V, Labbe SM, Blondin DP, Phoenix S, Guerin B, Haman F, Turcotte EE, Richard D, and Carpentier AC.** Brown adipose tissue oxidative metabolism contributes to energy expenditure during acute cold exposure in humans. *J Clin invest* 122: 545-552, 2012.
91. **Ouellet V, Routhier-Labadie A, Bellemare W, Lakhal-Chaieb L, Turcotte E, Carpentier AC, and Richard D.** Outdoor Temperature, Age, Sex, Body Mass Index, and Diabetic Status Determine the Prevalence, Mass, and Glucose-Uptake Activity of 18F-FDG-Detected BAT in Humans. *J Clin Endocrinol Metab* 96: 192-199, 2011.
92. **Park Y, Pendergast D, and Rennie D.** Decrease in body insulation with exercise in cool water. *Undersea Biomed Res* 11: 159-168, 1984.
93. **Passias TC, Meneilly GS, and Mekjavic IB.** Effect of hypoglycemia on thermoregulatory responses. *Journal of Applied Physiology* 80: 1021-1032, 1996.
94. **Pirnay F, Crielaard JM, Pallikarakis N, Lacroix M, Mosora F, Krzentowski G, Luyckx AS, and Lefebvre PJ.** Fate of exogenous glucose during exercise of different intensities in humans. *J Appl Physiol* 53: 1620-1624, 1982.
95. **Pohl H.** Temperature regulation and cold acclimation in the golden hamster. *J Appl Physiol* 20: 405-410, 1965.
96. **Rattigan S, Wheatley C, Richards SM, Barrett EJ, Clark MG.** Exercise and Insulin-mediated capillary recruitment in muscle. *Exerc Sport Sci Rev* 33: 43-48, 2005.
97. **Rennie D.** Tissue heat transfer in water: lessons from the Korean divers. *Med Sci Sports Exerc* 20: S177-S184, 1988.

98. **Rezende EL, Swanson DL, Novoa FF, and Bozinovic F.** Passerines versus nonpasserines: so far, no statistical differences in the scaling of avian energetics. *J Exp Biol* 205: 101-107, 2002.
99. **Richter EA and Hargreaves M.** Exercise, GLUT4, and skeletal muscle glucose uptake. *Physiol Rev* 93: 993-1017, 2013.
100. **Rochelle R and Horvath S.** Metabolic responses to food and acute cold stress. *J Appl Physiol* 27: 710-714, 1969.
101. **Rolfe DFS and Brown GC.** Cellular energy utilization and molecular origin of standard metabolic rate in mammals. *Physiol Rev* 77: 731-758, 1997.
102. **Romanovsky AA.** Thermoregulation: some concepts have changed. Functional architecture of the thermoregulatory system. *Am J Physiol Regul Integr Comp Physiol* 292: R37-46, 2007.
103. **Saito M, Okamatsu-Ogura Y, Matsushita M, Watanbe K, Yoneshiro T, Nio-Kobayashi J, Iwanaga I, Miyagawa M, Kameya T, Nakada K, Kawai Y, and Tsujisaki M.** High Incidence of Metabolically Active Brown Adipose Tissue in Healthy Adult Humans. *Diabetes* 58: 1526-1531, 2009.
104. **Sato H.** Fusimotor modulation by spinal and skin temperature changes and its significance in cold shivering. *Exp Neurol* 74: 21-32, 1981.
105. **Sato H, Hashitani T, Isobe Y, Furuyama F, and Nishino H.** Descending influences from nucleus raphe magnus on fusimotor neurone activity in rats. *J Therm Biol* 15: 259-265, 1990.
106. **Schepers RJ and Ringkamp M.** Thermoreceptors and thermosensitive afferents. *Neurosci Biobehav Rev* 34: 177-184, 2010.
107. **Schmidt-Nielsen K.** *Scaling: Why is animal size so important?* Cambridge, UK: Cambridge University Press, 1984.
108. **Scott E.** Nutrition of Alaskan Eskimos. *Nutri Rev* 14: 1-3, 1956.
109. **Shixian Q, VanCrey B, Shi J, Kakuda Y, and Jiang Y.** Green tea extract thermogenesis-induced weight loss by epigallocatechin gallate inhibition of catechol-O-methyltransferase. *Journal of Medicinal Food* 9: 451-458, 2006.
110. **Simoneau JA and Bouchard C.** Human variation in skeletal muscle fiber-type proportion and enzyme activities. *Am J Physiol* 257: E567-572, 1989.
111. **Simonides WS, Thelen MH, van der Linden CG, Muller A, and van Hardeveld C.** Mechanism of thyroid-hormone regulated expression of the SERCA genes in skeletal muscle: implications for thermogenesis. *Biosci Rep* 21: 139-154, 2001.
112. **Sinclair H.** The diet of Canadian Indians and Eskimos. *Proc Nutr Soc* 12: 69-82, 1953.
113. **Soderlund V, Larsson SA, and Jacobsson H.** Reduction of FDG uptake in brown adipose tissue in clinical patients by a single dose of propranolol. *Eur J Nucl Med Mol Imaging* 34: 1018-1022, 2007.
114. **Spriet LL.** Regulation of skeletal muscle fat oxidation during exercise in humans. *Med Sci Sports Exerc* 34: 1477–1484, 2002.
115. **Tanaka M, Owens NC, Nagashima K, Kanosue K, and McAllen RM.** Reflex activation of rat fusimotor neurons by body surface cooling, and its dependence on the medullary raphe. *J Physiol* 572: 569-583, 2006.
116. **Tappy L.** Thermic effect of food and sympathetic nervous system activity in humans. *Reprod Nutr Dev* 36: 391-397, 1996.

117. **Tarnopolsky MA.** Sex differences in exercise metabolism and the role of 17-beta estradiol. *Med Sci Sports Exerc* 40: 648-654, 2008.
118. **Teulier L, Rouanet JL, Letexier D, Romestaing C, Belouze M, Rey B, Duchamp C, and Roussel D.** Cold-acclimation-induced non-shivering thermogenesis in birds is associated with upregulation of avian UCP but not with innate uncoupling or altered ATP efficiency. *J Exp Biol* 213: 2476-2482, 2010.
119. **Tikuisis P, Eyolfson DA, Xu X, and Giesbrecht GG.** Shivering endurance and fatigue during cold water immersion in humans. *Eur J Appl Physiol* 87: 50-58, 2002.
120. **Tikuisis P and Giesbrecht GG.** Prediction of shivering heat production from core and mean skin temperatures. *Eur J Appl Physiol Occup Physiol* 79: 221-229, 1999.
121. **Vallerand AL, Frim J, and Kavanagh F.** Plasma glucose and insulin responses to oral and intravenous glucose in cold-exposed humans. *J Appl Physiol* 65: 2395-2399, 1988.
122. **Vallerand AL and Jacobs I.** Energy metabolism during cold exposure. *Int J Sports Med* 13: S191-S193, 1992.
123. **Vallerand AL, Schmegner IF, and Jacobs I.** Influence of the Cold Buster™ sports bar on heat debt, mobilization and oxidation of energy substrates: Department of National Defence: Defence and Civil Institute of Environmental Medicine. North York, Ontario. Report 92-60, 1992.
124. **Vallerand AL, Tikuisis P, Ducharme MB, and Jacobs I.** Is energy substrate mobilization a limiting factor for cold thermogenesis? *Eur J Appl Physiol* 67: 239-244, 1993.
125. **Vallerand AL, Wang LCH, and Jacobs I.** Influence of theobromine on heat production and body temperatures in cold-exposed humans: A preliminary report, edited by Department of National Defence: Defence and Civil Institute of Environmental Medicine. North York OR-R-. North York, Ontario, Canada, 1989.
126. **Vallerand AL, Zamecnik J, Jones PJ, and Jacobs I.** Cold stress increases lipolysis, FFA Ra and TG/FFA cycling in humans. *Aviat Space Environ Med* 70: 42-50, 1999.
127. **van der Lans AA, Hoeks J, Brans B, Vijgen GH, Visser MG, Vosselman MJ, Hansen J, Jorgensen JA, Wu J, Mottaghy FM, Schrauwen P, and van Marken Lichtenbelt WD.** Cold acclimation recruits human brown fat and increases nonshivering thermogenesis. *J Clin Invest* 123: 3395-3403, 2013.
128. **van Marken Lichtenbelt WD, Vanhommerig JW, Smulders NM, Drossaerts JM, Kemerink GJ, Bouvy ND, Schrauwen P, and Teule GJ.** Cold-activated brown adipose tissue in health men. *N Engl J Med* 360: 1500-1508, 2009.
129. **Veicsteinas A, Ferretti G, and Rennie DW.** Superficial shell insulation in resting and exercising men in cold water. *Journal of applied physiology: respiratory, environmental and exercise physiology* 52: 1557-1564, 1982.
130. **Vijgen GH, Bouvy ND, Teule GJ, Brans B, Hoeks J, Schrauwen P, and van Marken Lichtenbelt WD.** Increase in brown adipose tissue activity after weight loss in morbidly obese subjects. *J Clin Endocrinol Metab* 97: E1229-1233, 2012.
131. **Vijgen GH, Bouvy ND, Teule GJ, Brans B, Schrauwen P, and van Marken Lichtenbelt WD.** Brown adipose tissue in morbidly obese subjects. *PLoS One* 6: e17247, 2011.

132. **Virtanen KA, Lidell ME, Orava J, Heglind M, Westergren R, Niemi T, Taittonen M, Laine J, Savisto NJ, Enerback S, and Nuutila P.** Functional brown adipose tissue in healthy adults. *N Engl J Med* 360: 1518-1525, 2009.
133. **Vosselman MJ, van der Lans AA, Brans B, Wierts R, van Baak MA, Schrauwen P, and van Marken Lichtenbelt WD.** Systemic beta-adrenergic stimulation of thermogenesis is not accompanied by brown adipose tissue activity in humans. *Diabetes* 61: 3106-3113, 2012.
134. **Wang L, Hilliges M, Jernberg T, Wiegleb-Edstrom D, and Johansson O.** Protein gene product 9.5-immunoreactive nerve fibres and cells in human skin. *Cell Tissue Res* 261: 25-33, 1990.
135. **Webber J and Macdonald I.** The cardiovascular, metabolic and hormonal changes accompanying acute starvation in men and women. *Br J Nutr* 71: 437-447, 1994.
136. **Weber J-M and Haman F.** Oxidative fuel selection: adjusting mix and flux to stay alive. In: *Animals and Environments*, edited by Morris S and Vosloo A: Elsevier, 2004, p. 22-31.
137. **Weber JM and Haman F.** Fuel selection in shivering humans. *Acta Physiol Scand* 184: 319-329, 2005.
138. **Wells JC and Stock JT.** The biology of the colonizing ape. *Am J Phys Anthropol* Suppl 45: 191-222, 2007.
139. **Wenz M, Berend JZ, Lynch NA, Chappell S, and Hackney AC.** Substrate oxidation at rest and during exercise: effects of menstrual cycle phase and diet composition. *Journal of physiology and pharmacology : an official journal of the Polish Physiological Society* 48: 851-860, 1997.
140. **Westerterp-Plantenga M, Diepvens K, Joosen AM, Berube-Parent S, and Tremblay A.** Metabolic effects of spices, teas, and caffeine. *Physiol Behav* 89: 85-91, 2006.
141. **Wijers SL, Schrauwen P, Saris WH, and van Marken Lichtenbelt WD.** Human skeletal muscle mitochondrial uncoupling is associated with cold induced adaptive thermogenesis. *PLoS One* 3: e1777, 2008.
142. **Wissler EH.** Mathematical simulation of human thermal behavior using whole-body models. In: *Heat transfer in medicine and biology*, edited by Shitzer A and Eberhart RC. New York: Plenum Press, 1985, p. 347-355.
143. **Xu X, Tikuisis P, Gonzalez R, and Giesbrecht G.** Thermoregulatory model for prediction of long-term cold exposure. *Comput Biol Med* 35: 287-298, 2005.
144. **Yoneshiro T, Aita S, Kawai Y, Iwanaga T, and Saito M.** Nonpungent capsaicin analogs (capsinoids) increase energy expenditure through the activation of brown adipose tissue in humans. *Am J Clin Nutr* 95: 845-820, 2012.
145. **Yoneshiro T, Aita S, Matsushita M, Kameya T, Nakada K, Kawai Y, and Saito M.** Brown adipose tissue, whole-body energy expenditure, and thermogenesis in healthy adult men. *Obesity (Silver Spring)* 19: 13-16, 2011.
146. **Yoneshiro T, Aita S, Matsushita M, Kayahara T, Kameya T, Kawai Y, Iwanaga T, and Saito M.** Recruited brown adipose tissue as an antiobesity agent in humans. *J Clin Invest* 123: 3404-3408, 2013.
147. **Young AJ.** Homeostatic Responses to Prolonged Cold Exposure: Human Cold Acclimatization. *Comprehensive Physiology* Supplement 14: Handbook of Physiology 419-438, 2011.

148. **Young AJ, Castellani JW, O'Brien C, Shippee RL, Tikuisis P, Meyer LG, Blanchard LA, Kain JE, Cadarette BS, and Sawka MN.** Exertional fatigue, sleep loss, and negative energy balance increase susceptibility to hypothermia. *J Appl Physiol* 85: 1210-1217, 1998.
149. **Young AJ, Muza SR, Sawka MN, Gonzalez RR, and Pandolf KB.** Human thermoregulatory responses to cold air are altered by repeated cold water immersion. *J Appl Physiol* 60: 1542-1548, 1986.
150. **Young AJ, Sawka MN, Neufer PD, Muza SR, Askew EW, and Pandolf KB.** Thermoregulation during cold water immersion is impaired by low glycogen levels. *J Appl Physiol* 66: 1806-1816, 1989.
151. **Zderic TW, Coggan AR, and Ruby BC.** Glucose kinetics and substrate oxidation during exercise in the follicular and luteal phases. *J Appl Physiol* 90: 447-453, 2001.
152. **Zingaretti MC, Crosta F, Vitali A, Guerrieri M, Frontini A, Cannon B, Nedergaard J, and Cinti S.** The presence of UCP1 demonstrates that metabolically active adipose tissue in the neck of adult humans truly represents brown adipose tissue. *FASEB J* 23: 3113-3120, 2009.

Table 1. Studies on the effects of potentially thermogenic compounds on brown adipose tissue (BAT), skin temperature (Tskin), core temperature (Tcore), heat production (Hprod), fuel use, shivering intensity (ST) and norepinephrine (NE) measured in men during various cold exposures. Values are expressed as percent diffenrence from control values where a placebo was given.

Study *# participants* Average age (years)	Treatments (dose) i.v. intravenuous	T_{amb} (°C) *Time (min)* Wind speed	BAT	T_{skin} (°C)	T_{core} (°C)	H_{prod} % difference from placebo	Fuel use	ST	NE
Brown adipose tissue									
Yoneshiro *et al.*, (2012) BAT-positive (BAT+): 23, *n=10* BAT-negative (BAT-): 23, *n=8*	Capsinoids (orally, 9 mg)	27 120 min	----- -----	----- -----	----- -----	BAT+: +262% BAT-: - 66 %	----- -----	----- -----	----- -----
Cypess *et al.*, (2012) *n=10* (4 M/6 F) 27	Ephedrine (1 mg kg^{-1}), intramuscular injection	23 120 min	no diff	-----	-----	+9%	RER: - 6%	-----	+71%
Carey *et al.*, (2012) Lean: 25, *n=9* Obese: 27, *n=9*	Ephedrine hychloride (orally, 2.5 mg kg^{-1})	20-22 90 min	lean: ↑activity obese: no diff	----- ------	----- -----	lean: +18% obese: +13%	----- -----	----- -----	----- -----
Vosselman *et al.*, (2012) *n=10* 23	Isoprenaline (incr. i.v. dosage: 6, 12, 24 ng kg FFM^{-1} min^{-1}) Isoprenaline + acipomox (nicotinic acid derivative; 2 x 250 mg)	24-25 160 min	no diff no diff	+2% +2%	no diff no diff	+20% +13%	RER: - 6% no diff	----- -----	+20% +26%
Energy metabolism in the cold									
Wang (1986) *n=7* 22	Aminophyline (i.v., 3mg kg^{-1} over 45 min)	-2 to 15*, air *45*	-----	-----	no diff	no diff	-----	-----	-----
Vallerand, Wang and Jacobs, (1989) *n=8* Responders (R): 27 (*n=4*) Non-Responders (NR): 32 (*n=4*)	Theobromine (orally, 7.5 mg kg^{-1})	7, air *180* 1m/s	-----	R: +17 NR: +1	R: no diff NR: +52	R: no diff NR: no diff 20% higher in R than NR	no diff	-----	-----
Vallerand, Jacobs and Kavanagh, (1989) *n=9* 25	Ephedrine (orally, 1 mg kg^{-1}) Caffeine (orally, 2.5 mg kg^{-1})	10, air *180* 1m/s	-----	+11	+41	+19	+42 CHO no diff FAT no diff PROT	-----	no diff
Vallerand (1993)	Ephedrine (orally, 44 mg) Caffeine (orally, 60 mg) Theophyline (orally, 100 mg)		-----	+5	+24	+17	-----	-----	-----
MacNaughton *et al.*, (1990) *n=6* 22	Caffeine (orally, 5 mg kg^{-1})	5, air *120*	-----	no diff	no diff	+23 60-90 min	RER -10 at 5 min	-----	no diff
Graham *et al.*, (1991) *n=6* 22	Caffeine (orally, 5 mg kg^{-1})	5, air *120*	-----	no diff	no diff	no diff	no diff	-----	no diff
Gosselin and Haman (2013) *n=8* *23*	Caffeine (orally, 600 mg) Epigalo-cathechin-3-gallate (orally, 1600 mg)	15, LCS** *180*	-----	no diff	no diff	+10	no diff	-20	-----

* depending on individual differences in cold tolerance
** Liquid conditionned suit
T_{amb}, ambient temperature; BAT, brown adipose tissue; T_{skin}, skin temperature; T_{core}, core temperature; H_{prod}, heat production; ST, shivering thermogenesis; NE, norepinephrine

Figure legends

Figure 1. Anatomical conceptual illustration of neural networks that make up the somatosensory and autonomic thermoregulatory pathways. See ***Activating thermogenic pathways*** for details.

Figure 2. Relative changes in A. core temperature (T_{core}), B. average shivering intensity of 4 large muscles [*trapezius, latissimus dorsi, pectoralis major and rectus abdominis* expressed in % of maximal voluntary contraction(%MVC)] and C. oxygen consumption (L/min) as a function of the relative change in average skin temperature in men exposed to various cold conditions using an liquid conditioned garment. Values are adapted from (50-54, 90).

Figure 3. A. absolute rates ($mg \cdot min^{-1}$) and B. relative contributions to total thermogenic rate of carbohydrates (CHO, open bars) and lipids (black bars) in men exposed to the cold at various intensities [2.6, 3.5 or 4.7 times resting metabolic rate (X RMR)], following the ingestion of glucose and/or fructose at different rates and times as, well as following the depletion or loading of CHO reserves. Values are adapted from (11, 14, 15, 52-55).

Figure 4. Inter-individual differences in burst shivering rate and its effect on total CHO, muscle glycogen and plasma glucose utilization. Values are adapted from (51, 54).

Figure 5. A. absolute rates ($mg \cdot min^{-1}$) and B. relative contributions to total thermogenic rate of muscle glycogen (open bars) and plasma glucose (black bars) in men exposed to the cold at various intensities [2.6 and 3.5 times resting metabolic rate (X RMR)], following the ingestion of glucose alone or with fructose at different rates and times as, well as following the depletion or loading of CHO reserves. Values are adapted from (11, 14, 15, 52-54)

Cross-References

Young AJ. Homeostatic Responses to Prolonged Cold Exposure: Human Cold Acclimatization. *Comprehensive Physiology* Supplement 14: Handbook of Physiology 419-438, 2011.

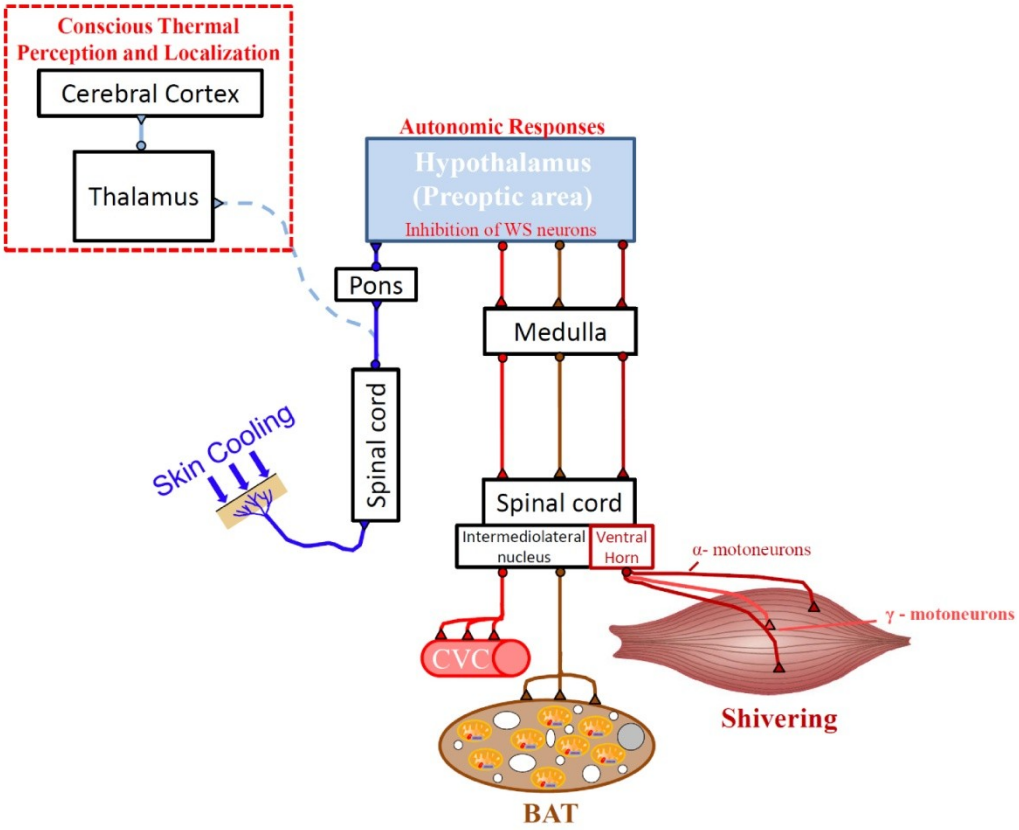
Conscious Thermal Perception and Localization
Cerebral Cortex
Thalamus
Autonomic Responses
Hypothalamus (Preoptic area)
Inhibition of WS neurons
Pons
Medulla
Spinal cord
Skin Cooling
Spinal cord
Intermediolateral nucleus
Ventral Horn
α- motoneurons
γ - motoneurons
CVC
Shivering
BAT

Figure 1

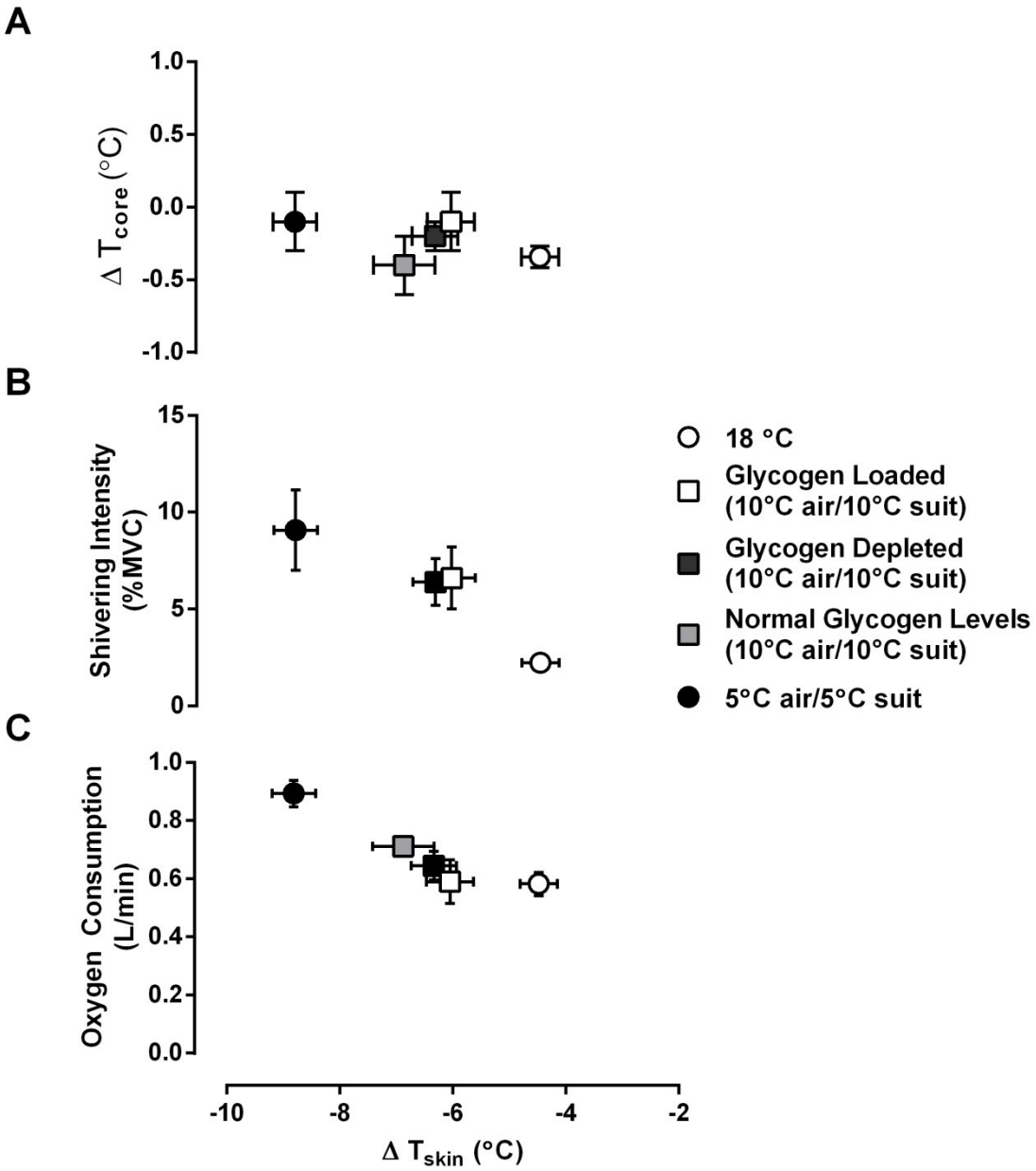
A
B
C
1.0
0.5
0.0
-0.5
-1.0
Δ T core (°C)
15
10
5
0
Shivering Intensity (%MVC)
1.0
0.8
0.6
0.4
0.2
0.0
Oxygen Consumption (L/min)
-10
-8
-6
-4
-2
Δ T skin (°C)
18 °C
Glycogen Loaded (10°C air/10°C suit)
Glycogen Depleted (10°C air/10°C suit)
Normal Glycogen Levels (10°C air/10°C suit)
5°C air/5°C suit

Figure 2

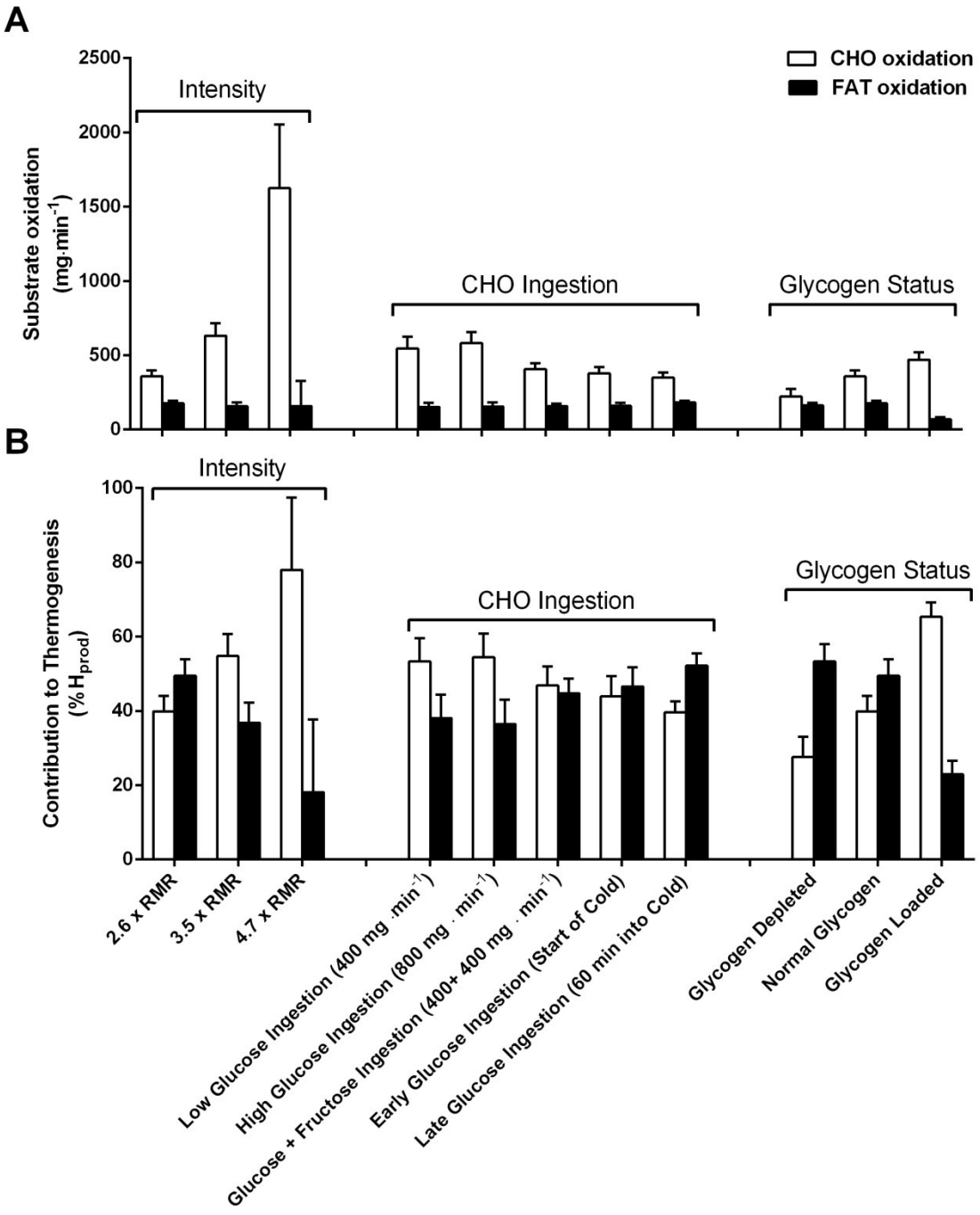
A
CHO oxidation
FAT oxidation
Substrate oxidation (mg·min-1)
2500
2000
1500
1000
500
0
Intensity
CHO Ingestion
Glycogen Status
B
Contribution to Thermogenesis (% Hprod)
100
80
60
40
20
0
Intensity
CHO Ingestion
Glycogen Status
2.6 x RMR
3.5 x RMR
4.7 x RMR
Low Glucose Ingestion (400 mg . min-1)
High Glucose Ingestion (800 mg . min-1)
Glucose + Fructose Ingestion (400+ 400 mg . min-1)
Early Glucose Ingestion (Start of Cold)
Late Glucose Ingestion (60 min into Cold)
Glycogen Depleted
Normal Glycogen
Glycogen Loaded

Figure 3

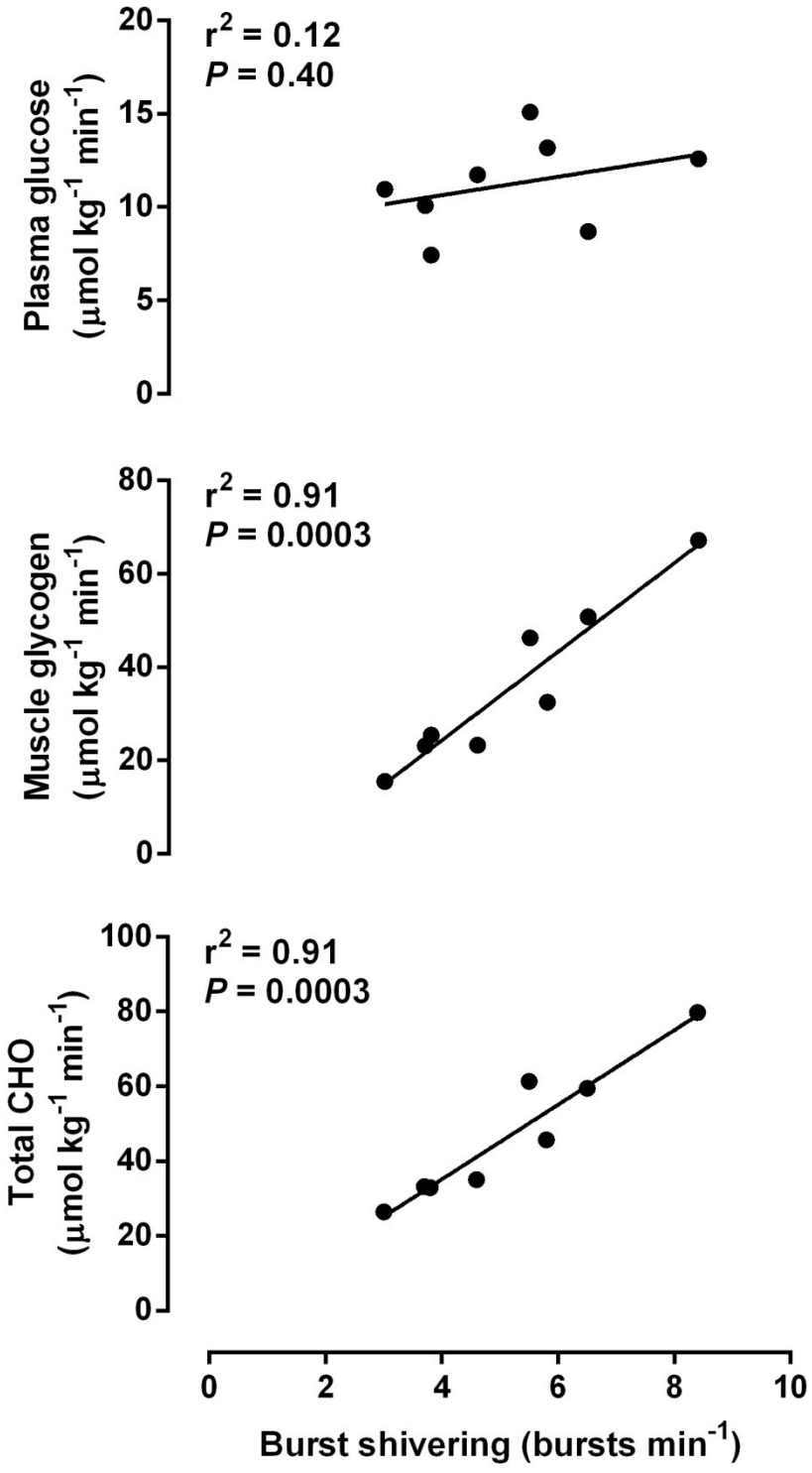
r² = 0.12
P = 0.40
Plasma glucose (µmol kg⁻¹ min⁻¹)
20
15
10
5
0
r² = 0.91
P = 0.0003
Muscle glycogen (µmol kg⁻¹ min⁻¹)
80
60
40
20
0
r² = 0.91
P = 0.0003
Total CHO (µmol kg⁻¹ min⁻¹)
100
80
60
40
20
0
0
2
4
6
8
10
Burst shivering (bursts min⁻¹)

Figure 4

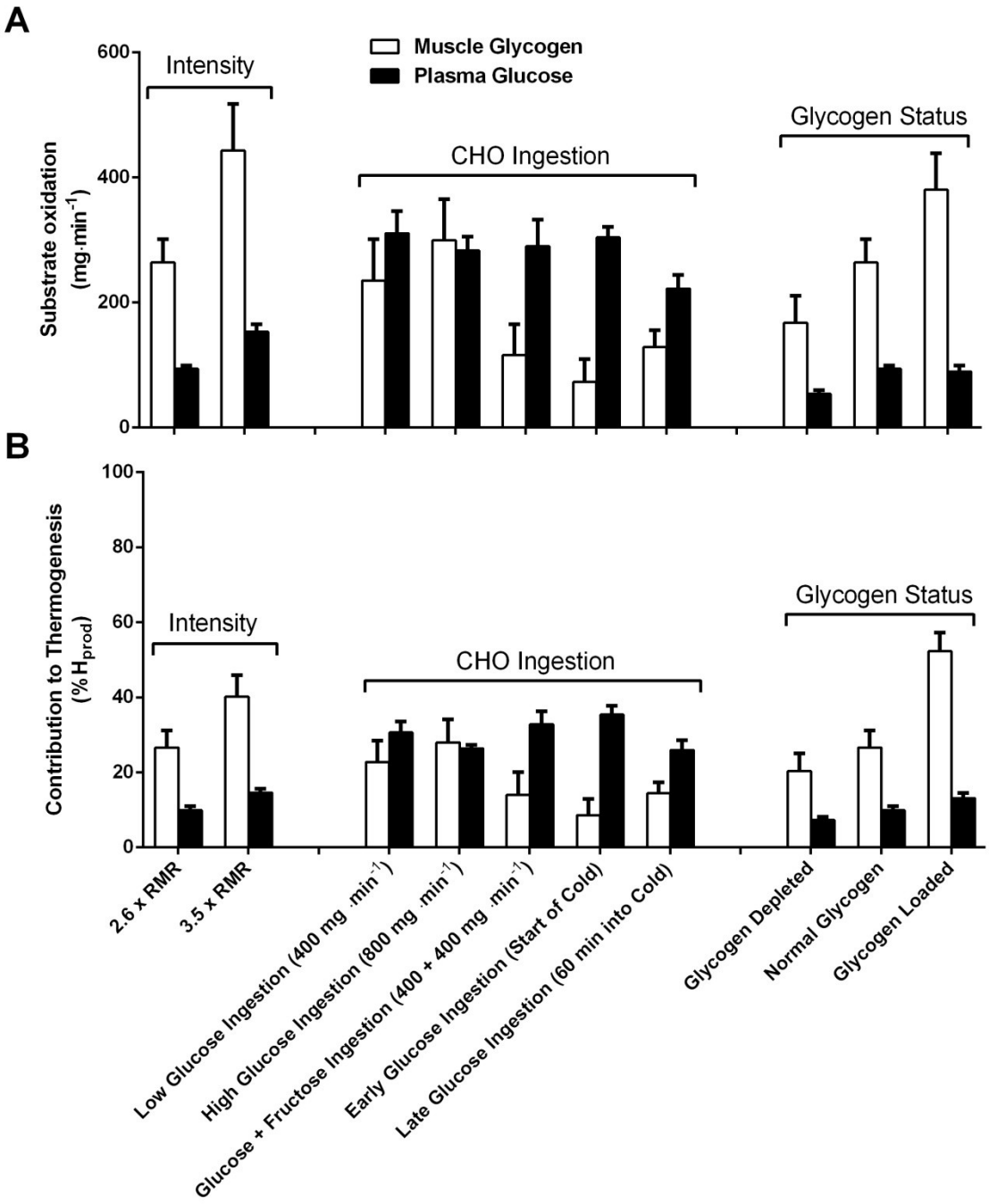
A
Muscle Glycogen
Plasma Glucose
Intensity
CHO Ingestion
Glycogen Status
Substrate oxidation (mg·min-1)
600
400
200
0
B
Contribution to Thermogenesis (%Hprod)
100
80
60
40
20
0
Intensity
CHO Ingestion
Glycogen Status
2.6 x RMR
3.5 x RMR
Low Glucose Ingestion (400 mg ·min-1)
High Glucose Ingestion (800 mg ·min-1)
Glucose + Fructose Ingestion (400 + 400 mg ·min-1)
Early Glucose Ingestion (Start of Cold)
Late Glucose Ingestion (60 min into Cold)
Glycogen Depleted
Normal Glycogen
Glycogen Loaded

Figure 5

APPENDIX C:

Final published version of ARTICLE I

Research article

Brown adipose tissue oxidative metabolism contributes to energy expenditure during acute cold exposure in humans

Véronique Ouellet,[1] Sébastien M. Labbé,[2] Denis P. Blondin,[3] Serge Phoenix,[2,4] Brigitte Guérin,[4] François Haman,[3] Eric E. Turcotte,[4] Denis Richard,[1] and André C. Carpentier[2]

[1]Centre de recherche de l'Institut universitaire de cardiologie et de pneumologie de Québec, Université Laval, Quebec City, Quebec, Canada.
[2]Department of Medicine, Centre de recherche clinique Etienne-Le Bel, Université de Sherbrooke, Sherbrooke, Quebec, Canada.
[3]Unité de recherche sur la nutrition et le métabolisme, Montfort Hospital, University of Ottawa, Ottawa, Ontario, Canada.
[4]Department of Nuclear Medicine and Radiobiology, Université de Sherbrooke, Sherbrooke, Quebec, Canada.

Brown adipose tissue (BAT) is vital for proper thermogenesis during cold exposure in rodents, but until recently its presence in adult humans and its contribution to human metabolism were thought to be minimal or insignificant. Recent studies using PET with ^{18}F-fluorodeoxyglucose (^{18}FDG) have shown the presence of BAT in adult humans. However, whether BAT contributes to cold-induced nonshivering thermogenesis in humans has not been proven. Using PET with ^{11}C-acetate, ^{18}FDG, and ^{18}F-fluoro-thiaheptadecanoic acid (^{18}FTHA), a fatty acid tracer, we have quantified BAT oxidative metabolism and glucose and nonesterified fatty acid (NEFA) turnover in 6 healthy men under controlled cold exposure conditions. All subjects displayed substantial NEFA and glucose uptake upon cold exposure. Furthermore, we demonstrated cold-induced activation of oxidative metabolism in BAT, but not in adjoining skeletal muscles and subcutaneous adipose tissue. This activation was associated with an increase in total energy expenditure. We found an inverse relationship between BAT activity and shivering. We also observed an increase in BAT radio density upon cold exposure, indicating reduced BAT triglyceride content. In sum, our study provides evidence that BAT acts as a nonshivering thermogenesis effector in humans.

Introduction

Brown adipose tissue (BAT) is a specialized tissue whose function is to produce heat (1, 2). Its thermogenic capacity is such that it allows mammals to live below thermoneutral conditions without having to rely on shivering muscles. The exceptional thermogenic potential of BAT is conferred by abundant well-developed mitochondria comprising uncoupling protein 1 (*UCP1*), a protein uncoupling mitochondrial respiration from ATP synthesis (2). BAT is highly vascularized and richly innervated by terminal fibers of the postganglionic neurons of the sympathetic nervous system (1–3).

PET/CT scanning investigations using ^{18}F-fluorodeoxyglucose (^{18}FDG) have revealed symmetrical cervical, supraclavicular metabolically active fat depots, which were suggested by Hany and colleagues to represent BAT (4–7). These fat depots comprise sympathetically innervated multilocular adipocytes expressing *UCP1* (8), the ultimate marker of brown fat cells. The magnitude of ^{18}FDG uptake by BAT was reported to increase with exposure to low temperature, to be higher in women than men, and to decrease with age and body fat mass (5, 7–12). These observations tend to support the idea that BAT substantially contributes to energy expenditure (2, 13, 14). As these observations have only been based on ^{18}FDG uptake, however, the studies carried out so far in humans have only allowed speculative conclusions regarding the oxidative capacity/activity of BAT.

The present study was thus designed to determine whether BAT is metabolically active and contributes to cold-induced nonshivering thermogenesis in humans. Using PET with ^{11}C-acetate (to determine tissue oxidative activity), ^{18}FDG (a glucose analogue), and ^{18}F-fluoro-thiaheptadecanoic acid (^{18}FTHA), a fatty acid tracer, BAT oxidative metabolism, glucose, and nonesterified fatty acid (NEFA) uptake were quantified in adult humans subjected to cold exposure conditions designed to minimize shivering.

Results

Six healthy men aged from 23 to 42 years, with a BMI of 23.7 to 31.0 kg/m^2, and taking no medication participated in the present study protocols (Figure 1). During cold exposure, average skin temperature was reduced by 3.8 ± 0.4°C without change in core body temperature, and VO_2, VCO_2, and resting energy expenditure increased approximately 1.8-fold (Table 1). Plasma glucose, triglycerides, triiodothyronine, thyroxin, thyroid-stimulating hormone, cortisol, and ACTH levels did not change significantly with cold exposure, whereas NEFA levels and NEFA rate of appearance in blood increased significantly (Table 1). By design, shivering was controlled and minimized to 1.6% ± 0.5% (range, 1.1% to 2.4%) of maximal voluntary contraction as continuously recorded by electromyography (EMG) in 4 large muscle groups known to contribute significantly to shivering during cold exposure (15–17).

^{18}FDG uptake during the cervicothoracic dynamic PET/CT acquisition upon cold exposure of 1 representative participant is shown in Figure 2A. During cold exposure, fractional uptake (K_i) of ^{18}FDG (Figure 2B) was higher in supraclavicular BAT compared with trapezius and deltoid muscles and subcutaneous adipose tissue but not compared with the longus colli (a small muscle

Authorship note: Véronique Ouellet and Sébastien M. Labbé contributed equally to the work.

Conflict of interest: The authors have declared that no conflict of interest exists.

Citation for this article: *J Clin Invest* doi:10.1172/JCI60433.

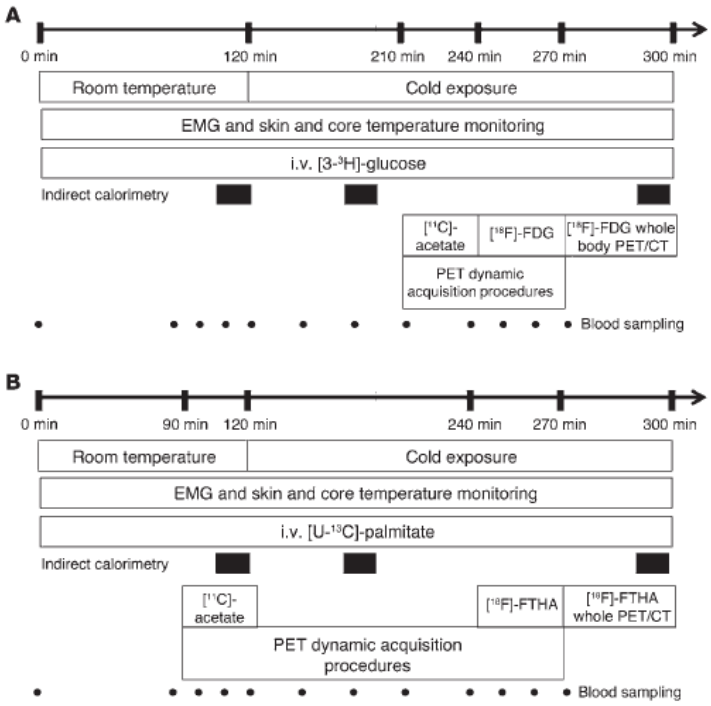

Figure 1
Study protocols. (**A**) Measurement of plasma glucose turnover and BAT ^{11}C-acetate and ^{18}FDG uptake during acute cold exposure. (**B**) Measurement of plasma NEFA turnover and BAT ^{18}FTHA during acute cold exposure and BAT ^{11}C-acetate uptake at room temperature.

located on the anterior surface of the cervical spine, between the atlas and the third dorsal vertebra). Net tissue glucose uptake (K_m) (Figure 2C) was higher in BAT vs. subcutaneous adipose tissue, trapezius, and deltoid, but not compared with the longus colli. Whole-body ^{18}FDG uptake in one of the participants at the end of the protocol is shown in Figure 2D. BAT mean total volume of activity was 168 ± 56 ml (range 31 to 329 ml) based on ^{18}FDG uptake. Glucose uptake by BAT amounted to 10.8 ± 4.5 μmol/min (range 1.3 to 28.7 μmol/min). Given a plasma glucose appearance rate of 1,493 ± 460 μmol/min, BAT glucose uptake accounted for 1.3% ± 0.8% of plasma glucose turnover (range 0.04% to 5.2%).

^{18}FTHA uptake during cervicothoracic dynamic PET/CT acquisition upon cold exposure of 1 representative participant is shown in Figure 3A. During cold exposure, fractional uptake (K_i) of ^{18}FTHA (Figure 3B) and net tissue NEFA uptake (K_m) (Figure 3C) were significantly higher in supraclavicular BAT compared with subcutaneous adipose tissue, trapezius, and deltoid, but not different from that of the longus colli. Whole-body ^{18}FTHA uptake at the end of the protocol in one of the participants is shown in Figure 3D. NEFA uptake by BAT amounted to 2.3 ± 0.8 μmol/min (range, 0.3 to 4.4 μmol/min). Given a plasma NEFA appearance rate of 1,002 ± 72 μmol/min, BAT NEFA uptake accounted for approximately 0.25% ± 0.08% of plasma NEFA turnover (range, 0.04% to 0.44 %).

After i.v. injection of ^{11}C-acetate, blood ^{11}C radioactivity over time was not significantly different during cold exposure compared with at room temperature (Figure 4A). BAT (Figure 4B), but not subcutaneous adipose tissue (Figure 4C), ^{11}C radioactivity was increased throughout exposure to cold. The longi colli (Figure 4D) and sternocleidomastoids (not shown) were the only cervical and upper thoracic muscles that displayed significant cold-induced increase in ^{11}C radioactivity over time. ^{11}C radioactivity over time in trapezius and deltoids is shown in Figure 4, E and F, respectively. The AUC of ^{11}C radioactivity, a marker of tissue oxidative and/or nonoxidative metabolism (acetate retention), was elevated in BAT and longus colli. The monoexponential decay slope from tissue peak ^{11}C activity (^{11}C-acetate k), a valid surrogate of tissue oxidative metabolism (18, 19), was, however, increased in BAT in all participants (Figure 4G) but not in longus colli (Figure 4H), demonstrating that the former tissue plays an important role in cold-induced nonshivering thermogenesis, whereas the latter tissue mostly retained acetate in nonoxidative pathways. BAT CT radio density (in Hounsfield units) increased in all participants (by 17% ± 5%; range, 6% to 41%; $P = 0.03$) (Figure 4I), whereas white adipose tissue (WAT) radio density did not change (3% ± 5%; $P = 1.00$). Supplemental Figure 1 (supplemental material available online with this article; doi:10.1172/JCI60433DS1) shows actual CT and PET/CT fusion images of the integrated tissue activity in the neck and upper chest area from dynamic list-mode acquisitions at room temperature and during cold exposure in one of the participants.

There was a significant inverse correlation between BAT volume of activity and shivering expressed as percentage of voluntary maximal contraction (Spearman $r = -0.89$; $P = 0.03$) (Supplemental Figure 2). We found no other significant correlations between BAT volume of activity and energy expenditure (Supplemental Table 1), although our small sample size severely limits the power of these analyses.

Table 1

Average body temperatures, indirect calorimetry, circulating metabolites and hormones, and plasma glucose and NEFA appearance rates at ambient temperature (warm) and during cold exposure (cold)

		1	2	3	4	5	6	Mean ± SEM
Skin temperature (°C)	Warm	32.9	33.1	32.6	34.2	33.1	32.7	33.1 ± 0.2
	Cold	28.2	30.5	28.5	30.7	29.2	28.2	29.6 ± 0.4[A]
Core temperature (°C)	Warm	37.0	37.0	37.4	37.0	36.6	36.6	37.0 ± 0.1
	Cold	36.4	36.4	37.4	36.8	36.2	36.7	36.6 ± 0.2
VO_2 (l/min)	Warm	0.318	0.346	0.356	0.375	0.386	0.441	0.370 ± 0.017
	Cold	0.563	0.661	0.473	0.615	0.678	0.923	0.652 ± 0.062[A]
VCO_2 (l/min)	Warm	0.275	0.302	0.320	0.324	0.310	0.390	0.320 ± 0.016
	Cold	0.503	0.643	0.431	0.497	0.535	0.893	0.584 ± 0.068[A]
TEE (kcal/min)	Warm	1.54	1.69	1.75	1.82	1.85	2.15	1.80 ± 0.08
	Cold	2.76	3.29	2.33	2.95	3.24	4.59	3.19 ± 0.31[A]
Glucose (mmol/l)	Warm	3.7	4.4	4.1	3.3	4.2	4.0	4.0 ± 0.2
	Cold	3.8	4.5	3.7	3.9	4.2	3.9	4.0 ± 0.1
$Ra_{glucose}$ (μmol/min)	Warm	ND	ND	ND	ND	ND	ND	ND
	Cold	950	957	1,133	1,703	3,661	556	1,493 ± 460
Insulin (pmol/l)	Warm	65	67	74	53	45	125	71 ± 11
	Cold	69	62	45	57	62	84	63 ± 5
TG (mmol/l)	Warm	0.88	0.87	1.52	0.69	0.49	1.15	0.93 ± 0.15
	Cold	0.89	0.78	1.61	0.62	0.57	1.06	0.92 ± 0.16
NEFA (μmol/min)	Warm	366	352	645	689	311	484	474 ± 66
	Cold	475	535	805	897	476	677	644 ± 73[A]
Ra_{NEFA} (μmol/min)	Warm	708	ND	740	845	759	813	773 ± 25
	Cold	901	ND	937	1,011	884	1,278	1,002 ± 72[A]
TSH (IU/l)	Warm	0.91	1.59	0.87	2.21	1.72	0.97	1.38 ± 0.22
	Cold	0.91	1.66	0.80	2.17	1.59	0.93	1.34 ± 0.22
Free T3 (pmol/l)	Warm	5.3	4.6	5.2	5.9	5.7	6.1	5.5 ± 0.2
	Cold	5.0	4.6	5.2	6.0	5.5	6.2	5.4 ± 0.2
Free T4 (pmol/l)	Warm	18.3	18.1	17.1	16.5	16.2	17.2	17.2 ± 0.4
	Cold	18.6	18.9	17.6	15.8	16.7	17.8	17.5 ± 0.5
Cortisol (nmol/l)	Warm	216	277	184	237	274	257	241 ± 15
	Cold	256	284	197	255	269	302	206 ± 15
BAT K_i ^{18}FDG	Warm	ND	ND	ND	ND	ND	ND	ND
	Cold	0.013	0.009	0.009	0.019	0.011	0.027	0.015 ± 0.003
BAT K_i ^{18}FTHA	Warm	ND	ND	ND	ND	ND	ND	ND
	Cold	0.018	0.013	0.015	0.022	0.020	0.023	0.018 ± 0.002
BAT volume of activity (ml)	Warm	ND	ND	ND	ND	ND	ND	ND
	Cold	329	57	51	244	31	296	168 ± 56

Values from all participants at ambient temperature (between times 80 and 120 minutes) and during cold exposure (between times 180 and 300 minutes) were averaged from both protocols (no difference between protocol A and B), except for $Ra_{glucose}$ and Ra_{NEFA}, which were only determined in protocol A and B, respectively, at isotopic steady-state enrichment (between times 100 and 120 minutes and times 280 and 300 minutes). [A]$P < 0.05$ by Wilcoxon's test. BAT, supraclavicular BAT; Ra, rate of appearance; T3, triiodothyronine; T4, thyroxine.

Discussion

Based on ^{11}C-acetate tissue kinetics, the present results demonstrate significant cold-induced activation of BAT oxidative metabolism in all subjects studied under well-controlled cold exposure conditions designed to minimize shivering. We also determined for what we believe is the first time in vivo in humans that plasma NEFA uptake is increased in cold-activated BAT compared with resting skeletal muscles and subcutaneous adipose tissues.

A cold-induced total BAT glucose uptake averaging 10.8 ± 2.9 μmol/min lies within the range reported by Virtanen et al. (6). In addition, the present results demonstrate the ability of human BAT to also increase its NEFA uptake during cold exposure. Whole-body ^{18}FTHA uptake at the end of the protocol predicts NEFA uptake by BAT amounting to 2.3 ± 0.8 μmol/min (range, 0.3 to 4.4 μmol/min). One limitation of our experimental design was the impossibility of assessing ^{18}FDG and ^{18}FTHA BAT uptake at ambient temperature, given the complexity of design and acceptable limits of radiation exposure of research participants. However, significant BAT glucose and NEFA uptake is not detectable in the vast majority of individuals at ambient temperature (12, 20). In rodents, the contribution from glucose and NEFA uptake has proven to be a relatively small fraction of total BAT metabolism during acute cold-induced thermogenesis compared with intracellular brown adipocyte triglycerides (21). Also, we did not assess BAT utilization of fatty acids from circulating lipoproteins, another potential source of BAT energy substrates (22). However, unlike what has been observed in mice in the latter study, we did not find any reduction in circulating triglycerides in the present study (Table 1). Assuming a volume of distribution of 0.45 dl/kg of body weight (23), with an average body weight of 80.7 kg and a plasma triglyceride level of 0.93 mmol/l (82 mg/dl), mean total circulating triglyceride content is estimated at approximately 3 g

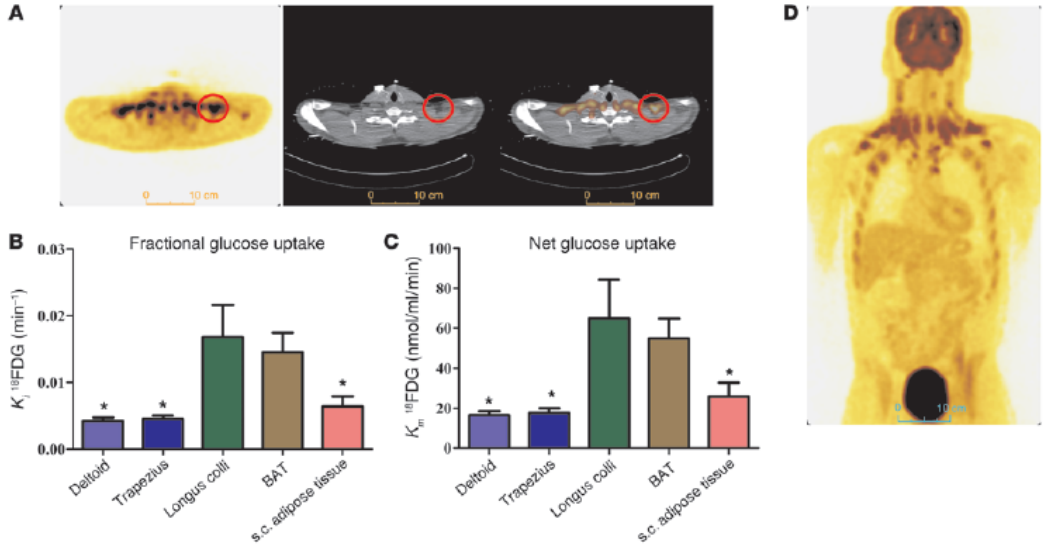

Figure 2
Tissue glucose uptake. (**A**) Transversal PET (left panel), CT (middle panel), and fusion scan (right panel) views of the cervicothoracic junction in one of the participants. Red circles denote supraclavicular BAT. (**B**) Fractional (K_i) and (**C**) net (K_m) glucose uptake in cervicothoracic tissues. (**D**) Coronal view (postero-anterior projection) of whole-body ^{18}FDG uptake during cold exposure. *$P < 0.05$ versus BAT, ANOVA with Dunnett's post-hoc test.

in the participants of the present study. As the half-life of circulating triglycerides during fasting (mostly VLDL) is relatively long (approximately 2 hours, i.e., a fractional clearance rate of 0.5/h; ref. 23) compared with the length of cold exposure in the present study, it is very unlikely that the pool of circulating triglycerides, even if it was fully utilized, could account for the 250 extra kcal of energy expenditure observed (i.e., approximately 28 g of triglycerides). It is also noteworthy that our subjects were not, in contrast with the mice in Bartelt's study (22), adapted to a temperature below thermoneutrality, which may render BAT adipocytes more prepared to clear circulating glucose and lipid.

The 6 subjects of the present study all exhibited increases in BAT metabolism upon cold exposure, albeit to varying degrees. The variability in the response occurred despite application of a cold exposure protocol that not only restricted shivering, but also dictated the strength of the cold response from strict body and skin temperature monitoring and indirect calorimetry measurements. Such variation would seem to be accounted for by interindividual differences in BAT capacity (volume). The wide interindividual differences in detectable BAT volume of activity (from to 31 to 329 ml) observed in young healthy men in the present study suggests that unknown factors may modulate BAT volume and thermogenic capacity in addition to age, sex, body mass index, and diabetes (24). Furthermore, we found a significant inverse relationship between BAT volume of activity and shivering. Interestingly, BAT precursor cells are present in supraclavicular fat independently of the presence of spontaneous ^{18}FDG uptake (25). Of note, a very recent publication demonstrated cold-induced increased blood flow in BAT that was associated with increased energy expenditure (26). The latter is consistent with the present results, which demonstrate cold-induced BAT thermogenesis in humans.

Our demonstration of BAT oxidative metabolism with trivial rates of plasma glucose and NEFA utilization and rapid increase in BAT radio density during cold exposure is suggestive of increased intracellular triglyceride utilization as the main source of energy for BAT thermogenesis. Intracellular triglycerides are the main fuel to sustain BAT energy metabolism during cold exposure in animal models (2, 27, 28). In room temperature–acclimated rats, short-term acute exposure to cold has been reported to lead to a near-complete depletion of BAT lipid (28). A similar depletion of BAT lipid has been reported at necropsy in newborn infants and adults who died from hypothermia (27). Intracellular brown adipocyte triglycerides represent half of the brown adipocyte volume (27). From a mass of 168 g (the average BAT mass seen in the present study), one can predict a BAT fat content of approximately 84 g. Mobilization of one-third of that lipid reserve (28 g), which seems possible based on previous investigations (28), would be sufficient to account for the extra energy (250 ± 45 kcal) expended during the 3-hour period of cold exposure in the present study. Although the 80% increase in total energy expenditure (TEE) that we observed during acute cold exposure appears important, it is therefore very likely that BAT thermogenesis accounted for an important fraction of this increase in TEE. Future studies will need to determine the contribution of intracellular triglycerides to BAT thermogenesis.

In addition, we cannot exclude the contribution of other tissues to cold-induced thermogenesis. We recorded increased glucose, NEFA, and acetate uptake in the longus colli. Nonetheless, the observation that significant cold-induced increase in ^{11}C-acetate oxidative metabolism was only seen in BAT demonstrates a signifi-

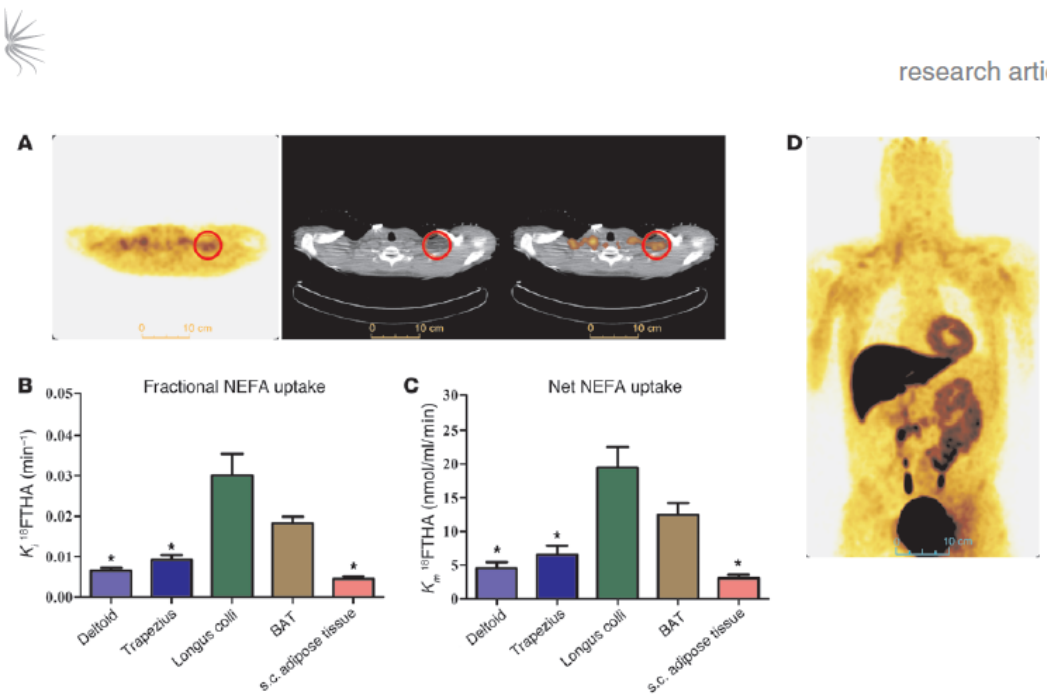

Figure 3
Tissue NEFA uptake. (**A**) Transversal PET (left panel), CT (middle panel), and fusion scan (right panel) views of the cervicothoracic junction in one of the participants. Red circles show supraclavicular BAT. (**B**) Fractional (K_i) and (**C**) net (K_m) NEFA uptake in cervicothoracic tissues. (**D**) Coronal view (postero-anterior projection) of whole-body ^{18}FTHA uptake during cold exposure. *$P < 0.05$ versus BAT, ANOVA with Dunnett's post-hoc test.

cant role of this tissue in the nonshivering thermogenic response to cold. The limited field of view of our PET/CT scanner (18 cm length) during dynamic acquisitions prevents us from assessing oxidative metabolism from the ^{11}C-acetate method in other internal organs, such as the heart and other deep central muscles that might have been activated by cold. The number of subjects in the present study is small due to the complexity of our measurements. Despite this limitation, we are nonetheless confident that our findings apply to other populations, since they were very consistent between subjects. Finally, it is not possible to exclude an effect of the 2-hour daily time difference in ^{11}C-acetate injection between the 2 protocols in the present study. To our knowledge, the effect of nycthemeral cycle on BAT metabolism has not been previously studied in humans.

The present findings support a role of BAT for nonshivering thermogenesis in humans with intracellular triglycerides as the main source of energy for this process, as observed in rodents. However, it remains to be demonstrated whether chronic and frequent bouts of cold exposure may contribute to increase BAT capacity and/or activity and may be a viable adjunct therapeutic strategy to other lifestyle interventions to prevent or treat obesity and its metabolic complications. It is also possible that energy substrate uptake by BAT could be substantially increased once intracellular triglyceride stores are depleted and/or BAT is fully cold adapted, as recently shown in rodents (22). Quantitative assessment of the contribution of intracellular triglyceride oxidation in BAT thermogenesis awaits further methodological developments.

In summary, the present study demonstrates that a cold-exposure stimulus designed to minimize muscle-mediated shivering thermogenesis enhances BAT oxidative metabolism as well as glucose and NEFA uptake in adult humans. The enhanced BAT activity was associated with a 1.8-fold increase in whole-body energy expenditure. We found a significant inverse relationship between BAT volume of activity and shivering and a significant increase in BAT radio density within 3 hours of cold exposure, indicating rapid reduction in BAT triglyceride content. The present results demonstrate that BAT is undoubtedly involved in nonshivering thermogenesis in humans.

Methods

Protocols A and B were 4.5-hour metabolic tests performed in random order, within an average of 20 days of each other (range, 7 to 36 days) and designed to assess whole-body and BAT-specific energy substrate turnover and oxidation and energy expenditure at room temperature (~25°C, time 0 to 120 minutes) and during acute exposure to cold (time 120 to 270 minutes) (Figure 1). Participants were instrumented and fitted with a liquid-conditioned tube suit (Allen-Vanguard Inc.). Following the room temperature period (time 0 to 120 minutes), the liquid-conditioned tube suit was perfused with approximately 18°C water using a temperature and flow-controlled circulation bath (Endocal, NESLAB, and Model 200-00; Micropump Inc.). Briefly, the same suit was used for all subjects to maintain consistent tubing density. In addition, the flow and temperature of water through the suit was produced with the same cooling bath. Based on pilot experiments, we determined that circulating water in the suit at 18°C minimized overt shivering in healthy participants while achieving a significant reduction in skin temperature of at least 2.5°C. We did not try to avoid the slight but significant increase in electromyographic (EMG) activity observed during the experiments. Therefore, EMG activity could

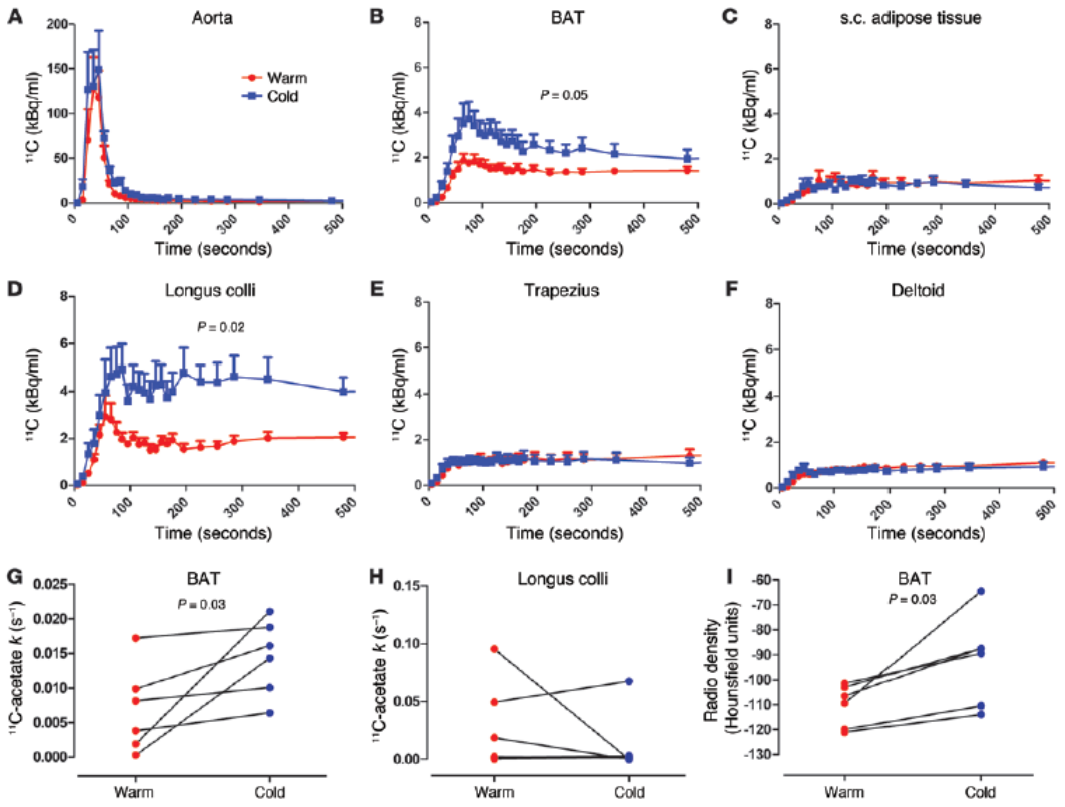

Figure 4

^{11}C-acetate kinetics. ^{11}C time-radioactivity curves over the first 500 seconds of acquisition after ^{11}C-acetate injection at room temperature (red) and during cold exposure (blue) in (**A**) blood in the aorta, (**B**) supraclavicular BAT, (**C**) subcutaneous adipose tissue, (**D**) longus colli, (**E**) trapezius, and (**F**) deltoid. ^{11}C time-radioactivity curves were different during cold exposure from those at room temperature in BAT (2-way ANOVA, $P = 0.05$; interaction with time, $P < 0.001$) and in longi colli (2-way ANOVA, $P = 0.02$; interaction with time, $P < 0.001$), but not in other organs. Monoexponential decay slope from peak tissue ^{11}C activity (^{11}C-acetate k) in (**G**) supraclavicular BAT and (**H**) longus colli. (**I**) BAT radio density by CT.

slightly differ among individuals despite similar cold exposure, depending on their degree of nonshivering thermogenesis. This difference in extent of EMG activity thus masked any possibility of discerning a correlation between nonshivering thermogenesis and TEE. Change in total heat production was calculated by indirect calorimetry (V_{max} 29n; Sensormedics) (29) at room temperature and between times of 180 to 200 minutes and 280 to 300 minutes (i.e., 60 to 80 minutes and 160 to 180 minutes after the beginning of cold exposure). TEE rapidly increased by time 180 to 200 minutes to approximately 79% of that recorded between times 280 and 300 minutes. Only indirect calorimetry and EMG measurements during the latter period are reported. Dry heat loss from the difference between water temperature entering and exiting the tube suit at a given flow rate was determined (30). Skin and core temperatures were monitored as previously described (31, 32). Changes in whole-body heat production, heat loss, and core and mean skin temperatures as well as muscle shivering intensity by EMG were determined as previously described (15, 16, 33, 34). This protocol achieved consistent skin temperature (difference = –0.2 ± 0.3°C) and energy expenditure (difference 2.2% ± 7.0%) between protocols A and B during cold exposure.

Plasma glucose appearance rate ($Ra_{glucose}$) was determined using a primed continuous infusion (0.33 × 10^6 dpm/min) of [3-^{3}H]-glucose during protocol A (23). Ra_{NEFA} was measured using i.v. administration of [U-^{13}C]-palmitate during protocol B using the Steele steady-state equation, as previously described (29, 35). Tissue oxidative metabolism was determined after i.v. bolus injection of ^{11}C-acetate (~185 MBq) at time 90 minutes (room temperature) and at time 210 minutes (i.e., 90 minutes after onset of cold exposure), followed by 30-minute list-mode dynamic PET acquisition, preceded by a 40 mAs CT acquisition centered at the cervicothoracic junction, as described (20). Tissue oxidative metabolism index (the rapid fractional tissue clearance of ^{11}C-acetate, k, in s^{-1}) was estimated from tissue ^{11}C activity over time using monoexponential fit from the time of peak tissue activity (36). This method is based on the following assumptions (37): (a) acetate enters the Krebs cycle freely after rapid conversion into acetyl-CoA; (b) other acetate metabolic fates (e.g., de novo lipogenesis) are relatively

slow compared with the Krebs cycle carbon fluxes; (c) carbon fluxes into the Krebs cycle through acetyl-CoA are directly coupled to the production of reducing equivalents; (d) the Krebs cycle contribution to the production of reducing equivalents is stable and accounts for approximately two-thirds of total production; and (e) the production of reducing equivalents is tightly coupled to oxygen consumption.

In protocol A, each participant received an i.v. bolus of ^{18}FDG (~185 MBq) at time 240 minutes (i.e., 2 hours after the onset of cold exposure), with 30 minutes list-mode dynamic PET acquisition centered at the cervicothoracic junction to determine tissue glucose uptake using Patlak graphical analysis (38). This was followed by a whole-body CT scan (16 mAs) to correct for attenuation and for definition of PET regions of interest, followed by whole-body PET acquisition to determine whole-body ^{18}FDG uptake. In protocol B, the same procedure was performed, but with i.v. bolus administration of ^{18}FTHA (~185 MBq) instead of ^{18}FDG to determine tissue NEFA uptake after correction for plasma metabolites using Patlak linearization (20, 38, 39). For dynamic PET acquisitions, mean value of pixels (mean standard uptake value [SUV]) for each frame was recorded. Regions of interest were drawn on the aortic arch for blood activity (input functions) and on supraclavicular BAT according to the following criteria: a tissue radio density between –10 and –100 Hounsfield units and ^{18}FDG uptake during cold exposure of more than 1 SUV unit (12). We also calculated total BAT volume of activity on whole-body scans according to the later criteria, as previously described (12). The regions of interest (ROI) were first defined from the transaxial CT slices, then copied to ^{18}FDG, and then to ^{11}C-acetate and ^{18}FTHA image sequences. For whole-body scans, mean values of pixels (mean SUV) for all tissues of interest were recorded. In the cervicothoracic dynamic sequences, ROI were drawn on the 2 largest muscles in the field of view (deltoid and trapezius, the latter also being electromyographically recorded), on posterior cervical subcutaneous adipose tissue, and on any muscle or tissue structures that showed significant (>1 SUV unit) ^{18}FDG uptake during cold exposure. The latter occurred systematically only in small paraspinal muscles of the neck (longi colli) within the field of view of dynamic scans.

Statistics. Data are expressed as mean + SEM. Wilcoxon's test was used to compare characteristics and averaged steady-state hormone and metabolite levels between room temperature and cold exposure. Two-way ANOVA for repeated measures with temperature, time, and interaction as the independent variables was used to analyze time- and temperature-dependent differences in blood and tissue PET-acquired activities throughout the protocols. ANOVA for repeated measures with Dunnett's post-hoc test were performed to compare fractional and net glucose and NEFA uptake between BAT and other tissues during cold exposure. Appropriate transformation of variables was performed when normal distribution was not observed for parametric statistical testing. A 2-tailed P value of less than 0.05 was considered significant. All analyses were performed with the GraphPad Prism version 5.00 for Windows.

Study approval. Informed written consent was obtained from all participants in accordance with the Declaration of Helsinki, and the protocol received approval from the Human Ethics Committee of the Centre de recherche clinique Etienne-LeBel.

Acknowledgments

This work was supported by a grant from the Canadian Diabetes Association (OG-3-10-2970-AC) and was performed at the Centre de recherche clinique Etienne-Le Bel, a research center funded by the Fonds de la recherche en santé du Québec (FRSQ). S.M. Labbé is the recipient of a Canadian Diabetes Association Doctoral Studentship Award. D. Richard is the recipient of the CIHR/Merck Frosst Research Chair on Obesity. A.C. Carpentier was the recipient of a FRSQ Senior Scholarship Award and is now the recipient of the CIHR-GlaxoSmithKline Chair in Diabetes.

Received for publication August 10, 2011, and accepted in revised form November 16, 2011.

Address correspondence to: André C. Carpentier, Division of Endocrinology, Centre hospitalier universitaire de Sherbrooke, Sherbrooke, Québec, Canada J1H 5N4. Phone: 819.564.5244; Fax: 819.564.5292; E-mail: andre.carpentier@usherbrooke.ca. Or to: Denis Richard, Centre de recherche de l'Institut universitaire de cardiologie et de pneumologie de Québec, Quebec City, Québec, Canada. Phone: 418.656.8711, ext. 11714; Fax: 418.656.4929; E-mail: Denis.Richard@criucpq.ulaval.ca.

1. Cannon B, Nedergaard J. Brown adipose tissue: function and physiological significance. *Physiol Rev*. 2004;84(1):277–359.
2. Richard D, Picard F. Brown fat biology and thermogenesis. *Front Biosci*. 2011;16:1233–1260.
3. Sell H, Deshaies Y, Richard D. The brown adipocyte: update on its metabolic role. *Int J Biochem Cell Biol*. 2004;36(11):2098–2104.
4. Hany TF, Gharehpapagh E, Kamel EM, Buck A, Himms-Hagen J, von Schulthess GK. Brown adipose tissue: a factor to consider in symmetrical tracer uptake in the neck and upper chest region. *Eur J Nucl Med Mol Imaging*. 2002;29(10):1393–1398.
5. Cypess AM, et al. Identification and importance of brown adipose tissue in adult humans. *N Engl J Med*. 2009;360(15):1509–1517.
6. Virtanen KA, et al. Functional brown adipose tissue in healthy adults. *N Engl J Med*. 2009; 360(15):1518–1525.
7. Saito M, et al. High incidence of metabolically active brown adipose tissue in healthy adult humans: effects of cold exposure and adiposity. *Diabetes*. 2009;58(7):1526–1531.
8. Zingaretti MC, et al. The presence of UCP1 demonstrates that metabolically active adipose tissue in the neck of adult humans truly represents brown adipose tissue. *FASEB J*. 2009;23(9):3113–3120.
9. Cohade C, Mourtzikos KA, Wahl RL. "USA-Fat": prevalence is related to ambient outdoor temperature-evaluation with 18F-FDG PET/CT. *J Nucl Med*. 2003;44(8):1267–1270.
10. Garcia CA, et al. Reduction of brown fat 2-deoxy-2-[F-18]fluoro-D-glucose uptake by controlling environmental temperature prior to positron emission tomography scan. *Mol Imaging Biol*. 2006;8(1):24–29.
11. Kim S, Krynyckyi BR, Machac J, Kim CK. Temporal relation between temperature change and FDG uptake in brown adipose tissue. *Eur J Nucl Med Mol Imaging*. 2008;35(5):984–989.
12. Ouellet V, et al. Outdoor temperature, age, sex, body mass index, and diabetic status determine the prevalence, mass, and glucose-uptake activity of 18F-FDG-detected BAT in humans. *J Clin Endocrinol Metab*. 2011;96(1):192–199.
13. Cannon B, Nedergaard J. Metabolic consequences of the presence or absence of the thermogenic capacity of brown adipose tissue in mice (and probably in humans). *Int J Obes (Lond)*. 2010;34(suppl 1):S7–S16.
14. Enerback S. Human brown adipose tissue. *Cell Metab*. 2010;11(4):248–252.
15. Haman F, Legault SR, Weber JM. Fuel selection during intense shivering in humans: EMG pattern reflects carbohydrate oxidation. *J Physiol*. 2004;556(pt 1):305–313.
16. Haman F, Legault SR, Rakobowchuk M, Ducharme MB, Weber JM. Effects of carbohydrate availability on sustained shivering II. Relating muscle recruitment to fuel selection. *J Appl Physiol*. 2004;96(1):41–49.
17. Haman F, Blondin DP, Imbeault MA, Maneshi A. Metabolic requirements of shivering humans. *Front Biosci (Schol Ed)*. 2010;2:1155–1168.
18. Brown M, Marshall DR, Sobel BE, Bergmann SR. Delineation of myocardial oxygen utilization with carbon-11-labeled acetate. *Circulation*. 1987; 76(3):687–696.
19. Ng CK, Huang SC, Schelbert HR, Buxton DB. Validation of a model for [1-11C]acetate as a tracer of cardiac oxidative metabolism. *Am J Physiol*. 1994; 266(4 pt 2):H1304–H1315.
20. Labbe SM, et al. Normal postprandial nonesterified Fatty Acid uptake in muscles despite increased circulating Fatty acids in type 2 diabetes. *Diabetes*. 2011;60(2):408–415.
21. Ma SW, Foster DO. Uptake of glucose and release of fatty acids and glycerol by rat brown adipose tissue in vivo. *Can J Physiol Pharmacol*. 1986;64(5):609–614.
22. Bartelt A, et al. Brown adipose tissue activity controls triglyceride clearance. *Nat Med*. 2011;17(2):200–205.
23. Carpentier A, et al. The effect of systemic versus portal insulin delivery in pancreas transplantation on insulin action and VLDL metabolism. *Diabetes*. 2001;50(6):1402–1413.
24. Richard D, Carpentier AC, Dore G, Ouellet V, Picard F. Determinants of brown adipocyte development and thermogenesis. *Int J Obes (Lond)*. 2010; 34(suppl 2):S59–S66.
25. Lee P, Swarbrick MM, Ting ZJ, Ho KK. Inducible

brown adipogenesis of supraclavicular fat in adult humans. *Endocrinology*. 2011;152(10):3597–602.
26. Orava J, et al. Different metabolic responses of human brown adipose tissue to activation by cold and insulin. *Cell Metab*. 2011;14(2):272–279.
27. Aherne W, Hull D. Brown adipose tissue and heat production in the newborn infant. *J Pathol Bacteriol*. 1966;91(1):223–234.
28. Baba S, Jacene HA, Engles JM, Honda H, Wahl RL. CT Hounsfield units of brown adipose tissue increase with activation: preclinical and clinical studies. *J Nucl Med*. 2010;51(2):246–250.
29. Carpentier A, et al. On the suppression of plasma non-esterified fatty acids by insulin during enhanced intravascular lipolysis in humans. *Am J Physiol Endocrinol Metab*. 2005;289(5):E849–E856.
30. Blondin DP, Depault I, Imbeault P, Peronnet F, Imbeault MA, Haman F. Effects of two glucose ingestion rates on substrate utilization during moderate-intensity shivering. *Eur J Appl Physiol*. 2010; 108(2):289–300.
31. Dubois D, Dubois EF. A formula to estimate the approximate surface area if height and weight be known. *Arch Intern Med*. 1916;17(62):863–871.
32. Hardy JD, Dubois EF. Regulation of heat loss from the human body. *Proc Natl Acad Sci U S A*. 1937; 23(12):624–631.
33. Haman F, et al. Effects of carbohydrate availability on sustained shivering I. Oxidation of plasma glucose, muscle glycogen, and proteins. *J Appl Physiol*. 2004;96(1):32–40.
34. Haman F, Peronnet F, Kenny GP, Massicotte D, Lavoie C, Weber JM. Partitioning oxidative fuels during cold exposure in humans: muscle glycogen becomes dominant as shivering intensifies. *J Physiol*. 2005;566(pt 1):247–256.
35. Carpentier AC, et al. Mechanism of insulin-stimulated clearance of plasma nonesterified fatty acids in humans. *Am J Physiol Endocrinol Metab*. 2007;292(3):E693–E701.
36. Buck A, et al. Effect of carbon-11-acetate recirculation on estimates of myocardial oxygen consumption by PET. *J Nucl Med*. 1991;32(10):1950–1957.
37. Klein LJ, et al. Carbon-11 acetate as a tracer of myocardial oxygen consumption. *Eur J Nucl Med*. 2001;28(5):651–668.
38. Menard SL, et al. Abnormal in vivo myocardial energy substrate uptake in diet-induced type 2 diabetic cardiomyopathy in rats. *Am J Physiol Endocrinol Metab*. 2010;298(5):E1049–E1057.
39. Ci X, et al. The effect of insulin on the intracellular distribution of 14(R,S)-[(18)F]fluoro-6-thia-heptadecanoic acid in rats. *Mol Imaging Biol*. 2006; 8(4):237–244.

APPENDIX D:

Final published version of ARTICLE III

JCEM ONLINE

Hot Topics in Translational Endocrinology—Endocrine Research

Increased Brown Adipose Tissue Oxidative Capacity in Cold-Acclimated Humans

Denis P. Blondin, Sébastien M. Labbé, Hans C. Tingelstad, Christophe Noll, Margaret Kunach, Serge Phoenix, Brigitte Guérin, Éric E. Turcotte, André C. Carpentier, Denis Richard, and François Haman

Faculty of Health Sciences (D.P.B., H.C.T., F.H.), University of Ottawa, Ottawa, Ontario, Canada K1N 6N5; Centre de Recherche de l'Institut Universitaire de Cardiologie et de Pneumologie de Québec (S.M.L., D.R.), Université Laval, Québec City, Québec, Canada G1V 4G5; Department of Medicine (C.N., M.K., S.P., A.C.C.), Centre de Recherche Clinique Etienne-Le Bel, Université de Sherbrooke, Sherbrooke, Québec, Canada; and Department of Nuclear Medicine and Radiobiology (S.P., B.G., E.E.T.), Université de Sherbrooke, Sherbrooke, Québec, Canada J1H 5N4

Context: Recent studies examining brown adipose tissue (BAT) metabolism in adult humans have provided convincing evidence of its thermogenic potential and role in clearing circulating glucose and fatty acids under acute mild cold exposure. In contrast, early indications suggest that BAT metabolism is defective in obesity and type 2 diabetes, which may have important pathological and therapeutic implications. Although many mammalian models have demonstrated the phenotypic flexibility of this tissue through chronic cold exposure, little is known about the metabolic plasticity of BAT in humans.

Objective: Our objective was to determine whether 4 weeks of daily cold exposure could increase both the volume of metabolically active BAT and its oxidative capacity.

Design: Six nonacclimated men were exposed to 10°C for 2 hours daily for 4 weeks (5 d/wk), using a liquid-conditioned suit. Using electromyography combined with positron emission tomography with [^{11}C]acetate and [^{18}F]fluorodeoxyglucose, shivering intensity and BAT oxidative metabolism, glucose uptake, and volume before and after 4 weeks of cold acclimation were examined under controlled acute cold-exposure conditions.

Results: The 4-week acclimation protocol elicited a 45% increase in BAT volume of activity (from 66 ± 30 to 95 ± 28 mL, $P < .05$) and a 2.2-fold increase in cold-induced total BAT oxidative metabolism (from 0.725 ± 0.300 to 1.591 ± 0.326 mL·s^{-1}, $P < .05$). Shivering intensity was not significantly different before compared with after acclimation (2.1% ± 0.7% vs 2.0% ± 0.5% maximal voluntary contraction, respectively). Fractional glucose uptake in BAT increased after acclimation (from 0.035 ± 0.014 to 0.048 ± 0.012 min^{-1}), and net glucose uptake also trended toward an increase (from 163 ± 60 to 209 ± 50 nmol·g^{-1}·min^{-1}).

Conclusions: These findings demonstrate that daily cold exposure not only increases the volume of metabolically active BAT but also increases its oxidative capacity and thus its contribution to cold-induced thermogenesis. (*J Clin Endocrinol Metab* 99: E438–E446, 2014)

In the 4 years since the seminal papers describing the presence of functional brown adipose tissue (BAT) in adult humans were published (1–3), significant progress has been made in characterizing its developmental origin (4, 5), function (6, 7), and distribution (8, 9). As in most mammals, BAT provides an important contribution to

ISSN Print 0021-972X ISSN Online 1945-7197
Printed in U.S.A.

Received October 24, 2013. Accepted December 30, 2013.
First Published Online January 13, 2014

Abbreviations: BAT, brown adipose tissue; CT, computed tomography; EMG, electromyography; ^{18}FDG, [^{18}F]fluorodeoxyglucose; NEFA, nonesterified fatty acid; NST, nonshivering thermogenesis; PET, positron emission tomography; SUV, standard uptake value; TG, triglyceride; UCP1, uncoupling protein-1.

doi: 10.1210/jc.2013-3901

thermoregulatory heat production in adult humans (6). The scarce amount of BAT found in individuals who are overweight or obese (10, 11) combined with the large BAT mass and lean phenotype exhibited by patients with pheochromocytoma (catecholamine-secreting tumors) (12, 13) have led to suggestions that it may also play an important part in energy homeostasis. Whether BAT can be induced to grow or increase its metabolic capacity and consequently be a therapeutic target for obesity and its related complications remains unclear. Evidence from animal models (14) and indirect support from human studies (15, 16) have suggested an inherent plasticity to this tissue, presenting signs of BAT recruitment. Furthermore, the differentiation of both types of brown adipocytes (classical and beige/brite) (4, 17, 18) and its activation (1, 3, 6) appear to be largely mediated by a sympathetic input. To date, the most potent and effective sympathetic stimulator of BAT differentiation and activation in humans has been cold exposure, as most sympathomimetics applied in vivo have shown little to no effect on BAT activation (19–21). Very recent studies have demonstrated that relative BAT glucose uptake as assessed by increased [^{18}F]fluorodeoxyglucose (^{18}FDG) standard uptake value (SUV) with positron emission tomography (PET) can be increased by repeated cold exposure in humans (22, 23). However, whether BAT oxidative capacity increases with the increase in BAT recruitment has not yet been demonstrated in adult humans. Six healthy lean men were invited to participate in a 4-week cold-acclimation protocol and undergo acute cold-exposure studies before and after the intervention to determine whether 4 weeks of daily cold exposure could increase both the volume of metabolically active BAT and its oxidative capacity.

Materials and Methods

Experimental protocol

Six healthy lean men aged 23 ± 1 year with a body mass index of 24.5 ± 1.2 kg/m^2 and body surface area of 2.01 ± 0.04 m^2 participated in 2 metabolic experimental sessions within a 4-week interval designed to assess whole-body and tissue-specific metabolism during an acute cold exposure (Figure 1). The cold acclimation protocol followed between these 2 experimental sessions consisted of daily cold exposure lasting 2 hours during which 10°C water was circulated through a liquid-conditioned suit (Three Piece; Allen-Vanguard), repeated 5 consecutive days per week for 4 consecutive weeks for a total of 18 acclimation sessions and 2 testing sessions. Participants were asked to maintain their current training regiment and refrain from drinking caffeinated or alcoholic beverages for the duration of the study.

Each acute cold exposure experimental session consisted of a 120-minute baseline period at ambient temperature (~25°C) followed by 180 minutes of exposure to a mild cold, elicited using the same liquid-conditioned suit. During cold exposure, 18.0°C water was circulated through the suit during the preacclimation visit and water at a temperature eliciting the same individualized inlet-outlet temperature difference as the preacclimation protocol (16.8°C ± 0.1°C) was circulated during the postacclimation visit using a temperature-controlled circulation bath (Endocal, NESLAB Model 200–00; Micropump). The postacclimation temperature was adjusted to induce a similar thermogenic rate between the 2 experimental sessions. The same suit was used for all subjects to maintain consistent tubing density and water flow. Experiments were conducted between 7:30 AM and 4:00 PM

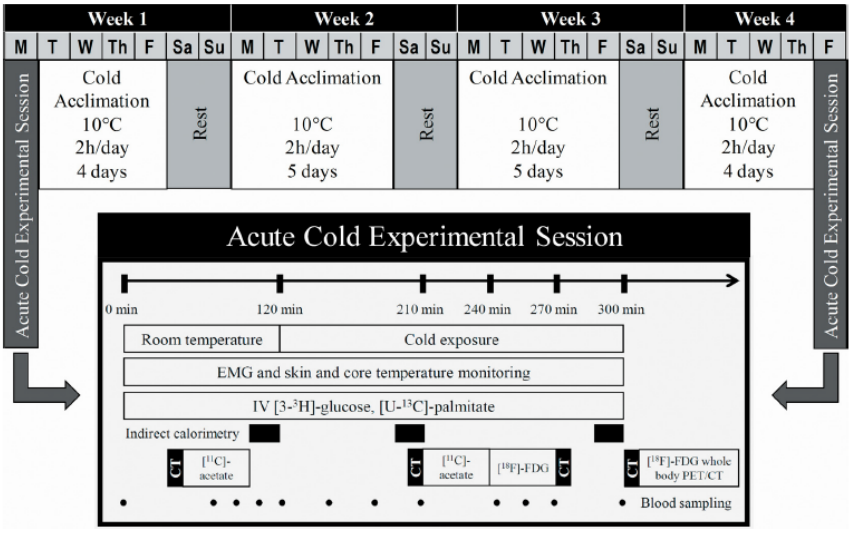

Figure 1. Study protocol.

hours, after 48 hours without strenuous physical activity. Upon their arrival in the laboratory, subjects wearing only shorts were weighed and instrumented with 12 autonomous wireless temperature sensors (Thermochron iButton model DS1922H, Maxim) fixed to the skin to measure mean skin temperature (24) and surface electromyography (EMG) electrodes (Delsys; EMG Systems) placed on the belly of 12 muscles. Participants were then fitted with the liquid-conditioned suit, ingested a telemetric thermometry capsule to measure core temperature (Vital Sense monitor and Jonah temperature capsule; Mini Mitter Co, Inc), and performed a series of exercises to estimate the maximal voluntary contraction of each of the muscles being measured for shivering activity. Whole-body metabolic heat production was determined by indirect respiratory calorimetry (Vmax 29n; Sensormedics) (25) at room temperature and between 180 to 200 minutes and 280 to 300 minutes (ie, 60 to 80 minutes and 160 to 180 minutes after the beginning of cold exposure). Whole-body and muscle-specific shivering intensity and pattern as well as mean skin and core temperatures were measured continuously from time 90 to 300 minutes as previously described (26). Only the means of the final 30 minutes of the ambient period and final 120 minutes of the cold exposure are reported. A weighted average of the ^{18}FDG uptake of 18 skeletal muscles, which includes deep muscles that are inaccessible using surface EMG, was also used as a shivering index to determine whether 1) shivering activity was modified based on muscle location (superficial vs deep) and 2) ^{18}FDG uptake in skeletal muscles could serve as a viable indicator of whole-body shivering activity. Plasma glucose appearance rate was determined using a primed continuous infusion (0.33 × 106 dpm/min) of [3-^{3}H]glucose (27). The rate of appearance of nonesterified fatty acids (NEFAs) was measured using iv administration of [U-^{13}C]palmitate using the Steele steady-state equation, as previously described (28).

PET/computed tomography protocol

Tissue oxidative metabolism was determined by first performing a computed tomography (CT) scan (40 milliAmpere-second) centered at the cervicothoracic junction to correct for attenuation and to define PET regions of interest. At 90 minutes (room temperature) and again at 210 minutes (ie, 90 minutes after onset of cold exposure), ~185 MBq of [^{11}C]acetate was injected iv followed by a 30-minute list-mode dynamic PET acquisition (24 × 10 seconds, 12 × 30 seconds, 4 × 300 seconds), as previously described (29). The tissue oxidative metabolism index (the rapid fractional tissue clearance of ^{11}C-acetate, k, in s^{-1}) was estimated from tissue ^{11}C activity over time using monoexponential fit from the time of peak tissue activity (30). This method is based on the following assumptions (31): 1) acetate enters the Krebs cycle freely after rapid conversion into acetyl-coenzyme A; 2) other acetate metabolic fates (eg, de novo lipogenesis) are relatively slow compared with the Krebs cycle carbon fluxes; 3) carbon fluxes into the Krebs cycle through acetyl-coenzyme A are directly coupled to the production of reducing equivalents; 4) the Krebs cycle contribution to the production of reducing equivalents is stable and accounts for approximately two-thirds of total production; and 5) the production of reducing equivalents is tightly coupled to oxygen consumption. Total oxidative metabolism index of BAT was determined by multiplying k (representing the oxidative metabolism of a particular depot) by the total volume of metabolically active BAT, as determined by ^{18}FDG uptake (described below). This calculation was performed to reflect the total oxidative metabolism of BAT located throughout the body.

To determine tissue glucose uptake, an iv bolus of ^{18}FDG (~185 MBq) was given at 240 minutes (ie, 2 hours after the onset of cold exposure), with a 40-minute list-mode dynamic PET acquisition (12 × 10 seconds, 8 × 30 seconds, 6 × 90 seconds, 5 × 300 seconds), followed by a CT scan (40 mAs) centered at the cervicothoracic junction to correct for attenuation and for definition of PET regions of interest. Plasma and tissue time-radioactivity curves were analyzed graphically using the Patlak linearization method (32), with the image-derived arterial input function taken from the aortic arch (33). The slope of the plot in the graphical analysis is equal to the tissue glucose extraction constant of ^{18}FDG (K_i in min^{-1} of ^{18}FDG). Tissue net glucose uptake (K_m) was then calculated by multiplying K_i by plasma glucose concentration, measured during the PET imaging protocol, which assumes a lump constant value of 1.0 compared with endogenous plasma glucose. After cold exposure (at 300 minutes), a whole-body CT scan (16 mAs) followed by a static whole-body PET acquisition was performed to determine whole body ^{18}FDG organ distribution and tissue SUV.

PET/CT image analyses

The regions of interest were first defined from the transaxial CT slices and then copied to ^{18}FDG and then to [^{11}C]acetate PET image sequences. For dynamic PET acquisitions, the mean value of pixels (mean SUV) for each frame was recorded. Regions of interest were drawn on the aortic arch for blood activity (input functions), the larger skeletal muscles in the field of view, posterior cervical sc adipose tissue, and the supraclavicular BAT according to the following criteria: a tissue radio density between −30 and −150 Hounsfield units and ^{18}FDG uptake during cold exposure of more than 1.5 SUV unit. The total BAT volume of activity on whole-body scans was also quantified according to the latter criteria. For whole-body scans, mean values of pixels (mean SUV) for all tissues of interest were recorded.

Statistical analysis

Data are expressed as mean ± SEM. Paired Student's t test was used to compare between acute cold exposure experimental sessions. Two-way ANOVA for repeated measures with acclimation status, temperature, and their interaction as the independent variables was used to analyze acclimation- and temperature-dependent differences in averaged steady-state hormone and metabolite levels and blood and tissue PET-acquired activities throughout the protocols. Bonferroni's multiple-comparisons post hoc test was used, where applicable. Appropriate transformations of variables were performed when a normal distribution was not observed for parametric statistical testing. Pearson correlation coefficients were used to determine correlation between variables. A 2-tailed P value $< .05$ was considered significant. All analyses were performed using SPSS for Windows version 16.0 or GraphPad Prism version 6.00 for Windows.

Study approval

Participants were fully informed of the risks and methodologies applied and provided their written consent to participate in this study, in accordance with the Declaration of Helsinki. This study received ethics approval from the Office of Research Ethics and Integrity at the University of Ottawa and the Institutional

doi: 10.1210/jc.2013-3901

Review Board for research on humans of the Centre Hospitalier Universitaire de Sherbrooke and Université de Sherbrooke.

Results

Effect of cold acclimation on thermal responses and plasma metabolites

The energy expenditure was individually matched between experimental sessions by maintaining the same difference in inlet and outlet temperature of the water circulating through the cooling garment (Δ2.8°C ± 0.2°C; Figure 2A) before and after the 4-week cold acclimation. This elicited a similar 1.9-fold increase in thermogenic rate (Figure 2B) in the acute cold experimental sessions. Using this approach, the cold stimulus produced by the liquid-conditioned cooling garment evoked a decrease in mean skin temperature that was the same between acute cold-exposure sessions (Figure 2C). Shivering intensity, which was purposely kept to a minimum, was not significantly different between experimental conditions, whether it was determined electromyographically (Figure 2D) or using a weighted average of the ^{18}FDG uptake of 18 skeletal muscles as a shivering index (Figure 2E). The significant relationship between shivering intensity and the shivering index (Pearson $r = 0.66$, $P = .02$) suggests that the latter may also represent a good indicator of whole-body shivering activity, which includes deep muscles that are inaccessible using surface EMG (Figure 2F).

To assess the whole-body metabolic consequences of daily cold exposure, hormonal and metabolite changes were examined. Insulin, triglyceride (TG), T_3, T_4, ACTH, and leptin levels did not change significantly with cold exposure or cold acclimation (Table 1). NEFA rate of appearance, oxidation rate, and concentration were similarly increased before and after cold acclimation during acute cold exposure. Only glucose and cortisol concentrations appeared to be influenced by acclimation state, with both being significantly lower after compared with before acclimation, regardless of temperature exposure. Glucose production rate was not significantly changed after cold acclimation, demonstrating that the reduced glucose level was caused by increased glucose clearance.

Daily cold exposure increases BAT volume of activity and fractional glucose uptake

To examine the effect of daily cold exposure on BAT volume, we determined the whole-body volume of ^{18}FDG uptake in BAT (ie, volume of BAT activity) after a whole-body PET/CT acquisition performed immediately upon completing the acute cold exposure. A whole-body PET/CT image of a representative participant before and after a 4-week cold acclimation protocol is shown in Fig-

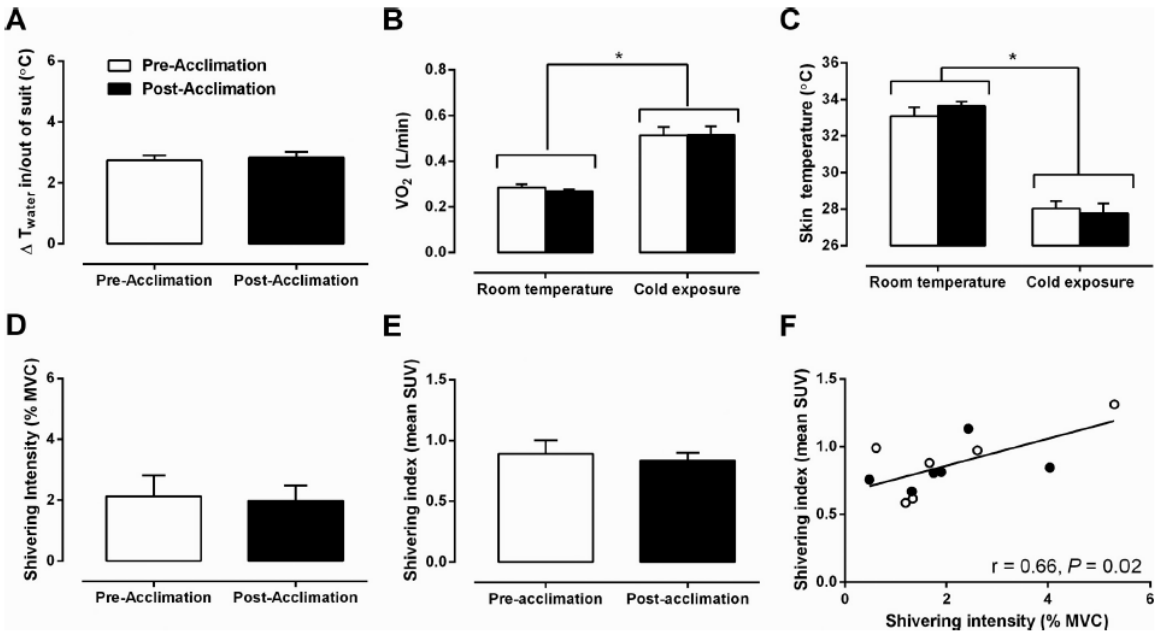

Figure 2. Thermal responses. A, Change in inlet and outlet water temperature of liquid-conditioned garment. B and C, Oxygen consumption (VO_2) (B) and mean skin temperature (C) during room temperature and cold exposure, before and after acclimation. D and E, Shivering intensity (D) and shivering intensity index (E) before and after acclimation. F, Relationship between mean shivering intensity and shivering intensity index (Pearson $r = 0.66$, $P = .02$). *, $P < .05$ vs room temperature, ANOVA with Bonferroni's post hoc test.

Table 1. Hormone and Metabolite Concentrations at Room Temperature and Cold Exposure, Before and After Cold Acclimation

	Before Acclimation		After Acclimation	
	Room Temperature	Cold Exposure	Room Temperature	Cold Exposure
Energy expenditure, kcal/min	1.4 ± 0.1	2.7 ± 0.2[b]	1.3 ± 0.0	2.5 ± 0.2[b]
Glucose, mmol/L	4.8 ± 0.2	4.8 ± 0.1	4.6 ± 0.1[c]	4.5 ± 0.1[c]
$Ra_{glucose}$, μmol/min		1707 ± 166		2059 ± 100
Insulin, pmol/L	67 ± 13	53 ± 8	57 ± 14	53 ± 9
TG, mmol/L	1.20 ± 0.47	1.13 ± 0.41	0.95 ± 0.36	1.02 ± 0.41
NEFA, μmol/L	398 ± 53	687 ± 110[b]	411 ± 69	691 ± 132[b]
Ra_{NEFA}, μmol/min	485 ± 71	756 ± 96[b]	448 ± 111	665 ± 119[b]
Rox_{NEFA}, μmol/min	326 ± 77	601 ± 89[b]	319 ± 65	631 ± 128[b]
TSH, IU/L	2.56 ± 0.73	1.96 ± 0.54[b]	1.98 ± 0.34	1.82 ± 0.47[b]
Free T_3, pmol/L	6.0 ± 0.4	5.8 ± 0.4	5.8 ± 0.3	7.0 ± 1.1
Free T_4, pmol/L	16.2 ± 0.8	16.7 ± 0.7	16.8 ± 0.4	16.0 ± 1.5
ACTH, pmol/L	4.2 ± 0.7	3.4 ± 0.4	3.8 ± 0.2	3.4 ± 0.4
Cortisol, nmol/L	374 ± 25	308 ± 37	299 ± 48[c]	280 ± 27[c]
Leptin, ng/mL	2.5 ± 0.9	2.4 ± 1.0	2.6 ± 0.9	2.3 ± 0.7

Abbreviations: Ra, rate of appearance; Rox, oxidation rate.

[a] Values are means ± SEM; n = 6 subjects.

[b] Different from room temperature, $P < .05$.

[c] Different from Pre-acclimation, $P < .05$.

ure 3A. Total BAT volume of activity increased by 45% after 4 weeks of cold acclimation (66 ± 30 mL before acclimation vs 95 ± 28 mL after acclimation; $P = .05$; Figure 3B). BAT attenuation, determined using CT and expressed in Hounsfield units, was the same at room temperature and increased to a similar degree in all participants after an acute cold exposure, independent of acclimation status (Figure 3C). To examine cold-stimulated BAT and skeletal muscle quantitative glucose uptake, a cervicothoracic dynamic PET/CT acquisition was performed after the iv injection of a bolus of ^{18}FDG during the acute cold exposure. Fractional uptake (K_i) of ^{18}FDG (Figure 3D) was significantly greater in supraclavicular BAT compared with the longus colli, sternocleidomastoid, trapezius, pectoralis major, and deltoid muscles as well as sc adipose tissue. The K_i of ^{18}FDG in supraclavicular BAT was significantly greater after acclimation compared with before acclimation to cold (Figure 3D). Similarly, net tissue glucose uptake (K_m) (Figure 3E) was significantly higher in BAT vs longus colli, sternocleidomastoid, trapezius, pectoralis major, and deltoid muscles as well as sc adipose tissue. The K_m of ^{18}FDG in supraclavicular BAT was not significantly different between acclimation states ($P = .08$). Given a total glucose uptake by BAT of 20.1 ± 15.2 μmol/min before acclimation and 26.2 ± 11.8 μmol/min after acclimation ($P = .08$) and a plasma glucose appearance of 1707 ± 166 and 2059 ± 100 μmol/min, respectively, BAT glucose uptake accounted for 1.1% ± 0.8% and 1.4% ± 0.7% of plasma glucose turnover, respectively. There was a significant direct relationship between the radiodensity of BAT and the fractional and net glucose uptake by the tissue (Pearson $r = 0.71$, $P = .01$; and Pearson $r = 0.72$, $P = .008$, respectively; Figure 3, F and G).

Daily cold exposure increases BAT oxidative metabolism

To investigate the oxidative capacity of cold-stimulated BAT, a cervicothoracic dynamic PET/CT acquisition was performed after the iv injection of a bolus of [^{11}C]acetate during the acute cold exposure. After the iv injection of [^{11}C]acetate, BAT ^{11}C radioactivity over time was significantly higher during cold exposure compared with room temperature, both before and after a cold acclimation intervention (Figure 4, A and E). Pectoralis major was the only muscle displaying a significant cold-induced increase in ^{11}C radioactivity over time (Figure 4, C and G). The monoexponential decay slope from tissue peak ^{11}C activity ([^{11}C]acetate k), a surrogate of tissue oxidative metabolism (34, 35), increased significantly during cold exposure in BAT (effect of temperature $P = .001$; Figure 4I), demonstrating an increase in cold-induced oxidative metabolism. The monoexponential decay slope from tissue peak ^{11}C activity was also presented as a function of the total BAT volume of activity to demonstrate the total oxidative metabolism of BAT. The total BAT oxidative metabolism increased significantly in the cold with the increase being significantly greater after the cold acclimation (temperature × acclimation interaction $P = .02$; Figure 4J).

doi: 10.1210/jc.2013-3901

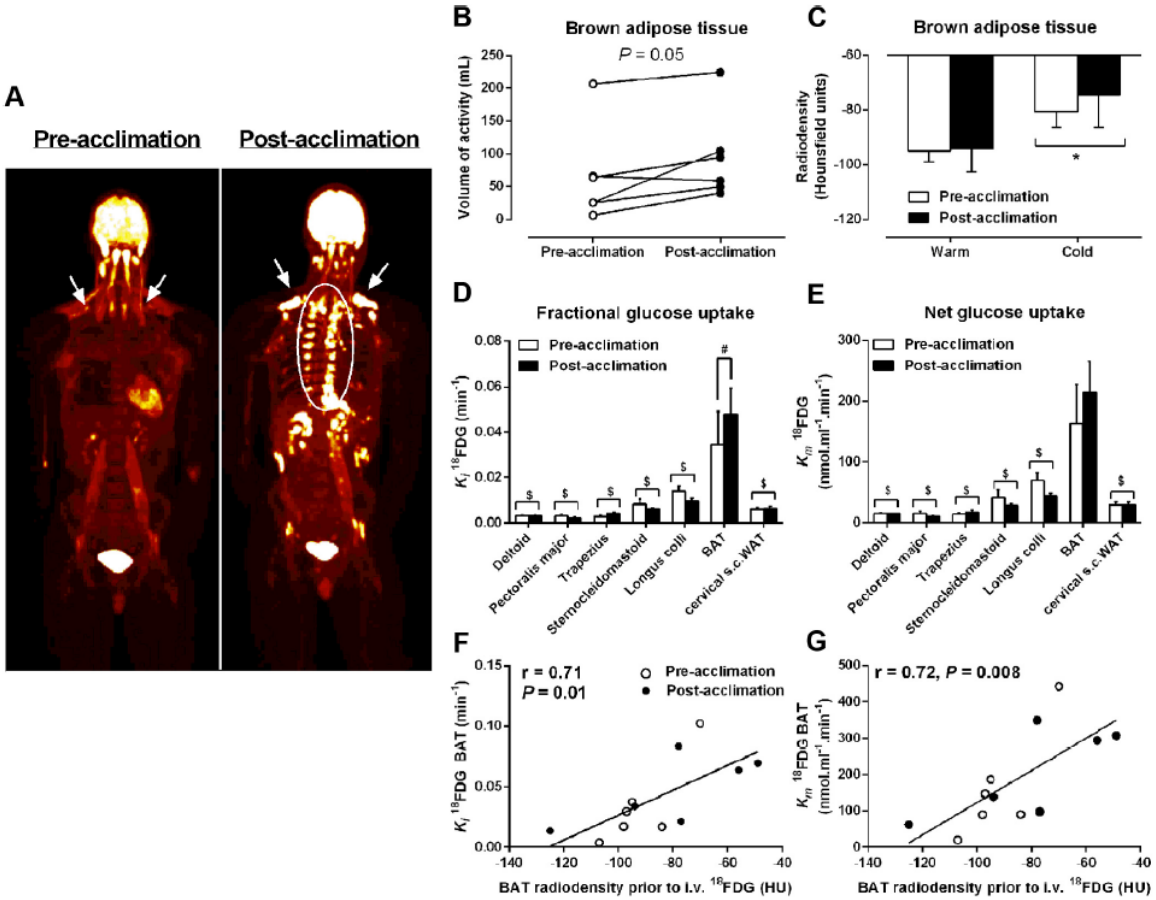

Figure 3. Tissue glucose uptake. A, Coronal view (anterior-posterior projection) of whole-body ^{18}FDG uptake during cold exposure before and after acclimation. B, Volume of BAT ^{18}FDG activity before and after acclimation. C, BAT radiodensity by CT during room temperature and cold exposure before and after acclimation. D and E, Fractional (K_i) (D) and net (K_m) (E) glucose uptake in cervicothoracic tissues. F and G, Relationship between BAT radiodensity from CT taken before iv ^{18}FDG injection in the cold and K_i ^{18}FDG (Pearson r = 0.71, $P = .01$) (F) and K_m ^{18}FDG (Pearson $r = 0.72$, $P = .008$) (G). *, $P < .05$ vs room temperature; $, $P < .005$ vs BAT; #, $P < .05$ vs before acclimation, ANOVA with Bonferroni's post hoc test.

Discussion

Based on the PET tracers ^{18}FDG and [^{11}C]acetate, this study demonstrates for the first time that daily cold exposure not only increases the volume of metabolically active BAT by 45% but also doubles its cold-induced oxidative capacity in adult humans. Within the [^{11}C]acetate PET acquisition field of view including the neck and upper thorax, BAT was the only tissue demonstrating a significant increase in the total oxidative metabolism in the cold with the increase being significantly greater after the cold acclimation. [^{11}C]Acetate as PET tracer has proved to be instrumental in assessing BAT (6) and other tissue metabolism in vivo (31, 32, 36, 37).

Thirty years ago, Huttunen et al (16) described the greater presence of multilocular adipocytes after necropsy in adipose tissue samples excised from the neck region of Finnish outdoor workers exposed to the cold compared with indoor workers. Until recently, this was the only evidence suggesting that chronic cold exposure induces increases in BAT mass in adult humans. However, the hypothesis that chronic cold activation stimulates BAT recruitment in vivo in adult humans has only recently explicitly been investigated (22, 23), while the present study was in progress. We and others (22) have observed that daily exposure to a mild cold, an unequivocal and to date most potent and safe stimulus to activate BAT in humans, does indeed increase whole-body BAT volume of activity, as defined by the volume of ^{18}FDG uptake in BAT. Recent studies have demonstrated that most BAT depots in humans exhibit molecular signatures and histological features resembling the inducible brown adipocytes (known as beige, brown-in-white, or brite) clustered within white

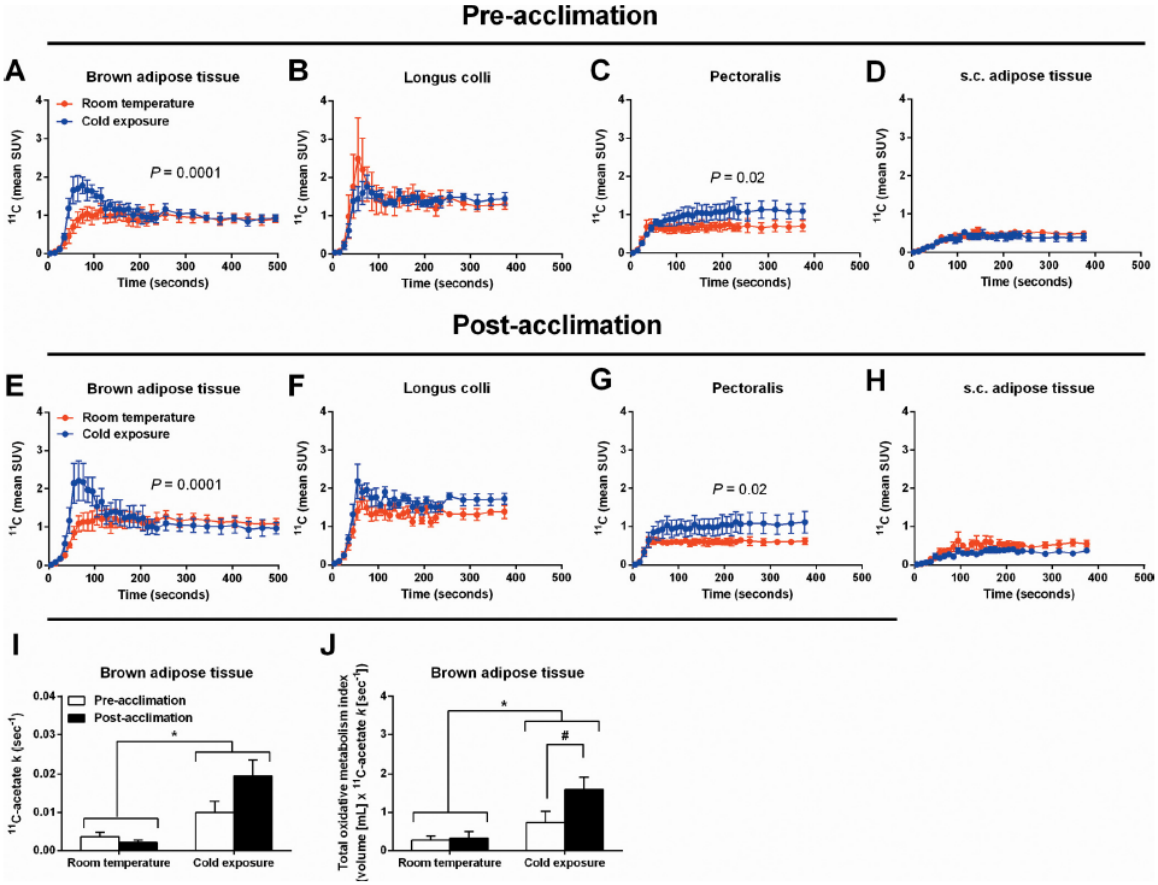

Figure 4. [^{11}C]Acetate kinetics. A–H, ^{11}C time-radioactivity curves over the first 500 seconds of acquisition after [^{11}C]acetate injection at room temperature (red) and during cold exposure (blue) in BAT (A and E), longus colli (B and F), pectoralis (C and G), and cervical sc white adipose tissue (D and H) before and after acclimation. I, Tissue oxidative metabolism index ([^{11}C]acetate *k*) in cervicothoracic BAT before and after acclimation. J, Total BAT oxidative metabolism index before and after acclimation. *, $P < .05$ vs room temperature; #, $P < .05$ vs before acclimation, ANOVA with Bonferroni's post hoc test.

adipose tissue depots of cold-exposed rodents (4, 5) but may also contain classical BAT (9, 38). Whether the increased volume of glucose uptake observed herein is a result of proliferation of classical brown adipocytes, a de novo recruitment of brite adipocytes from white adipose tissue precursors (4), or simply a direct interconversion of mature white adipocytes into a brown adipocyte phenotype or browning (39, 40), is unclear. These findings imply that the thermogenic potential of BAT has increased as a result of the 4-week cold acclimation. Due to the requirement of using radioactive isotopes to assess BAT metabolism in vivo in humans and limits in radioactivity exposure, the time course of both BAT recruitment and atrophy after the end of the intervention are not possible to determine in a within-subject design such as this.

The decreases in BAT radiodensity and the low levels of glucose uptake, averaging 20.1 ± 15.2 and 26.2 ± 11.8 μmol/min, under both experimental cold conditions lends further support to the notion that intracellular TGs are likely the predominant substrate fueling BAT oxidative metabolism in humans. Although intracellular TG depots decrease during the acute cold exposure, the similar radiodensity of BAT observed under unstimulated conditions (eg, room temperature) before and after acclimation would suggest that they replete rapidly after the acute cold exposure. The time course of this repletion, including the role of BAT in postprandial metabolism, requires further investigation and may shed some light on the metabolic regulatory function of BAT. The significant inverse relationship between BAT radiodensity and its fractional and net glucose uptake suggests that, similar to skeletal muscle, circulating substrates may supply and complement the intracellular depots to meet the energy demand under stimulated conditions. The metabolic fate of glucose taken up by BAT has yet to be clearly established in humans. However, with BAT thermogenesis dependent on fatty

doi: 10.1210/jc.2013-3901

acids for the activation of uncoupling protein-1 (UCP1) and as a substrate to fuel thermogenesis (14), glucose is likely supplying the carbon backbone for fatty acid synthesis, which can be subsequently oxidized. The reduced concentration of circulating glucose after acclimation, despite a greater glucose rate of appearance, combined with a trend toward a greater glucose clearance by BAT also suggests that this tissue may play a greater role in glucose metabolism than previously suspected. The detailed characterization of the fuel utilization and substrate handling of this tissue in humans warrants further investigation if it is to be further pursued as a therapeutic target for metabolic diseases.

The metabolic impact of the increased BAT oxidative capacity that occurred after repetitive cold exposures may have contributed to an increase in the nonshivering thermogenesis (NST) of our subjects. Nonetheless, our cold acclimation protocol was insufficient to promote the recruitment of BAT-mediated NST to the extent necessary to completely abolish the shivering response (Figure 2). More prolonged and/or intense cold acclimation could be necessary to fully recruit BAT-mediated NST in humans, or exposure to a colder acute thermal challenge may be required for BAT-mediated NST to fully manifest. Furthermore, although EMG was monitored in 12 muscle groups, it remains that this method measures superficial EMG activity and provides some insight on fiber recruitment and fuel selection. Consequently, it is possible that deeper muscle groups, not accessible by EMG, were most influenced by the changes in BAT-mediated NST or that changes in skeletal muscle bioenergetics were also modified. In the only cold acclimation study quantifying shivering activity in humans, and thus de facto NST, 20 days of daily exposure to 12°C (8 h/d) was required to observe a near abolishment of shivering activity in men previously acclimated to summer conditions (41). It is noteworthy that even in rodents subjected to aggressive cold-exposure protocols (often 24 hours exposure for several days at 4°C), NST develops progressively (42). In rats, cold exposure leads to an initial (a few hours) increase in BAT thermogenic activity associated with an increase in UCP1 stimulation, which is followed after a few days by a progressive increase in the thermogenic capacity, revealed through increases in UCP1 expression, mitochondriogenesis, and brown adipocyte protein content (43). In rats, cold adaptation has been reported to tremendously increase the thermogenic capacity of BAT, which can account for more than 60% of the total heat produced in response to noradrenaline with little contribution from skeletal muscle (44). In the present study, because we did not have access to BAT samples, we cannot determine the cause of the increase in BAT thermogenic capacity (ie, increase in expression of UCP1 and accessory thermogenic genes or mitochondriogenesis). Another important limitation of the present study is the inability to assess the relative contribution of BAT and muscle as well as organs such as the heart and liver to total thermogenesis. Nevertheless, based on the present [^{11}C]acetate oxidative metabolism and BAT radiodensity data, one can be confident of some contribution of BAT to energy metabolism after 4 weeks of acclimation, which is in line with evidence showing that human brown adipocytes are metabolically active and share similarities with classic brown adipocytes seen in laboratory rodents (9).

In summary, we showed that total BAT volume of activity increases significantly as a result of repeated controlled daily cold exposure and that this change in mass is paralleled by an increase in BAT oxidative capacity. Therefore, the contribution of BAT to NST must necessarily increase during cold acclimation in humans.

Acknowledgments

We acknowledge the excellent technical assistance provided by Diane Lessard, Caroll-Lynn Thibodeau, Maude Gérard, Éric Lavallée, and Frédérique Frisch. We also thank the subjects of this study for their collaboration and Allen-Vanguard Inc (Kevin Semeniuk) for providing the liquid-conditioned suits.

Address all correspondence and requests for reprints to: Dr François Haman, Faculty of Health Sciences, University of Ottawa, Ottawa, Ontario, Canada K1N 6N5. E-mail: fhaman@uottawa.ca; or Dr. Denis Richard, Centre de Recherche de l'Institut Universitaire, de Cardiologie et de Pneumologie de Québec, Québec City, Québec, Canada G1V 4G5. E-mail: Denis.Richard@criucpq.ulaval.ca.

This work was supported by a grant from the Canadian Diabetes Association (OG-3–10-2970-AC) and the Natural Sciences and Engineering Research Council of Canada (NSERC Canada) to F.H. and was performed at the Centre de recherche clinique Etienne-Le Bel, a research center funded by the Fonds de la recherche Québec-Santé. D.P.B. is the recipient of the NSERC Postgraduate Scholarship. S.M.L. is the recipient of a Canadian Institutes of Health Research (CIHR) Postdoctoral fellowship. D.R. is the recipient of the CIHR/Merck Frosst Research Chair on Obesity. A.C.C. is the recipient of the CIHR-GlaxoSmithKline Chair in Diabetes.

Author contributions: conception and design of the experiments, F.H., D.R., A.C.C., E.E.T., and B.G.; collection, analysis, and interpretation of data, D.P.B., S.M.L., H.T., C.N., M.K., S.P., F.H., E.E.T., D.R., A.C.C., and S.P.; drafting the article or revising it critically for important intellectual content, D.P.B., S.M.L., H.T., F.H., A.C.C., D.R., E.E.T., B.G., C.N., and M.K.

Disclosure Summary: The authors have declared that no conflict of interest exists related to the content of this manuscript.

References

1. **van Marken Lichtenbelt WD, Vanhommerig JW, Smulders NM, et al.** Cold-activated brown adipose tissue in healthy men. *N Engl J Med*. 2009;360:1500–1508.
2. **Cypess AM, Lehman S, Williams G, et al.** Identification and importance of brown adipose tissue in adult humans. *N Engl J Med*. 2009; 360:1509–1517.
3. **Virtanen KA, Lidell ME, Orava J, et al.** Functional brown adipose tissue in healthy adults. *N Engl J Med*. 2009;360:1518–1525.
4. **Wu J, Boström P, Sparks LM, et al.** Beige adipocytes are a distinct type of thermogenic fat cell in mouse and human. *Cell*. 2012;150: 366–376.
5. **Sharp LZ, Shinoda K, Ohno H, et al.** Human BAT possesses molecular signatures that resemble beige/brite cells. *PLoS One*. 2012; 7:e49452.
6. **Ouellet V, Labbé SM, Blondin DP, et al.** Brown adipose tissue oxidative metabolism contributes to energy expenditure during acute cold exposure in humans. *J Clin invest*. 2012;122:545–552.
7. **Vosselman MJ, Brans B, van der Lans AA, et al.** Brown adipose tissue activity after a high-calorie meal in humans. *Am J Clin Nutr*. 2013;98:57–64.
8. **Ouellet V, Routhier-Labadie A, Bellemare W, et al.** Outdoor temperature, age, sex, body mass index, and diabetic status determine the prevalence, mass, and glucose-uptake activity of ^{18}F-FDG-detected BAT in humans. *J Clin Endocrinol Metab*. 2011;96:192–199.
9. **Cypess AM, White AP, Vernochet C, et al.** Anatomical localization, gene expression profiling and functional characterization of adult human neck brown fat. *Nat Med*. 2013;19:635–639.
10. **Vijgen GH, Bouvy ND, Teule GJ, Brans B, Schrauwen P, van Marken Lichtenbelt WD.** Brown adipose tissue in morbidly obese subjects. *PLoS One*. 2011;6:e17247.
11. **Orava J, Nuutila P, Noponen T, et al.** Blunted metabolic responses to cold and insulin stimulation in brown adipose tissue of obese humans. *Obesity (Silver Sping)*. 2013;21(11):2279–2287.
12. **Lean ME.** Brown adipose tissue in humans. *Proc Nutr Soc*. 1989; 48:243–256.
13. **Ricquier D, Nechad M, Mory G.** Ultrastructural and biochemical characterization of human brown adipose tissue in pheochromocytoma. *J Clin Endocrinol Metab*. 1982;54:803–807.
14. **Cannon B, Nedergaard J.** Brown adipose tissue: function and physiological significance. *Physiol Rev*. 2004;84:277–359.
15. **Vijgen GH, Bouvy ND, Teule GJ, et al.** Increase in brown adipose tissue activity after weight loss in morbidly obese subjects. *J Clin Endocrinol Metab*. 2012;97:E1229–E1233.
16. **Huttunen P, Hirvonen J, Kinnula V.** The occurrence of brown adipose tissue in outdoor workers. *Eur J Appl Physiol Occup Physiol*. 1981;46:339–345.
17. **Schulz TJ, Huang P, Huang TL, et al.** Brown-fat paucity due to impaired BMP signalling induces compensatory browning of white fat. *Nature*. 2013;495:379–383.
18. **Yin H, Pasut A, Soleimani VD, et al.** MicroRNA-133 controls brown adipose determination in skeletal muscle satellite cells by targeting Prdm16. *Cell Metab*. 2013;17:210–224.
19. **Carey AL, Formosa MF, Van Every B, et al.** Ephedrine activates brown adipose tissue in lean but not obese humans. *Diabetologia*. 2013;56:147–155.
20. **Vosselman MJ, van der Lans AA, Brans B, et al.** Systemic β-adrenergic stimulation of thermogenesis is not accompanied by brown adipose tissue activity in humans. *Diabetes*. 2012;61:3106–3113.
21. **Cypess AM, Chen YC, Sze C, et al.** Cold but not sympathomimetics activates human brown adipose tissue in vivo. *Proc Natl Acad Sci U S A*. 2012;109:10001–10005.
22. **van der Lans AA, Hoeks J, Brans B, et al.** Cold acclimation recruits human brown fat and increases nonshivering thermogenesis. *J Clin Invest*. 2013;123:3395–3403.
23. **Yoneshiro T, Aita S, Matsushita M, et al.** Recruited brown adipose tissue as an antiobesity agent in humans. *J Clin Invest*. 2013;123: 3404–3408.
24. **Hardy JD, Dubois EF.** The technic of measuring radiation and convection. *J Nutr*. 1938;15:461–475.
25. **Haman F, Péronnet F, Kenny GP, et al.** Effect of cold exposure on fuel utilization in humans: plasma glucose, muscle glycogen, and lipids. *J Appl Physiol*. 2002;93:77–84.
26. **Haman F, Legault SR, Weber JM.** Fuel selection during intense shivering in humans: EMG pattern reflects carbohydrate oxidation. *J Physiol*. 2004;556:305–313.
27. **Carpentier A, Patterson BW, Uffelman KD, et al.** The effect of systemic versus portal insulin delivery in pancreas transplantation on insulin action and VLDL metabolism. *Diabetes*. 2001;50:1402–1413.
28. **Carpentier AC, Frisch F, Cyr D, et al.** On the suppression of plasma nonesterified fatty acids by insulin during enhanced intravascular lipolysis in humans. *Am J Physiol Endocrinol Metab*. 2005;289: E849–E856.
29. **Labbé SM, Croteau E, Grenier-Larouche T, et al.** Normal postprandial nonesterified fatty acid uptake in muscles despite increased circulating fatty acids in type 2 diabetes. *Diabetes*. 2011;60:408–415.
30. **Buck A, Wolpers HG, Hutchins GD, et al.** Effect of carbon-11-acetate recirculation on estimates of myocardial oxygen consumption by PET. *J Nucl Med*. 1991;32:1950–1957.
31. **Klein LJ, Visser FC, Knaapen P, et al.** Carbon-11 acetate as a tracer of myocardial oxygen consumption. *Eur J Nucl Med*. 2001;28:651–668.
32. **Ménard SL, Croteau E, Sarrhini O, et al.** Abnormal in vivo myocardial energy substrate uptake in diet-induced type 2 diabetic cardiomyopathy in rats. *Am J Physiol Endocrinol Metab*. 2010;298: E1049–E1057.
33. **Croteau E, Lavallée E, Labbe SM, et al.** Image-derived input function in dynamic human PET/CT: methodology and validation with ^{11}C-acetate and 18F-fluorothioheptadecanoic acid in muscle and 18F-fluorodeoxyglucose in brain. *Eur J Nucl Med Mol Imaging*. 2010;37:1539–1550.
34. **Brown M, Marshall DR, Sobel BE, Bergmann SR.** Delineation of myocardial oxygen utilization with carbon-11-labeled acetate. *Circulation*. 1987;76:687–696.
35. **Ng CK, Huang SC, Schelbert HR, Buxton DB.** Validation of a model for [1-^{11}C]acetate as a tracer of cardiac oxidative metabolism. *Am J Physiol*. 1994;266:H1304–H1315.
36. **Labbé SM, Grenier-Larouche T, Noll C, et al.** Increased myocardial uptake of dietary fatty acids linked to cardiac dysfunction in glucose-intolerant humans. *Diabetes*. 2012;61:2701–2710.
37. **van den Hoff J, Burchert W, Börner AR, et al.** [1-^{11}C]Acetate as a quantitative perfusion tracer in myocardial PET. *J Nucl Med*. 2001; 42:1174–1182.
38. **Jespersen NZ, Larsen TJ, Peijs L, et al.** A classical brown adipose tissue mRNA signature partly overlaps with brite in the supraclavicular region of adult humans. *Cell Metab*. 2013;17:798–805.
39. **Frontini A, Vitali A, Perugini J, et al.** White-to-brown transdifferentiation of omental adipocytes in patients affected by pheochromocytoma. *Biochim Biophys Acta*. 2013;1831:950–959.
40. **Rosenwald M, Perdikari A, Rülicke T, Wolfrum C.** Bi-directional interconversion of brite and white adipocytes. *Nat Cell Biol*. 2013; 15:659–667.
41. **Davis TR.** Chamber cold acclimatization in man. *J Appl Physiol*. 1961;16:1011–1015.
42. **Nedergaard J, Cannon B.** UCP1 mRNA does not produce heat. *Biochim Biophys Acta*. 2013;1831:943–949.
43. **Trayhurn P, Ashwell M, Jennings G, Richard D, Stirling DM.** Effect of warm or cold exposure on GDP binding and uncoupling protein in rat brown fat. *Am J Physiol*. 1987;252:E237–243.
44. **Foster DO, Frydman ML.** Tissue distribution of cold-induced thermogenesis in conscious warm- or cold-acclimated rats reevaluated from changes in tissue blood flow: the dominant role of brown adipose tissue in the replacement of shivering by nonshivering thermogenesis. *Can J Physiol Pharmacol*. 1979;57:257–270.

APPENDIX E:

Additional results from ARTICLE IV

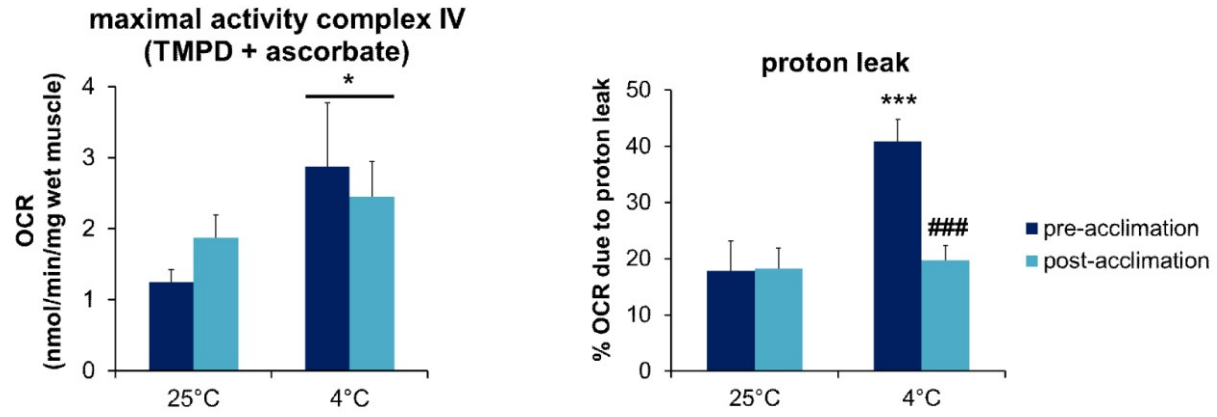

Figure 5. Left panel: Maximal complex IV activity (cytochrome C oxidase). * 4°C *vs.* 25°C, P = 0.05. OCR: oxygen consumption rate. Right panel: Proton leak measured after ATP synthase inhibition by oligomycin. *** 4°C *vs.* 25°C, $P < 0.00$; ###, pre- *vs.* post-acclimation at 4°C. ***All measures performed by Céline Aguer, PhD*** on permeabilized muscle fibers before (25°C)and after (4°C) an acute cold exposure, pre- and post-acclimation. Values are Mean ± SEM, n = 6.

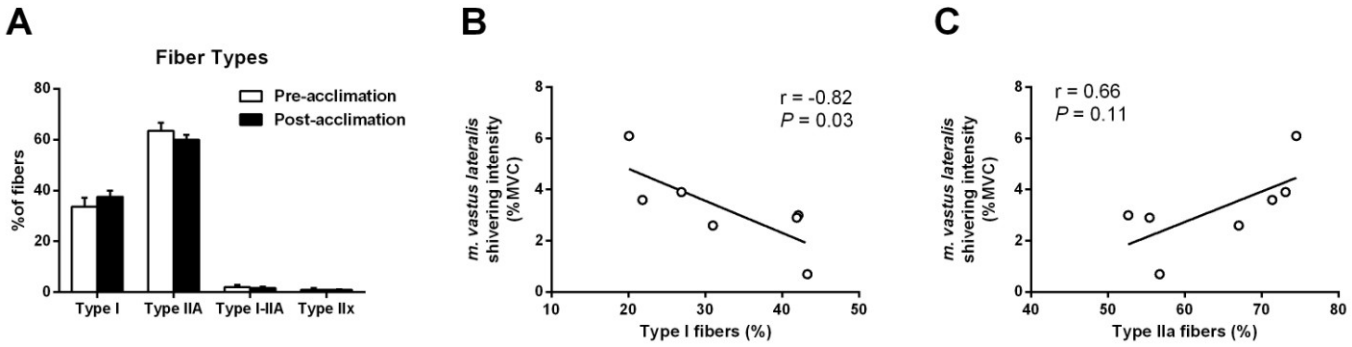

Figure 6. (A) Muscle fiber composition measured pre- and post- acclimation in *m. vastus lateralis*. Relationship between shivering intensity of *m. vastus lateralis* and percentage of Type I fibers (B) and Type IIa fibers (C). Values are Mean ± SEM, n = 6. ***Fiber typing performed by laboratory of Dr. Mary-Ellen Harper.***

APPENDIX F:

Abstracts related to thesis

International Conferences

Aguer C, **Blondin DP**, Taylor T, Taylor AW, Harper M-E, Haman F.
Cold acclimation in healthy young men results in metabolic modifications in skeletal muscle.
The Obesity Society Annual Scientific Meeting, Atlanta, GA, November 11-16, 2013.
Poster Presentation.

Blondin DP, Labbé SM, Noll C, Kunach M, Phoenix S, Guérin B, Turcotte EE, Haman F, Richard D, Carpentier AC.
Acute cold exposure elicits increases in BAT oxidative metabolism in individuals with Type 2 Diabetes.
NIH Workshop: Exploring the role of brown fat in humans, Bethesda, MD, October 15-16, 2013.
Oral Presentation.

Blondin DP, Labbé SM, Richard D, Turcotte É, Carpentier AC, Haman F.
Cold acclimation increases the contribution of brown adipose tissue-derived thermogenesis in adult humans.
Experimental Biology, Boston, USA, April 19-24, 2013.
Oral Presentation.

Blondin DP, Labbé SM, Richard D, Turcotte É, Carpentier AC, Haman F.
Brown adipose tissue volume correlates inversely to shivering intensity in cold-exposed men.
Recent Advances and Controversies in the Measurement of Energy Metabolism, Maastricht, The Netherlands, November 2-4, 2011.
Oral Presentation.

Blondin DP, Labbé SM, Richard D, Turcotte É, Carpentier AC, Haman F.
Muscle recruitment and muscle-specific substrate uptake in cold-exposed humans evaluated by electromyography and positron emission tomography coupled to computed tomography (PET/CT).
Obesity 2011, 29th Annual scientific meeting, Orlando, FL, October 1-5, 2011.
Poster Presentation no 162-P

Blondin DP, Ouellet V, Carpentier AC, Richard D, Turcotte É, Haman F.
Cold exposure methodology for investigating brown adipose tissue activation in humans.
Obesity 2010, 28th Annual scientific meeting, San Diego CA, October 8-12, 2010.
Poster Presentation no 766-P

Ouellet V, Labbé SM, **Blondin DP**, Haman F, Turcotte É, Richard D,Carpentier AC.
Cold-activated brown adipose tissue metabolism in healthy men.
Obesity 2010, 28th Annual scientific meeting, San Diego CA, October 8-12, 2010.
Late-Breaking Abstracts *Poster Presentation* 33-LB-P

Richard D, Ouellet V, Ménard S, **Blondin DP**, Turcotte E, Haman, F, Carpentier AC.
Brown adipose tissue in humans.
11th International Congress on Obesity*, July 11-15, 2010, Stockholm, Sweden*

National Conferences

Blondin DP, Labbé SM, Richard D, Turcotte É, Carpentier AC, Haman F.
Daily cold exposure increases brown adipose tissue-derived thermogenesis in adult humans.
16th Annual Canadian Diabetes Association/Canadian Society of Endocrinology and Metabolism Professional Conference and Annual Meetings, Montreal, QC, October 17-20, 2013.
Poster Presentation.

Blondin DP, Labbé SM, Noll C, Kunach M, Turcotte É, Carpentier AC, Richard D, Haman F.
La contribution thermogénique du tissu adipeux brun augmente suite à un protocole d'acclimatation au froid chez des hommes sains.
5ème Réunion annuelle de la plate-forme COLosSUS, Sherbrooke, Canada, Feb. 14-15 2013.
Oral Presentation.

Labbé SM, **Blondin DP,** Noll C, Kunach M, Turcotte É, Haman F, Carpentier AC, Richard D.
L'exposition aigue au froid n'induit pas l'activation du tissu adipeux brun chez le patient diabétique.
5ème Réunion annuelle de la plate-forme COLosSUS, Sherbrooke, Canada, Feb. 14-15 2013.
Poster Presentation.

Aguer C, **Blondin DP**, Taylor T, Taylor AW, Harper M-E, Haman F.
Effet d'une exposition aigue et chronique au froid sur le métabolisme du muscle squelettique chez l'homme sain.
5ème Réunion annuelle de la plate-forme COLosSUS, Sherbrooke, Canada, Feb. 14-15 2013.
Poster Presentation.

Blondin DP, Labbé SM, Richard D, Turcotte É, Carpentier AC, Haman F.
Le recrutement musculaire et le transport intramusculaire du ^{18}Fluorodeoxyglucose (^{18}FDG) et l'acide ^{18}Fluoro-6-thia-heptadécanoïque (^{18}FTHA) lors d'une exposition au froid mesurer par la tomodensitométrie couplée à la tomography par emission de positrons (TEP/CT).
3ème Réunion annuelle de la plate-forme COLosSUS, 17-18 février 2011, Sherbrooke.
Oral Presentation

Ouellet, V, Labbé SM, **Blondin DP,** Haman F, Turcotte É, Richard D, Carpentier AC.
Métabolisme du tissu adipeux brun en réponse à une exposition au froid chez des hommes en santé.
3ème Réunion annuelle de la plate-forme COLosSUS, 17-18 février 2011, Sherbrooke.

Blondin, D.P., Robidoux, M., Imbeault, P., Blais, J., O'hearn, K., Kruemmel, E., Seabert, T., Pal, S. and Haman, F.
Effects of dietary behaviour on exogenous glucose kinetics in 2 Oji-Cree communities of northwestern Ontario.
Canadian Obesity Network's 1st National Obesity Summit.

Blondin, D.P., Imbeault, P., Péronnet, F., and Haman, F.
Exogenous glucose oxidation during shivering: effects of carbohydrate ingestion timing and type.
Canadian Society of Exercise Physiology Annual Scientific Conference. Banff, Alberta
Oral presentation

Maneshi, A., **Blondin, D.P.**, Imbeault, M-A., Haman, F.
Effects of the menstrual cycle on substrate utilization during low-intensity shivering.
Canadian Society of Exercise Physiology Annual Scientific Conference. Banff, Alberta